Retinoic acid and mouse development: identification of retinoic acid receptor target genes involved in axial patterning

By

Deborah M. Allan

Department of Medicine, Division of Experimental Medicine
McGill University, Montreal
July 2001

A thesis submitted to the Faculty of Graduate Studies and Research in partial fulfillment of the requirements of the degree of doctorate of philosophy.

Table of Contents

Chapter 2. Materials and Methods

Abstract

Retinoic acid (RA), the major biologically active form of vitamin A, is required for normal development of the mouse embryo. In particular, RA is necessary for the correct anteroposterior specification of the embryonic axis. Exposure to RA at certain stages of development leads to premature truncation of the vertebral column, accompanied by spina bifida. In contrast, embryos that are homozygous null for *RARγ* do not exhibit these defects, indicating that this receptor specifically mediates this teratogenic effect. Differential display PCR and suppression subtractive hybridization were employed using the *RARγ* null embryos in an attempt to identify downstream targets that may be involved in the formation of these abnormalities. As a result of this process, a full-length cDNA molecule encoding a novel member of the aldo-keto reductase family (*AKR1A4*) was cloned. Although RA does not regulate the expression of this gene, its developmental expression pattern and substrate specificity suggests a potential role for this enzyme in the protection of certain rapidly growing embryonic structures from harmful metabolites.

A precise level of RA signaling is also required for proper specification of vertebral identity. Exposure to excess RA during the early stages of gastrulation results in posterior homeotic transformations of several vertebrae. These transformations are correlated with shifts in the anterior boundaries of *Hox* expression. In contrast, the loss of functional RARs leads to anterior vertebral transformations. Although retinoic acid response elements have been identified in *Hox* promoters, it is likely that RA regulates the expression of some *Hox* genes through intermediary factors. Cdx1 is a homeobox-containing transcription factor that influences vertebral patterning in a manner similar to RARs, and is directly regulated by RA in the mouse embryo. Analysis of an allelic series of *RARγ/Cdx1* null mutant mice demonstrated that *Cdx1* and *RARγ* act synergistically to pattern certain cervical vertebrae. In addition, *Cdx1* is required for the full effect of RA treatment on the vertebral column. However, Cdx1 does not mediate all of the effects of RARγ as the incidence of a thoracic to cervical vertebral transformation is significantly higher in *RARγ/Cdx1* double mutants as compared to either single null mouse.

Résumé

L'acide rétinoïque (AR), le metabolite actif de la vitamine A, est requis pour le développement normal de l'embryon de souris, tout particulièrement pour la formation de l'axe antéro-posterieur. A certains stades du développement, l'exposition à l'AR exogène entraîne la troncation de la colonne vertebrale, accompagnée de spina bifida. Toutefois, les embryons deficients en récepteur de l'AR γ (RARγ) ne présentent pas ces défauts, indiquant que RARγ est nécessaire à l'expression de ce phénotype. Des techniques d'expression différentielle par PCR et de soustraction par hybridation ont été employées, en utilisant des embryons déficients en RARγ, afin d'identifier des gènes cibles qui seraient responsables de l'apparition de ces malformations. Ces études ont mené à l'identification et au clonage d'un nouvel ADNc encodant une proteine de la famille des aldo-céto réductases (AKR1A4). Bien que l'expression d'*AKR1A4* ne semble pas régulée par l'AR, son patron d'expression au cours du développement ainsi que sa spécificité pour certains substrats suggèrent que cet enzyme jouerait un rôle dans la protection de certaines structures de l'embryon en croissance rapide contre des métabolites nocifs.

Un niveau précis de signalisation par l'AR est requis pour une spécification normale de l'identité vertébrale. L' exposition à un excès d'AR durant les premiers stades de la gastulation cause des transformations homéotiques postérieures de plusieures vertèbres. Ces transformations sont accompagnées d'un déplacement de la limite antérieure d'expression des gènes *Hox*. Par contre, une perte de RAR fonctionnel se traduit par des transformations antérieures des vertèbres. Bien que des éléments de réponse à l'AR aient été identifiés dans le promoteur de quelques gènes *Hox*, il est fort probable que l'AR régule l'expression de certains *Hox* via des facteurs intermédiaires. Cdx1 est un facteur de transcription à boîte homéo qui influence l'identité des vertèbres d'une manière similaire aux RARs, en plus d'être une cible directe de l'AR chez l'embryon de souris. L'analyse d'une série allélique de souris mutantes pour *RARγ/Cdx1* a montré que *Cdx1* et *RARγ* agissaient en synergie afin de conférer l'identité de certaines vertèbres cervicales. De plus, *Cdx1* est requis pour observer le plein effet du traitement avec l'AR sur la colonne vertébrale. Cependant, Cdx1 n'est pas la cible unique du RARγ, comme l'indique l'incidence de la transformation d'une vertèbre thoracique en cervicale

qui est beaucoup plus élevée chez les doubles mutants *RARγ/Cdx1* que chez les mutants simples.

Acknowledgments

First and foremost, I would like to thank Dr. David Lohnes for his support and guidance throughout my graduate training. His consistent encouragement, unfailing sense of humour, and patience regarding the preparation of this thesis were especially appreciated.

I would also like to thank the past and present members of the Lohnes laboratory for their thoughtful comments and suggestions regarding the work presented in this thesis. I would especially like to acknowledge the invaluable technical assistance of Marie-Claude Marchand, Nathalie Bouchard, and Wei Wang. The contributions made by Martin Houle are also greatly appreciated, particularly the continuation of the work presented in Chapter 5. I would also like to thank Martin Houle and Sylwia Wasiak for translation of the abstract. Finally, I would like to thank all of the lab members, and neighbors, for their friendship.

The support and guidance received from Dr. Gerald Price and Ms. Dominique Besso is greatly appreciated. I would also like to thank Dr. Mark Featherstone, Dr. Muriel Aubry, Dr. Jean Vacher, and Dr. Martine Raymond for sitting on my thesis committee.

I would like to acknowledge the assistance provided by the staff of the mouse facilities at the IRCM. In particular, Julie Turcotte was invaluable in the care of the mice that contributed to the work presented in this thesis. I would also like to thank Christian Charbonneau for assistance with photography and slide preparation, and Marco Raposo for sequencing services. Additionally, I would like to thank Claire Crevier for sectioning the embryos presented in Chapter 4.

The *Cdx1* null mice described in Chapter 5 were obtained through a collaboration with Dr. Barbara Meyer and Dr. Peter Gruss. The templates for probes and riboprobes used throughout these studies were kindly provided by Drs. Mark Featherstone (*Hoxd4*),

Mario Cappechi (*Hoxd3*), Martin Petkovich (*P450RAI*), Bernard Hermann (*Brachyury*), and Peter Gruss (*Cdx1*).

Financial support provided by the Faculty of Graduate Studies and Research at McGill University, and by the National Sciences and Engineering Research Council of Canada is gratefully acknowledged.

Finally, I would like to thank my family and friends for their unconditional support and love. The sincere encouragement and optimistic outlook of my parents was especially appreciated. I would also like to thank my dear friend, Julia Brain, for her assistance in the deposition of this thesis. I am most deeply grateful for the generous patience, understanding, and support that my fiancé Andrew was able to provide from both near and afar.

Abbreviations

AAA	anterior arcus atlantis
ADH	alcohol dehydrogenase
ADR	aldose reductase
AF	activation function
AGE	advanced glycation end product
AKR	aldo-keto reductase
ALDH	aldehyde dehydrogenase
ALR	aldehyde reductase
AP	anteroposterior
AP-1	activated protein 1
BCIP	X-phosphate/5-Bromo-4-chloro-3-indolyl phosphate
CBP	CREB-binding protein
cdk	cyclin dependent kinase
CNS	central nervous system
c.p.m.	counts per million
CRABP	cellular retinoic acid-binding protein
CRAD	*cis*-retinoid/androgen dehydrogenase
CRBP	cellular retinoid binding protein
CTE	carboxy terminal extension
DBD	DNA-binding domain
DD-PCR	differential display polymerase reaction
DEPC	diethyl pyrocarbonate
D-MEM	Dulbecco's Modified Eagle Medium
DMSO	dimethyl sulfoxide
DR	direct repeat
DRIP	vitamin D receptor interacting proteins
DTT	dithiothreitol
E	embryonic day of development
EST	expressed sequence tag
FABP	fatty acid binding protein
FAS	fetal alcohol syndrome
HAT	histone acetyltransferase
HDAC	histone deacetyltransferase
HPLC	high pressure liquid chromatography
IPTG	isopropylthio-β-D-galactoside
JNK	jun N-terminal kinase
LBD	ligand binding domain
LRAT	lethicin:retinol acetyltransferase
MAPK	mitogen activated protein kinase
MEM	minimal essential medium
MKP	map kinase phosphatase
NBT	4-Nitro blue tetrazolium chloride
N-CoR	nuclear receptor corepressor
ONPG	o-Nitrophenyl-β-D-Galactopyranoside

PBS	phosphate-buffered saline
PCR	polymerase chain reaction
PFA	paraformaldehyde
PKC	protein kinase C
PPAR	peroxisome proliferator-activated proteins
RA	retinoic acid
RAL	retinaldehyde
RALDH	retinaldehyde dehydrogenase
RAR	retinoic acid receptor
RARE	retinoic acid response element
RBP	retinol binding protein
RDA	representational difference analysis
REH	retinyl ester hydrolase
RoDH	retinol dehydrogenase
ROL	retinol
RXR	retinoid X receptor
SAGE	serial analysis of gene expression
SDR	short chain dehydrogenase/reductase
SMRT	silencing mediator for retinoic acid and thyroid hormone receptors
TA	tuberculum anterium
TR	thyroid hormone receptor
TRAP	TA-associated proteins
UTR	untranslated region
VAD	vitamin A deficiency
VDR	vitamin D receptor

Table of Figures

Table of Tables

Chapter 1

Literature Review

1.1 Introduction

Vitamin A (retinol) is required for normal development, vision, homeostasis, reproduction, and survival. In addition, various natural and synthetic derivatives of vitamin A (retinoids) are presently employed in the treatment of various skin disorders and some cancers. A critical amount of vitamin A is required for normal embryogenesis, as vitamin A deficiency leads to severe congenital abnormalities. In contrast to vision, which requires 11-*cis*-retinaldehyde as a light sensitive chromophore, all other physiological and developmental processes require carboxylic acid derivatives of vitamin A; retinoic acid (RA). The discovery of two families of retinoid receptors has provided insight as to how such diverse processes in the embryo and adult are influenced by a single vitamin. These receptors act as ligand-activated transcription factors that participate in the transcriptional regulation of various target genes involved in growth, differentiation, and patterning. The aim of this Chapter is to provide an overview of retinoid signaling, with special emphasis on the roles of retinoids in mouse development, in particular the process of axial patterning.

1.2 Vitamin A metabolism

1.2.1 Vitamin A uptake, storage, and mobilization

Vitamin A is ingested in the form of carotenoids (i.e. β-Carotene) or preformed vitamin A from plant and animal products, respectively (reviewed in Sporn *et al.*, 1994). β-Carotene is converted to retinol in the intestine by two consecutive steps. First, oxidative cleavage of β-Carotene results in the formation of two molecules of retinaldehyde, which are subsequently reduced to retinol by aldehyde reductases (see Figure 1.1). Retinol is a substrate for lecithin:retinol acyltransferase (LRAT), an enzyme with catalyzes the formation of retinyl esters, the primary storage form of vitamin A. Retinyl esters can also be formed from serum retinol in tissues that express LRAT, for example the liver (Ong *et al.*, 1988; Yost *et al.*, 1988). The liver stellate cells are the major storage sites for retinyl esters, however other tissues such as the kidneys, adipose

tissue, testis and bone marrow are also sites of retinyl ester accumulation (Williams *et al.*, 1984).

Each molecule of retinol is bound to a retinol binding protein (RBP), which is complexed in a 1:1 molar ratio with transthyretin (TTR). *Rbp* null mutant mice exhibit low plasma retinol levels and impaired retinal function during the first month of life, the latter of which can be corrected by 5 months of age by a diet sufficient in vitamin A (Quadro *et al.*, 1999). However, under vitamin A deficient conditions, defective retinal function persists and plasma retinol declines to undetectable levels, despite the fact that retinol levels in the liver are higher than in wild type animals. Therefore, RBP appears to be necessary for neonatal vision and the mobilization of stored hepatic retinol. In addition to retinol, a small amount of RA (4-14 nmol/L; 0.2%-0.7% of plasma retinol concentrations) normally circulates in the plasma and appears to be preferentially internalized by certain tissues (Kurlandsky *et al.*, 1995).

1.2.2 Distribution of retinoic acid during development

Several experimental approaches have been employed to identify areas of RA localization during development. Transgenic mouse embryos that carry a β-galactosidase reporter gene under the control of RA-responsive elements do not exhibit any evidence of bioactive RA before E7.0 (Rossant *et al.*, 1991). The first appearance of RA signaling occurs in the posterior region of the E7.0-E7.5 embryo, in all three germ layers. By E8.5, high levels of RA can be detected in the trunk tissues up to the level of the first somite, as well as in the retina and craniofacial tissues (Rossant *et al.*, 1991). At this stage very little RA is detected in the tissues caudal to the last formed somite. At later stages of development, RA is abundant in the spinal cord, adrenal gland, kidney, and intestine, and is present at lower levels in the brain, heart and liver (Wagner *et al.*, 1992; Ang *et al.*, 1996b; Moss *et al.*, 1998). Some of these findings have been confirmed by HPLC analysis, which detected high levels of all-*trans*-RA in the spinal cord, hindbrain, somites and the forelimb bud (Scott *et al.*, 1994; Horton and Maden, 1995). The predominant isoforms of RA during embryogenesis are species specific, as 3,4-*didehydro*-RA is the major form of RA in the chick, while only all-*trans*-RA is detected in the mouse (Horton and Maden, 1995; Maden *et al.*, 1998).

1.2.3 Enzymes involved in vitamin A metabolism

Retinoic acid is generated from retinal in a two-step process that involves consecutive enzymatic oxidations (reviewed in Napoli, 1999; Ross *et al.*, 2000; Duester, 2000). The first of these two reactions is reversible and results in the conversion of retinol to retinaldehyde. Several members of two distinct families of enzymes, the alcohol dehydrogenase (ADH) and short-chain dehydrogenase/reductase (SDR) families, can perform this function. This step is followed by a non-reversible oxidation of retinaldehyde to retinoic acid, which is catalyzed by retinaldehyde specific dehydrogenases (RALDH). The positions of these enzymes in the vitamin A metabolic pathway (based on substrate specificity and co-factor requirements) are shown in Figure 1.1.

1.2.3a Alcohol dehydrogenases (ADH)

The ADH family consists of 8 cytosolic, zinc-dependent enzymes that catalyze the oxidation of several alcohols to their corresponding aldehydes in a NAD-dependent fashion (Duester *et al.*, 1999; Peralba *et al.*, 1999). While a retinol-specific ADH has not been identified, five members of this family (ADH1, 2, 4, 7, and 8) are able to utilize retinol as a substrate. ADH1 catalyzes the oxidation of both all-*trans*- and 9-*cis*-retinol to the corresponding retinaldehydes (Bliss, 1951). During development, *Adh1* expression is restricted to the developing kidneys in the mouse and *Xenopus*, and is therefore an unlikely candidate for total RA production in the embryo (Vonesch *et al.*, 1994; Ang *et al.*, 1996a; Hoffmann *et al.*, 1998). Moreover, *Adh1* null mice are viable and exhibit no detectable developmental or histological abnormalities, although they are not as efficient as wild type mice at metabolizing a large dose of retinol (Deltour *et al.*, 1999a). ADH4 exhibits the highest catalytic efficiency for conversion of all-*trans*-retinol to all-*trans*-retinaldehyde when compared to other members of the ADH family (Yang *et al.*, 1994). In contrast to the *Adh1* expression pattern, many *Adh4* expression domains overlap with areas of RA production (i.e. primitive streak mesoderm, neuroepithelium, and limb buds), suggesting that this enzyme may contribute to embryonic RA synthesis (Rossant *et al.*, 1991; Ang *et al.*, 1996 Section 1.2.2). However, targeted disruption of *Adh4*

Figure 1.1. Schematic diagram of vitamin A metabolism. See text for details. **Abbreviations**: ADH, alcohol dehydrogenase; CRAD, *cis*-retinoid/androgen dehydrogenase; LRAT, lethicin:retinol acyltransferase; RALDH, retinaldehyde dehydrogenase; REH, retinyl ester hydrolase; RoDH, retinol dehydrogenase; SDR, short-chain dehydrogenase/reductase.

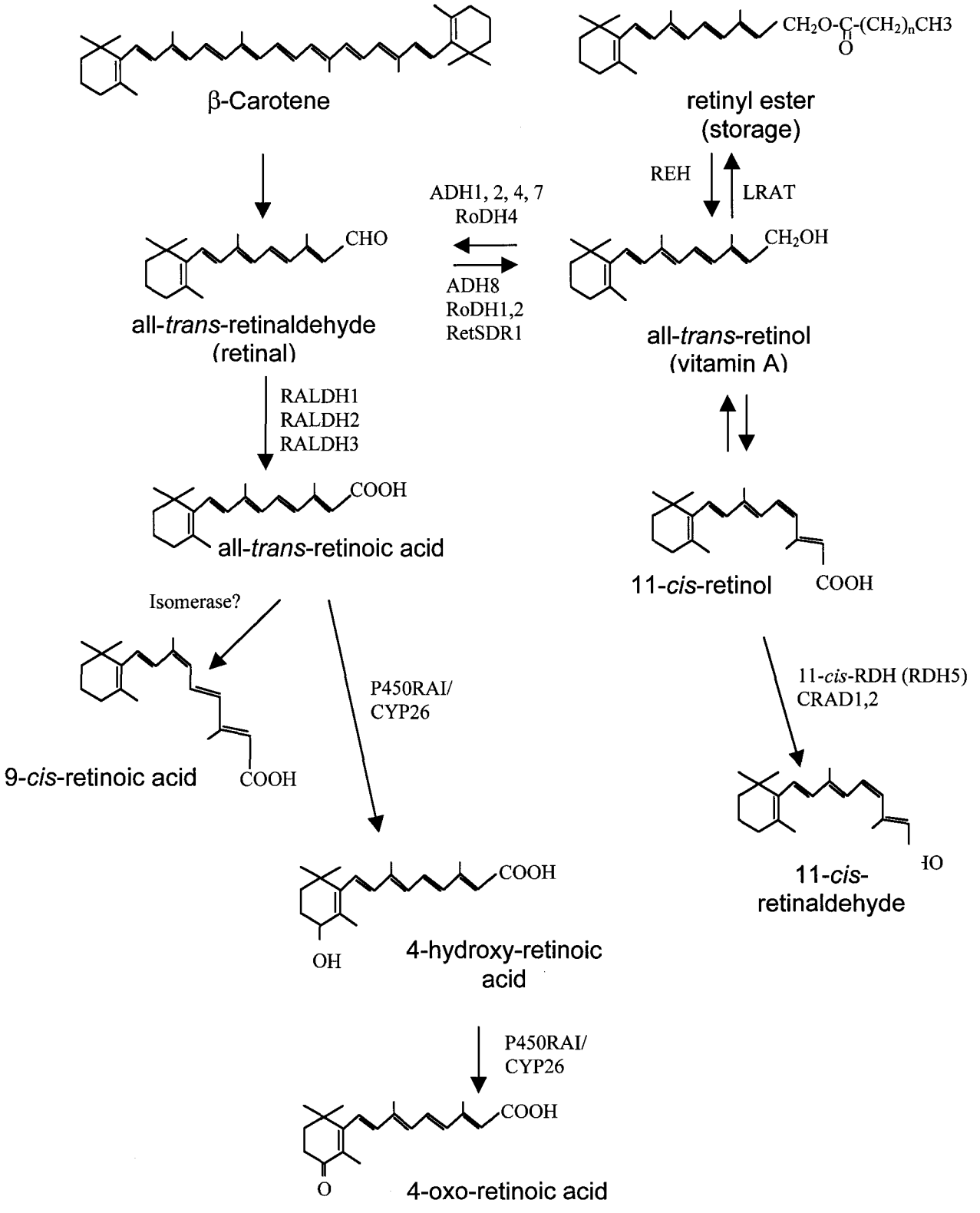
β-Carotene
retinyl ester
(storage)
REH
LRAT
ADH1, 2, 4, 7
RoDH4
ADH8
RoDH1,2
RetSDR1
CHO
all-trans-retinaldehyde
(retinal)
all-trans-retinol
(vitamin A)
RALDH1
RALDH2
RALDH3
COOH
all-trans-retinoic acid
11-cis-retinol
COOH
Isomerase?
9-cis-retinoic acid
COOH
P450RAI/
CYP26
11-cis-RDH (RDH5)
CRAD1,2
11-cis-
retinaldehyde
COOH
OH
4-hydroxy-retinoic
acid
P450RAI/
CYP26
COOH
O
4-oxo-retinoic acid

demonstrates that this enzyme is dispensable for development under normal conditions, although it is required for wild type fetal survival rates under vitamin A deficient conditions (Deltour *et al.*, 1999b). Although *Adh1* and *Adh4* are not critically required for RA production in the embryo, it is possible that there may be functional redundancy between these enzymes and/or other retinol oxidizing enzymes (see below).

1.2.3b Short chain dehydrogenases/reductases (SDR)

A wide variety of alcohols and aldehydes, including retinoids, are substrates for short chain dehydrogenases/reductases (SDRs). This family is evolutionarily related to the ADH family, although SDRs do not have a requirement for metal ions (Persson *et al.*, 1995). Eight different SDR family members have been identified that utilize retinoids as substrates; RoDH1, -2, -3, -4, CRAD1, CRAD2, RDH5, and retSDR1 (Napoli, 1999; Duester, 2000; and references therein). Some members have higher affinity for all-*trans*-retinol and retinaldehyde (RoDH1, RoDH2, RoDH4 and retSDR1), while others exhibit a preference for the *cis*-isomers (RDH5, CRAD1, and CRAD2). For example, RDH5 (11-*cis*-retinol dehydrogenase) is expressed at high levels in the eye and is required for the production of 11-*cis*-retinaldehyde, the visual chromophore in the retina (Simon *et al.*, 1995). Whether each of the SDRs function primarily as retinoid oxidases or reductases *in vivo* is not yet clear. Moreover, the role(s) of the SDRs in development remains to be established as their expression patterns during embryogenesis have not been examined.

1.2.3c Aldehyde dehydrogenases (ALDH)

Similar to the ADH and SDR families, the ALDH family consists of a large number of related enzymes, some of which are able to use retinoids as substrates (Yoshida *et al.*, 1998). In the mouse embryo there are three ALDH enzymes that oxidize retinaldehyde to retinoic acid: RALDH1, -2 and, -3. RALDH1 (also known as ALDH1, AHD2) can catalyze the oxidation of all-*trans*-retinaldehyde and 9-*cis*-retinaldehyde, and is encoded by genes found in human, rat, chick, mouse, and frog (Lee *et al.*, 1991; Dockham *et al.*, 1992; Godbout, 1992; Labrecque *et al.*, 1995; Penzes *et al.*, 1997; Ang and Duester, 1999). In the mouse embryo between E7.5 and E10.5, *Raldh1* is expressed in the midbrain, otic vesicles, mesonephros, thymic primordia, and the dorsal retina,

(Haselbeck *et al.*, 1999; McCaffery *et al.*, 1999). The role of RALDH1 has been studied most extensively in the developing retina where it is proposed to participate in the establishment of RA gradients, in conjunction with RALDH3 and P450/CYP26 (McCaffery *et al.*, 1999; Li *et al.*, 2000).

RALDH2 is likely the predominant aldehyde dehydrogenase required for RA synthesis in the mouse embryo, based on its pattern of expression during development, substrate specificity, zymography assays, and the severe congenital defects that occur in the absence of this enzyme (Dräger and McCaffery, 1995; Wang *et al.*, 1996; Zhao *et al.*, 1996; Neiderreither *et al.*, 1997, 1999, 2000). Indeed, RA activity cannot be detected in the *Raldh2* null mutant mouse embryo, with the exception of the region surrounding the eye where RA is likely produced by RALDH1 or RALDH3 (Neiderreither *et al.*, 1999; Li *et al.*, 2000). *Raldh2* transcripts are first detected between E7.0 and E7.5 in the posterior region of the embryo, coinciding with the initial detection of RA activity (Rossant *et al.*, 1991). During somite formation and differentiation *Raldh2* has a varied pattern of expression: it is initiated in somites that have recently formed, elevated in somites that are slightly older, and diminished in somites that have commenced differentiation. Additional sites of expression during these stages of development are the trunk mesoderm, the posterior end of the embryo, and the eye region. At slightly later stages, *Raldh2* expression can be detected in the spinal cord adjacent to the developing limbs, regions of the face, midgut, mesonephric mesenchyme, and the limb buds.

RALDH3 has recently been identified as the mouse homologue of ALDH6, a human aldehyde dehydrogenase capable of oxidizing retinaldehyde (Yoshida *et al.*, 1998), and is the enzyme responsible for the retinaldehyde oxidizing activity in the ventral retina (previously known as V1 activity; McCaffery *et al.*, 1993; Li *et al.*, 2000).

1.2.4 Retinoic acid catabolism

In order for normal embryogenesis to occur, a critical level of active vitamin A must be maintained in developing tissues. In addition, both excess and deficient levels of RA-signaling are detrimental to the adult organism. Therefore, a mechanism is required to ensure that active RA is cleared from tissues that no longer require its function. Cytochrome P450 activity has been correlated with RA catabolism for some time, as

inhibitors of P450 activity also reduce the production of RA metabolites (Roberts *et al.*, 1979). Recently, a gene encoding a novel RA-inducible cytochrome P450 enzyme (P450RAI-1, or CYP26A) was identified in zebrafish, mice, humans, chick, and *Xenopus* (White *et al.*, 1996, 1997; Fujii *et al.*, 1997; Ray *et al.*, 1997; Abu-Abed *et al.*, 1998; Hollemann *et al.*, 1998; Swindell *et al.*, 1999). A gene encoding a second member of this novel family (P450RAI-2) has also been cloned from the human brain (White *et al.*, 2000a). Both of these enzymes catalyze the conversion of all-*trans*-RA to more polar metabolites, such as 4-OH-RA, 18-OH-RA and 4-*oxo*-RA. It is not clear whether the polar metabolites produced by P450RAI-1 and -2 are merely intermediates in the RA catabolic pathway or whether they have unique biological roles. For example, in *Xenopus* 4-*oxo*-RA modifies axial specification in the developing embryo and can bind to and activate RARβ (Pijnappel *et al.*, 1993).

P4*50RAI-1* expression is rapidly inducible by RA treatment in several cell lines and in the embryo (White *et al.*, 1996, 1997; Ray *et al.*, 1997; Hollemann *et al.*, 1998; Iulianella *et al.*, 1999; Swindell *et al.*, 1999). This regulation is direct as F9 cells lacking functional *RARγ* and *RXRα*, alone or in combination, exhibit lower levels of *P450RAI-1* induction by RA, and a conserved retinoic acid response element (RARE) has recently been identified in the promoter of several species (Abu-Abed *et al.*, 1998; Loudig *et al.*, 2000). An increased level of *P450RAI-2* message is also observed in response to RA treatment of several cell lines (White *et al.*, 2000a). Ectopic expression of *P450RAI* in the *Xenopus* embryo results in anteriorization of the hindbrain, a phenotype similar to that induced by dominant-negative RARs (Blumberg *et al.*, 1997; Kolm *et al.*, 1997; van der Wees *et al.*, 1998). Moreover, ectopic *P450RAI* specifically rescues the teratogenic effects of excess RA, suggesting that this enzyme mediates RA inactivation *in vivo* (Hollemann *et al.*, 1998).

P450RAI-1 expression domains in the embryo vary in a spatiotemporal manner and are typically complementary to sites of RA activity (Fujii *et al.*, 1997; Iulianella *et al.*, 1999; de Roos *et al.*, 1999; McCaffery *et al.*, 1999). For example, at E8.5 RA is produced in the trunk, to the level of the most recently formed somite, by RALDH2 (Rossant *et al.*, 1991; Neiderreither *et al.*, 1999). In contrast, *P450RAI-1* transcripts are localized to the region of the open caudal neuropore, where little bioactive RA is

detectable. As, this region is highly sensitive to exogenous RA, it has been proposed that P450RAI-1 may function to control the amount, and/or timing of RA-exposure to these tissues (Iulianella *et al.*, 1999). Similar roles for P450RAI-1 in the formation of RA "boundaries" have been proposed with regard to the developing *Xenopus* brain and mouse retina (Hollemann *et al.*, 1998; McCaffery *et al.*, 1999; Ross *et al.*, 2000). Indeed, *P450RAI* homozygous null mice exhibit several defects characteristic of RA excess, including caudal truncation, posterior transformation of the vertebrae, and abnormal patterning of the hindbrain (Abu-Abed *et al.*, 2001; Sakai *et al.*, 2001).

1.3 Vitamin A and embryogenesis

1.3.1 Vitamin A deficiency

The relationship between vitamin deficiency, congenital birth defects, and fetal death was first observed over 60 years ago (Mason, 1935; Hale, 1937). Following this initial discovery, the effect of maternal vitamin A deficiency (VAD) on the developing rat embryo was carefully studied, and a reproducible spectrum of congenital abnormalities described (Warkany and Schraffenberger, 1946; Wilson and Warkany, 1948, 1949; Wilson *et al.*, 1953). In summary, a sufficient level of vitamin A during development is required for proper formation of the eye, respiratory system, heart and aortic arches, diaphragm, limbs, and urogenital system. More recent studies of VAD rat fetuses have demonstrated additional requirements of vitamin A in correct patterning of the hindbrain, cranial nerve development, and development of the frontonasal/maxillary region (Dickman *et al.*, 1997; White *et al.*, 1998, 2000b).

As completely VAD female rats are infertile, it has been difficult to assess the full effect of vitamin A deficiency on the developing embryo. Recently, targeted disruption of the *Raldh2* gene in the mouse has resulted in offspring that are devoid of RA, as assessed by two RA-responsive reporter transgenes (Neiderreither *et al.*, 1999). These mice are much more severely affected than previously described VAD mice and fail to survive past midgestation (E10.5). Congenital defects exhibited by *Raldh2*$^{-/-}$ embryos include a shortened axis, small somites, hindbrain patterning abnormalities, the absence

of limb buds, neural tube defects, a truncated frontonasal region, and severe heart defects (Neiderreither *et al.*, 1999, 2000). The affected tissues in *Raldh2* null mutant mice are nearly identical to those of VAD mice, rats and quails, supporting a role for RA as the biologically active metabolite of vitamin A (Dersch and Zile, 1993; Maden *et al.*, 1996; Morriss-Kay and Sokolova, 1996; Sokolova, 1996; Maden *et al.*, 1997; Stratford *et al.*, 1999; Maden *et al.*, 2000).

In rats, VAD-associated abnormalities can be prevented by vitamin A supplementation during distinct windows of development (Wilson *et al.*, 1953). However, whether RA can fulfill all of the requirements of vitamin A during embryogenesis is not clear. For example, retinoids can prevent VAD-induced defects in the quail embryo when administered at very early stages of development (Dersch and Zile, 1993). Contradictory results have been reported in RA supplemented VAD rats. When examined at E12.5-13.5, VAD rat fetuses orally dosed with RA (140-200 μg RA/rat/day) appeared to be normal (Dickman *et al.*, 1997). However, another group observed several morphological abnormalities including limb, hindbrain, and eye defects, when the experiments were performed in the same manner, indicating an incomplete rescue by RA (White *et al.*, 1998). This discrepancy may be due to insufficient depletion of vitamin A stores, or to contaminating retinol in the RA preparation. RA supplementation in the diet, or by oral dosing, may not be sufficient to rescue the VAD-induced abnormalities simply because a general increase in RA levels may not mimic the endogenous localization and gradients of RA in the developing embryo. This is supported by the attempted RA-rescue of *Raldh2* mutant embryos. Although some of the morphological defects, such as axis truncation and the absence of heart looping, were reduced or eliminated by maternal dosing (2.5 mg/kg body weight every 12 hours), other defects, such as abnormal hindbrain patterning, persisted (Neiderreither *et al.*, 1999).

In addition to its vital role in embryogenesis, vitamin A is also required for homeostasis in the adult. A diet deficient in vitamin A leads to blindness, squamous metaplasia of various epithelial tissues, sterility, and eventual death (Wolbach and Howe, 1925; see Sporn *et al.*, 1994 and Blomhoff, 1994 for reviews and references). All of the defects that arise due to VAD in the adult, with the exception of blindness, can be

reversed or prevented by administration of retinoic acid (Howell, *et al.*, 1963; Thompson *et al.*, 1964).

1.3.2 Retinoid excess

In addition to the spectrum of congenital abnormalities that arise due to maternal VAD, an excess of vitamin A during development also results in severe malformation of the embryo (Cohlan, 1953). In general, retinoic acid is a more potent teratogen than vitamin A, however this effect is isoform-specific and varies from species to species (Soprano and Soprano, 1995). The structures that are affected by exogenous retinoids vary according to the dose and time of exposure, however, a common set of target structures includes the limbs, heart, axial skeleton, eyes, skull, brain, and central nervous system (Shenefelt, 1972; Lammer *et al.*, 1985; Webster *et al.*, 1986; Kessel and Gruss, 1991; Kessel, 1992; Creech Kraft, 1992; Morriss-Kay, 1993). Human embryos are sensitive to retinoids in the first trimester of pregnancy (Hathcock *et al.*, 1990). Infants exposed to 13-*cis*-RA during this period are afflicted with craniofacial defects, heart malformations, and abnormalities of the thymus, eye, and CNS (Lammer *et al.*, 1985). As 13-*cis*-RA is commonly used to treat various skin conditions, it is imperative that systemic retinoids not be used during pregnancy. The specific effects of exogenous RA on anteroposterior patterning of the embryo axis will be discussed in Section 1.6.

1.4 Retinoid binding proteins

Two classes of proteins have been implicated in the regulation of retinoid signaling. The first (fatty-acid binding protein family; FABP) is comprised of small intracellular proteins that bind hydrophobic molecules (reviewed in Ong *et al.*, 1994). Included in this family are the cellular retinol-binding proteins (CRBP type I, type II, and type III), and the cellular retinoic acid-binding proteins (CRABP type I and type II). These proteins are thought to be involved in storage, transport, and metabolism of the retinoids. The second superfamily is composed of nuclear proteins that act as ligand-inducible transcription factors (reviewed in Mangelsdorf *et al.*, 1995). Within this superfamily are two distinct families of RA receptors, the retinoic acid receptors (RARs)

and retinoid X receptors (RXRs), which act together to regulate the transcription of many diverse target genes.

1.4.1 Cellular retinoid binding proteins

1.4.1a CRBPI, -II, and -III

The cellular retinol-binding proteins are thought to be involved in delivery of retinol and retinaldehyde to the appropriate enzymes involved in RA production or retinol esterification, and protection of their substrates from oxidation by non-specific dehydrogenases (Ong *et al.*, 1994; Vogel *et al.*, 2001). During development, *CrbpI* is expressed in several tissues including the spinal cord, motor neurons, liver, lung and placenta (Dollé *et al.*, 1990; Maden *et al.*, 1990; Ruberte *et al.*, 1991; Gustafson *et al.*, 1993), *CrbpII* is expressed in the yolk sac and late liver (Sapin *et al.*, 1997; Ghyselinck *et al.*, 1999), and *CrbpIII* is expressed in the developing heart and myotome (Vogel *et al.*, 2001). Inactivation of *CrbpI* in mice does not result in congenital abnormalities, indicating that this enzyme is dispensable for embryogenesis (Ghyselinck *et al.*, 1999). Likewise, *CrbpI* null mutant adult mice appear normal, with the exception of reduced levels of retinyl esters in the liver. However, under conditions of dietary vitamin A deprivation, these retinyl ester stores become rapidly depleted, leading to severe vitamin A deficiency.

1.4.1b CRABPI and CRABPII

Crabp genes are found in all vertebrates and have been highly conserved throughout evolution (reviewed in Donovan *et al.*, 1995). Both CRABPI and CRABPII bind all-*trans*-RA, but not 9-*cis*-RA, with high affinity (Bailey and Siu, 1988; Aström *et al.*, 1991; Siegenthaler *et al.*, 1992; Fiorella *et al.*, 1993). It has been proposed that a role for the CRABPs may be to sequester RA such that the free, and thus active, levels are kept very low. This is supported by the observations that the expression pattern of *Crbp1* is largely complementary to that of *CrabpI*, suggesting that tissues that require RA express *CrbpI*, while tissues that are sensitive to excess RA express *CrabpI* (Perez-Castro *et al.*, 1989; Dollé *et al.*, 1990; Gustafson *et al.*, 1993). Alternatively, it has been

hypothesized that RA-dependent cells, which are incapable of RA-synthesis, express *CrabpI* in order to capture RA (Ross *et al.*, 2000 and references therein). Additionally, CRABP:RA complexes have been shown to interact with RA-metabolizing enzymes, suggesting that CRABPs may be involved in RA catabolism (Fiorella and Napoli, 1991). Hence, it is rather surprising that targeted disruption of *CrabpI* and *CrabpII* individually or in combination does not adversely affect mouse development or adult life, with the exception of postaxial polydactyly in *CrabpII* null mice (Gorry *et al.*, 1994; Fawcett *et al.*, 1995; Lampron *et al.*, 1995). Furthermore, all combinations of *CrabpI* and *CrabpII* null mutant mice do not display increased sensitivity to exogenous RA during embryogenesis.

1.4.2 The nuclear receptor superfamily

The molecular mechanisms behind the pleiotrophic effects of vitamin A were uncovered through the cloning of the retinoid receptors. Comparison of the nucleotide sequences encoding the estrogen receptor, glucocorticoid receptor, and thyroid hormone receptor allowed the identification of a highly conserved region required for DNA binding (Giguère *et al*, 1986). This domain was used to screen cDNA libraries for related molecules and ultimately resulted in the identification of a receptor for RA (RAR; Giguère *et al.*, 1987: Petkovich *et al.*, 1987). Similar experiments led to the discovery of the retinoid X receptor (RXR; Mangelsdorf *et al.*, 1990), which was subsequently demonstrated to bind the 9-*cis* isoform of RA (Heyman *et al.*, 1992; Levin *et al.*, 1992).

The nuclear receptor superfamily is a large group of related molecules that function as ligand-activated transcription factors (reviewed in Mangelsdorf *et al.*, 1995). This superfamily can be divided into four classes based on ligand binding, DNA binding, and dimerization properties. The first class consists of the steroid receptors, which bind hormones derived from cholesterol such as estrogen, androgens, and glucocorticoids. These receptors recognize and bind to palindromic DNA sequences as homodimers. The ligands of nonsteroid receptors, the second class of nuclear receptors, are small lipophilic molecules such as retinoic acid, vitamin D_3 and thyroid hormone. In contrast to the steroid hormone receptors, receptors in this class form heterodimeric complexes with the

retinoid X receptors (RXRs) and bind to direct DNA repeats. The remaining receptors are so-called 'orphan receptors', which have no known ligands. The orphan receptors can be divided into two classes based on whether they form dimers or bind to DNA elements as monomers. While some of these orphan receptors may have as yet unidentified ligands, it is thought that their activity may also be controlled by post-translational modification (Mangelsdorf and Evans, 1995).

All nuclear receptors exhibit a similar structural organization that can be divided into six distinct regions (A-F), as shown in Figure 1.2. The DNA-binding domain (DBD) and ligand-binding domain (LBD) are located in regions C and E, respectively. The DBD is highly conserved among all nuclear receptors and is composed of two zinc-fingers and a carboxy-terminal extension (CTE) (Evans, 1988; Green and Chambon, 1988; Rastinejad *et al.*, 1995). An α-helix of one of these zinc fingers (the recognition helix) makes contact with specific bases in the DNA major groove and the CTE forms contacts with bases in the minor groove (Luisi *et al.*, 1991; Schwabe *et al.*, 1993). The DBD is also involved in receptor dimerization (Perlman *et al.*, 1993; Zechel *et al.*, 1994; Rastinejad *et al.*, 1995).

In addition to its ligand binding properties, region E is also required for ligand-dependant transcriptional activation (AF-2; Nagpal *et al.*, 1992), transcriptional repression in the absence of ligand (Baniahmad *et al.*, 1992), and receptor dimerization (Forman *et al.*, 1989; Bourguet *et al.*, 2000). The crystal structure solutions of several nuclear receptor LBDs have resulted in the identification of a common fold, arranged as an anti-parallel, 3-layered 'sandwich', composed of 12 α-helices (reviewed in Egea *et al.*, 2000). The ligand is located within an internal hydrophobic cavity, making specific contacts with several residues of the α-helices. A conformational change of the LBD is induced upon ligand-binding, such that the orientation of the C-terminal α-helix (H12 or AF-2 helix), which is protruding into the solvent in the absence of ligand, is repositioned towards the LBD, in a mechanism that is analogous to a 'mouse-trap' (reviewed in Moras and Gronemeyer, 1998). The repositioning of the AF-2 helix, along with conformational changes of other helices, results in the formation of a hydrophobic groove, which is critical for binding transcriptional coactivators and the dissociation of transcriptional corepressors (Section 1.4.4; Torchia *et al.*, 1998).

The N-terminal A/B region is the most variable between receptor types (i.e. RARα vs. RARγ), and contains a second activation function (AF-1), which is ligand-independent and functions in a cell and promoter-specific manner (Nagpal *et al.*, 1992, 1993; Folkers *et al.*, 1993). The hinge region (D) allows movement of the DBD relative to the LBD, and is also involved in corepressor binding. The C-terminal region (F) is weakly conserved between receptor types and has no recognized function.

1.4.3 RARs and RXRs

The RAR family of nuclear receptors comprises three RAR types; α, β and γ, encoded by three genes located on mouse chromosomes 11, 14, and 15, respectively (Mattei *et al.*, 1991; Nadeau *et al.*, 1992). Each of these genes produces multiple isoforms (α_1 and α_2, β_1,-β_4, γ_1 and γ_2) as a result of differential promoter usage (P1 and P2), alternate splice sites, and alternate translation initiation codons (reviewed in Giguère, 1994). All isoforms differ only with respect to the 5' UTR and N-terminal A domain. For example, the A/B domain of the RARβ3 isoform is composed of 115 amino acids, while only 32 residues comprise this domain in the RARβ4 isoform (Zelent *et al.*, 1991). The conservation between RAR isoforms from different species is greater than that of the individual RAR genes in a given organism, suggesting functional conservation (reviewed in Lohnes *et al.*, 1992).

Similar to the RAR family, there are three subtypes of RXRs; α, β, and γ, encoded by genes located on mouse chromosomes 2, 17 and 1, respectively (Hoopes *et al.*, 1992). Several RXR isoforms also exist, although their physiological significance has not been examined in any detail (Liu and Linney, 1993; Nagata *et al.*, 1994; Sugawara *et al.*, 1995; Brocard *et al.*, 1996). While RARs bind to and are activated by both all-*trans*- and 9-*cis*-RA, RXRs are activated only by the 9-*cis* isoform (Heyman *et al.*, 1992; Levin *et al.*, 1992).

RXRs are required as DNA binding partners for RARs to bind tightly to, and transactivate from, response elements *in vitro* (reviewed in Leid *et al.*, 1992). Moreover, these heterodimers appear to be the functional units that transduce the RA signal *in vivo* (Section 1.5.3; Kastner *et al.*, 1997). In addition to acting as binding partners for RARs, RXRs can also bind to certain DNA response elements as homodimers (Zhang *et al.*,

Figure 1.2. Structural organization of the nuclear receptors. The nuclear receptors can be divided into six domains, A-F. The NH_2-terminal A/B region contains the ligand-independent activating function (AF-1) and the only variable region between receptor isoforms. Region C contains the DNA-binding domain and also plays a role in receptor dimerization when bound to DNA. Region D is the linker, or hinge, region that allows flexibility between the ligand-binding and DNA-binding domains. Region E contains the ligand-binding domain, the ligand-dependent activating function (AF-2), and a DNA-independent dimerization domain. The C-terminal domain, F, has no known function and is not highly conserved between receptor types. **Abbreviations**: AF, activating function; DBD, DNA-binding domain, LBD, ligand-binding domain.

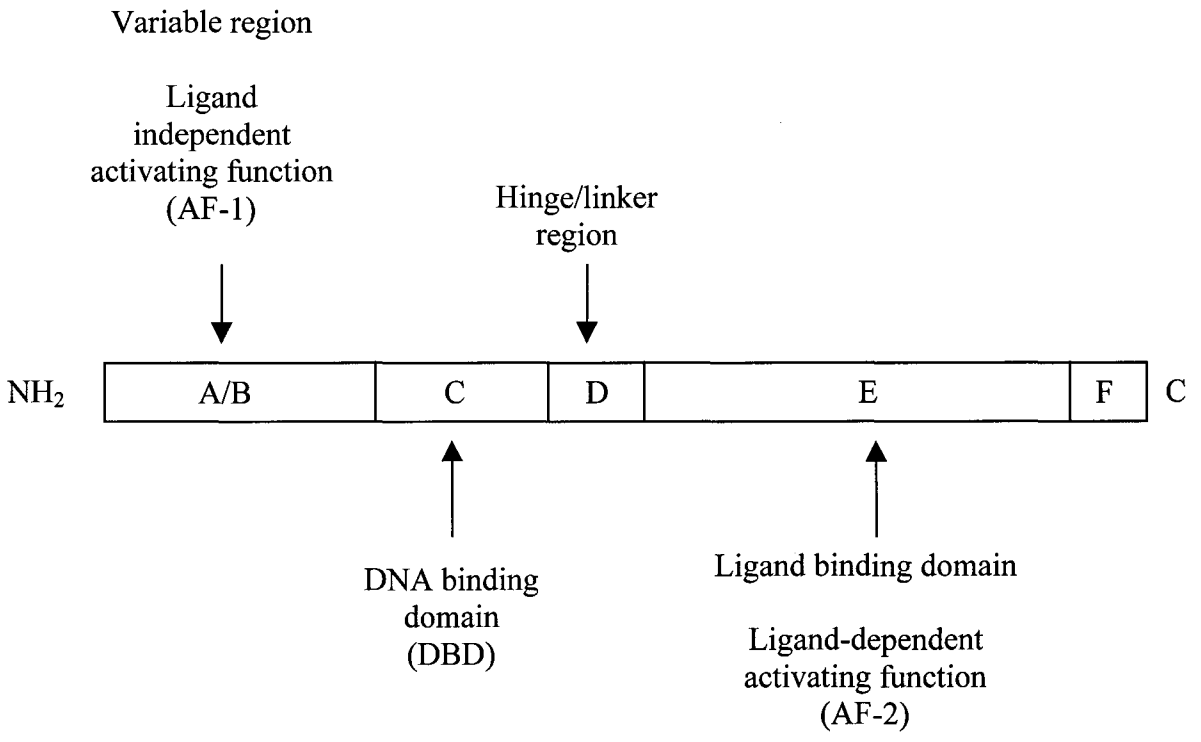
Variable region
Ligand independent activating function (AF-1)
Hinge/linker region
NH2
A/B
C
D
E
F
C
DNA binding domain (DBD)
Ligand binding domain
Ligand-dependent activating function (AF-2)

1992), and as heterodimers with several other members of the nuclear receptor superfamily, including the thyroid hormone receptor (TR), vitamin D receptor (VDR), peroxisomal proliferator activated receptor (PPAR), NGFI-B, NURR1, and COUP-TF (reviewed in Mangelsdorf and Evans, 1995).

Further complexity is added to the retinoid signaling pathway by the observation that the RARs and RXRs can also affect the activity of other transcription factors through transrepression (reviewed in Göttlicher *et al.*, 1998). For example, the reduction of AP-1 transcriptional activity by RAR activation is thought to occur by sequestration of common cofactors (i.e.CBP/p300; see Section 1.4.4c), or by inhibition of JNK signaling (Kamei *et al.*, 1996; Caelles *et al.*, 1997; Lee *et al.*, 1998, 1999). Additionally, the transcriptional activity, and degradation, of RARs can be modulated by phosphorylation (Rochette-Egly *et al.*, 1997; Delmotte *et al.*, 1999; Bastien *et al.*, 2000).

1.4.4 Mechanism of transcriptional regulation

1.4.4a Retinoic acid response elements (RAREs)

The DBDs of all nuclear receptors recognize, and bind to, a 6-bp consensus sequence (AGGTCA for non-steroid receptors). This hexamer is termed a 'half-site' as it is typically found in duplicate, such that each member of the hetero- or homodimeric pair binds to one site. The orientation of the half-sites, and the spacing between them, dictates which type of nuclear receptor will bind to a particular response element. For example, most steroid hormone receptors form homodimers and bind to response elements consisting of palindromes separated by three nucleotides (Beato *et al.*, 1995). On the other hand, receptors that form heterodimers with RXR bind to direct half-site repeats (Manglesdorf and Evans, 1995). When bound to the response element, heterodimeric partners are always arranged in the same orientation. That is, the RXR is always bound to the 5' half-site, while the RAR, VDR, or TR partner binds downstream (Perlmann *et al.*, 1993; Kurokawa *et al.*, 1993; Zechel *et al.*, 1994). As an exception to this rule, RAR-RXR heterodimers bind to the DR1 element in the opposite orientation. However, this configuration results in transcriptional repression (Mangelsdorf *et al.*, 1991; Kurokawa *et al.*, 1995).

The number of nucleotides that separate the repeats (ranging from 1 to 5) determines which combination of RXR and nuclear receptor will be able to bind. For example, RAR-RXR heterodimers bind to direct repeats separated by 2 or 5 nucleotides (DR2 or DR5 elements), while VDR-RXR and TR-RXR heterodimers bind to DR3 and DR4 elements, respectively. Furthermore, RXRs are able to bind to DR1 elements both as homodimers, and as heterodimers with RARs (as mentioned above). Functional DR1, DR2 and DR5 RAREs have been identified in the promoters of several genes. However, non-consensus, complex RAREs, including palindromic and everted repeats, have also been described (for examples see Giguère, 1994; Ross *et al.*, 2000).

In vitro, RXRs are able to form heterodimers with their various partners in solution through highly conserved residues in their LBDs (Rosen *et al.*, 1993; Bourguet *et al.*, 2000; Egea *et al.*, 2000; Gampe *et al.*, 2000). However, the DBDs alone are able to direct heterodimerization on the appropriate DNA response elements, indicating that an additional dimerization interface is located within this domain. Indeed, molecular modeling has suggested that these dimerization interfaces are responsible for discriminating between direct repeats separated by different numbers of nucleotides (Rastinejad *et al.*, 1995). A two-step dimerization model has been proposed where the heterodimeric partners first dimerize though their LBDs in solution, thus bringing the DBDs into close proximity. The hinge, or linker region (D) provides flexibility, allowing the DBD to move with respect to the LBD, thereby facilitating heterodimer binding to the appropriate response element (i.e. DR2 *vs*. DR5; Manglesdorf *et al.*, 1995).

1.4.4b Transcriptional repression

RAR and TR, in complex with RXR, are able to actively repress transcription when bound to DNA in the absence of ligand. This is accomplished through recruitment of the SMRT (silencing mediator for retinoic acid and thyroid hormone receptors) and N-CoR (nuclear receptor corepressor) corepressors (Figure 1.3; Chen and Evans, 1995; Hörlein *et al.*, 1995; Kurokawa *et al.*, 1995). Although they were originally identified as molecules associated with TR and RAR, N-CoR and SMRT also act as corepressors for other nuclear receptors (i.e. COUP-TF, DAX1, and antagonist-bound ER), and several other transcription factors (i.e. Mad, CBF-1/RBP-JK, Pit-1; Glass and Rosenfeld, 2000).

Figure 1.3 Models of corepressor and coactivator function. See text for details. (**A**) In the absence of RA the RAR/RXR heterodimers are associated with N-CoR/SMRT and the HDAC complex. Note that this interaction can occur directly, or through mSIN3. The HDAC activity results in deacetylation of the histones, which is correlated with a decrease in transcriptional activity. (**B**) The SWI/SNF complex associates with the RAR/RXR heterodimer and promotes tighter binding to the DNA. Upon ligand activation (indicated by the white diamond), the coactivators are recruited to the AF2 domain. The histone acetylase (HAT) may enable other transcription factors (TFs) to bind to the promoter, or may regulate the activity of the TFs themselves. The DRIP/TRAP complex associates with the liganded RAR/RXR heterodimers and appears to be involved in recruiting the RNA-pol II transcriptional machinery. The net effect of coactivator binding is an increase in transcriptional activity.

A) Repression

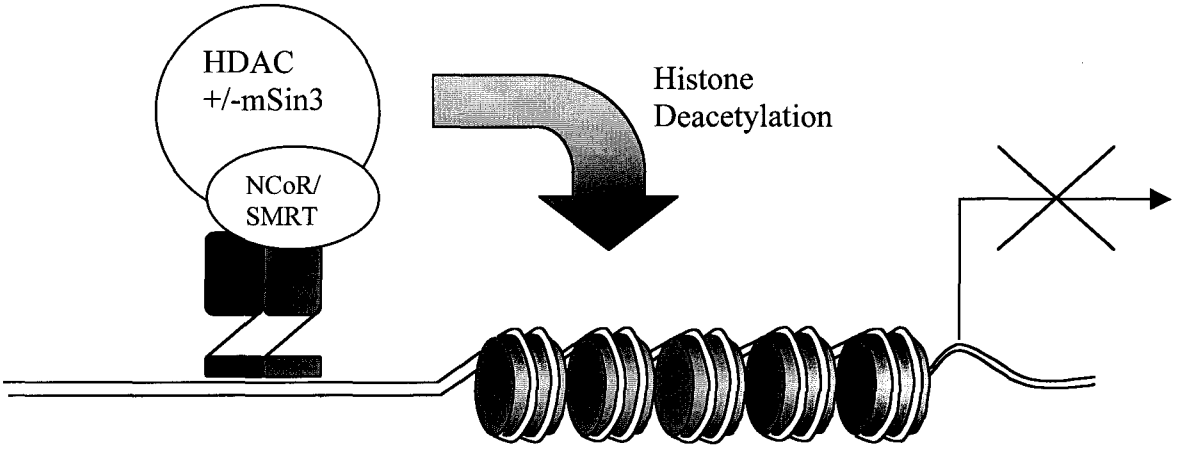

B) Activation

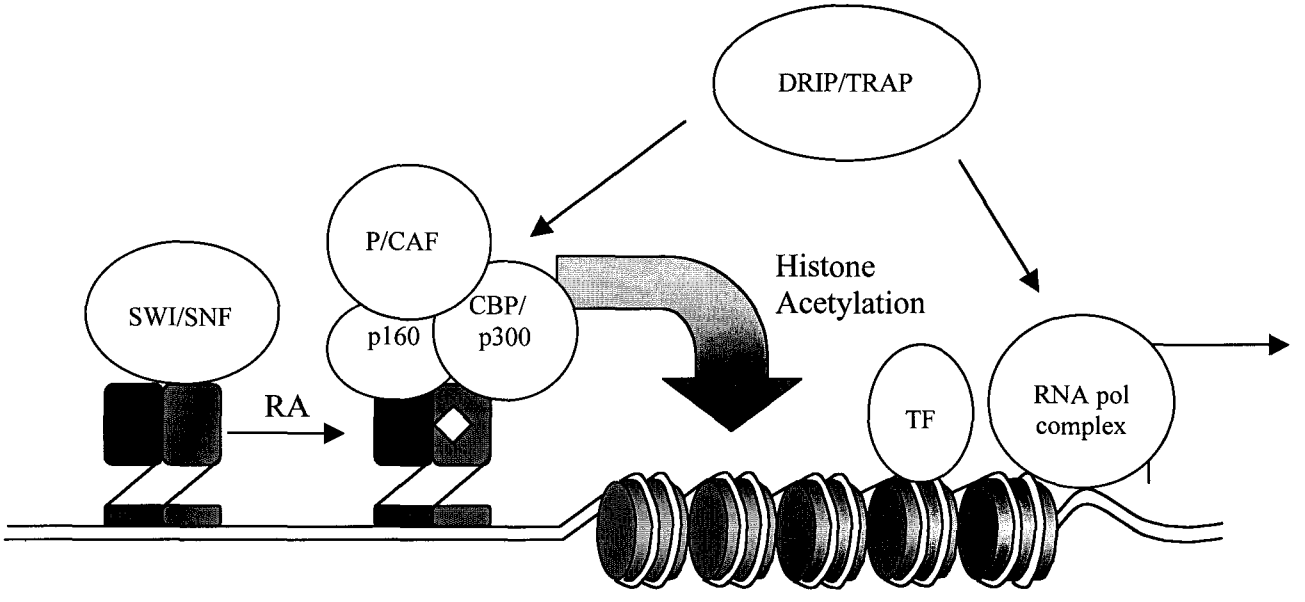

SMRT and N-CoR are highly related molecules of ~270 kD that have two nuclear receptor interacting domains in the C-terminal portion of the protein. These domains contain a conserved sequence known as the CoRNR box (Perissi *et al.*, 1999; Zhu *et al.*, 1999), which forms an extended helix that binds to a hydrophobic groove in the unliganded LBD of nuclear receptors (Glass and Rosenfeld, 2000). When tethered to DNA, SMRT and N-CoR bestow active transcriptional repression via recruitment of the Sin3 complex by one of several repressor domains located in the NH_2-terminus of the protein. The Sin3 complex consists of several components, including histone deacetylase enzymes (HDACs; Heinzel *et al.*, 1997; Nagy *et al.*, 1997). Histone hypoacetylation is correlated with gene repression, and presumably results in a highly ordered chromatin structure that limits the access of transcription factors and transcriptional machinery to the promoters of target genes (Pazin and Kadonaga, 1997; Xu *et al.*, 1999). It is also possible that HDACs may deacetylate other transcription factors, which may affect their activity.

In the mouse there are seven known HDACs which can be divided into two groups based on homology to two yeast HDACs that are found in distinct complexes (Rpd3 and Hda-1). Class I (Rpd3-like) includes HDAC1, -2, and -3, while class II (Hda1-like) includes HDAC4 to HDAC7 (Wen *et al.*, 2000 and references therein). Only HDAC1 and HDAC2 copurify with the Sin3 complex (Zhang *et al.*, 1997b; Laherty *et al.*, 1998). Recently, it was demonstrated that N-CoR and SMRT directly interact with HDAC4, HDAC5, and HDAC7 (Huang *et al.*, 2000; Kao *et al.*, 2000). Moreover, the complex associated with SMRT/N-CoR and HDAC4 and HDAC5 does not include mSin3 or HDAC1 (Huang *et al.*, 2000). Additionally, N-CoR and SMRT are both part of a HDAC3 complex, and interact with this enzyme through regions that are distinct from those involved in HDAC4, -5, and -7 binding (Wen *et al.*, 2000). Therefore, N-CoR and SMRT are able to recruit both classes of HDACs through several different repressor domains. It is not yet clear whether different HDAC complexes are recruited in a cell- or promoter-specific manner, although it is tempting to speculate that this may be the case.

1.4.4c Transcriptional activation

Several types of coactivating molecules are able to associate with ligand-bound nuclear receptors. Most of these coactivators interact with more than one type of nuclear receptor, suggesting a common mechanism of transcriptional activation. The p160 family of coactivators comprises several molecules, all of which possess a highly conserved bHLH PAS domain in the NH_2-terminal region that mediates protein-protein interactions (Glass and Rosenfeld, 2000). Members of this family include SRC/NCoA-1, TIF2/GRIP1/NCoA2, and pCIP/ACTR/AIB1/RAC/TRAM1. All of these proteins contain multiple LXXLL motifs which form short α-helices that are able to bind the hydrophobic groove in the LBD of nuclear receptors following ligand binding (Darimont *et al.*, 1998; Feng *et al.*, 1998). Repositioning of the AF-2 helix mediated by ligand binding (and additional conformational changes) results in the formation of a 'charged clamp' that forms interactions with the LXXLL α-helix (Moras and Gronemeyer, 1998). Several members of the p160 family contain intrinsic histone acetylase (HAT) activity (Chen *et al.*, 1997; Spencer *et al.*, 1997) which results in the acetylation of histones and is correlated with an increase in transcriptional activity (Pazin and Kadonaga, 1997). The mechanism by which this occurs has not been elucidated, however it is thought that histone acetylation results in an 'opening' of the chromatin structure, such that additional transcription factors and the transcriptional machinery may access the DNA and promote transcription.

A second class of coactivators capable of direct interaction with the nuclear receptors includes the CBP (CREB-binding protein) and p300 proteins. These proteins are highly related, yet exhibit distinct functions *in vitro* and during development (reviewed in Goodman and Smolik, 2000). Like the p160 proteins, CBP/p300 also have intrinsic HAT activity (Bannister and Kouzarides, 1996; Ogryzko *et al.*, 1996). In addition to direct interaction with the nuclear receptors, CBP/p300 also directly associates with SRC-1, and together they synergistically increase transcriptional activation (Yao *et al.*, 1996). A third factor involved in nuclear receptor coactivation that possesses HAT activity is P/CAF, the mammalian homologue of yeast Gcn5 (Yang *et al.*, 1996). This protein is part of a larger complex containing several TAF-like proteins, and

mediates direct interactions with CBP, p160 co-activators, and ligand-activated nuclear receptors, including RARs (Chen *et al.*, 1997; Blanco *et al.*, 1998; Korzus *et al.*, 1998).

Two large complexes were independently found to copurify with ligand-bound VDR and TR (Fondell *et al.*, 1996; Rachez *et al.*, 1998). These complexes (DRIP/TRAP) are very similar to one another, as well as to other complexes associated with transcription factors such as SREBP, NFκB, and Sp1 (Glass and Rosenfeld, 2000). One component of this complex, TRAP220/DRIP205/TRIP2/mPIP1, interacts specifically with the nuclear receptors through two LXXLL motifs (Yuan *et al.*, 1998; Malik and Roeder, 2000). As opposed to the coactivators described above, the DRIP/TRAP complexes do not possess intrinsic HAT activity (Yuan *et al.*, 1998). Instead, they may be involved in recruitment of the RNA-pol II transcriptional machinery to the promoter (reviewed in Malik and Roeder, 2000).

A distinct class of factors that enhance the transcriptional activation of nuclear receptors is the SWI/SNF ATP-dependent nucleosome remodeling complex (reviewed in Kadonaga, 1998). It has recently been demonstrated that this complex, in the presence of ATP, acts prior to the recruitment of coactivators containing HAT activity, and is required for the unliganded RAR-RXR heterodimer to bind tightly to its response element (Dillworth *et al.*, 2000). Following ligand binding, coactivators are recruited through the AF-2 domain of the receptors and acetylate the histones surrounding the response element (and possibly other proteins). These events take place before the assembly of the transcriptional machinery, suggesting that the DRIP/TRAP complex may function downstream of the coactivators that contain HAT activity.

In summary, there are several types of coactivators that are capable of interacting with the nuclear receptors either directly, or via other 'scaffold' proteins (see Figure 1.3). Similar to the corepressors, it is likely that some of these coactivators may function in a tissue-, promoter-, or receptor-specific manner *in vivo*. In this regard, the amino acid sequences flanking the LXXLL motif have been demonstrated to be important in receptor specificity (Darimont *et al.*, 1998; Feng *et al.*, 1998).

1.4.5 RAR expression patterns during development

The expression patterns of the *RARs* have been analyzed by *in situ* hybridization from E6.5 to E15.5 in the mouse embryo (Dollé *et al.*, 1989, 1990; Ruberte *et al.*, 1990, 1991, 1993; Mollard *et al.*, 2000). A detailed description of all of the domains of *RAR* expression throughout embryogenesis is beyond the scope of this introduction. A general summary of transcript localization for each of the *RARs* is provided below, with special emphasis placed on the expression patterns at earlier stages of development.

1.4.5a RARa

RARα is not expressed, or is expressed at very low levels, until E8.0, when it appears to accumulate at slightly increased levels in the epiblast and mesoderm of the primitive streak (Ruberte *et al.*, 1991). At E8.5 (8 to 10 somites) *RARα* is expressed in the neuroepithelium of the forebrain, and in the hindbrain at the level of the preotic sulcus. *RARα* transcripts are also detected in neural crest cells migrating from the latter region, as well as in neural crest cells located in the frontonasal mass and mandibular arch. Slightly later in development (10 to 14 somites), *RARα* becomes almost ubiquitously expressed, but appears to have a rostral limit at the boundary of presumptive rhombomeres 3 and 4, and is excluded from the developing heart.

1.4.5b RARβ

RARβ transcripts are detectable at an earlier stage than those of *RARα* or *RARγ* (Ruberte *et al.*, 1990). At the presomitic stage (E7.5 to E8.0) *RARβ* are detected ubiquitously throughout the embryo, with the exception of the most rostral portion where they are localized to the mesenchyme, and excluded from the overlying neuroectoderm. At E8.5, *RARβ* messages are present in the neuroepithelium of the caudal hindbrain, foregut endoderm, lateral plate mesoderm, frontonasal mesenchyme, and in the sinous venosus region of the heart. Additionally, expression of this receptor isoform is detected in the neural tube epithelium from the anterior level of the first somite to the posterior level of the open neuropore. Notably, *RARβ* transcripts are never detected in the open neural folds of the caudal neuropore. *RARβ* is also expressed in the mesenchyme of the frontonasal mass and the first branchial arch. At E10.5, *RARβ* expression commences in

frontonasal mass and the first branchial arch. At E10.5, *RARβ* expression commences in the proximo-dorsal mesenchyme of the limb bud, and can later be detected at high levels throughout the interdigital mesenchyme.

1.4.5c RARγ

Similar to *RARα* transcripts, *RARγ* messages are not detected by *in situ* hybridization until E8.0, at which time they are observed only in the caudal portion of the embryo. *RARγ* transcripts are found in all three germ layers in the region of the posterior neuropore including the open neural folds, presomitic and lateral mesoderm, and endoderm (Ruberte *et al.*, 1990). However, *RARγ* transcripts are not detected in neural tissues following neural tube closure, or in paraxial mesoderm following somite formation. *RARγ* expression persists in this region of the embryo (and at later stages in the tailbud) until the formation of the body axis is complete. Beginning at E8.5 and continuing until E10.5, *RARγ* transcripts can be detected in the head region, specifically in the mesenchyme of the branchial arches and the frontonasal mass. As the limb buds begin to develop at E9, *RARγ* is expressed homogeneously throughout these structures, however this expression becomes restricted to the mesenchyme by E10.5. Upon mesenchymal condensation in the limbs, expression of *RARγ* becomes further restricted to these precartilaginous condensations, where it persists until ossification occurs. Similarly, the sclerotomal portion of the somite begins to express *RARγ* at E10.5. This expression continues throughout the formation of the prevertebrae, and is extinguished as the prevertebral cartilage undergoes ossification. All other cartilaginous structures including the mesenchymal derivatives of the frontonasal and first branchial (mandibular) arch; the precartilage of the otic capsule: and the tracheal, bronchial, and laryngeal cartilages; also express *RARγ*.

1.5 Phenotypes of RAR and RXR null mice

1.5.1 Targeted disruption of *RAR* genes

Null mutations have been generated in each of the *RAR* genes, individually and in combination (See Table 1.1 for details and references). In general, mice that lack a given *RAR* isoform (i.e. *RARα1*, *RARβ2*, and *RARγ2*) do not exhibit developmental abnormalities and are completely viable and fertile. Although evolutionary conservation and tissue specific expression during development would suggest that the isoforms have unique roles, the remaining receptors appear able to compensate for the loss, at least in a laboratory setting. One exception is *RARγ1*, as mice null for this isoform exhibit mild developmental abnormalities, including homeotic transformations, malformations of the laryngeal cartilage, and growth deficiency (Subbarayan *et al.*, 1997). Disruption of *RAR* types (i.e. *RARα* and *RARγ*) in the mouse leads to relatively minor congenital abnormalities, a high rate of postnatal lethality, and sterility in males. While the postpartum abnormalities reflect those observed in VAD animals, none of the fetal VAD defects are observed in any of the single *RAR* mutants. This finding was quite surprising and suggested a high degree of functional redundancy between the different RAR types.

In order to address this, the single *RAR* mutants were interbred to generate various combinations of double mutants (Lohnes *et al.*, 1994; Mendelsohn *et al.*, 1994a). The simultaneous disruption of two *RARs* has a dramatic effect on postnatal viability, and leads to embryonic death in some *RARα/γ* double mutants. Furthermore, all of the double mutants exhibit congenital defects that are much more severe, and penetrant, than those observed in the corresponding single null mice. The developmental abnormalities characteristic of vitamin A deficient fetuses are also recapitulated by the various combinations of *RAR* double mutants (VAD-related defects are marked with an asterix in Table 1.1). These findings provide strong support that RA is the biologically active form of vitamin A and functions through the RARs to control gene expression. Additionally, several defects included in the *RAR* mutant phenotypes, such as homeotic transformations of the vertebrae and exencephaly, were never observed in VAD fetuses. It is likely that

Table 1.1 Congenital abnormalities of RAR and RXR single and double mutant mice

Receptor	Phenotype	References
Single mutants		
RARα	-*RARα1*: no detectable phenotype -*RARα*: neonatal lethality* -interdigital webbing (60%) -male sterility due to degeneration of testicular germinal epithelium (100%)* -low frequency of vertebral homeotic transformations -pteroquadrate element (10%)	Lufkin *et al.*, 1993; Li *et al.*, 1993; Lohnes *et al.*, 1994 Kastner *et al.*, 1997
RARβ	-*RARβ1/3* and *RARβ3*: no detectable phenotype -*RARβ*: growth deficiency* -eye defects: retrolenticular membrane* (85%; also in 70% of *RARβ2* null mice) -cervical homeotic transformations	Mendelsohn *et al.*, 1994b; Luo *et al.*, 1995; Grondona *et al.*, 1996; Ghyselinck *et al.*, 1997, 1998
RARγ	-*RARγ2*: no detectable phenotype -*RARγ*: neonatal lethality* -growth deficiency* (less severe in *RARγ1* null mice) -malformed tracheal and laryngeal cartilage (100%) (latter also observed in 60% of *RARγ1* null mice) -agenesis of Harderian gland epithelium (50%) -male sterility due to squamous metaplasia and/or keratinization of the seminal vesicle and prostate gland epithelia (100%)* -interdigital webbing -homeotic transformations and malformations of the vertebrae (86%) (13% of *RARγ1* null mice) -complete resistance to RA induced truncation of the vertebral column (100%)	Lohnes *et al.*, 1993; Kastner *et al.*, 1997 Subbarayan *et al.*, 1997
RXRα	-embryonic lethality (100% between E13.5 and E16.5) -heart defects: ventricular hypoplasia*, defects in ventricular septation* -eye defects: retrolenticular membrane*, shortening of the ventral retina*, close origin of eyelids*, thickened corneal stroma*, agenesis of anterior eye chamber* -delayed development of embryonic liver -placental defects -complete resistance to RA induced limb malformations -interdigital webbing (5%)	Sucov *et al.*, 1994, 1995; Kastner *et al.*, 1994
RXRβ	-some *in utero* and perinatal lethality* -male sterility due to abnormal spermatogenesis, accompanied by lipid accumulation in the sertoli cells and eventual degeneration of the germinal epithelium (100%)	Kastner *et al.*, 1996

Table 1.1 Congenital abnormalities of RAR and RXR single and double mutant mice		
Receptor	**Phenotype**	**References**
RXRγ	-no detectable abnormalities	Krezel *et al.*, 1996
Double mutants		
RARα/RARβ	*RARα1/RARβ2* -reduced viability following cesarean section at E18.5 compared to either single mutant -craniofacial skeletal abnormalities: fusion of incus to alisphenoid* -abnormalities of the hyoid bone -abnormal tracheal and laryngeal cartilages -heart and aortic arch abnormalities: persistent truncus arteriosus*, dextroposed aorta*, ventricular septal defect*, abnormal patterning of the aortic arches* -absence of esophagotracheal septum* -abnormalities of thymus, thyroid and parathyroid glands -genitourinary defects: kidney hypoplasia, ureter abnormalities*, agenesis of the uterus and cranial vagina*	Lohnes *et al.*, 1994; Mendelsohn *et al.*, 1994a
	RARα/RARβ2 -all defects observed in *RARα1/RARβ2* null mice -further reduced viability following cesarean section -vertebral homeotic transformations and malformations -hypoplasia or agenesis of lungs* -diaphragmatic hernia* -absence of anal canal -increased penetrance of heart and aortic arch abnormalities compared to *RARα1/β2* null mice	Lohnes *et al.*, 1994; Mendelsohn *et al.*, 1994a
	RARα/β3 -80% perinatal lethality (none in either single mutant) -no additional abnormalities compared to *RARα* null mice	Ghyselinck *et al.*, 1998
	RARα/RARβ -all defects observed in *RARα/RARβ2* null mice -agenesis of the spleen and thymus	Ghyselinck *et al.*, 1997
RARα/RARγ	*RARα1/RARγ* -reduced viability following cesarean section at E18.5 compared to either single mutant -craniofacial skeletal defects: ectopic cartilaginous and bony nodules, supernumerary cranial skeletal elements -abnormalities of intraorbital glands and ducts: agenesis of the Harderian glands and nasolachrymal duct, cystic dysplasia of the sublingual gland, shortening of the sublingual and	Lohnes *et al.*, 1994; Mendelsohn *et al.*, 1994a

Table 1.1 Congenital abnormalities of RAR and RXR single and double mutant mice		
Receptor	**Phenotype**	**References**
	submandibular ducts, and absence of the sublingual caruncle -increased frequency of homeotic transformations and vertebral malformations compared to RARγ null mice	
	RARα1/RARγ/RARα2$^{+/-}$ -all defects observed in *RARα1/RARγ* null mice -further reduced viability following cesarean section at E18.5 -increased severity of craniofacial skeletal defects: -cystic dysplasia of the submandibular gland, and agenesis of the sublingual gland and duct -brain abnormalities -eye defects: unfused eyelids*, corneal-lenticular stalk -heart and aortic arch abnormalities: dextroposed aorta*, ventricular septal defect*, and abnormal patterning of the aortic arches* -abnormalities of thymus, thyroid and parathyroid glands -genitourinary defects: kidney hypoplasia, agenesis or dysplasia of the vas deferens*	Lohnes *et al.*, 1994; Mendelsohn *et al.*, 1994a
	RARα/RARγ -all defects of above *RARα/RARγ* isoform specific null mice -partial embryonic lethality (absence of both *RARγ* isoforms required) -reduced size at birth -eye defects: coloboma of retina and optic nerve*, fibrous retrolenticular membrane*, small conjunctival sac*, abnormal corneal stroma, absence of the anterior chamber*, abnormal lens fibers*, agenesis of the cornea, conjunctiva, and lens -severe deficiencies and malformations of most skeletal elements derived from the frontonasal mesectoderm and the first, second, and third pharyngeal arches (some defects in *RARα/RARγ2* null mice) -exencephaly -agenesis of the Harderian gland (also in *RARα/RARγ2* null mice), submandibular gland and duct -severe malformations of all cervical vertebrae (absence of either RARγ isoform from the RARα null background results in increased homeotic transformations and malformations of the vertebrae) -umbilical hernia -limb abnormalities -heart and aortic arch abnormalities: persistent atrioventricular canal*, thin myocardium*, persistent truncus arteriosus* (some heart defects also seen in *RARα/RARγ1* null mice) -genitourinary defects: kidney agenesis and aplasia (hypoplasia in *RARα/RARγ1* or *RARα/RARγ2* null mice), agenesis of the ureter*, urinary bladder, uterus*, and cranial vagina*, agenesis or dysplasia of the seminal vesicles*	Lohnes *et al.*, 1994; Mendelsohn *et al.*, 1994a; Subbarayan *et al.*, 1997

Table 1.1	Congenital abnormalities of RAR and RXR single and double mutant mice	
Receptor	**Phenotype**	**References**
RARβ/RARγ	*RARβ/RARγ1* -unilateral kidney agenesis	Subbarayan *et al.*, 1997
	RARβ2/RARγ2 -eye defects: retinal dysplasia*, agenesis of choroid and sclera*, small eyelids*, retrolenticular membrane*	Grondona *et al.*, 1996
	RARβ1/3/RARγ -70% perinatal lethality none in either single mutant -eye defects: retrolenticular membrane*, agenesis of choroids and sclera*, retinal degeneration*	Ghyselinck *et al.*, 1998
	RARβ2/RARγ -reduced viability following cesarean section at E18.5 compared to either single mutant -eye defects: coloboma of retina and optic nerve*, small conjunctival sac*, abnormal corneal stroma*, absence of anterior chamber* -abnormalities of intraorbital glands and ducts: agenesis of the nasolachrymal duct, shortened sublingual duct -increased frequency of vertebral malformations compared to RARγ null mice	Lohnes *et al.*, 1994; Mendelsohn *et al.*, 1994a
	RARβ/RARγ -all abnormalities previously described for disruption of specific *RARβ/RARγ* isoforms -eye defects: shortening of the ventral portion of the retina*	Ghyselinck *et al.*, 1997
RXRα/RARα	*RXRα$^{+/-}$/RARα* -increased penetrance and expressivity of interdigital webbing in double heterozygotes (55%) -pterygoquadrate element (50%) -increased penetrance of vertebral homeotic transformations and malformations with the loss of *RARα* alleles -malformations of the anterior tracheal rings	Kastner *et al.*, 1994, 1997 Kastner *et al.*, 1994, 1997
	RXRα/RARα -genitourinary defects: kidney hypoplasia or agenesis*, ureter abnormalities*, partial (*RARα$^{+/-}$*) or complete (*RARα$^{-/-}$*) agenesis of uterus and cranial vagina* -lung hypoplasia* and absence of esophagotracheal septum* -heart and aortic arch abnormalities: persistent truncus arteriosus*, abnormal arteries*, conotruncal ventricular septal defect* (penetrance and expressivity increases with the loss of *RARα* alleles)	

Table 1.1 Congenital abnormalities of RAR and RXR single and double mutant mice		
Receptor	**Phenotype**	**References**
RXRα/RARβ	<u>*RXRα*$^{+/-}$*/RARβ*</u> -eye defects: increased penetrance of retrolenticular membrane* in double heterozygotes compared to single heterozygotes	Kastner *et al.*, 1994, 1997
	<u>*RXRα/RARβ*</u> -eye defects: increased thickening of corneal stroma compared to *RXRα* null mice (also seen in *RXRα/RARβ2* mice) -heart and aortic arch abnormalities: persistent truncus arteriosus*, abnormal arteries*, conotruncal ventricular septal defect* (100%; also in 30% of *RXRα/RARβ2* null mice) -thymic agenesis (also in *RXRα/RARβ2* null mice) -genitourinary defects: ureter abnormalities* and partial agenesis of the caudal portion of the Müllerian duct* (both also in *RXRα/RARβ2* null mice)	
RXRα/RARγ	<u>*RXRα*$^{+/-}$*/RARγ*</u> -increased penetrance and expressivity of interdigital webbing with the loss of *RARγ* alleles -increased penetrance of vertebral homeotic transformations and malformations compared to either single mutant -increased expressivity of tracheal ring malformations compared to *RARγ* null mice	Kastner *et al.*, 1994, 1997
	<u>*RXRα/RARγ*</u> -heart and aortic arch abnormalities: persistent truncus arteriosus*, abnormal arteries*, conotruncal ventricular septal defect* (penetrance and expressivity increases with the loss of RARγ alleles) -hypoplasia of the submandibular gland -eye defects: increased penetrance and expressivity of *RXRα* eye phenotype (shortening or absence of the ventral retina, increased severity of eyelid and anterior segment defects with loss of *RARγ* alleles) -duplication of the nasal septum -malformed scapula -genitourinary defects: ureter abnormalities*, partial agenesis of the caudal portion of the Müllerian duct*	
RXRβ or γ* and any *RAR	-no increase in the penetrance or expressivity of congenital malformations characteristic of each single *RAR* mutant	Kastner *et al.*, 1997

* VAD-associated defects

different levels of RA signaling are required for distinct morphological processes, and a deficiency that would result in the above non-VAD associated defects would not be compatible with maternal or embryonic survival. This is supported by the findings that *RARα/γ* double mutants exhibit 50% lethality *in utero* and *Raldh2* null mice do not survive past midgestation (Lohnes *et al.*, 1994; Neiderreither *et al.*, 1999).

1.5.2 Targeted disruption of RXR genes

As RXRs are DNA-binding partners for several members of the nuclear receptor superfamily, including RARs (reviewed in Mangelsdorf and Evans, 1995), it could be anticipated that the disruption of *RXR* genes would affect numerous signaling pathways and consequently have a dramatic effect on the developing embryo. Therefore, it appears quite remarkable that the targeted disruption of *RXRβ*, or *RXRγ* genes results in relatively mild phenotypes. In fact, disruption of *RXRγ* has no detectable effect on the developing embryo or adult (Krezel *et al.*, 1996). This is unexpected as *RXRγ* expression is highly restricted in the adult and is localized to developing skeletal muscles during embryogenesis (Dollé *et al.*, 1994). *RXRβ* null males are sterile due to lipid accumulation in the Sertoli cells and abnormal spermatogenesis, a phenotype likely due to modification of the PPAR signaling pathway (Kastner *et al.*, 1996). In contrast, *RXRα* null mice are more severely affected and die *in utero* between E13.5 and E16.5. These null embryos exhibit congenital abnormalities of the eye and heart that are similar to those observed in VAD embryos, as well as placental defects and delayed development of the embryonic liver (Kastner *et al.*, 1994; Sucov *et al.*, 1994, 1995; Sapin *et al.*, 1997). As RARs are functionally redundant during development, various combinations of *RXR* double mutant mice were generated to assess whether functional compensation was a feature common to both receptor families. Strikingly, both *RXRα/RXRγ* and *RXRβ/RXRγ* double mutants did not display any additional abnormalities compared to *RXRα* and *RXRβ* single mutants, respectively. Moreover, $RXR\alpha^{+/-}RXR\beta^{-/-}RXR\gamma^{-/-}$ mice are completely viable indicating that one copy of *RXRα* is sufficient to fulfill all of the RXR requirements during embryogenesis and adulthood (Krezel *et al.*, 1996). Further analysis of the *RXRβ* and *RXRγ* null mice demonstrated that these animals were in fact compromised. Both *RXRβ* and *RXRγ* single null mice are significantly deficient incertain

locomotor skills, and this deficiency is more pronounced in the double mutants (Krezel *et al.*, 1998). Such defects may not affect the lifespan of a mouse in a laboratory environment, however they could significantly impair survival in the wild.

1.5.3 RAR and RXR compound mutants

Given the relatively minor phenotypic effects following null mutation of the *RXR* genes it was questioned whether these receptors played a significant role in transducing the retinoid signal *in vivo*. As RARs require RXRs for tight binding to RAREs *in vitro* (Leid *et al.*, 1992), mice null for various combinations of *RARs* and *RXRs* were generated and analyzed for evidence of cooperation between these receptors during development (Kastner *et al.*, 1994, 1997). Synergistic interaction is observed between *RXRα* and all of the *RARs* such that all of the defects observed in *RAR* double mutants are recapitulated in *RAR/RXR* compound mutants (see Table 1.1 for details and references). In some cases, abnormalities that are never observed in single *RAR* or *RXR* mutants become apparent when both receptors are absent. For example, genitourinary defects (hypoplasia or agenesis of the kidney, uterus and cranial vagina) were never observed in *RARα* or *RXRα* single mutants but were frequently observed in *RARα/RXRα* double mutants.

Similar to the findings following targeted disruption of the *RXRγ* gene in the *RXRα* or *RXRβ* null backgrounds (Krezel *et al.*, 1996), the loss of functional *RXRγ* and *RXRβ* genes from various *RAR* null backgrounds has no effect on the penetrance or expressivity of congenital malformations in the developing embryo. Therefore, the loss of *RXRα* in combination with one of the three *RAR* types is sufficient to produce the entire spectrum of defects observed in VAD fetuses.

1.5.4 Resistance to RA-induced malformations

In developing mice, exposure to high concentrations of RA during development results in severe malformations of structures that are undergoing morphogenesis at that time (see Section 1.3.2). As described above, analysis of the congenital defects that arise due to the loss of a specific RAR or RXR has provided valuable information regarding the role of these receptors in normal morphogenesis. These mice have also been used to determine whether specific receptors are involved in mediating the teratogenic outcomes

that are caused by RA excess. For example, the developing limbs of the mouse embryo are sensitive to exogenous RA between E10.5 and 11.5, and such exposure results in truncation of the long bones, and truncations, fusions, and reductions in the number of digits (Kochhar *et al.*, 1973, 1985). *RXRα* null embryos are completely resistant to these truncations and malformations (Sucov *et al.*, 1995). Moreover, RA-treated *RXRα* heterozygotes exhibit milder defects than treated wild type embryos, therefore this rescue is dependent on gene dosage.

Excess RA administered around the eighth day of development results in a high degree of embryonic lethality, and the surviving fetuses exhibit craniofacial malformations, and severe truncation of the body axis accompanied by spina bifida (Tibbles and Wiley, 1988: Kessel and Gruss, 1991; Kessel, 1992). The anteroposterior level at which the axial truncation occurs is dependent on the dose of RA, and the developmental stage at which it is administered. Treatment with lower doses and/or at later stages of development results in progressively more posterior truncations (Kessel, 1992; Shum *et al.*, 1999). *RARγ*, but not *RARα* or *RARβ*, homozygous null mice, administered a dose of 100mg/kg all-*trans*-RA at E8.5 are completely resistant to both the caudal truncations and neural tube defects observed in their wild type littermates (See Figure 1.4; Lohnes *et al.*, 1993). Moreover, *RARγ* heterozygous fetuses treated in the same manner display an intermediate phenotype, indicating that transduction of the RA signal is gene dosage-dependent.

The expression of a panel of molecular markers has been examined in the *RARγ* null mice to determine which tissues are targeted by excess RA in the caudal embryo (Iulianella *et al.*, 1999). Transcript levels of *Brachyury*, *Cdx4*, and *Wnt3a*, are diminished in the nascent mesoderm of RA-treated wild type but not RA-treated *RARγ* null embryos. The diminished level of these transcripts in the RA-treated nascent mesoderm population is not due to widespread cell death in this tissue, as the decline is observed before any morphological abnormalities are apparent, and before the induction of apoptosis (Iulianella *et al.*, 1999). Additionally, the message levels of other genes

Figure 1.4. RARγ null mutant mice are resistant to RA-induced caudal truncation. (**A**) Wild type E18.5 mouse skeleton. (**B-D**) E18.5 skeletons treated with 100 mg/kg RA at E8.5. (**B**) Wild type (**C**) *RARγ*$^{+/-}$ (**D**) *RARγ*$^{-/-}$ Note that *RARγ*$^{-/-}$ mice are completely resistant to the caudal truncations elicited by RA-treatment in wild type skeletons, and that *RARγ*$^{+/-}$ mice exhibit an intermediate phenotype, indicating a gene-dosage effect. This figure was adapted from Lohnes *et al.*, 1993. **Abbreviations**: C, cervical vertebrae; T, thoracic vertebrae; L, lumbar vertebrae, S, sacral vertebrae.

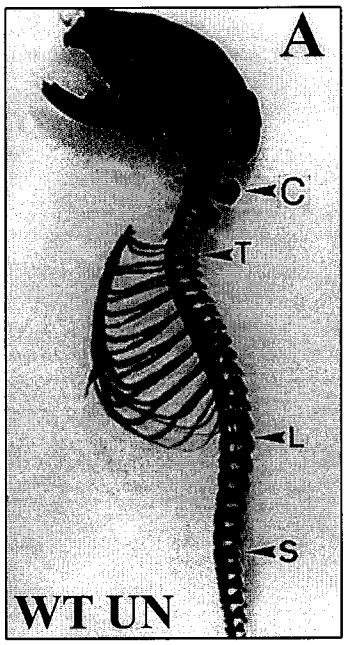
A
C
T
L
S
WT UN

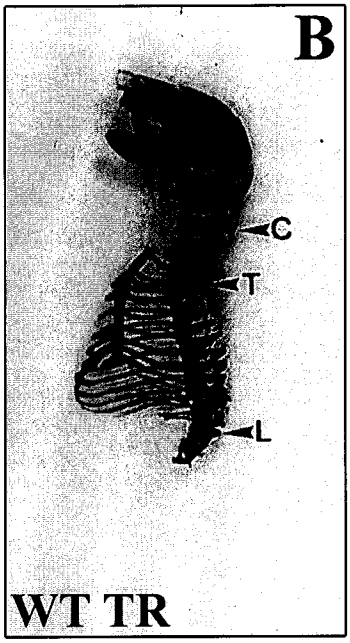
B
C
T
L
WT TR

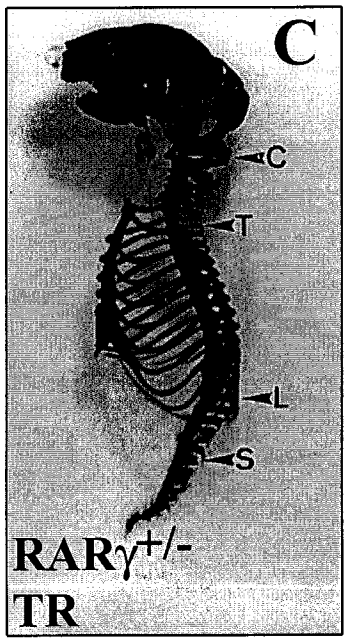
C
C
T
L
S
RARγ+/-
TR

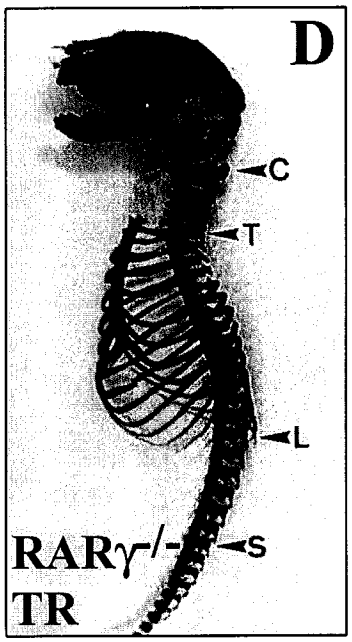
D
C
T
L
S
RARγ-/-
TR

expressed in this tissue, such as *Cdx1* (Houle *et al.*, 2000) and *P450RAI* (Iulianella *et al.*, 1999), are dramatically increased following a similar length of RA exposure.

Recently, it was demonstrated that RA treatment at E9.5 and E10.5 also results in downregulation of *Wnt3a* expression in the tailbud as early as 2 hours post maternal treatment (Shum *et al.*, 1999). These authors also demonstrated that RA excess results in a phenotype that is highly similar to that observed in the *vestigial tail* mutant mice (a hypomorphic allele of *Wnt3a*; Greco *et al.*, 1996). In both cases ectopic neural tube-like structures are formed ventral to the endogenous neural tube, and the amount of ectopic neural tissue generated is proportional to the dose of RA administered. Repression of WNT3a signaling by RA is further supported by the observation that *Brachyury*, which is downregulated by RA treatment at E8.5, is a direct target of this pathway (Iulianella *et al.*, 1999; Yamaguchi *et al.*, 1999, Arnold *et al.*, 2000).

1.6 Retinoic acid signaling and anteroposterior patterning

1.6.1 Hox genes

1.6.1a The Hox gene clusters

In the mouse, a total of 39 *Hox* genes are organized into four clusters (A through D) located on different chromosomes, each cluster spanning approximately 120 kb (reviewed in Krumlauf, 1994). Comparison of the genomic organization of the *Hox* genes in vertebrates to that of other species has led to the hypothesis that the vertebrate *Hox* clusters arose as a result of two duplications of an ancestral *Hox* complex (for reviews see Krumlauf, 1992; Kenyon, 1994). In *Drosophila* the analogous complex (*HOM-C*) appears to have diverged along an independent pathway, compared to vertebrates, as the original cluster of genes has been separated into two smaller components, the *Bithorax* and *Antennapedia* complexes (Lewis, 1978; Kaufman *et al.*, 1990). Based on homology to the *Drosophila HOM* genes, and to their genomic location in each of the four clusters, the vertebrate *Hox* genes have been grouped into 13 families. Members in each of these families are referred to as paralogues and tend to be highly conserved with respect to function, time of expression, and domain of expression during development.

A conserved feature of the *HOM/Hox* gene complexes is the correlation between the physical order of the genes along the chromosome and their order of expression in the developing embryo. This phenomenon, termed colinearity, was first noted in *Drosophila* (Lewis, 1978) and was later observed in mouse embryos (Duboule and Dollé, 1989; Graham *et al.*, 1989). *Hox* genes that are located at the 3' end of the structure tend to be expressed at earlier stages and more anteriorly in the embryo than *Hox* genes located in more 5' regions of the cluster. In the mouse, the result is a nested set of *Hox* expression domains such that distinct anteroposterior levels possess a unique assortment of these transcripts. The specific combination of *Hox* gene expression in the developing CNS, vertebral column, organs and limbs is thought to influence the developmental fate of that particular region or structure. Indeed, both ectopic, and loss of expression of the *Hox/HOM* genes during development result in malformations and homeotic transformations. Hence, it is apparent that *Hox* expression must be strictly controlled, both spatially and temporally, in order for embryogenesis to proceed correctly.

The highly conserved genomic organization of the *Hox* gene cluster is suggestive of a structural mechanism necessary for proper transcriptional regulation. Transgenic analysis in the mouse embryo has demonstrated that a relatively small region of flanking DNA is capable of directing a normal expression pattern of certain *Hox* genes (Krumlauf 1994, and references therein). These findings imply that the position of a *Hox* gene in the cluster is not as important as its 5' and 3' regulatory regions. As the expression of several *Hox* genes is maintained through auto- and cross-regulatory interactions it has been suggested that shared regulatory elements between neighboring *Hox* genes has ensured that the genomic organization was conserved. However, insertion of *Hox* transgenes at different locations within the *HoxD* cluster has provided clear evidence that a higher order of *Hox* regulation also exists. For example, relocation of a *Hox* transgene to the 5'-most region of the cluster results in delayed activation of transgene expression, and induction of an expression pattern more characteristic of the 5' *Hoxd* genes (van der Hoeven *et al.*, 1996). Recently, a region located within 40 kb 5' of the *HoxD* cluster has been demonstrated to be essential for preventing the early expression of the more 5' located *Hox* genes (Kondo and Duboule, 1999). Deletion of this silencing element results in premature expression of the 5' *Hoxd* genes, in regions more anterior to their normal

boundaries of expression. Moreover, colinear expression is lost, as expression of the transgenes, and endogenous *Hoxd10* and *Hoxd4* genes, are initiated at the stage when *Hoxd1* expression normally commences. Ectopic expression of these genes is transient as at later stages of development a normal pattern of expression is observed. Therefore it appears that additional factors, not present in these ectopic domains, are necessary for the maintenance of *Hox* expression. The 5' *HoxD* silencer is not equally effective on all transposed *Hox* genes, as the *Hoxb1* transgene retains some of its early expression patterns when transposed to the region 5' of *Hoxd13* (Kmita *et al.*, 2000). Additionally, in this ectopic position, the *Hoxb1* transgene can induce premature expression of *Hoxd13*. Therefore, it appears that more than one level of transcriptional control is operating on the *Hox* clusters, and that both the position of the *Hox* gene within the cluster and its flanking sequences are important for colinear expression.

1.6.1b RA regulation of Hox expression in the embryo

There are three phases of *Hox* gene expression in the developing mouse embryo; initiation, establishment and maintenance (reviewed by Deschamps *et al.*, 1999). Expression of the 3' most *Hox* genes is initiated at E7.5 in the region of the primitive streak during gastrulation. Sequential activation of the progressively more 5' *Hox* genes continues to take place in the posterior region of the embryo until E9.5. Following initiation, the expression domains spread forward in the CNS, paraxial mesoderm, and lateral plate mesoderm until a predetermined rostral limit is reached. This mechanism is thought to be intrinsic to the cells that have completed gastrulation, as spreading occurs in the absence of cell mixing, and can traverse a physical barrier implanted into the embryo (Deschamps and Wijgerde, 1993; Gaunt and Strachan, 1994, Gaunt *et al.*, 1999). Once the appropriate boundaries have been reached, expression of some *Hox* genes is maintained through auto- and cross-regulation by other transcription factors and the *Hox* products themselves (See Table 1.2 and references therein). In Drosophila, *HOM* expression is maintained through chromatin remodeling by *Polycomb*-group and *Trithorax*-group proteins. These factors have mammalian homologues, and evidence provided by null mutation of the corresponding genes implies that a similar mechanism

of long-term maintenance has been conserved in vertebrates (reviewed in Schumacher and Magnuson, 1997).

Retinoic acid is likely involved in initiation of *Hox* gene expression. RA is present in the posterior portion of the E7.5 mouse embryo, in a domain that overlaps the region where *Hox* genes are first expressed (Rossant *et al.*, 1991). In addition to the temporal and spatial colinearity of *Hox* gene expression discussed in the previous section, *Hox* genes are also responsive to RA treatment in a manner that reflects their position in the cluster. This was first discovered in F9 cells, where 3' *Hox* genes respond more rapidly, and at a lower concentration of RA, than the more 5' members of the cluster (Simeone *et al.*, 1990, 1991). This effect appears to be restricted to *Hox* genes located in the 3' half of the cluster, as genes located more 5' either do not respond to, or are inhibited by RA treatment. In the mouse embryo, RA-treatment at certain stages of development results in anteriorization of *Hox* expression domains in the CNS, mesoderm, prevertebrae, and gut (Kessel and Gruss, 1991; Morriss-Kay *et al.*, 1991; Conlon and Rossant, 1992; Marshall *et al.*, 1992; Wood *et al.*, 1994; Huang *et al.*, 1998). Furthermore, the stage at which the 3' *Hox* genes become responsive to exogenous RA is correlated with their location in the cluster. For example, the expression domains of *Hoxb1* and *Hoxb2* in the CNS are anteriorized following exposure to RA at E7.25 (Conlon and Rossant, 1992), while *Hoxb4* does not respond to RA treatment until E8.5 (Morrison *et al.*, 1997).

RAREs have been identified in the regulatory regions of *Hox* genes in paralogue groups 1 and 4 (see Table 1.2 for examples). Deletion and point mutation of these elements in transgenic mice results in delayed or abolished expression in various structures including the hindbrain, spinal cord, lateral plate and paraxial mesoderm, and gut, indicating that retinoids are involved in endogenous *Hox* expression. Regulation of *Hox* genes through the RAREs appears to be complex, as individual RAREs located in the same *Hox* gene can control expression in different tissues (i.e. the two RAREs located 3' of *Hoxb1* direct expression in the neuroectoderm and the foregut, respectively). Furthermore, some RAREs are required for the expression of neighboring *Hox* genes. For example, the 3' RARE of *Hoxa1* is necessary for expression of *Hoxa2* in rhombomere 5. However, it is not clear whether the RARE is acting directly on *Hoxa2*,

or indirectly through *Hoxa1* (Dupé *et al.*, 1997). Gould *et al.* (1998) elegantly demonstrated that the type of RARE is extremely important in defining the rostral boundary of *Hox* gene expression. When the DR5 RARE located 5' to *Hoxb4* is replaced by the DR2 RARE normally located 3' of *Hoxb1,* the rostral limit of *Hoxb4* expression is shifted anteriorly from the rhombomere 6/7 boundary to the rhombomere 3/4 boundary. Therefore, simply changing the type of RARE can alter the rostral limit of *Hoxb4* expression in the CNS.

1.6.2 Retinoic acid and hindbrain patterning

The developing CNS of the mouse is divided into four regions: the forebrain, midbrain, hindbrain, and spinal cord. The hindbrain is further segmented into eight regions, termed rhombomeres, each of which is uniquely specified with respect to anteroposterior identity. *Hox* genes are expressed in the CNS up to the level of the hindbrain, and their boundaries of expression coincide with the divisions of the rhombomeres. It is widely accepted that the *Hox* genes are largely responsible for conferring AP identity to specific rhombomeres (reviewed in Rijli *et al.*, 1998).

It has been proposed that RA is a posterior transforming factor in the Nieuwkoop 'activation-transformation' model, in which the neural tissue is first activated to form anterior (forebrain) structures, and is subsequently transformed to more posterior structures by signals in the posterior mesoderm (reviewed in Conlon, 1995). In this model, excess RA signaling would result in the posteriorization of more anterior structures. For example, when the mouse embryo is exposed to excess RA at E7.5 rhombomeres 2 and 3 assume the molecular identity of rhombomeres 4 and 5 (Marshall *et al.*, 1992). In these RA-treated embryos, expression of *Hoxb1* is detected in both rhombomeres 2 and 4 at E9.5, while in untreated embryos, it is specifically restricted to rhombomere 4. Posterior transformation of the neural tissue by exposure to RA during gastrulation has also been observed in *Xenopus* and zebrafish, and is accompanied by anteriorized expression boundaries of certain *Hox* genes (Durston *et al.*, 1989; Holder and Hill, 1991; Ruiz i Altaba and Jessel, 1991; Conlon and Rossant, 1992; Hill *et al.*, 1995).

Evidence from several species has demonstrated that attenuation of endogenous RA signaling also has a dramatic effect on the developing hindbrain. For example,

Table 1.2	Transcription factors and enhancer elements involved in Hox regulation		
Factor/ Element	**Hox genes regulated**	**Comments**	**References**
RA	*Hoxb1, Hoxb2, Hoxa3, Hoxd3, Hoxb4, Hoxd4, Hoxb5, Hoxa7, Hoxc8, Hoxa10, Hoxd10, Hoxa11*	-*Hoxb1*, -*b2*, -*d3*, -*b4*, -*d4*, and –*b5* are anteriorized in the hindbrain by RA-treatment	Conlon and Rossant, 1992; Marshall *et al.*, 1992; Folberg *et al.*, 1997, 1999b
		-*Hoxa3*, -*a7* and -*c8* are anteriorized in the prevertebrae following RA treatment at E7.5	Kessel and Gruss, 1991
		-*Hoxa10*, -*d10* and -*a11* are repressed or posteriorized in the prevertebrae following RA treatment at E8.5	Kessel, 1992
Raldh2	*Hoxa1, Hoxb1, Hoxa3, Hoxb3, Hoxa4, Hoxd4*	-*Hoxa1* expression is reduced at E7.75, and abolished at E8.5 in *Raldh2*$^{-/-}$ embryos -*Hoxb1*, -*a3* and –*b3* expression is weak and diffuse in the hindbrain of *Raldh2*$^{-/-}$ embryos -*Hoxd4* expression is absent from the hindbrain and *Hoxa4* expression is absent from the gut mesoderm in *Raldh2*$^{-/-}$ embryos	Neiderreither *et al.*, 1999, 2000
RARβ	*Hoxb4, Hoxd4*	-*RARβ* is required for full anteriorization the *Hoxa4* and *Hoxd4* expression domains in response to RA-treatment	Folberg *et al.*, 1999b
RARE	*Hoxa1*	-*Hoxa1* 3' (DR5) RARE is required for normal initiation of endogenous expression at E7.5 -*Hoxa1* 3' RARE also mediates some effects of RA excess, and is required for *Hoxa1* expression in the paraxial mesoderm and neural tube	Langston and Gudas, 1992; Frasch *et al.*, 1995; Dupé *et al.*, 1997;
	Hoxb1	-*Hoxb1* 3' (DR2) RARE is required for normal levels of *Hoxb1* expression in neuroectoderm and mesoderm at E7.5 -*Hoxb1* 5' DR2 RARE is required for repression of *Hoxb1* transgene expression in r3 and r5	Marshall *et al.*, 1994; Studer *et al.*, 1998 Studer *et al.*, 1994
		-*Hoxa1* 3' DR5 RARE and *Hoxb1* 3' DR2 RARE together are required for *Hoxb1* expression in the primitive streak and r4	Studer *et al.*, 1998

Table 1.2	Summary of transcription factors and enhancers involved in Hox regulation cont'd.		
Factor/ Element	**Hox genes regulated**	**Comments**	**References**
RARE cont'd	*Hoxb1* cont'd	-*Hoxb1* 3' DR5 RARE is required for transgene expression and response to RA in the foregut	Huang *et al.*, 1998
	Hoxa4	-*Hoxa4* 5' RARE is required for transgene expression in the lung, metanephros, gut and peripheral nerves, and is required for RA-response of transgene in the CNS	Packer *et al.*, 1998
	Hoxb4	-*Hoxb4* 3' RARE is required for initiation of transgene expression in the CNS (early neural enhancer)	Gould *et al.*, 1998
	Hoxd4	-*Hoxd4* 3' RARE is required for timely initiation, normal levels, and correct rostral limit of transgene expression in the CNS, also mediates a subset of the RA-response -*Hoxd4* 5' RARE increases the efficiency of transgene expression in the absence of a mesodermal enhancer	Moroni *et al.*, 1993; Pöpperl and Featherstone, 1993; Morrison *et al.*, 1996, 1997; Zhang *et al.*, 1997a, 2000
HRE	*Hoxb1*	-direct autoregulatory loop required for maintenance of expression in r4 -*Hoxa1* is required to set the correct rostral limit of *Hoxb1* expression in the presumptive hindbrain and maintain expression of *Hoxb1* in r4	Pöpperl *et al.*, 1995; Studer *et al.*, 1996, 1998; Barrow *et al.*, 2000
	Hoxb2	-expression of *Hoxb2* in r4 is maintained by direct *Hox*b1 cross-regulation	Maconochie *et al.*, 1997
	Hoxa4	-expression of *Hoxa4* transgene is not maintained at later stages of development in *Hoxa4* null embryos -*Hoxa4* is required for maintenance of RA-induced expression of the *Hoxa4* transgene	Packer *et al.*, 1998
	Hoxb4	-the *Hoxb4* late neural enhancer (shared with *Hoxb3*) is auto- and cross-regulated by HOX proteins from paralogues 4 and 5 (possibly 6 and 7 as well)	Gould *et al.*, 1997
	Hoxd4	-autoregulatory element has been identified in the region 5' to *Hox*d4 -in vivo function has not been examined	Pöpperl and Featherstone, 1992

Table 1.2 Summary of transcription factors and enhancers involved in Hox regulation cont'd.			
Factor/ Element	**Hox genes regulated**	**Comments**	**References**
AP-2	*Hoxa2*	-AP-2 binding sites are necessary for *Hoxa2* transgene expression in cranial neural crest cells	Maconochie *et al.*, 1999
***Krox20/* KROX20**	*Hoxa2, Hoxb2, Hoxb3*	-KROX20 directly regulates *Hoxa2* and -*b2* expression in r3 and r5 -*Krox20* is required for normal expression of *Hoxb3* in r5	Nonchev *et al.*, 1996 Sham *et al.*, 1993; Vesque *et al.*, 1996; Seitanidou *et al.*, 1997
KRML1 (*Kreisler*)	*Hoxb1, Hoxa3, Hoxb3, Hoxb4, Hoxd4*	-KRML1 directly regulates expression of *Hoxa3* and *Hoxb3* in r5, and r5 and 6, respectively -expression domains of *Hoxb1*, -*b4*, and *d4* are altered in the hindbrain of *Kreisler* mutants	Frohman *et al.*, 1993; McKay *et al.*, 1994; Manzanares *et al.*, 1997, 1999
Cdx1	*Hoxd3, Hoxc5, Hoxc6, Hoxa7, Hoxc8*	-required for setting the normal rostral limit of *Hoxd3* in the somites, and *Hoxc5*, -*c6*, -*a7*, and -*c8* in the prevertebrae -putative CDX binding sites in the promoter of *Hoxa7* and *Hoxb8* -mutation of these sites *in vivo* has not been reported	Subramanian *et al.*, 1995; Charité *et al.*, 1998

rhombomeres 4 to 8 are completely lacking in vitamin A deficient quail embryos, and evidence suggests that the AP patterning of rhombomere 3 is also abnormal (Maden *et al.*, 1996; Gale *et al.*, 1999). Overexpression of dominant-negative RARs in *Xenopus* embryos results in a reduction in the length of the presumptive hindbrain, and anterior transformations of the more posterior rhombomeres (Blumberg *et al.*, 1997; Kolm *et al.*,1997; van der Wees *et al.*, 1998). Several *RAR* double mutant mice exhibit abnormalities in structures derived from the cranial neural crest cells that migrate from the presumptive hindbrain (Lohnes *et al.*, 1994; Mendelsohn *et al.*, 1994a; Luo *et al.*, 1996; Ghyselinck *et al.*, 1997). Moreover, the developing hindbrain of *RARα/RARβ* double null embryos are abnormally patterned and segmented (Dupé *et al.*, 1999), and targeted disruption of the *Raldh2* gene in the mouse, which prevents most RA synthesis in the embryo, also alters the patterning, growth and segmentation of the hindbrain region including presumptive rhombomeres 3 to 8 (Neiderreither *et al.*, 2000). Taken together, these data suggest that RA is required for posteriorization of the developing caudal hindbrain.

1.6.3 Anteroposterior patterning of the vertebral column

Although the somites are visually indistinguishable prior to and during differentiation, each of these structures gives rise to morphologically distinct vertebrae, which perform specific functions based on their location in the axial column. For example, the anterior somites form occipital and cervical (neck) vertebrae, while those located immediately posterior form thoracic vertebrae, which bear ribs. In order for correct patterning to occur, molecular differences must exist between somites located at distinct anteroposterior positions. Similar to the developing rhombomeres, the anteroposterior identity of each vertebra is largely determined by the expression of particular combination of *Hox* genes.

1.6.3a Hox genes and vertebral patterning

Over the past decade, several murine *Hox* genes have been individually disrupted by targeted homologous recombination. The effects of these null mutations appear to coincide with the anterior limits of expression of the particular *Hox* gene during

development. In the developing vertebral column *Hox* genes are expressed in the paraxial mesoderm, and maintained in the somites and the prevertebrae. The anterior boundary of expression appears to be established prior to segmentation of the somites, as transplantation of segmental plate mesoderm to locations respectively more anterior or posterior in the axial column does not alter the fate of the transplanted tissue (Kieny, 1972; Nowicki and Burke, 2000). For example, if presumptive cervical somites are transplanted to the thoracic region they will not develop ribs and continue to express *Hox* genes that are characteristic of cervical somites. In general, targeted disruption of a *Hox* gene leads to anterior transformations of the vertebrae. However, in some cases both anterior and posterior transformations are observed in the same *Hox* mutant mouse (reviewed in Krumlauf, 1994).

Although vertebral anterior transformations are a common result of *Hox* inactivation, the cellular processes that underlie these transformations may be different. For example, targeted disruption of *Hoxd3* results in fusion of the first vertebra to the occipital bones of the skull, and loss of the anterior portion of the second vertebra (Condie and Capecchi, 1993). Furthermore, inactivation of *Hoxd3* and *Hoxa3*, or *Hoxd3* and *Hoxb3*, in combination results in complete loss of the first vertebra (Condie and Capecchi, 1994; Manley and Capecchi, 1997). In contrast, targeted mutation of *Hoxb4* or *Hoxd4* results in the appearance of ectopic structures. A ventrally located structure, termed the anterior arcus atlantis (AAA) is normally present on the first cervical vertebra. In *Hoxb4,* and *Hoxd4* null mice an AAA is also present on the second cervical vertebra, indicating a partial anterior transformation of vertebra 2 (Ramírez-Solis *et al.*, 1993; Horan *et al.*, 1995a). Combined inactivation of three group 4 *Hox* (*Hoxa4*, *-b4*, and *-d4*) genes results in the appearance of ectopic AAAs on up to 4 cervical vertebrae (Horan *et al.*, 1995b). These results indicate that *Hox* genes of the same paralogous group are functionally redundant, and that *Hox* genes that belong to different paralogous groups may control different cellular processes in the developing embryo. For example, it has been hypothesized that group 3 *Hox* genes may strongly promote proliferation while group 4 *Hox* genes may be less efficient at this process (Condie and Capecchi, 1993; Folberg *et al.*, 1999a). Therefore, a loss of group 3 *Hox* genes may lead to a decrease in proliferation of certain vertebral precursor cells, which would result in the deletion of

vertebral elements. On the other hand, loss of group 4 *Hox* genes may allow the remaining HOX proteins to stimulate proliferation, resulting in the appearance of structures that are normally repressed.

1.6.3b RA signaling and vertebral patterning

Exogenous RA, administered to the mouse embryo at E7.5, causes posterior transformations of several cervical vertebrae, such that a particular vertebra acquires the physical characteristics of the next caudal vertebra. These morphological changes are correlated with anteriorized expression domains of several *Hox* genes in the prevertebrae (Kessel and Gruss, 1991). Conversely, inactivation of RARs and RXRs leads to anterior homeotic transformations of the cervical vertebrae (Section 1.5). Combined inactivation of more than one *RAR*, or one *RAR* and one *RXR*, generally results in increased penetrance and expressivity of homeotic transformations, suggesting that the *RARs* are partially redundant with respect to vertebral patterning (Lohnes *et al.*, 1994; Kastner *et al.*, 1997).

There are several similarities in the phenotypes of certain *Hox* null mutant mice and *RAR* null mutant mice. For example, as described above, *Hoxb4* and *Hoxd4* null mice display an ectopic AAA on the second cervical vertebra. Additionally, an ossified bridge between the basioccipital bone of the skull and the AAA of the fist cervical vertebra is also evident in these mice (Ramírez-Solis *et al.*, 1993; Horan *et al.*, 1995a). Both of these defects are also observed in *RARγ* null mice (Lohnes *et al.*, 1993; Kastner *et al.*, 1997). Moreover, *Hoxd4* and *RARγ* act synergistically in the patterning of these two vertebrae, as a dramatic increase in the penetrance of these transformations is observed in the *RARγ/Hoxd4* double mutants (Folberg *et al.*, 1999a). However, neither *Hoxb4* nor *Hoxd4* expression is altered in *RARγ* mutant mice, and *Hoxb4* expression is not changed in *RARγ/Hoxd4* double mutant mice at E9.5 (Folberg *et al.*, 1999a). Therefore, it appears that in some instances, RARs and HOX proteins may act in parallel to influence specification of the same vertebrae. Nevertheless, *Hox* expression boundaries in the prevertebrae are anteriorized following RA treatment, and this is correlated with posterior transformations of the vertebrae, indicating that RA-signaling does influence the expression of at least some *Hox* genes in the developing vertebrae. In

addition to direct *Hox* regulation through RAREs, it is likely that RA may also control *Hox* expression though an intermediary factor. In this regard, RA directly regulates the transcription of another homeobox-containing gene, *Cdx1*.

1.6.4 Cdx genes

1.6.4a The caudal gene family

The *Drosophila caudal* (*cad*) gene was first isolated in a screen for homeobox-containing genes using the *ultrabithorax* homeobox as a probe (Mlodzik *et al.,* 1985; Levine *et al.*, 1985). Homologues of *cad* were subsequently identified in amphioxus (*AmphiCdx*), *C.elegans* (*ceh-3*), silk moth (*B mori caudal*), *Xenopus* (*Xcad1*, *Xcad2*, and *Xcad3*), zebrafish (*cad*[*zf-cad1*]), chick (*Cdx-A*, *Cdx-B*, and *Cdx-C*), mouse (*Cdx1*, *Cdx2*, and *Cdx4*), hamster (*Cdx2/3*) and humans (*Cdx1*, *Cdx2*, and *Cdx4*) (Freund *et al.*, 1998 and references therein). Recently, the amphioxus *caudal* gene (*AmphiCdx*) was suggested to be a member of the *ParaHox* gene cluster (Brooke *et al.*, 1998). The *ParaHox* cluster is thought to have arisen by duplication of the same cluster of genes (*ProtoHox*) that is ancestral to the *Hox* cluster. Hence, certain members of the *ParaHox* cluster are considered to be paralogues of certain *Hox* genes. It was originally proposed that *Cdx/cad* is the *ParaHox* paralogue of *AbdB* (Brooke *et al.*, 1998). However, more recent findings regarding the role of *cad* in *Drosophilia* development suggests that *Cdx/cad* is the paralogue of *Evx/eve* which is located 5' of the *Hox* cluster in vertebrates and cnidarians (Moreno and Morata, 1999).

1.6.4b Expression of Cdx genes during embryogenesis

Expression of *caudal*-related genes in all developing organisms studied to date is localized to the posterior end of the embryo. In the mouse, the three *Cdx* genes are expressed in nested domains in the posterior region of the embryo. *Cdx1* transcripts and protein are first detected at E7.5 in the ectodermal and nascent mesodermal cells of the primitive streak (Meyer and Gruss, 1993). Shortly thereafter, at E7.75, *Cdx1* can be detected anterior to the node in the ectoderm and paraxial mesoderm. The anterior boundary of expression at this stage is at the level of the preotic sulcus (presumptive hindbrain) in the neural ectoderm, and slightly more posterior in the mesoderm. As

development proceeds, the anterior boundary of *Cdx1* expression in the neural tube becomes progressively more posterior, and at later stages is positioned in the spinal cord. Within the neural ectoderm, *Cdx1* appears to be localized to the dorsal region of the neural folds, and in the newly migrating neural crest cells. *Cdx1* is also detected in the nascent paraxial mesoderm and weakly in the somites. As the somites differentiate (E9.0-9.5), *Cdx1* is localized to the dorsal region, the presumptive dermomyotome. This dorsal localization is only evident in the first 16 to 17 somites at E10.5. The more posterior somites (somites 18 to 30) exhibit significantly reduced levels of this protein, with the exception of somites 24 to 30 (opposite the hindlimb bud), which express slightly higher levels. *Cdx1* is also expressed in the mesenchyme of the developing forelimb bud at E9.5, and also later in the hindlimb bud, albeit at reduced levels. Specific expression of *Cdx1* is also detected in the nephrogenic cord and later in the mesonephric ducts.

Cdx2 is first detected in the trophectoderm at E3.5 and continues to be expressed in the placenta through at least E12.5 (Beck *et al.*, 1995). In the embryo proper, *Cdx2* is not detected until E8.5, where it is localized to the posterior region of the embryo. Specifically, *Cdx2* is found in all tissues of the primitive streak region including the ectoderm, mesoderm, and hindgut endoderm. At this stage, *Cdx2* is also present in the neural plate, the posterior region of the neural tube and notochord, and in unsegmented paraxial mesoderm. The levels of *Cdx2* in the neural tube and notochord decrease gradually in the anterior direction, with no distinct rostral boundary. At later stages, *Cdx2* is maintained in the tail bud and by E12.5 is localized to the very tip of the tail and the gut endoderm. A sharp anterior boundary of *Cdx2* is detected in the gut epithelium slightly proximal to the junction of the foregut and midgut. The amount of *Cdx2* in this tissue gradually declines in the caudal direction until the level of the rectum, where it can no longer be detected.

Compared to *Cdx1* and *Cdx2*, the temporal and spatial expression pattern of *Cdx4* is more restricted (Gamer and Wright, 1993). Low levels of expression can be detected at E7.5 in the allantios and the posterior tip of the primitive streak. By early neurulation stages, *Cdx4* is observed in all tissues of the primitive streak region with increasing levels towards the posterior end. Expression in the paraxial mesoderm reaches an anterior limit

approximately two somite-lengths posterior to the last formed somite. The rostral limit of expression in the neural tube is slightly more anterior, however for both tissues a sharp boundary is not apparent. *Cdx4* is also expressed in the lateral plate mesoderm, intermediate mesoderm, and the hindgut endoderm from E8.5 to E9.5. After E10.5 *Cdx4* transcripts and protein can not be detected.

In summary, the mouse *Cdx* genes are expressed in nested domains along the developing anteroposterior axis (summarized by Deschamps *et al.*, 1999). The rostral limit of *Cdx1* expression is most anterior, followed sequentially by that of *Cdx2* and *Cdx4*. A similar nested expression pattern of the *caudal* genes has also been observed in *Xenopus* (Pillemer *et al.*, 1998) and chick (Marom *et al.*, 1997), suggesting a conserved role for these genes in the control of anteroposterior identity of the vertebrate axis through individual and overlapping gradients. It is interesting to note that *Cdx1* and *Cdx2* genes also have non-overlapping domains of expression. For example, *Cdx1* is expressed in the somites, limb buds, and the developing mesonephros, while *Cdx2* is expressed in the placenta and the posterior notochord.

1.6.4c The role of caudal-related genes during development

Translational repression of *cad* in the anterior region of the *Drosophila* embryo is performed by the *bicoid* gene product (Rivera-Pomar *et al.*, 1996), and is necessary for proper development of the anterior structures. Ubiquitous expression of *cad* early in embryogenesis leads to defects in head formation and segmentation (Mlodzik *et al.*, 1990). Conversely, loss of maternal *cad* expression results in the deletion and malformation of posterior segments (Macdonald and Struhl, 1986), and loss of zygotic and adult *cad* expression causes an anterior transformation of the tenth abdominal segment. The structures that are normally derived from this segment (anal tuft, parts of anal pads, terminal sense organs) are absent (Macdonald and Struhl, 1986; Moreno and Morata, 1999). Moreover, expression of *cad* in the head and wing discs of the Drosophila larvae results in the formation of ectopic analia structures (Moreno and Morata, 1999). Taken together *cad* appears to have two separate functions; the first is to ensure proper anteroposterior patterning and segmentation of the embryo; and the second is to direct the formation of the posterior-most structures.

The anteroposterior patterning function of *cad* in *Drosophila* appears to have been conserved in at least two of the vertebrate *Cdx* genes. Mice bearing null mutations in *Cdx1* and *Cdx2* have been generated by homologous recombination (Subramanian *et al.*, 1995; Chawengsaksophak *et al.*, 1997). *Cdx1* homozygous null mice survive until adulthood and are fertile. Externally, these mice appear normal however their vertebrae have undergone a series of anterior homeotic transformations. These transformations are most highly penetrant in the cervical region, although additional transformations are also observed in the thoracic region. Despite the specific expression of *Cdx1* in the limb buds and mesonephros no apparent abnormalities are observed in either of these structures.

Cdx2 homozygous null embryos fail to implant, and do not survive past E3.5 (Chawengsaksophak *et al.*, 1997). This is most likely due to a defect in the trophectoderm, where *Cdx2* is first expressed, although this defect has not been characterized. *Cdx2* heterozygotes, on the other hand, are viable and fertile. However, like the *Cdx1* null mice, the *Cdx2* heterozygotes exhibit anterior homeotic transformations of the vertebral column, and also have a shortened and/or kinky tail. The homeotic transformations in the *Cdx2* heterozygous skeletons occur in the posterior cervical vertebrae and the anterior thoracic vertebrae, a region that overlaps, yet is distinctly posterior to that affected in the *Cdx1* homozygous null skeletons. This may reflect their graded levels of expression during development, as *Cdx1* is expressed more anteriorly than *Cdx2*. It is interesting to note that *Cdx2* heterozygous null mice also exhibit AP patterning defects of the intestine (Chawengsaksophak *et al.*, 1997; Beck *et al.*, 1999). Several polyp-like lesions develop in the intestines of $Cdx2^{+/-}$ mice, which are composed of tissues with more anterior characteristics (i.e. stomach and small intestine). As *Cdx2* is expressed specifically in the posterior gut endoderm, it has been proposed that the loss of *Cdx2* leads to a deficiency in posterior specification. Although *Cdx1* is also expressed in the intestine, *Cdx1* null mice do not have any reported intestinal defects.

The generation of a *Cdx4* null mouse has not been reported, however studies of the *Xenopus* homologue (*Xcad3*) suggest that this gene may also have a role in anteroposterior patterning. Similar to that observed in Drosophila, ectopic expression of a highly active form of *Xcad3* inhibits anterior development, while expression of a

dominant-negative *Xcad3* construct results in the loss of trunk and tail structures (Isaacs *et al.*, 1998).

1.6.4d Regulation of Hox gene expression by Cdx proteins

Given the homeotic transformations observed in the vertebral columns of *Cdx1* null skeletons, Subramanian *et al.* (1995) examined the expression patterns of several *Hox* genes. A posterior shift in the expression domain by one somite or one or two prevertebrae was observed for *Hoxd3*, *Hoxa7*, *Hoxc5*, *Hoxc6* and *Hoxc8*. As a null mutation of a particular *Hox* gene typically affects a limited region of the vertebral column, the misregulation of *Hox* genes from several different paralogous groups could account for the series of vertebral homeotic transformations observed in the *Cdx1* null skeletons.

As homeobox-containing genes, the *caudal* family members encode transcription factors. Drosophila *caudal* can directly regulate the transcription of *fushi-tarazu* (Dearolf *et al.*, 1989). In the mammalian intestine, several direct target genes have been identified for *Cdx2/3* (reviewed in Freund *et al.*, 1998). From this information, and *in vitro* binding assays of chick *CdxA* on random oligonucleotides (Margalit *et al.*, 1993), a consensus DNA element (A/CTTTATA/G) recognized by the *caudal* family members has been identified. One or more copies of this element are present in the promoters and/or enhancers of several *Hox* genes (Subramanian *et al.*, 1995). Moreover, expression of *Cdx1 in vitro* is able to induce transcription from a portion of the *Hoxa7* promoter that contains two putative CDX binding sites, and a deletion that includes one of these putative sites reduces this induction by 50% (Subramanian *et al.*, 1995). This region of the promoter is necessary for the correct specification of the anterior limit of *Hoxa7* expression *in vivo* (Knittel *et al.*, 1995). Additionally, ectopic expression of *Cdx* genes result in anteriorized expression of a reporter gene, which is under the control of a portion of the *Hoxb8* promoter that contains several putative CDX-binding sites (Charité *et al.*, 1998). Taken together, these data suggest that CDX may be a direct regulator of endogenous *Hox* gene expression.

1.6.4e Regulation of Cdx expression by retinoic acid

The expression level of *Cdx1* in the embryo is dramatically increased following a short treatment with RA from E7.5-E9.5 (Houle *et al.*, 2000). RA-induction of *Cdx1* has also been observed in F9 cells, and is at least partially dependent on the expression of *RARγ* (Tanjea *et al.*, 1995; Chiba *et al.*, 1997). In the embryo, both endogenous and RA-induced expression of *Cdx1* is dependent on the presence of RARα1 and RARγ (Houle *et al.*, 2000). *RARα1/RARγ* double mutant embryos have much lower than wild type levels of *Cdx1* transcript at E7.5, however a difference can not be detected by E8.5, suggesting that the RARs play a role in the early stage of endogenous *Cdx1* expression. RA-regulation of *Cdx1* is direct as a RARE that is necessary for RA induction in F9 cells has been identified in the mouse and human promoters (Houle *et al.*, 2000). Additionally, RA-treatment negatively affects the transcript levels of *Cdx2* and *Cdx4* in the mouse embryo, (Iulianella *et al.*, 1999; Prinos *et al.*, manuscript in preparation).

1.7 Summary

RA plays a significant role in anteroposterior patterning of the mouse embryo. Some of these roles, such as RA-induced caudal truncations, are mediated specifically by RARγ. In order to identify possible downstream targets of this receptor that may be involved in transducing the teratogenic effect of RA, differential display and suppressive subtractive hybridization approaches were employed. The results of these efforts are described in Chapter 3 of this thesis. These experiments led to the identification of a novel member of the aldo-keto reductase superfamily. The isolation of the corresponding full-length cDNA, and the expression pattern of this gene during development, and in adult tissues, are described in Chapter 4. Finally, *RARγ* and *Cdx1* null mice exhibit similar anterior homeotic transformations of the vertebral column. As RARs are direct regulators of *Cdx1* expression, it was proposed that RARγ may act upstream of CDX1 in vertebral patterning. Chapter 5 describes the generation, and skeletal analysis, of a complete allelic series of *RARγ/Cdx1* mutant mice. Additionally, the role of *Cdx1* in mediating RA-induced posterior transformations and malformations is examined in this Chapter.

Chapter 2

Materials and Methods

2. Materials and Methods

2.1 Animals.

All crosses were maintained on a C57BL/6/SV129 mixed background unless otherwise stated. CD-1 mice (Charles River) were used as additional wild type controls for certain experiments.

2.1a. RARα1 and RARγ null mice.

The generation of mice lacking functional genes for *RARα1* or *RARγ* was previously described (Lohnes *et al.*, 1993; Lufkin *et al.*, 1993). *RARα1γ* double null mice were derived, and maintained with the appropriate crosses.

2.1b. Cdx1 null mice.

The generation of mice lacking a functional *Cdx1* gene was previously described (Subramanian *et al.*, 1995). An allelic series of *RARγ/Cdx1* mutant mice (wild type, $RAR\gamma^{+/-}$, $RAR\gamma^{-/-}$, $Cdx1^{+/-}$, $Cdx1^{-/-}$, $Cdx1^{+/-}RAR\gamma^{+/-}$, $Cdx1^{+/-}RAR\gamma^{-/-}$, $Cdx1^{-/-}RAR\gamma^{+/-}$, and $Cdx1^{-/-}RAR\gamma^{-/-}$) was derived from the appropriate crosses. All of the mice in this allelic series were maintained on the same (C57BL/6/SV129 mixed) background.

2.2. Collection and storage of mouse embryos and fetuses

Mating females were checked daily for evidence of a vaginal plug. Embryos were considered to be E0.5 at noon on the day of plug detection. Female mice were sacrificed by cervical dislocation at the appropriate stage of gestation. For differential display PCR and suppressive subtractive hybridization whole embryos, or caudal portions, were dissected free of maternal tissues in phosphate-buffered saline (PBS), snap frozen on dry ice, and stored at –80°C. Yolk sacs were collected for genotyping where appropriate. For skeletal analysis E18.5 fetuses and newborn mice were collected, euthanized with CO_2, and stored at –20°C until processed. For whole mount *in situ* hybridization, E7.5 to E14.5 embryos were dissected as described above and fixed in 4% paraformaldehyde (PFA) in PBS overnight. Embryos were dehydrated by a graded series of methanol in

PBS and stored in 100% methanol at –20°C. All embryos were used for *in situ* hybridization within 2 months of dissection.

2.3. Isolation of genomic DNA

2.3a. Tail tips and skin samples from fetuses.

Mouse tail samples (approximately 1 to 3 weeks of age), or dorsal skin samples from full-term fetuses, were digested with protease (Sigma) and genomic DNA was isolated using standard phenol:chloroform extraction methods. DNA was resuspended in 500 μl of water and 1 μl was used for genotypic analysis by PCR.

2.3b. Yolk sacs.

Yolk sacs were processed for genotypic analysis as previously described (Hogan *et al.*, 1994). Small pieces of embryonic yolk sac, dissected in PBS, were collected and snap-frozen on dry ice. Yolk sacs were digested in 20 μl of homogenization buffer [0.5 M KCl, 0.1 M Tris-HCl (pH 8.3), 0.1 mg/ml gelatin, 0.45% Nonidet P-40, and 0.45% Tween-20] containing 0.5 mg/ml of proteinase k (GibcoBRL). Digested samples were boiled for 10 minutes and 2 μl of lysate was used for genotypic analysis by PCR.

2.4. Genotypic analysis by PCR

DNA for genotypic analysis was obtained as described in Section 2.3. All PCR reactions were performed in a 25 μl volume containing 200 μm dNTPs, 50 mM KCl, 10 mM Tris-HCl (pH 8.3), 1.5 mM $MgCl_2$, and 2 units of Taq DNA polymerase (GibcoBRL). Wild type and targeted alleles amplified simultaneously required 0.125 μg of each primer specific for the wild type and targeted allele and 0.25 μg of primer common to both alleles. Individually amplified alleles required 0.125 μg of primer specific for either the wild type or targeted allele and 0.125 μg of primer common to both alleles. Amplifications were performed using a DNA Thermal Cycler® (Perkin Elmer) or a Genius® (Techne) PCR machine as described below. PCR products were resolved on a 1.5% agarose gel in the presence of ethidium bromide and visualized by exposure to UV light.

2.4a. Cdx1.

Simultaneous amplification of wild type and targeted alleles of the *Cdx1* locus was accomplished using primers specific for the wild type allele (CA29: 5'-CCCCACAGGTAAAGATCTGG-3'), and the targeted allele (PD129: 5'-GGCCGGAGA ACCTGCGTGCA-3') and a third primer common to both alleles (CA36: 5'-CCCCAAAGGCAGCAGCAGGG-3'). DNA fragments were amplified using the following program: 94°C for 30 seconds; 62°C for 10 seconds; and 72°C for 2 minutes, for a total of 30 cycles. Amplification with CA29 and CA36, or PD129 and CA36, resulted in 342 bp (wild type) and 570 bp (targeted) products, respectively.

2.4b. RARα1.

Wild type and targeted alleles of the *RARα1* isoform were amplified separately using primers BB6 (5'-GTTGGGCTGACCACCCAACC-3') and CA22 (5'-GGGAAAGAAGAAGGCGTAGG-3'), and BB6 and PD129 (Section 2.4a.), respectively. DNA fragments were amplified using the following program: 94°C for 30 seconds; 60°C for 30 seconds; and 72°C for 2 minutes, for a total of 35 cycles. Amplification of the wild type allele generated a 200 bp product, whereas amplification of the targeted allele resulted in a product of 700 bp in size.

2.4c. RARα.

Separate amplification of the wild type and targeted alleles of the *RARα* locus (both isoforms) was accomplished using primers NX21 (5'-ATCGAGACCCAGAGCAG CAG-3') and RB156 (5'CGCTGACCCCATAGTGGTAG-3'), and NX21 and PD129 (Section 2.4a.), respectively. DNA fragments were amplified using the following program: 94°C for 30 seconds; 62°C for 10 seconds; and 72°C for 2 minutes, for a total of 25 cycles. Amplification of the wild type and targeted alleles resulted in products of 150 and 800 bp in size, respectively.

2.4d. RARγ.

Simultaneous amplification of wild type and targeted alleles of the RARγ locus was accomplished using primers specific for the wild type allele (RB155: 5'-CTTCACAGGAGCTGACCCCA-3'), and the targeted allele (PD129; Section 2.4a.) and a primer common to both alleles (RB154: 5'-CAGAGCACCAGCTCGGAGGA-3'). DNA fragments were amplified using the following program: 94°C for 30 seconds; 55°C for 10 seconds; and 72°C for 2 minutes, for a total of 35 cycles. The amplified DNA products were 120 (wild type) and 600 (targeted) bp in size, respectively.

2.5. Retinoic acid treatment of mice

Pregnant female mice were dosed by oral gavage with 10 mg/kg all-*trans*-retinoic acid (RA) (Sigma) at E7.5, or 100 mg/kg all-*trans*-RA at E8.5 or E9.5. RA was dissolved in 10% DMSO with corn oil as a vehicle. Control mice were left untreated. Mice were sacrificed by cervical dislocation after the appropriate length of RA-treatment and embryos or fetuses were collected for *in situ* hybridization, differential display, subtractive hybridization, or skeletal analysis as described in Section 2.2.

2.6 Skeletal preparations

Newborn mouse skeletons were processed and bone and cartilage tissues stained as previously described (Iulianella and Lohnes, 1997). Euthanized mice were skinned, eviscerated, and dehydrated in 95% ethanol. Cartilage was stained overnight with 0.3 mg/ml of alcian blue 8GN in a 4:1 solution of ethanol:glacial acetic acid. Skeletons were soaked in 95% ethanol overnight and cleared with 2% KOH for 4 to 5 hours. Bone was subsequently stained overnight with 0.1% aqueous alizarin red S and decolorized up to 1 week in 20% glycerol/1% KOH. Skeletons were cleared for 1-2 weeks, and stored, in a 1:1 solution of glycerol:ethanol.

2.7 Whole mount *in situ* hybridization

2.7a. Generation of riboprobes.

Sense and anti-sense digoxygenin-labeled riboprobes were synthesized with the appropriate RNA polymerase using 10 μg of plasmid DNA linearized with the

appropriate restriction enzyme as a template. Quantities of riboprobe were estimated by electrophoresis of an aliquot on an agarose gel alongside a standard control. The plasmids used to generate the *Hoxd3*, *Hoxd4* and *Hoxb6* riboprobes were gifts from Drs. Mario Cappechi (University of Utah, Salt Lake City), Mark Featherstone (McGill University, Montreal), and Guy Sauvageau (IRCM, Montreal), respectively. The *Hoxb5* riboprobes were generated from an EST obtained from the IMAGE Consortium, IMAGE number 421728, GenBank accession number AI893993. The *AKR1A4* riboprobes were synthesized from the full-length cDNA obtained from an E8.5 cDNA library.

2.7b. Whole mount in situ hybridization protocol 1.

This protocol was used for all *Hox* riboprobes and certain riboprobes generated from differential display PCR-, and suppressive subtractive hybridization-, isolated clones. Whole mount *in situ* hybridization was performed essentially as described by Wilkinson (1992). Alkaline phosphatase-anti-digoxygenin antibody (Boehringer Mannheim) was diluted 1:4000. The colorimetric reaction was performed in the dark with 0.34 mg/ml 4-nitro blue tetrazolium chloride (NBT) and 0.35 mg/ml x-phosphate/5-bromo-4-chloro-3-indolyl-phosphate (BCIP) in NTMT [0.1 M NaCl, 0.1 M Tris-HCl (pH 9.5), 50 mM $MgCl_2$, and 0.1% Tween-20] for 2 hours to overnight. The color reaction was terminated by several washes with PBT (pH 5.5), and the embryos were stored at 4°C. To clear the embryos, and to reduce background staining, the embryos were dehydrated, and then rehydrated in a graded series of methanol in TBST [0.14 M NaCl, 2.5 mM KCl, 25 mM Tris-HCl (pH 7.5) and 0.1% Tween-20]. After two washes with CMFET (0.14 M NaCl, 2.5 mM KCl, 7.5 mM Na_2HPO_4, 0.9 mM KH_2PO_4, 0.7 mM EDTA, and 0.1% Tween-20) the embryos were incubated in a 1:1 solution of glycerol:CMFET for 2 hours, followed by a 4:1 solution of glycerol:CMFET for 2 hours. The embryos were stored in this solution at 4°C.

2.7c. Whole mount in situ hybridization protocol 2.

Whole mount *in situ* hybridization using riboprobes generated from *AKR1A4* cDNA was performed on E7.5 to E14.5 mouse embryos and E13.5 and E14.5 mouse lungs according to Henrique *et al.*, (1995). Alkaline phosphatase-anti-digoxygenin

antibody was diluted 1:2000. The colorimetric reaction was performed in the dark with 0.225 mg/ml NBT and 0.115 mg/ml BCIP in NTMT for 2 hours to overnight. The reaction was terminated and embryos were cleared as described in Section 2.7b.

2.7d. Sectioning of embryos.

After clearing, embryos were rinsed twice with PBS, and fixed in 4% PFA/0.1% glutaraldehyde in PBS for 30 minutes at 4°C. Embryos were washed twice with PBS, and were dehydrated by a graded series of ethanol in PBS. The embryos were washed twice with 100% ethanol, and incubated for 5 minutes in a 1:1 ethanol:benzene solution. The mixture was replaced with benzene and the embryos were incubated at 60°C for five minutes. The embryos were then incubated in three changes of paraplast at 60°C for 20 minutes each and embedded in the desired orientation. The blocks were sectioned by microtome at 7 μm, and the paraffin wax was removed from the sections by two washes with xylene. The rehydrated sections were counterstained with 1% eosin B, dehydrated in ethanol, incubated in xylene for 5 minutes, and mounted with Permount (Fisher).

2.8. RNA isolation and quantitation

2.8a. Total RNA.

Trizol® reagent (GibcoBRL) was used to isolate total RNA from tissues, cells, and embryos according to the manufacturer's instructions. Individual embryos were homogenized in 0.8 ml Trizol®, whereas cell pellets, tissues, and pooled embryos were homogenized in 1 ml of Trizol®. The RNA pellet was resuspended in an appropriate volume of RNase-free H_2O and stored at –80°C.

2.8b. Poly A^+ RNA.

Poly A^+ RNA was isolated from caudal portions of E8.5 mouse embryos using the QuickPrep™ Micro mRNA Purification Kit (Amersham Pharmacia Biotech, Inc.) according to the manufacturer's instructions. Poly A^+ RNA was stored at –80°C.

2.8c. Quantitation of total RNA from individual embryos.

Mouse liver total RNA was serially diluted 1:2 from 500 ng/μl to 12.5 ng/μl for a total of eight standard samples. One microliter of each standard and two microliters of E8.5 embryo RNA were transferred onto a GeneScreen Plus (NEN Life Sciences Products Inc.) nylon membrane with a slot-blot apparatus according to the manufacturer's instructions (Schleicher and Schuell). The membrane was hybridized in SSC-based buffer (6x SSC, 5x Denhardt's, 0.5% SDS, 80 mg/ml yeast RNA, and 100 μg/ml denatured salmon sperm DNA) at 65°C with a randomly labeled cDNA fragment encoding 18S RNA (prepared with ^{32}P-α-dCTP, Oligolabelling Kit, Amersham Pharmacia Biotech, Inc.). Membranes were washed at 65°C to a final stringency of 0.2x SSC/0.1% SDS and exposed to X-Omat™ autoradiographic film (Kodak) for 16-24 hours. Portions of the membrane corresponding to RNA standards and samples were excised with a scalpel and radioactivity quantitated using a scintillation counter. The amount of embryo RNA was extrapolated from a standard curve constructed from the liver RNA values.

2.9. Differential display polymerase chain reaction (DD-PCR)

Differential display was performed as described by Liang and Pardee (1992), with minor modifications. In brief, 0.5 μg of total RNA was combined with 0.5 μg of T_{11}MN oligonucleotide primer (where M is either A, C, or G, and N is either A, C, G or T), 10 μM dNTPs, 10 mM DTT, 1x First Strand Synthesis Buffer (GibcoBRL), and 36 units of RNase inhibitor (Amersham Pharmacia Biotech Inc.) in a total volume of 20 μl. MMLV-reverse trancriptase (300 units, GibcoBRL) was added to the reaction mix following a two minute pre-incubation at 37°C. Reverse transcription was allowed to proceed for 1 hour, and was terminated by heating to 95°C for 5 minutes. PCR amplification was performed using 2 μl of the reverse transcription reaction, 6.25 μCi ^{35}S-dATP (Amersham Pharmacia Biotech Inc.), 1 μm dNTPs, 0.22 μg of T_{11}MN reverse primer, 0.16 μg of random decamer oligonucleotide, 1x PCR buffer [50 mM KCl, 10 mM Tris-HCl (pH 8.3), 1 mM $MgCl_2$] and 2 units of Taq DNA polymerase (GibcoBRL) in a final volume of 20 μl. cDNA fragments were amplified using the following PCR program:

94°C for 30 seconds, 41°C for 2 minutes, and 72°C for 30 seconds, for 40 cycles. The last cycle was followed by an additional 10 minute incubation at 72°C to extend the cDNA fragments. Four microliters of PCR products were resolved on a denaturing polyacrylamide gel (6% polyacrylamide/50% urea), dried, and exposed to XOmat™ autoradiographic film (Kodak) for 72 hours. Gel areas corresponding to differentially expressed bands were excised with a scalpel and re-hydrated in 10 μl of water. DNA was eluted from the acrylamide gel by boiling for 10 minutes. Two microliters of the cDNA eluent were re-amplified by PCR as described above, with an increased dNTP concentration (10 μM) and omission of ^{35}S-dATP. Reverse Northern analysis (Section 2.15) {Chalifour *et al.*, 1994) was used to screen amplified PCR products for true positives. Positive PCR products were ligated into the pGEM®-T vector (Promega) according to the manufacturer's instructions. *E.coli* was transformed with the ligated DNA by electroporation, and plasmid DNA was isolated using standard alkali lysis techniques, Qiagen-tip 500 columns, or the Concert™ Rapid Plasmid Miniprep System (GibcoBRL) according to the manufacturer's directions. Clones of interest were end-sequenced using the T7 Sequencing™ Kit (Amersham Pharmacia Biotech Inc.) or by automated sequencing.

2.10. Suppressive subtractive hybridization

Poly A^+ RNA was isolated from 131 untreated (driver), and 119 RA-treated (tester), caudal embryo pieces as described in Section 2.8b. PCR amplified representative cDNA was synthesized from 0.5 μg of poly A^+ RNA using the SMART™ PCR cDNA Synthesis Kit (Clontech) according to the manufacturer's instructions. The amplified cDNA was used as starting material for the Clontech PCR-Select™ cDNA Subtraction Kit. The subtraction and subsequent PCR amplification were carried out according to the manufacturer's instructions. Virtual northern blots were used to assess the efficiency of the subtraction (Section 2.11). Subtracted cDNA fragments were randomly cloned into the pGEM® TA-cloning vector as described in Section 2.9 and screened for true RA-regulation by reverse northern analysis (Section 2.12). Positive clones were sequenced as described in Section 2.9.

2.11. Virtual northern blots

Two hundred micrograms of cDNA (unsubtracted tester, unsubtracted driver, and subtracted) generated by the suppressive subtractive hybridization protocol (Section 2.10) were run on a 1.5% agarose gel. The cDNA was denatured by two washes of 45 minutes each in 0.5 M NaOH, and was transferred onto Hybond N^+ nylon membrane overnight. The membrane was neutralized with 6x SSC and hybridized with ^{32}P-dCTP-labelled cDNA fragments. The cDNA probes used to confirm efficient subtraction included *Brachyury*, *Cdx1*, *P450RAI,* and *β-actin.* The cDNA fragments were released from the vector by the appropriate restriction enzyme digestions, resolved on an agarose gel, and purified using the Concert™ Matrix gel extraction system (GibcoBRL) according to the manufacturer's instructions. Five hundred nanograms of the cDNA fragment were labeled with 30 μCi of ^{32}P-α-dCTP by random priming (Amersham Pharmacia Inc.). The membranes were hybridized overnight with approximately $1x10^6$ c.p.m./ml of the labeled cDNA in formamide-based buffer [40% deionized formamide, 0.9 M NaCl, 50 mM sodium phosphate buffer (pH 6.5), 2 mM EDTA, 4x Denhardt's, and 1% SDS] at 42°C. The membranes were washed as described in Section 2.8c and exposed to XOmat™ autoradiographic film (Kodak) for 1 to 3 days.

2.12. Reverse northern blots

2.12a. Reverse northern; Slot blots.

Ten microliters of PCR product, or plasmid DNA containing the sub-cloned PCR product as an insert, were transferred in duplicate onto GeneScreen Plus nylon membranes using a slot-blot apparatus according to the manufacturer's instructions. The membranes were hybridized in a formamide-based buffer (Section 2.11), at 42°C, with $1x10^6$ c.p.m./ml of ^{32}P-α-dCTP labeled cDNA generated from either untreated, or RA-treated, embryos as follows: 3 μg of pooled-embryo RNA (Section 2.8a), in a total volume of 12 μl, was denatured at 70°C and placed on ice. The RNA was reverse transcribed with 300 units of MMLV-reverse transcriptase in a mixture of 1x First Strand Buffer, 10 mM DTT, 0.5 mM dNTPs, and 18 units of RNAguard™ RNase inhibitor, at 37°C for 1 hour. One half of the reverse transcription reaction was labeled with 50 μCi of ^{32}P-α-dCTP as described in Section 2.8c, except the reaction was incubated at 37°C

for 4 hours. The membranes were washed as described in Section 2.8c and exposed to autoradiographic film. The signal intensities from membranes hybridized with the untreated cDNA probe were compared to those from membranes hybridized with the RA-treated cDNA probe in order to identify RA-regulated clones.

2.12b. Reverse northern; Agarose gels.

Rsa I-digested plasmid DNA was resolved on a 1.5% agarose gel, in duplicate. The DNA was denatured, and transferred to Hybond N^+ nylon membranes as described in Section 2.11. One microgram of amplified cDNA generated from either untreated, or RA-treated, caudal embryo portions (Section 2.10) was labeled with ^{32}P-dCTP, the membranes hybridized, washed, and signal detected as described in Section 2.12a.

2.13. Northern blots

Fifteen micrograms of total RNA were resolved on a denaturing gel (1.85% deionized formaldehyde, 1x MOPS) and transferred to GeneScreen Plus (NEN Life Sciences Products Inc.) nylon membranes with 10x SSC overnight. RNA was fixed to the membrane by baking at 80°C for 2 hours under vacuum. The blots were hybridized overnight with approximately 10^6cpm/ml of ^{32}P-α-dCTP labeled cDNA in formamide-based buffer (Section 2.11) at 42°C. Loading of RNA was normalized by hybridization at 42°C with an 18S ribosomal RNA oligonucleotide probe (5'-ACGGTATCTGATCGTCTTCGAACC-3') in SSC-based buffer (Section 2.8.c.). Membranes were washed as described in Section 2.11, except membranes hybridized with the 18S oligonucleotide probe were washed at 37°C. Blots were exposed to autoradiographic film for 1 to 10 days (cDNA probes) or 1 to 10 minutes (18S oligonucleotide probe).

2.14. Library plating and screening

A mouse E8.5 cDNA library in λZAP II phage arms (a gift from Dr. Brigid Hogan) was used to isolate cDNA molecules homologous to differential display PCR products. A total of $2x10^5$ phage in 300 μl of SM buffer were combined with an equal

volume of Y1090 *E.coli* plating bacteria and incubated without shaking at 37°C for 20 minutes. Ten milliliters of molten 0.7% top agarose was added and the mixture plated onto LB agar in 150-mm petri dishes. Twenty plates were prepared in this manner and incubated overnight at 37°C to produce a total of $1x10^6$ bacteriophage plaques. Phage DNA was transferred onto supported nitrocellulose membranes (Hybond™-C extra), in duplicate, according to the manufacturer's instructions. DNA was fixed to the membrane by baking at 80°C for 2 hours under vacuum. Membranes were hybridized with $1x10^6$ c.p.m./ml of ^{32}P-α-dCTP labeled DC43 cDNA in an SSC-based buffer (Section 2.8c.) at 65°C overnight. The membranes were washed as described in Section 2.11 and exposed to autoradiographic film for 3 days. Positive plaques were picked and bacteriophage were eluted in 1 ml of SM buffer containing 1 drop of chloroform. The bacteriophage eluent was serially diluted (10-fold), plated onto LB agar in 100-mm petri dishes, and DNA was transferred onto nitrocellulose membranes, fixed, and hybridized as described above. Serial dilutions and hybridizations were repeated until single plaques containing positive clones were isolated, usually a total of three times. pBluescript SK^- plasmids containing the cDNA insert of interest were isolated by *in vivo* excision (Section 2.15).

2.15. *In vivo* excision

In vivo excision was performed using the Uni-Zap™ XR Cloning Kit (Stratagene) in order to isolate pBluescript SK^- plasmid DNA (containing the cDNA insert of interest) from λZAP II phage DNA. Minor modifications were made to the manufacturer's protocol and are described below. Single plaques (see Section 2.14) were picked and phage allowed to diffuse from the agar for 48 hours in 250 μl of SM buffer at 4°C. Two hundred microliters of eluted phage were combined with 200 μl of XL1-Blue *E.coli* ($O.D._{600}$ = 1, resuspended in 10 mM $MgSO_4$) and 1 μl R408 helper phage (~$1x\ 10^5$ pfu) in a 50 ml conical tube and incubated without shaking at 37°C for 15 minutes. Three milliliters of 2x YT media (90 mM NaCl, 16 g/l bacto-tryptone, and 10 g/l bacto-yeast extract) were added and the tube was incubated at 37°C overnight with shaking. The culture was heated to 70°C for 20 minutes and centrifuged at 3000 r.p.m. for 5 minutes. The supernatant was decanted into a sterile tube and stored at 4°C. Various amounts (10, 20, 50 and 200 μl) of supernatant were combined with 200 μl XL1-Blue *E.coli* bacteria

and the mixture was incubated at 37°C for 15 minutes. Three hundred microliters of LB broth (0.17 M NaCl, 10 g/l bacto-tryptone, and 5 g/l bacto-yeast extract) were added and the cultures were incubated at 37°C with shaking for 45 minutes. Two hundred microliters were plated onto LB agar containing 50 μg/ml ampicillin, in 100-mm petri dishes, and incubated at 37°C overnight. Single colonies were picked and cultured overnight in 2 ml of LB broth. The pBluescript SK^- plasmid containing the cDNA insert of interest was isolated from single colonies by standard alkali lysis methods. Sequencing was as described in Section 2.9.

2.16. Culture of established cell lines

2.16a. F9 cells.

Wild type F9 teratocarcinoma cells were grown in gelatinized 10-cm tissue culture dishes (Nunc) in Dulbecco's Modified Eagle Medium (D-MEM, GibcoBRL) supplemented with 10% heat-inactivated fetal bovine serum, 100 units/ml penicillin, 100 μg/ml streptomycin, 10 μg/ml gentamicin, 2 mM glutamine and 20 μM sodium pyruvate. F9 teratocarcinoma cells stably transfected with the Sil-REM/β-gal-Neo construct (Wagner *et al.*, 1992) were grown in the above media except 15% heat-inactivated fetal bovine serum was included and G418 was added. The cells were incubated at 37°C in the presence of 5% CO_2 and passed at a ratio of 1:20 when confluent.

2.16b. P19 cells.

P19 embryocarcinoma cells were grown in 10-cm tissue culture dishes in Minimal Essential Medium (MEM) α Medium (GibcoBRL) supplemented with 10% heat-inactivated fetal bovine serum, 100 units/ml penicillin, and 100 μg/ml streptomycin. Cells were incubated at 37°C in the presence of 5% CO_2 and were passed at a ratio of 1:20 when confluent.

2.17 Retinoid preparation and treatment of mammalian cells

Retinoic acid, retinaldehyde, and retinol (retinoids) were prepared, under reduced light, as 10^{-2} M stocks in DMSO and stored at –20°C. At the time of treatment, the retinoid was diluted to the appropriate concentration in tissue culture media and added

immediately to the cells. For time course studies, all cells were treated with the retinoid simultaneously and were harvested at specific time points thereafter. Cells treated with DMSO as a control were harvested at the same time as the cells with the longest retinoid treatment. For dose response studies, all cells were treated simultaneously with different concentrations of the retinoid, ranging from 10^{-5} to 10^{-10} M, and were harvested 24 hours later. Control cells were treated for the same amount of time with a 1/1000 dilution of DMSO (equivalent to the amount found in 10^{-5} M of retinoid).

2.18. Transfection of DNA into mammalian cells

2.18a. Transient transfections.

Cells were transfected with 30 μg of plasmid DNA by calcium phosphate precipitation. The transfected cells were then subjected to time course and dose response experiments with the retinoids (Section 2.17). After the appropriate treatments, the levels of β-galactosidase activity were measured (Section 2.19) and corrected for protein concentration (Section 2.20).

2.18b. Stable transfections.

The full-length *AKR1A4* cDNA was directionally cloned (HindIII/PstI) into a modified pSG5 eukaryotic expression vector (Green *et al.*, 1988). F9-RARE-β-gal reporter cells (60-70% confluent) were electroporated (0.25 V, 0.4 cm electrode gap) in the presence of 5 μg of the linearized (XbaI) *AKR1A4*/pSG5 construct, and 50 μg of a plasmid conferring puromycin resistance (pD503), linearized with HindIII. As a negative control, the cells were electroporated with 5 μg of pSG5 vector alone, and 50 μg of pD503. After electroporation, the cells were plated into two 100-mm tissue culture dishes. Puromycin was added to the media after 1-2 days, in order to select for pD503 transfected clones. Following one week of selection, the puromycin-resistant clones were pooled, plated in 96-well cluster plates and subjected to time course and dose response experiments with retinoids (Section 2.17). After the appropriate treatments, the levels of β-galactosidase activity were measured (Section 2.19) and corrected for protein concentration (Section 2.20).

2.19 β-galactosidase assays

F9 cells stably transfected with the SIL 15.4 RARE-β-galactosidase reporter construct (Wagner *et al.*, 1992) were used to assess the potential effect of AKR1A4 on the vitamin A metabolic pathway. Following transfections (Section 2.18), and/or retinoid-treatment (Section 2.17), cells plated in 96-well cluster plates were washed twice with ice-cold PBS and fixed in 50 μl of ice-cold 4% PFA in PBS for 10 minutes. Following fixation, the cells were rinsed twice with PBS and 100 μl of β-galactosidase buffer (23 nM NaH_2PO_4, 77 nM Na_2HPO_4, 0.1 mM $MnCl_2$, 2 mM $MgSO_4$, 40 mM β-mercaptoethanol) was added to each well. Following a 10 minute incubation at 37°C, 25 μl of 4 mg/ml o-Nitrophenyl β-D-Galactopyranoside (ONPG) (pre-warmed to 37°C) were added to each well, the solutions mixed, and the reaction allowed to proceed at 37°C. Following the colorimetric reaction the supernatant was transferred to a new 96-well cluster plate and the absorbance read at a wavelength of 405 nm. All values were corrected for amount of protein (Section 2.20)

2.20. Protein assays

The concentration of protein in cell lysates was determined using the Bio-Rad *DC* Protein Assay according to the manufacturer's instructions. Protein concentrations were used to correct the values obtained from the β-galactosidase assays (Section 2.19).

Chapter 3

Identification of retinoic acid regulated genes in the mouse embryo by differential display and suppression subtractive hybridization

3.1 Abstract

Vitamin A and its derivatives, collectively termed retinoids, are potent teratogens in both animal models and the human population. At E8.5, pregnant mice administered a dose of 100mg/kg of retinoic acid give rise to offspring that uniformly exhibit severe caudal truncation of the vertebral column, accompanied by spina bifida. In contrast, RARγ, but not RARβ or RARα, homozygous null embryos are completely resistant to this teratogenic insult, suggesting that this receptor specifically mediates the RA-induced caudal malformations. The identification of RARγ target genes involved in this process was approached using two techniques, namely differential display PCR and suppression subtractive hybridization. The optimization of these techniques for use with mouse embryos is presented, along with a preliminary characterization of several candidate RA-regulated cDNA fragments. Homology searches identified three genes corresponding to RA-regulated fragments: TI-227; a novel gene (DC16); and NADH dehydrogenase subunit 6. The possible roles of these genes in RA-induced caudal truncation and spina bifida are discussed.

3.2 Introduction

Vitamin A and its metabolic derivatives (retinoids) are potent teratogens when present in excess during embryonic development. Various congenital abnormalities, including malformations of the limbs, craniofacial features, neural tube, and heart, are induced by retinoids in the human population and in animal models (reviewed by Ross *et al.*, 2000). In the mouse, two such RA-induced defects: 1) limb malformations and 2) caudal truncation of the anterior-posterior axis coupled with spina bifida do not occur if RXRα or RARγ, respectively, are non-functional (Lohnes *et al.*, 1993; Sucov *et al.*, 1995). There are no reports that targeted disruption of any of the remaining *RAR* or *RXR* genes confers resistance to the effects of exogenous RA. Therefore, although certain receptors are functionally redundant in some instances, as demonstrated by the phenotypes of compound *RAR* and *RXR* null mutations, other pharmacological events can be mediated by only one receptor type (Kastner *et al.*, 1997). Whether this is due to the specific recognition of a RA response element in the promoter of target genes by distinct RAR/RXR heterodimers, or tissue restricted expression of either the receptors themselves or transcriptional co-activators, is not yet clear. Regardless of how this differential control is established, it is apparent that the expression levels of RXRα or RARγ target genes that mediate the RA-induced malformations must not be influenced by RA-excess in the absence of these receptors. Therefore, it follows that the mRNA levels of genes implicated in the formation of these defects would be different in RA-treated wild type embryos compared to RA-treated receptor null embryos.

Several techniques have been developed that allow the identification of genes that contain different sequences, or are differentially expressed between various tissue types, or are differentially affected by exogenous treatments or genetic alterations. These include differential display PCR (DD-PCR; Liang and Pardee, 1993), subtractive hybridization (Welcher *et al.*, 1986), suppression subtractive hybridization (SSH; Diatchenko *et al.*, 1996), serial analysis of gene expression (SAGE; Velculescu *et al.*, 1995), representational difference analysis (RDA; Lisitsyn *et al.*, 1993), and DNA arrays (Chalifour *et al.*, 1994). Each of these techniques offers slight variations that may be more relevant to the particular question being addressed. For example, DD-PCR allows

the comparison of a profile of gene expression across several different samples, while subtractive hybridization restricts the comparison to only two samples at a time.

In this chapter, the use of both DD-PCR and SSH to identify RA-regulated genes will be described. The RA-induced caudal truncation and accompanying spina bifida phenotype elicited in wild type, but not *RARγ* null, embryos was used as a model. This model is advantageous in that it allows not only the identification of RA-responsive genes, but also genes that may be regulated by a specific RAR. Moreover, RARγ target genes isolated in this manner may potentially be involved in eliciting RA-induced malformations. As neural tube defects (including spina bifida) occur quite frequently in the human population, identification of genes involved in this process would be beneficial with respect to prevention, early diagnosis, and potential *in utero* treatment of these birth defects.

In the first stage of this project DD-PCR was used to compare gene expression levels between four different groups of embryos: 1) untreated wild type, 2) RA-treated wild type, 3) RA-treated *RARα1* null, and 4) RA-treated *RARα1γ* double null. It was hypothesized that the expression of a gene implicated in RA-induced caudal truncation would be altered (increased or decreased) in wild type treated embryos compared to untreated controls. This hypothetical gene would also respond in RA-treated *RARα1* null embryos, which are susceptible to treatment, but not in resistant *RARα1γ* double mutants.

The second stage of this project utilized a more restricted approach to the identification of genes involved in RA-induced caudal malformations. Suppression subtractive hybridization (SSH) was used to study RA-regulation of genes expressed in the caudal portion (all tissues posterior to the last formed somite) of E8.5 embryos. By restricting the tissue used in the analysis to that known to be directly affected by RA treatment (Iulianella *et al.*, 1999), it was hypothesized that a higher proportion of the RA-regulated genes identified may be involved in eliciting caudal defects. As subtractive hybridization restricts the comparison of gene expression to two populations, only wild type embryos (control and RA-treated) were examined.

3.3. Results

3.3a Differential display PCR (DD-PCR)

The differential display PCR (DD-PCR) technique, used to identify genes that are diferentially expressed between two samples, was first described by Liang and Pardee (1992). In brief, RNA is isolated from tissues or cells of interest and cDNA is synthesized by reverse transcription using one of twelve different oligonucleotides as a primer (Reverse primers; Table 3.1). These primers are composed of eleven dTTP nucleotides followed by two anchoring nucleotides at the 3' end, designated M and N, where M is dATP, dCTP, or dGTP, and N is dATP, dCTP, dGTP or dTTP, for a total of 12 possible primers. ^{35}S-dATP-labeled fragments are generated by PCR amplification of the cDNA using a given reverse primer in combination with one random decamer (Table 3.1), resolved on a polyacrlyamide gel, and visualized by exposure to autoradiagraphic film. Bands corresponding to differentially expressed fragments can be excised from the gel and re-amplified using the same set of primers for further analysis.

3.3b. Application of DD-PCR to mouse embryos

Prior to the initiation of this project DD-PCR had only been described using RNA from adult tissues or cell lines, and typically employed 2 μg of RNA for reverse transcription, an amount not attainable from an individual E8.5 mouse embryo. Additionally, standard methods for isolation of high quality RNA (i.e. CsCl gradient) are not applicable to tissues of this size. Pooling several embryos would alleviate these problems, however, slight differences in developmental stage may skew the representation of certain transcripts. Hence, diminishing quantities of RNAisolated from mouse skin by two different procedures, CsCl gradient and Trizol®, were compared to determine whether significant differences in DD-PCR-generated patterns would occur. DD-PCR was performed with one reverse primer in combination with one of five different random primers using RNA isolated by either technique (Figure 3.1A). Each primer pair generated a unique pattern of cDNA fragments that was essentially identical using RNA isolated by either method (compare lanes 1 through 5 to lanes 6 through 10). Nearly identical results were obtained using 1, 0.5, or 0.25 μg of RNA (Figure 3.1B; compare lanes 1, 2 and 3, or lanes 7, 8, and 9). Note that additional PCR products, not

Table 3.1. Differential display PCR primer sequences

Reverse Primers

DD1	5′ TTTTTTTTTTTAA 3′
DD2	5′ TTTTTTTTTTTAC 3′
DD3	5′ TTTTTTTTTTTAG 3′
DD4	5′ TTTTTTTTTTTAT 3′
DD5	5′ TTTTTTTTTTTCA 3′
DD6	5′ TTTTTTTTTTTCC 3′
DD7	5′ TTTTTTTTTTTCG 3′
DD8	5′ TTTTTTTTTTTCT 3′
DD9	5′ TTTTTTTTTTTGA 3′
DD10	5′ TTTTTTTTTTTGC 3′
DD11	5′ TTTTTTTTTTTGG 3′
DD12	5′ TTTTTTTTTTTGT 3′

Random Primers

DD13	5′ ACTGATGCAG 3′
DD14	5′ CGTGCTATTC 3′
DD15	5′ ACGTCTGACA 3′
DD16	5′ TTCGGACCAT 3′
DD17	5′ GTCAGACTAC 3′
DD18	5′ GCTAGTCACA 3′
DD19	5′ TCAAGGTAGC 3′
DD20	5′ CTCATGACTG 3′
DD21	5′ ACTTGCAGGT 3′
DD22	5′ CTTCTTCGAG 3′
DD23	5′ TAGCGATACC 3′
DD24	5′ CTCATATCGG 3′
DD25	5′ GTTCCATGTC 3′
DD26	5′ AGATGTGGAG 3′
DD27	5′ AAGTCTTCCG 3′
DD28	5′ CTTCTACCGT 3′
DD29	5′ TCAACTGCGA 3′
DD30	5′ GCAGCATCAT 3′
DD31	5′ ACGCATGTTC 3′
DD32	5′ CCTGGTCCAT 3′

Figure 3.1. Analysis of DD-PCR results obtained by decreasing quantities of starting material and number of PCR cycles. (**A**) DD-PCR was performed as described (above text and Chapter 2, Section 2.9) using RNA isolated from mouse skin by CsCl gradient or Trizol®. Two micrograms of RNA were reverse transcribed with DD6 (see Table 3.1 for primer sequences) and amplified by PCR for a total of 50 cycles with DD6 and either DD13 (lanes 1 and 6), DD14 (lanes 2 and 7), DD15 (lanes 3 and 8), DD16 (lanes 4 and 9), or DD17 (lanes 5 and 10). Comparison of samples revealed only minor differences between the patterns of cDNA fragments produced for a given primer pair, irrespective of the means of RNA isolation (**B**) DD-PCR was performed using different amounts of RNA isolated from mouse skin (Trizol) and 40 (lanes 1 to 6) or 50 cycles (lanes 7 to 12) of PCR amplification. Lanes 1-3 and 7-9: Varying amounts of input RNA (lanes 1 and 7: 1 μg; lanes 2 and 8, 0.5 μg; lanes 3 and 9, 0.25 μg). All reverse transcription reactions were performed with DD6 and PCR amplifications were performed with DD6 and DD13. Lanes 4 and 10: use of oligo (dT) primer with only one anchoring nucleotide instead of two ($T_{11}G$). Lanes 5 and 11: PCR amplification of no-reverse transcriptase control reaction. Lanes 6 and 12: PCR reactions with only the random decamer (DD13).

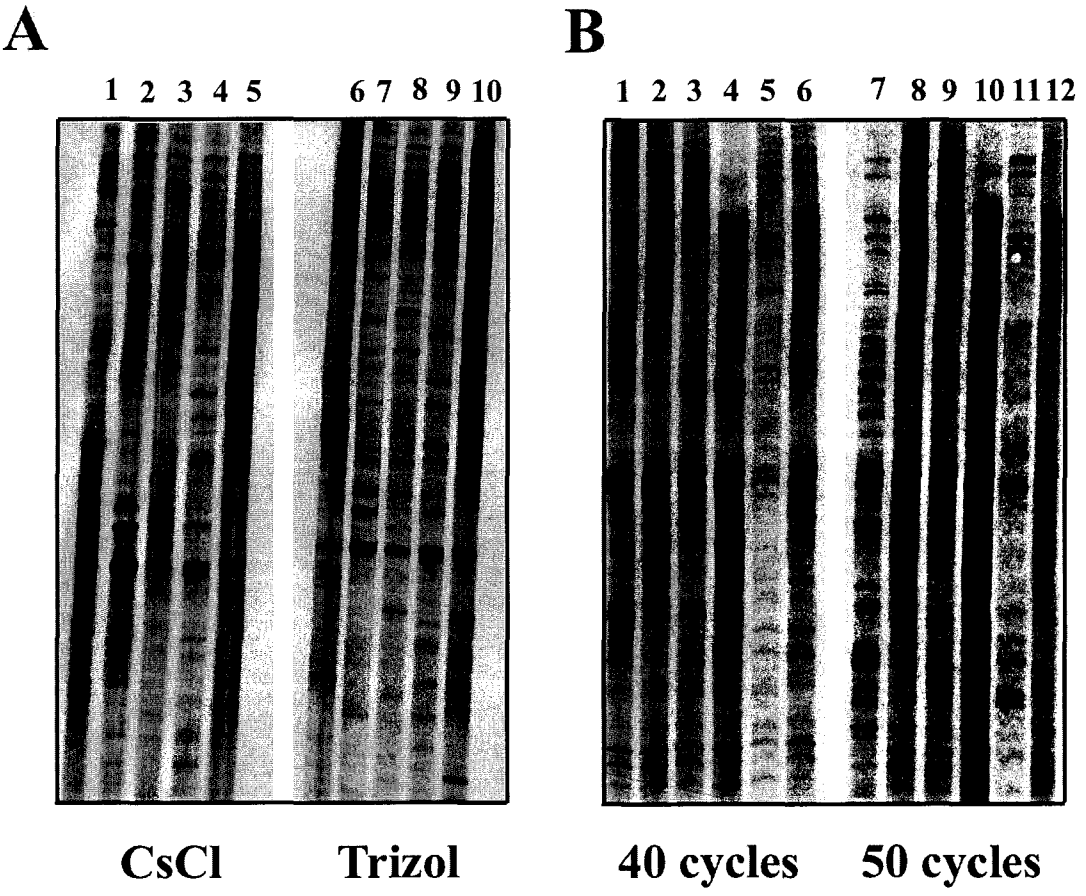
A
1 2 3 4 5 6 7 8 9 10
B
1 2 3 4 5 6 7 8 9 10 11 12
CsCl
Trizol
40 cycles
50 cycles

present under any other condition, appeared when 1 μg of RNA was used and the cDNA was amplified for 50 cycles (Figure 3.1B, lane 6). This may be due to over-amplification, and therefore may no longer be representative of the endogenous mRNA levels. From these results it was concluded that 0.5 μg of input RNA, and 40 cycles of PCR amplification was optimal.

The contribution of each primer to the amplification of a particular set of cDNA fragments was also tested by using a reverse primer that had only one anchoring nucleotide ($T_{11}G$) instead of two. As expected, the number of cDNA fragments generated increased when the $T_{11}G$ primer was used (Figure 3.1B, lanes 4 and 10). Although more cDNA fragments could be analyzed per gel using such primers, the complexity of the pattern precluded clear interpretation of expression levels. Intriguingly, when only the random decamer was used in the PCR reaction, several cDNA fragments were generated (Figure 3.1B; lanes 6 and 12). Many of these bands were identical to those produced when both primers were present in the PCR reaction, indicating that a significant portion of the cDNA fragments were generated solely from these decamers. The few bands produced from controls that did not contain reverse transcriptase (Figure 3.1B; lanes 5 and 10), are most likely a result of contaminating DNA.

In order to quantitate the amount of RNA isolated from individual embryos it was necessary to use a method other than spectrophotometry as the quantity of RNA obtained was typically below the limits of detection. To this end, a series of serially diluted mouse liver RNA samples and aliquots of RNA from mouse embryos were immobilized, in duplicate, on a nylon membrane using a slot blot apparatus and hybridized with ^{32}P-labeled 18s RNA cDNA. A representitive autoradiograph is shown in Figure 3.2. A standard curve was constructed from the liver RNA values and the amount of embryo RNA was extrapolated. In general, a single E8.5 embryo yielded 0.1 to 4.5 μg of total RNA, with a mean of 1.3 μg (50 samples).

For a given experiment, duplicate samples from each embryo group (untreated wild type, RA-treated wild type, RA-treated *RARα1* null, and RA-treated *RARα1γ* double null) was subjected to DD-PCR for a total of eight samples. Embryos were stage-matched based on somite number in order to reduce differences related to developmental

stage. Pregnant females were orally gavaged with RA in the morning of E8 and were sacrificed six hours post-treatment. This relatively short length of treatment was used as an attempt to identify genes that exhibit a rapid response to RA-treatment. Ideally, many of these genes would be direct RAR targets. Further details describing the collection of embryos can be found in Chapter 2, Section 2.2.

3.3c. Identification of differentially amplified cDNA fragments

A complete list of differentially amplified cDNA candidates isolated from E8.5 mouse embryos, and the primers used, can be found in Table 3.2. The generation of these candidates was acccomplished using three reverse primers (DD7, DD10 and DD11) and twenty random decamers (DD13 – DD32) for a total of sixty different combinations. By comparing the relative intensity of the cDNA bands generated from the different groups of mouse embryos a total of one-hundred-and-seven differentially amplified candidates were identified. Table 3.3 provides a summary of the types, and representation, of cDNA patterns observed. It should be noted that fourteen of the differentially amplified bands were identified by comparison of only RA-treated wild type to RA-treated *RARα1γ* double null samples (DC29 to DC42, marked with a number sign in Table 3.2). These candidates were not included in the summary of cDNA amplification patterns (Table 3.3).

Only 39% of the candidate fragments displayed differential amplification in RA-treated wild type samples as compared to untreated control samples. In particular, nine of these candidates exhibited a pattern characteristic of a gene that might be involved in RA-induced caudal truncation (marked with an asterisk in Table 3.2). The levels of amplified cDNA of the remaining 61% of the candidates were altered only in the RA-treated *RAR* mutant samples. As these candidates were not likely to be involved in RA-induced malformations, the characterization of this category was not pursued.

It is important to note that although the differential levels of amplificaiton of certain cDNA fragments may correlate with RA-treatment and/or loss of a particular RAR, this is not evidence that the genes corresponding to these fragments are actually regulated by these factors *in vivo*. Several explanations could account for differential amplification of a cDNA fragment, other than differential expression, including slight differences in the quantity of input cDNA, or preferential amplification of a particular

Figure 3.2. Quantitation of RNA isolated from individual embryos. A standard curve was prepared in duplicate from total RNA isolated from mouse liver. One-tenth of the RNA isolated from four individual E8.5 mouse embryos was loaded, in duplicate, alongside the standard samples, and the membrane was hybridized with a ^{32}P-labeled 18s RNA cDNA probe. The amount of RNA isolated from individual embryos was extrapolated from a standard curve constructed using c.p.m. values obtained from the liver samples (not shown).

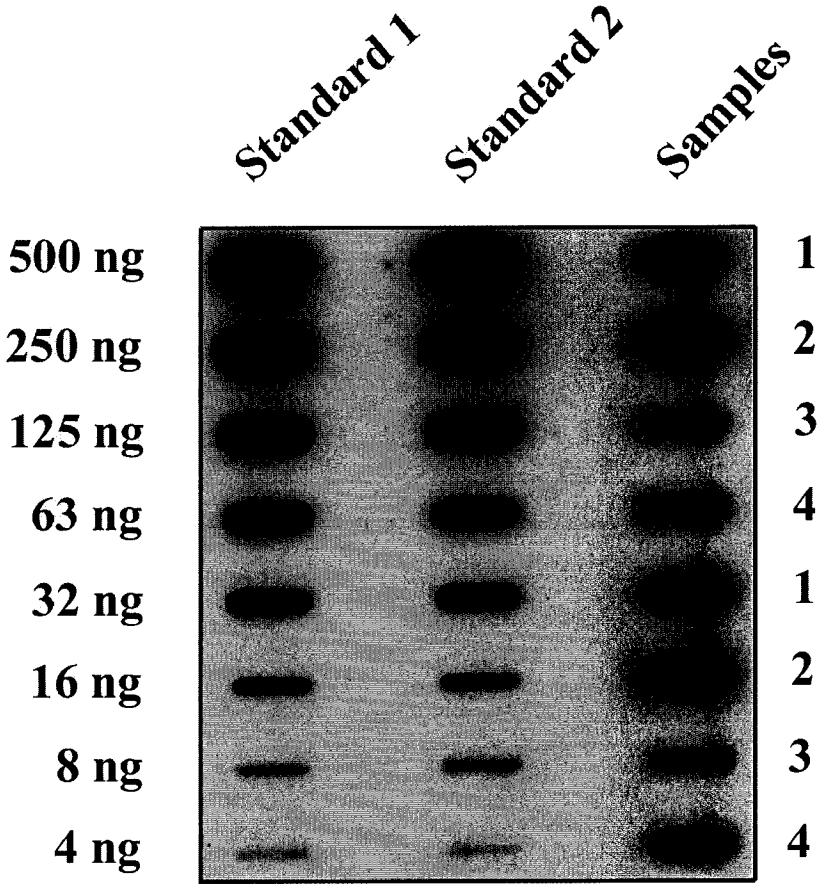
Standard 1
Standard 2
Samples
500 ng
250 ng
125 ng
63 ng
32 ng
16 ng
8 ng
4 ng
1
2
3
4
1
2
3
4

Table 3.2. cDNA fragments identified by DD-PCR

Differential Clone	Reverse Primer	Random Primer	Expression Pattern
DC1	DD10	DD16	Up in WT TR and $\alpha1^{-/-}$ TR *
DC2	DD10	DD16	Up in WT TR and $\alpha1^{-/-}$ TR *
DC3	DD10	DD16	Up in WT TR and $\alpha1^{-/-}$ TR *
DC4	DD10	DD16	Up in DM TR
DC5	DD10	DD16	Up in WT TR
DC6	DD10	DD16	Up in $\alpha1^{-/-}$
DC7	DD10	DD14	Down In DM TR
DC8	DD10	DD14	Down in DM TR
DC9	DD10	DD19	Down in WT TR, $\alpha1^{-/-}$ TR and DM TR
DC10	DD10	DD18	Down in DM TR
DC11	DD10	DD18	Up in WT TR
DC12	DD10	DD23	Down in WT TR
DC13	DD10	DD22	Up in WT TR
DC14	DD10	DD22	Down in WT TR
DC15	DD10	DD26	Up in WT TR
DC16	DD10	DD25	Up in WT TR and $\alpha1^{-/-}$ TR *
DC17	DD10	DD31	Up in WT TR, $\alpha1^{-/-}$ TR and DM TR
DC18	DD10	DD32	Down in WT TR and $\alpha1^{-/-}$ TR*
DC19	DD10	DD29	Down in DM TR
DC20	DD10	DD28	Up in $\alpha1^{-/-}$ TR and DM TR
DC21	DD10	DD28	Down in $\alpha1^{-/-}$ TR and DM TR
DC22	DD10	DD27	Down in $\alpha1^{-/-}$ TR
DC23	DD10	DD27	Up in $\alpha1^{-/-}$ TR
DC24	DD11	DD16	Up in WT TR
DC25	DD11	DD16	Up in DM TR
DC26	DD11	DD17	Down in WT TR, $\alpha1^{-/-}$ TR and DM TR
DC27	DD11	DD14	Down in WT TR, $\alpha1^{-/-}$ TR and DM TR
DC28	DD11	DD16	Up in WT TR
DC29#	DD11	DD16	Down in DM TR
DC30#	DD11	DD17	Up in DM TR
DC31#	DD11	DD17	Up in DM TR
DC32#	DD11	DD17	Up in DM TR
DC33#	DD11	DD17	Up in DM TR
DC34#	DD11	DD17	Up in DM TR
DC35#	DD11	DD18	Down in DM TR
DC36#	DD11	DD27	Up in DM TR
DC37#	DD11	DD27	Up in DM TR
DC38#	DD11	DD14	Down in DM TR

Table 3.2. cont'd cDNA fragments identified by DD-PCR			
Differential Clone	**Reverse Primer**	**Random Primer**	**Expression Pattern**
DC39#	DD11	DD14	Down in DM TR
DC40#	DD11	DD14	Down in DM TR
DC41#	DD11	DD14	Down in DM TR
DC42#	DD11	DD14	Up in DM TR
DC43	DD11	DD21	Up in WT TR, $\alpha1^{-/-}$ TR and DM TR
DC44	DD11	DD21	Down in DM TR
DC45	DD11	DD24	Down in DM TR
DC46	DD11	DD24	Down in DM TR
DC47	DD11	DD24	Up in DM TR
DC48	DD11	DD24	Up in WT TR
DC49	DD11	DD25	Up in DM TR
DC50	DD11	DD25	Down in DM TR
DC51	DD11	DD22	Up in DM TR
DC52	DD11	DD25	Up in WT TR and $\alpha1^{-/-}$ TR *
DC53	DD11	DD26	Down in $\alpha1^{-/-}$ TR and DM TR
DC54	DD11	DD27	Up in $\alpha1^{-/-}$ TR and DM TR
DC55	DD11	DD28	Down in DM TR
DC56	DD11	DD28	Down in DM TR
DC57	DD11	DD28	Down in WT TR
DC58	DD11	DD28	Down in WT TR
DC59	DD11	DD28	Down in $\alpha1^{-/-}$ TR and DM TR
DC60	DD11	DD28	Down in $\alpha1^{-/-}$ TR and DM TR
DC61	DD11	DD29	Down in $\alpha1^{-/-}$ TR and DM TR
DC62	DD11	DD29	Down in WT TR
DC63	DD11	DD29	Down in WT TR
DC64	DD11	DD29	Up in WT TR
DC65	DD11	DD26	Down in WT TR
DC66	DD11	DD27	Down in WT TR
DC67	DD11	DD27	Down in DM TR
DC68	DD11	DD27	Up in WT TR
DC69	DD11	DD30	Down in DM TR
DC70	DD11	DD30	Up in WT TR and $\alpha1^{-/-}$ TR *
DC71	DD11	DD30	Down in DM TR
DC72	DD11	DD30	Up in DM TR
DC73	DD11	DD30	Up in DM TR
DC74	DD11	DD30	Down in DM TR
DC75	DD11	DD30	Down in DM TR

Table 3.2. cont'd cDNA fragments identified by DD-PCR			
Differential Clone	**Reverse Primer**	**Random Primer**	**Expression Pattern**
DC76	DD11	DD30	Down in DM TR
DC77	DD7	DD14	Up in $\alpha1^{-/-}$ TR
DC78	DD7	DD14	Up in WT TR and $\alpha1^{-/-}$ TR *
DC79	DD7	DD15	Down in $\alpha1^{-/-}$ TR
DC80	DD7	DD15	Down in $\alpha1^{-/-}$ TR
DC81	DD7	DD15	Down in $\alpha1^{-/-}$ TR and DM TR
DC82	DD7	DD15	Down in $\alpha1^{-/-}$ TR and DM TR
DC83	DD7	DD15	Down in $\alpha1^{-/-}$ TR and DM TR
DC84	DD7	DD15	Up in WT TR
DC85	DD7	DD15	Down in $\alpha1^{-/-}$ TR
DC86	DD7	DD16	Up in $\alpha1^{-/-}$ TR and DM TR
DC87	DD7	DD16	Up in $\alpha1^{-/-}$ TR and DM TR
DC88	DD7	DD16	Down in $\alpha1^{-/-}$ TR and DM TR
DC89	DD7	DD16	Down in $\alpha1^{-/-}$ TR and DM TR
DC90	DD11	DD31	Up in $\alpha1^{-/-}$ TR and DM TR
DC91	DD11	DD31	Down in DM TR
DC92	DD11	DD31	Down in WT TR and $\alpha1^{-/-}$ TR*
DC93	DD11	DD31	Down in $\alpha1^{-/-}$ TR and DM TR
DC94	DD11	DD32	Down in DM TR
DC95	DD11	DD32	Down in $\alpha1^{-/-}$ TR and DM TR
DC96	DD11	DD32	Up in $\alpha1^{-/-}$ TR and DM TR
DC97	DD11	DD32	Down in DM TR
DC98	DD7	DD17	Up in $\alpha1^{-/-}$ TR
DC99	DD7	DD17	Down in $\alpha1^{-/-}$ TR and DM TR
DC100	DD7	DD17	Down in $\alpha1^{-/-}$ TR and DM TR
DC101	DD7	DD17	Up in WT TR, $\alpha1^{-/-}$ TR and DM TR
DC102	DD7	DD17	Down in $\alpha1^{-/-}$ TR and DM TR
DC103	DD7	DD17	Down in $\alpha1^{-/-}$ TR and DM TR
DC104	DD7	DD17	Down in $\alpha1^{-/-}$ TR and DM TR
DC105	DD7	DD18	Down in $\alpha1^{-/-}$ TR
DC106	DD7	DD19	Up in $\alpha1^{-/-}$ TR and DM TR
DC107	DD7	DD21	Up in $\alpha1^{-/-}$ TR

* cDNA fragments that are candidates for involvement in the RA-induced caudal truncation and spina bifida phenotype.
# Differentially expressed cDNA fragments that were isolated by comparison of RA-treated wild type and RA-treated *RARα1γ* double null samples only.

Table 3.3.	DD-PCR cDNA fragments categorized according to RA and RAR regulation*

Expression altered by RA treatment	
Induced by RA:	
WT only	10 (11%)
WT and RARα1$^{-/-}$	7 (8%)
WT, RARα1$^{-/-}$ and RARα1$^{-/-}$γ$^{-/-}$	3 (3%)
Repressed by RA:	
WT only	8 (9%)
WT and RARα1$^{-/-}$	2 (2%)
WT, RARα1$^{-/-}$ and RARα1$^{-/-}$γ$^{-/-}$	6 (6%)

Expression altered due to RAR status#	
Induced in RAR null embryos:	
RARα1$^{-/-}$ only	5 (5%)
RARα1$^{-/-}$γ$^{-/-}$ only	7 (8%)
RARα1$^{-/-}$ and RARα1$^{-/-}$γ$^{-/-}$	7 (8%)
Repressed in RAR null embryos:	
RARα1$^{-/-}$ only	5 (5%)
RARα1$^{-/-}$γ$^{-/-}$ only	19 (20%)
RARα1$^{-/-}$ and RARα1$^{-/-}$γ$^{-/-}$	14 (15%)

* cDNA fragments that were identified by comparison of RA-treated wild type and RA-treated *RARα1γ* double null embryos only (DC29 to DC42) were not included in this summary.

Expression of cDNA fragments in this category was not altered by RA treatment in wild type embryos, but did change in a particular RA-treated RAR null background.

cDNA fragment due to minor differences in PCR conditions. Although several precautionary measures were taken in each step of this screen, such as amplification of each sample type in duplicate, false positives were anticipated. Therefore, it was imperative that the differential expression of these candidate cDNA fragments be verified by other methods.

3.3d. Confirmation of RA-regulation (DD-PCR)

Northern blot analysis is not practical for screening the candidate genes identified here for two reasons. First, the large number of cDNA fragments typically isolated necessitates a rapid method of screening. Second, the amount of RNA needed for the preparation of one northern blot (15 to 20 μg per lane) is not readily obtainable from E8.5 embryos, especially considering that RAR mutant embryos are limiting.

A technique described by Mou *et al.* (1994) that allows rapid evaluation of many cDNA fragments, using a smaller amount of RNA than needed for northern analysis, was assessed using the candidates isolated from this screen. The differentially expressed PCR products were eluted, re-amplified, and immobilized on nylon membranes using a slot blot manifold, in duplicate. The membranes were hybridized with ^{32}P-dCTP labeled cDNA synthesized from total RNA isolated from untreated or RA-treated E8.5 embryos. However, it was difficult to determine whether a particular cDNA fragment was in fact differentially expressed due to high, and often variable, levels of background signal (data not shown). As a variation of this method, the PCR products were resolved on an agarose gel, transferred to nylon membranes, and hybridized as described in Chapter 2, Section 2.12. This "reverse northern" approach greatly reduced background and provided a more reliable method for assessing potential RA-regulation of candidates. Typical results are shown in Figure 3.3.

Of the forty-eight PCR product samples that were re-screened twenty-five (52%) did not produce detectable signals, even upon extensive exposure (represented by lanes 1 to 3 in Figure 3.3.). This suggests that many of these cDNAs are present in low abundance in the mouse embryo. Due to the nature of the probe used for hybridization, genes that are expressed at low levels may not be represented as ^{32}P-labeled cDNA. Although this is not unexpected, it greatly restricts the analysis of putative RA-regulated

Figure 3.3. Confirmation of differential expression by reverse northern analysis. Equal amounts of PCR product generated by re-amplification of excised differentially expressed bands were run on two agarose gels and transferred to nylon membranes. The duplicate blots were hybridized with equivalent c.p.m. of ^{32}P-labeled cDNA generated from total RNA extracted from untreated or RA-treated E8.5 mouse embryos. Comparison of the blots demonstrates that some of the re-amplified PCR products (lanes 4 to 6) are false positives while others (lane 7) appear to be RA-regulated. PCR products in lanes 1 to 3 are not detectable by this method. *β-actin* serves as a non RA-regulated control.

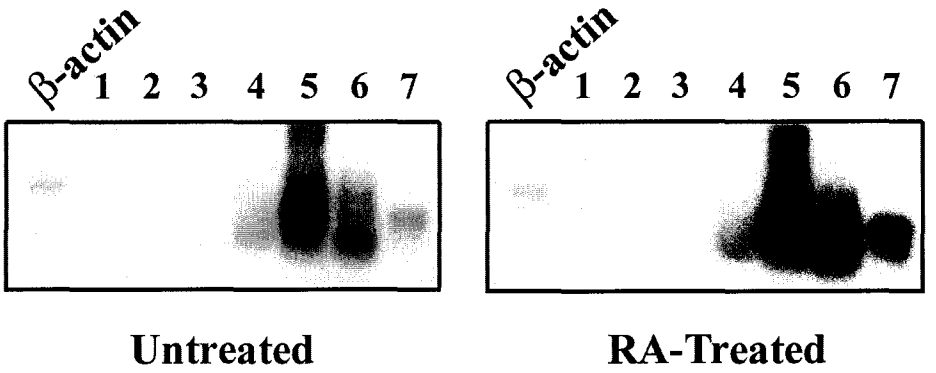
β-actin
1 2 3 4 5 6 7
β-actin
1 2 3 4 5 6 7
Untreated
RA-Treated

genes. Only two (DC16 and DC28) of the twenty-three visible PCR products appeared to be clearly up-regulated by RA (lane 7, Figure 3.3.). In summary, only 4% of the cDNA fragments identified as potentially RA-regulated (9% of those visible by reverse northern analysis) proved to be true positives after re-screening.

In parallel with re-screening of the cDNA fragments, some of the PCR products were cloned into vectors, end-sequenced and analyzed by whole mount *in situ* hybridization. Although apparently single bands were excised from the DD-PCR polyacrylamide gel, multiple PCR products of similar size were, in fact, present. This was determined by restriction enzyme analysis of several individual subclones isolated from a given PCR product. Typically, at least two and sometimes up to four different species of PCR product were identified in this manner, necessitating a second reverse northern analysis. As a result, a positively RA-regulated cDNA fragment was isolated from the DC16 PCR product mixture. Although many subclones were screened from the DC28 PCR product mixture, a RA-regulated clone was not identified.

3.3e. DC16 is a RA-regulated cDNA fragment

A 155 bp sequence of DC16, and its expression pattern in untreated and RA-treated embryos, is shown in Figure 3.4. DC16 is weakly expressed at this stage of development, and its levels are dramatically increased after six hours of RA-treatment *in utero* (compare Figure 3.4B to 3.4C). In contrast, hybridization with the sense control did not produce a detectable signal (data not shown). A comparison of DC16 sequences deposited in GenBank indicated that there was no significant homology to any known genes. However, nearly perfect homology was found with several ESTs cloned from various embryonic, neonatal and adult tissues. To isolate a longer cDNA fragment an E8.5 mouse library was screened with the DC16 fragment. Five positive clones were identified and end-sequenced. Three of the clones had identical sequences at one end of the insert. Digestion with several restriction enzymes revealed that two of the clones (# 2 and #4) were identical to one another, while the third (#3) was slightly longer (approximately 2 kb vs. 1.5 kb in length). A fourth clone (#1) was slightly shorter than #2 and #4 (approximately 1 kb in length) and was homologous to these clones at one end of the insert. The final clone (#5) contained the longest insert (approximately 2.5 kb in

length) however, there was no homology between the end-sequences of this cDNA fragment and any of the other clones. None of the end-sequences exhibited any homology to DC16 or any previously cloned genes.

The above sequence information was used to screen mouse EST sequences for homology. Five overlapping ESTs were identified and their combined sequence of 1385 nucleotides is shown in Figure 3.5. The complete sequence of clone #1 from the E8.5 cDNA library is located within the constructed sequence (shown in bold) and overlaps with the DC16 cDNA fragment (underlined). An arrow indicates the beginning of the homologous sequence found in clones #2, #3, and #4. Although ESTs that could extend the 5' or 3' ends of this construct were not identified, and a poly-A stretch was found at the 3' end, the possibility that the endogenous cDNA is longer than that shown may not be excluded. This is supported by the fact that no sequence homology was found for the opposite end of clones 2, 3, and 4, and both ends of clone 5. Additionally, hybridization of a northern blot of F9 cell RNA with the ^{32}P-labeled DC16 fragment resulted in the visualization of two bands approximately 1 kb and 7 kb in size (data not shown). The size of the smaller band is in concordance with that predicted by the overlapping EST sequences and therefore may be the full-length cDNA. An alternate explanation is that the DC16 locus is subject to to alternate promoter or polyadenylation signal usage, or variant splice site recognition, resulting in two transcripts of different length.

Homology searches using this cDNA sequence again revealed no significant homology to any previously cloned gene. Moreover, only very short open reading frames (ORFs) were found. Although it is possible that one of these encodes a functional product, this sequence may contain only the 3' or 5' untranslated regions. As DC16 appeared to be ubiquitously expressed, and uniformly RA-responsive, in the E8.5 embryo, it was considered unlikely that this gene product plays a role in the RA-induced caudal malformations, and additional characterization was not pursued.

Another cDNA fragment (DC43) isolated by DD-PCR was down regulated by RA treatment in the caudal region of the embryo (data not shown). Therefore, the corresponding full-length cDNA was isolated and its expression pattern during development characterized. During these analyses, DC43 proved to be a false positive, however, its interesting pattern of expression during embryogenesis and significant

Figure 3.4. Sequence and embryonic expression pattern of a RA-regulated cDNA fragment; DC16. (**A**) Complete sequence of the 155-bp cDNA fragment isolated by DD-PCR. The reverse (DD10) and random (DD25) primer sequences used in the PCR amplification are underlined. (**B**) Wild type untreated E8.5 mouse embryo hybridized with antisense DC16 riboprobe. (**C**) An E8.5 mouse embryo treated with RA for 6 hours hybridized with the same riboprobe and under the same conditions as in (B). Note the dramatic increase in expression due to RA-treatment. The sense riboprobe did not produce a detectable signal (data not shown).

A

```
        DD10
  1     TTTTTTTTTT TGCCAATATA TCTTTTAGTA TAATGACAGG

 41     GAGAATTACA ATAAAAAAAT CAAAGATACA ACAANATAAG

 81     CATGAAAAGC AACATTTACA TGAGNGCAAA TTATTAAGTA

121     TACATGTACA GTAAGAACAG CTTGTGACAT GGAAC
                                      DD25
```

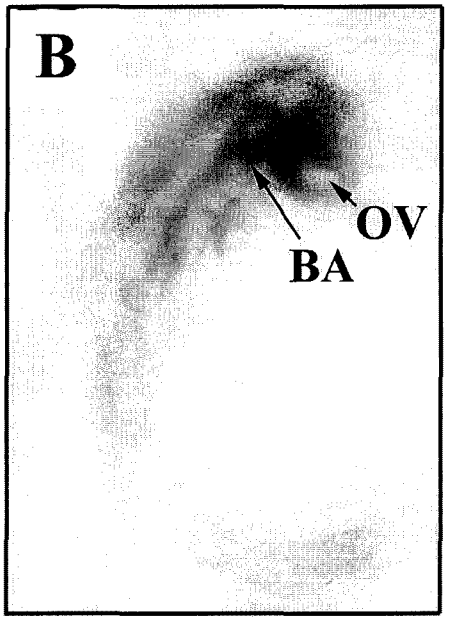

Figure 3.5. Complementary DNA sequence derived from overlapping ESTs with homology to DC16. DC16 was used as a probe to identify homologous cDNA clones from an E8.5 mouse library. The identified clones were end sequenced and the sequences used to screen an EST database. Several overlapping EST clones were identified that had nearly perfect homology to the end sequences of one particular cDNA clone (#1), shown in bold. The sequence of the DC16 cDNA fragment is located near the 3' end of this sequence (underlined). Five overlapping EST fragments were used to create this continuous sequence. The Genbank accession numbers are as follows: AA689827 (nucleotides 1 to 519), AW990341 (nucleotides 237 to 739), AW912670 (nucleotides 709 to 1119), BB364201 (nucleotides 997 to 1281), and BE651215 (nucleotides1144 to 1385). When compared to the EST sequence, the 3' end of the DC16 fragment, corresponding to DD25 (Figure 3.5A), is not the same. It appears that only the five 3'-most nucleotides of the random primer were homologous to the endogenous cDNA.

1 TCACATTAAA TGAAAGAAGC CAGCTCAGCC AACACAGCCT GTGTTTTAGC
51 ATACACAGAC TCTAGTAGGC AAAAGAGAGA CTCTAAGGGT CTACTTGTGA
101 GGAAATGAGG ACCATTAGGC AGAGGGAAGG GGTTGGGAGA TAGGAAAAAA
151 AAATGGGTGA AGAGAGTCAA ATATGTAGAA CTGTCAAAAT ATCATGACAA
201 AAACCATTAC TTTGCTCAAT AATACATGCC ATTTTTTTTA ATTTAAAGCT
251 AAAAGTAATA TGCATAAGAA ATTACTTCGC CCTATCTGGG CCTAATGTAA
301 GAGACCTGGA AATGCCTAAA GTTTCATGTT CAATAGGTTG AGTACAATTT
351 CTTGCTATGG TTACCCTTTC ATTGCTATGG CTACCC**TTTC ATTGCTATGG**
401 TTACCCTTTC ATTGCTATGG CTACCCCTTG CATTGGTTAT GAGAACATAA
451 CCAATGGGTA ATTAGGAACA TTTGCATTTG TTAAGACTAG CAACCAATAT
501 ATTGGAGGAA ATATTGTGTT GGTATAGAAA CTCTGAAAGG TTAAAAACTG
551 GCCCAGAACA CAGGTGTTCA AAGCAAAGGC CAGTCTTCGG CTATGAAGGC
601 AGGTGTCCCA AACTAGGACA AAAGAAAAGG CCACCCTGTA AAGTTGTCCG
651 TAAATCCAAC AAAACGTAAA ACATCCTGAG TCATGAAAGT GAGCAAAGTA
701 CCCTCTCCTC ACTAACGTGC CGAGCTATGC TCATGGATTA AAGCTTCCTG
751 CACTGCACTG TTTGAGGACC TCCAAATAAT AACCACAATT AACAAATATG
801 GAATTATACT CACATCTCAG TACATTCAAG AGGCACCTAA CTATATCTAA
851 CGAATCCCAT AAAGCCTTAT AAGCTAACCA CCAATACCTG CAGAACATTT
901 ATGCAATGTT CTCACAGATG AGGCATACTT AGCTACTATA TATATATATA
951 TATATATATA TATATATAGT ATATATGTAT GTATATGTAT ATATATGGAG
1001 AGATTGACTA TGATTTATTA CACGGTGCTT AGTCTTTGGC AAGAAGCCAG
1051 TAATGCCAAT ATATCTTTTA GTATAATGAC AGGAGAAATT ACAATAAAAA
1101 AATCAAAGAT ACAACAAAAT AAGCATGAAA AGCAACATTT ACATGAGAGC
1151 AAATTATTAA GTATACATGT ACAGTAAGAA CAGCTTGTGA CATGGAAACA
1201 ACTTCTAAAT GTGATGTCAA TCTATGATTA TAGAGCGACA TTTATACCTA
1251 CCTTCTACAT AGACAAGAGT TAACATTTGA TAACCTAAAA GTGTTTTGAA
1301 AGTTGTGTAA AGGGCATGGC GACAAGAAAT GTTAGAAAAA AACATCAGGT
1351 AGAGAGAAAA GTTAA**CAAAA AAAAAAAAAA AAAAA**

homology to the aldehyde reductase genes cloned from human, rat and pig tissues warranted further study. A full description of the characterization of this novel gene comprises Chapter 4 of this thesis.

3.3f. Suppression subtractive hybridization

The second technique used to identify RA-regulated genes in the mouse embryo is suppression subtractive hybridization (SSH). This PCR–based technique, originally described by Diatchenko *et al.* (1996), is designed such that following the subtraction of tester and driver cDNA samples, only those fragments that are more abundant in the tester population are amplified exponentially.

In contrast to DD-PCR, the amount of RNA required to perform SSH (2 μg of poly A^+ RNA) exceeds the amount that can be readily derived from an E8.5 mouse embryo. Additionally, limiting the analysis of differential gene expression to the caudal embryo (posterior to the last formed somite) would be advantageous for identification of genes involved in RA-induced caudal truncation and spina bifida. As this reduces the amount of tissue that can be utilized per embryo by approximately 80%, a large number of mouse embryos would be needed to isolate 2 μg of poly A^+ RNA. To circumvent this, poly A^+ RNA from the caudal portions of approximately 100 embryos (untreated and RA-treated) was amplified using the SMART™ PCR cDNA Synthesis kit (Clontech). As a result, several micrograms of cDNA could be generated from only 0.5 μg of poly A^+ RNA.

To ensure that the amplified cDNA was indeed representative of the endogenous mRNA population, the PCR products were hybridized with ^{32}P-labeled cDNA fragments corresponding to known RA-regulated genes. The results of this analysis are shown in Figure 3.6A. *Cdx1* and *P450RAI* transcripts are both increased in the caudal portion of the E8.5 embryo following RA-treatment. This is reflected by the increased abundance of these sequences in the RA-treated cDNA sample relative to the untreated cDNA pool. *Brachyury (T)* levels are decreased in response to RA in the nascent mesoderm at E8.5, which is also represented in the amplified cDNA products. These results suggest that the PCR amplified cDNA pools are representative.

Figure 3.6 Confirmation of mRNA representation in amplified cDNA and test of subtraction efficiency. Equivalent amounts of amplified cDNA fragments from untreated and treated caudal embryo **(A)** and amplified cDNA fragments from untreated and treated caudal embryo, and the subtracted cDNA pool **(B)** were resolved on an agarose gel, transferred to nylon membranes, and hybridized with ^{32}P-labeled cDNAs corresponding to known RA-regulated genes. *β-actin* was used as a negative control. Abbreviations: M, marker; UN, untreated; TR, treated; S, subtracted.

A

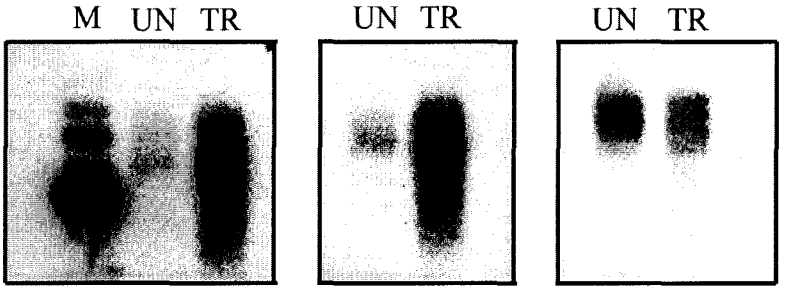

p450RAI **Cdx1** **Brachyury**

B

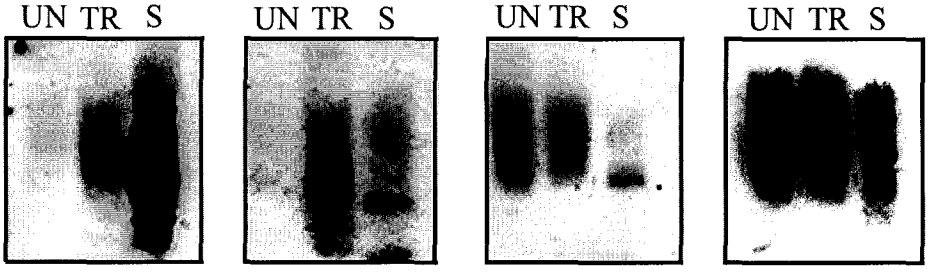

p450RAI **Cdx1** **Brachyury** **β-actin**

3.3g. Identification of RA-regulated cDNA fragments

SSH was performed using the PCR amplified cDNA, with the RA-treated sample as the tester population, and the untreated sample as the driver. This subtraction should enrich for transcripts that are increased in the caudal portion of E8.5 mouse embryos as a result of RA-treatment. The subtracted and unsubtracted cDNAs were compared as described in Section 3.3f. Figure 3.6B shows that both *Cdx1* and *P450RAI* cDNA fragments were present in the subtracted cDNA population, and that *P450RAI* fragments were greatly enriched. The levels of *Cdx1* transcripts were not enriched in the subtracted population, indicating that the subtraction was not effective for all RA-regulated transcripts in the pool. Conversely, *brachyury* was decreased relative to untreated and treated unsubtracted samples. *β-actin* was expressed at the same level, irrespective of RA treatment, in the unsubtracted samples, and should theoretically be undetectable after subtraction. Although *β-actin* transcripts in the subtracted cDNA pool were diminished, they were not eliminated, indicating that the subtraction was not completely efficient. However, the fact that both *P450RAI* and *Cdx1* transcripts were found at significant levels in the subtracted cDNA pool, and *brachyury* levels were reduced, indicates that this pool was enriched for RA-induced genes.

3.3h. Confirmation of regulation (SSH)

RA-regulation of subtracted cDNA clones was assessed by reverse northern analysis as described in Chapter 2, Section 2.12b, using DNA isolated from individual colonies. The probes were derived from the same pools used to perform the initial subtraction. Four hundred-and-thirty-eight cDNA containing plasmids were screened in this manner and two hundred and two generated signals after exposure for 7 to 10 days (Table 3.4). As with the DD-PCR technique, cDNA fragments that are presumably low in abundance could not be detected by this method. Of the 202 detectable clones, 63 (31%) gave a more intense signal using the probe derived from the RA-treated cDNA population.

As the clones were screened with the same cDNA population that was used to identify them initially, it is possible that false positive clones may have been generated. This could occur if the cDNA populations were not truly representative of the

Table 3.4. Suppression Subtractive Hybridization Results

Primary Screen	
Total number of clones screened	438
Total number of clones visible by reverse northern analysis	202
Total number of clones that appeared to be up-regulated by RA	63
Percentage of total clones	14.4%
Percentage of visible clones	31.1%
Secondary Screen	
Total number of clones screened	63
Total number of clones visible by reverse northern analysis	57
Total number of clones that appeared to be up-regulated by RA	21
Percentage of total clones	33%
Percentage of visible clones	36.8%
Total number of clones that appeared to be down regulated by RA	9
Percentage of total clones	14.5%
Percentage of visible clones	15.7%
Total number of clones that appeared to be unaffected by RA treatment	27
Percentage of total clones	43%
Percentage of visible clones	47.4%

Table 3.5. Candidate RA-regulated cDNA fragments

Clone Number	RA-regulation in secondary screen	Sequence homology
1	Not visible	Human 7TM domain protein
2	Not regulated	Cdc2
3	Up-regulated	EST (from RA-treated P19 cells)
4	Down-regulated	B2 repetitive element
5	Not regulated	N.D.
6	Not regulated	Ribosomal protein L5
7	Not regulated	Ribosomal protein L5
8	Not regulated	B2 repetitive element
9	Not visible	Human mRNA (unknown function)
10	Up-regulated	ESTs
11	Up-regulated	Human CGI-48 protein (C.elegans homologue)
12	Up-regulated	Human TAF2K
13	Down-regulated	Glucose regulated protein
14	Up-regulated	TI-227
15	Up-regulated	Unr mRNA (Rat and Human)
16	Up-regulated	NADH dehydrogenase subunit 1
17	Not regulated	N.D.
18	Not visible	Ubiquitin C-terminal hydrolase
19	Not visible	ESTs
20	Up-regulated	Cellular nucleic acid binding protein
21	Not regulated	HMG-1
22	Up-regulated	Tax RE binding protein 107
23	Not regulated	NADH dehydrogenase subunit 1
24	Up-regulated	NADH dehydrogenase subunit 6
25	Up-regulated	EF1α
26	Up-regulated	B2 repetitive element
27	Not regulated	Human mRNA (KIAA0101)
28	Up-regulated	Spermidine/spermine N1-acetyltransferase
29	Not regulated	Midkine
30	Not regulated	No strong homologies
31	Down regulated	ESTs (sim. To ubiquitin activating enzyme)
32	Up regulated	No strong homologies
33	Up regulated	N.D.
34	Not visible	N.D.
35	Down regulated	Nedd-4/Ubiquitin protein ligase
36	Up regulated	ESTs
37	Down regulated	Human nuclear cap binding protein 1
38	Not regulated	BCNT/cp27/Craniofacial dev. Protein1
39	Not Regulated	B2 repetitive element

Table 3.5. cont'd Candidate RA-regulated cDNA fragments

Clone Number	RA-regulation in secondary screen	Sequence homology
40	Not regulated	N.D.
41	Up regulated	EST
42	Down regulated	N.D.
43	Up regulated	N.D.
44	Not regulated	Ribosomal protein L27
45	Down regulated	B2 repetitive element
46	Not regulated	Heat shock protein 86
47	Not regulated	N.D.
48	Not regulated	No strong homologies
49	Not regulated	NADH dehydrogenase subunit 4
50	Down regulated	B2 repetitive element
51	Not regulated	ESTs
52	Not regulated	N.D.
53	Not regulated	N.D.
54	Not visible	No strong homologies
55	Not regulated	Human β1 catenin
56	Up regulated	ESTs
57	Not regulated	ESTs
58	Not regulated	Phosphoglycerate kinase
59	Not regulated	ESTs
60	Down regulated	Replacement variant histone H3.3
61	Not regulated	Mitochondrial stress-70 protein
62	Up regulated	Human DEK mRNA
63	Up regulated	N.D.

endogenous mRNA pool. Although the amplified cDNA was confirmed to be representative with respect to known RA-regulated genes, the levels of other genes may have been skewed, and therefore biased. To address this, a second pool of cDNA was amplified using poly A^+ RNA isolated from independent caudal embryos (untreated and RA-treated), and the 63 putative RA-regulated clones re-screened using these new cDNAs. As shown in Table 3.4, 57 of the 63 clones were visible after exposure to film for the same length of time described above. Of the 57 clones, 21 (37%) were present at higher levels in the RA-treated cDNA pool. Surprisingly, nine of the clones (16%) that appeared to be induced by RA treatment in the first screen were repressed in the second. The remaining 27 clones (47%) exhibited no detectable difference between untreated and RA-treated cDNA populations. These results indicate that there are indeed substantial variations in cDNA amplification from these different RNA samples. Nonetheless, 21 of the 63 clones were present at higher levels in the RA-treated cDNA pool in both screens. A summary of RA-regulation and sequence homologies of the cDNA fragments identified is displayed in Table 3.5.

Whole mount *in situ* hybridization analysis was performed on untreated and RA-treated E8.5 mouse embryos using the cDNA fragments isolated by SSH as probes. Unfortunately, only a small fraction of the cDNA fragments tested provided any information regarding embryonic expression pattern. This could be due to the fact that this technique by nature generates small cDNA fragments, which may be inappropriate for *in situ* analysis. As an alternative approach, the cDNA fragments were used to probe northern blots prepared from F9 and P19 cells. These embryocarcinoma cell lines are a frequently used model of RA-regulation of gene expression and are often reflective of in vivo regulation. Each cell line was treated with 10^{-6} M RA and cells were harvested at specific time points thereafter ranging from 30 minutes to 8 hours. In total, twenty-one fragments were used to probe the northern blots and only two (#14 and #24) showed regulation by RA. The remaining 19 messages were either not visible by this method or were not regulated by RA in these cell lines; examples can be found in Figure 3.7. The expression of clones #12, #20 and #22 were not altered while clones #14 and #24 were induced by RA in both cell lines.

Clone #14 is homologous to a gene called *TI-227* that was found to be differentially expressed between melanoma cell lines that exhibit different metastatic behaviours (Ishiguro *et al.*, 1996). Although little information is available regarding this gene, a recent publication reports that *TI-227* is not detectable in normal tissues and therefore may be specifically associated with tumors that have a particular metastatic ability (Ishiguro *et al.*, 2000). In F9 and P19 cells the expression of this gene appears to be rapidly induced by RA treatment, with increased transcripts seen after as little as 30 minutes post-exposure (F9 cells). This response is transient in both cell lines and returns to untreated levels after 4 hours. Whole mount *in situ* hybridization using this clone did not produce a signal (data not shown).

The second SSH clone regulated by RA in the F9 and P19 cell lines (#24) is homologous to *NADH dehydrogenase subunit 6 (ND6)*, an enzyme encoded by the mitochondrial genome. The pattern of RA regulation of this clone was different than that of clone #14 and also varied between the two cell lines (Figure 3.7). The expression of clone #24 in P19 cells was induced after 30 minutes, and peaked following 4 hours of RA treatment. In F9 cells, increased levels of expression were detected after 1 hour of RA treatment and levels continued to rise throughout the 8 hour analysis. Whole mount *in situ* hybridization analysis at E8.5 showed that ND6 is RA-responsive in vivo (compare 3.8A to 3.8B). This increased level of expression can be clearly observed in the caudal region of the embryo (Figure 3.8C).

Figure 3.7 Northern blot analysis of candidate RA-regulated genes. Northern blots prepared from F9 and P19 cells were hybridized with the indicated ^{32}P-labeled cDNA fragments isolated by SSH. **(A)** TAF2K **(B)** TI-227 **(C)** Cellular nucleic acid binding protein (CNBP) **(D)** Tax responsive element binding protein 107 (TAX RE BP 107) **(E)** Agarose gel demonstrating RNA loading for blots shown in A-D **(F)** *NADH dehydrogenase subunit 6 (ND6)* **(G)** Agarose gel demonstrating RNA loading for the blot shown in F. The first lane (unlabeled) on each autoradiograph and gel is a size marker.

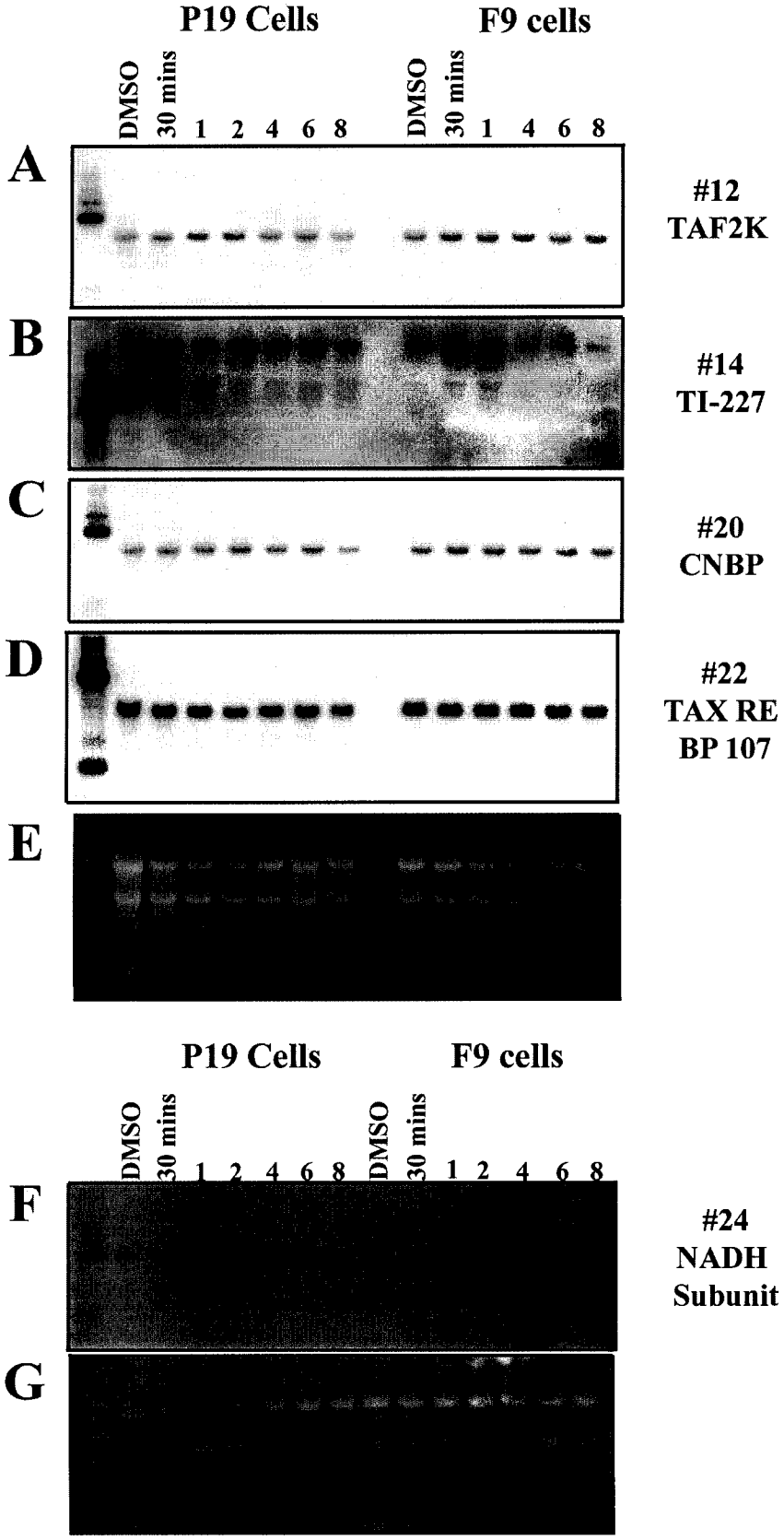
P19 Cells
F9 cells
DMSO
30 mins
1 2 4 6 8
DMSO
30 mins
1 4 6 8
A
#12
TAF2K
B
#14
TI-227
C
#20
CNBP
D
#22
TAX RE
BP 107
E
P19 Cells
F9 cells
DMSO
30 mins
1 2 4 6 8
DMSO
30 mins
1 2 4 6 8
F
#24
NADH
Subunit
G

Figure 3.8. The NADH dehydrogenase subunit 6 mRNA is elevated by RA-treatment in the E8.5 mouse embryo. Clone #24 (*NADH dehydrogenase subunit 6 (ND6))* was used as a riboprobe for whole mount *in situ* hybridization of untreated (**A**) and RA-treated (**B**) mouse embryos. Note the increased expression elicited by a 6 hour RA treatment. (**C**) The RA induced expression of *ND6* in the caudal embryo. Note the caudal flexion (arrow) that occurs in RA-treated embryos as a precursor to axial truncation.

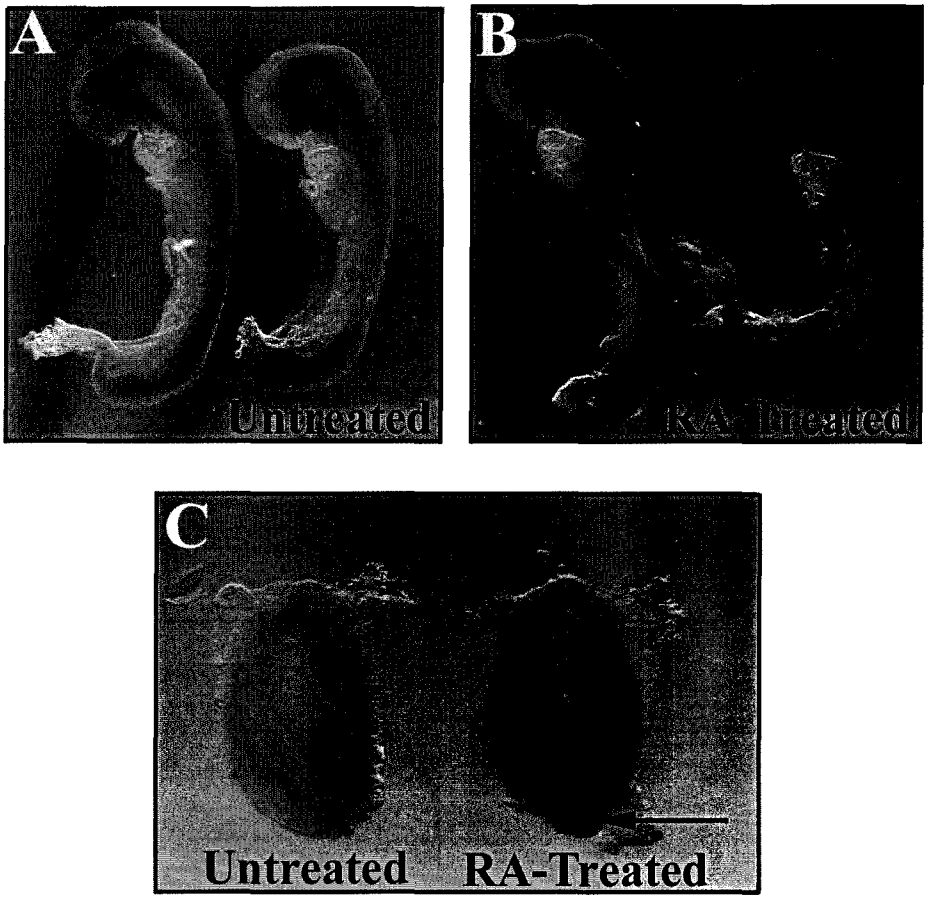
A
Untreated
B
RA-Treated
C
Untreated
RA-Treated

3.4 Discussion

3.4a. Differential display vs. suppression subtractive hybridization

Several methods for identification of differentially expressed genes have recently been described. In this chapter the use of two such techniques, differential display PCR (DD-PCR) and suppression subtractive hybridization (SSH), to identify genes that are regulated by RA in the E8.5 mouse embryo is described. The identification of candidate RA-regulated genes was initially approached using DD-PCR as it allows the simultaneous comparison of cDNA fingerprints generated from several different sample types. However, reverse northern analysis suggested that the vast majority of candidate cDNA fragments identified were false positives. In fact, only two out of the forty-eight PCR product mixtures tested exhibited any RA regulation, although the true number of RA-regulated genes may have been higher since 52% of the PCR product mixtures were not visible by this method. Additionally, as several species of PCR product were frequently found within a single band, it is possible that an abundant transcript could mask the signal of a less abundant, but differentially expressed gene. Therefore, although it is clear that weakly expressed genes can be visualized by DD-PCR, it was difficult to isolate the appropriate cDNA fragment and confirm regulation.

The second technique used to identify RA-regulated genes, suppression subtractive hybridization (SSH), has one main advantage over DD-PCR; the amplified cDNA fragments are subcloned prior to determination of differential expression. This eliminates the problem of resolving which particular PCR product is the correct fragment. However, the same limitations encountered with DD-PCR, with respect to confirmation of weakly expressed genes, are also applicable to SSH. By restricting the SSH analysis to the caudal portion of the embryo the possibility of identifying RA-regulated genes that are not involved in the axial truncation phenotype is reduced. However, the large number of embryos needed to isolate a sufficient amount of caudal poly A^+ RNA is a major disadvantage. The use of the SMART cDNA synthesis kit enabled the generation of a large quantity of cDNA from a relatively small amount of input mRNA. Unfortunately, it also provided an additional mechanism for the generation of false positives as many of the cDNA fragments were not representatively amplified.

It is interesting to note that Cdx1 and p450RAI, transcripts that are positively regulated by RA, were not identified in either screen. This is likely due to the relatively low number of clones screened from this complex library as both of these trancripts were detectable in the subtracted pool by reverse northern analysis. A more successful means to identify RA-regulated genes in the embryo by SSH would be to use unamplified cDNA generated from the tissue(s) of interest. Although this would require the collection of a large number of embryos, it would eliminate any bias introduced by PCR. Alternatively, several pools of amplified cDNA could be generated from different samples (i.e. 5 different collections of 50-100 caudal embryo pieces) and each pool could be used to screen the subtracted library of cDNA fragments. Clones that are differentially expressed in the majority of amplified cDNA pools could be further considered as potential RA-regulated genes.

3.4b. DC16

One candidate isolated by DD-PCR, DC16, was confirmed to be RA-regulated *in vivo*. DC16 appeared to be weakly expressed in the wild type embryo, and was evident mainly in the branchial arch and fronto-nasal mass. After 6 hours of RA treatment *in utero*, the expression level of this gene was dramatically increased throughout the entire embryo. DC16, and related cDNA clones, exhibited no homology to any previously cloned gene, however they were nearly identical to several overlapping ESTs. The continuous cDNA sequence constructed using these ESTs again exhibited no homology to any sequences deposited in GenBank. Therefore, DC16 appears to correspond to a novel, RA-regulated gene expressed during mouse development. As the ORFs identified within the assembled sequence are very short, it is likely that the full-length sequence of this cDNA has not been isolated, and that the sequence analyzed contains only the 3' or 5' UTR.

All things considered, DC16 cannot be excluded as a candidate for RA-induced caudal truncation, that is upregulated in the affected tissues specifically by RARγ. In order to determine this unequivocally, whole mount *in situ* hybridization with embryos of all of genotypes and treatments initially used to perform the DD-PCR analysis must be carried out.

3.4c. NADH dehydrogenase subunit 6 (ND6)

Using reverse northern analysis, the mRNA levels of twenty-one clones isolated by SSH appeared to be consistently induced by retinoic acid treatment in the caudal embryo. Although several such clones were evaluated for RA-regulation by whole mount *in situ* hybridization, only two (#24 and #25; *NADH dehydrogenase subunit 6 (ND6)* and *EF-1α*, respectively) resulted in any detectable signal. *EF-1α*, a translation factor, was very strongly expressed in the caudal region of the mouse embryo but was not affected by RA-treatment (data not shown). Conversely, the expression level of ND6 was increased by RA-treatment *in vivo*. NADH dehydrogenase (or NADH: ubiquinone oxidoreductase) is the first, and largest, enzyme complex in the respiratory chain, which is located in the mitochondrial inner membrane and is responsible for electron transfer from NADH to ubiquinone (reviewed by Weiss at al., 1991). Intriguingly, Ruiz-Lozano *et al.* (1998) found the transcript levels of another subunit (14.5b) of this same complex to be reduced in E13.5 *RXRα* null embryos. The normal transcription of this gene appears to be dependent on both copies of *RXRα* as expression levels are reduced by 50% in heterozygotes. Additionally, mRNA levels of subunit 14.5b of *NADH dehydrogenase* were diminished in vitamin A deficient rat hearts at E13.5 (Ruiz-Lozano *et al.*, 1998). This is significant as *RXRα* null embryos die around E14.5 due to cardiac failure (Sucov *et al.*, 1994; Kastner *et al.*, 1994; Dyson *et al.*, 1995; Gruber at al., 1996) and vitamin A deficient embryos exhibit similar cardiovascular abnormalities (Wilson and Warkany, 1949; Dersch and Zile, 1993; Dickman *et al.*, 1997). Therefore it appears that the expression of *NADH dehydrogenase subunit 14.5b* is dependent on retinoid signaling.

Preliminary whole mount *in situ* hybridization experiments indicated that both the endogenous, and RA-induced, expression of *ND6* is dependent on RARγ (data not shown). Moreover, similar to *RXRα* and *NADH dehydrogenase subunit 14.5b* in the E13.5 mouse heart, the loss of one functional *RARγ* gene results in a decrease of *ND6* message (data not shown). These results imply that retinoid regulation of genes involved in electron transport may be a common mechanism throughout embryonic development. Hence, it is important to note that in addition to subunit 6 of *NADH dehydrogenase*, this SSH screen also identified subunits 1 and 4 of this complex as RA-responsive in caudal

embryo tissues (clones #16, #23 and #49), although these clones have not yet been tested by northern blot analysis or *in situ* analysis.

Both RA and NADH dehydrogenase appear to play significant roles in governing apoptosis and it is tempting to speculate that the RA induction of *ND6* may promote apoptosis in the caudal embryo. Examples can be found in the literature supporting a role for NADH dehydrogenase both in apoptotic induction and resistance, depending on the cell type and the experimental conditions. The majority of evidence suggests that a decrease in NADH dehydrogenase activity results in apoptosis. For example, inhibition of this enzyme complex by rotenone results in apoptosis of dopaminergic nerve terminals and is used as a model to study Parkinson's disease (Greenamyre *et al.*, 1999). On the other hand, Kataoka *et al.* (1997) found that a mutant HL-60 cell line that is resistant to apoptosis exhibits decreased expression of *NADH dehydrogenase subunit 5*. This finding is in concordance with the preliminary *in situ* hybridization results that show a reduction of *ND6* expression in *RARγ* null embryos, which are resistant to RA-induced caudal truncation and associated apoptosis.

3.4d. TI-227

Due to the limited success of *in situ* hybridization for analysis of the SSH clones, northern blots of F9 and P19 cell RNA were used to identify RA-responsive clones that may also be regulated in the embryo. Only two SSH clones (#14 and #24) of the twenty-one tested were found to be RA regulated in F9 and P19 cell lines. Clone #24 (*ND6*) was also found to be RA-regulated in mouse embryos as described above. Clone #14 (*TI-227*) did not produce a signal detectable above background levels in either untreated or RA-treated embryos by *in situ* analysis. *TI-227* was originally identified by a differential display screen comparing gene expression of two melanoma cell lines with different metastatic properties (Ishiguro *et al.*, 1996). As neither the function of this gene product, nor its pattern of expression during embryogenesis, has been determined it is not presently possible to suggest a role for *TI-227* in RA-induced caudal malformations.

3.4e. B2 repetitive elements

A cDNA fragment that was isolated in the SSH screen a total of six times (#4, #8, #26, #39, #45 and #50) was 92.7% homologous to a 124-bp segment of the 180-bp consensus B2 element sequence (Krayev *et al.*, 1982; Rogers, 1985). The B2 family of short interspersed repetitive elements (SINEs) is found at high copy number (50,000 to 100,000) throughout the rodent genome (Kramerov *et al.*, 1979; Krayev *et al.*, 1982). The elements are either transcribed as part of the non-coding region of a gene, usually in the UTRs or introns, or individually by RNA polymerase III (Haynes and Jelinek, 1981; Kramerov *et al.*, 1985; Singh *et al.*, 1985). B2 transcripts are abundant in embryonic and transformed cell lines, and transcription of these elements tends to decline upon differentiation (Murphy *et al.*, 1983; Bennett *et al.*, 1984; Rigby *et al.*, 1984). Additionally, high levels of B2 transcripts are found in the mouse embryo from the second-cleavage stage until at least mid-gestation (Vasseur *et al.*, 1985; Bachvarova, 1988). Despite the widespread expression of these transcripts during development and cellular transformation, a biological function has yet to be assigned. Nonetheless, several potential roles for these short messages have been proposed including an involvement in splicing, mRNA transport, transcriptional regulation, DNA replication, and evolution (Krayev *et al.*, 1982; Vasseur *et al.*, 1985; Clemens, 1987; Bladon and McBurney, 1991).

Intriguingly, the expression of B2 elements in P19 embryonal carcinoma cells is affected by RA treatment (Bladon *et al.*, 1990). RA causes a transient increase of B2 element expression that peaks around four hours of treatment and is followed by a sharp decline over several days to levels below that of untreated P19 cells. This timeframe corresponds to the length of RA treatment of mouse embryos used in the SSH screen. Therefore, RA may regulate the expression of this repetitive element not only in embryonic cell lines, but also in the developing embryo itself. Alternatively, the SSH fragments with B2 element homology may correspond to the UTR of another message induced by RA treatment. As the six SSH clones contain no additional sequence information outside of the B2 element it is not possible to determine which, if any, potential RA-regulated gene is the true target. It is important to note that RA-regulation of the B2 element in the embryo was not confirmed by *in situ* hybridization. Therefore the possibility that RA does not regulate B2 elements in embryonic tissues, and that these

six SSH clones are false positives identified due to their natural abundance in the developing embryo, remains.

3.4f Conclusions

The identification of differentially expressed genes in mouse embryos using techniques such as DD-PCR and SSH appears to be especially prone to the generation of false positives. This is due, in part, to the small size of the embryo and the need for a relatively large amount of RNA to perform such techniques. Additionally, levels of gene expression in the embryo are naturally more dynamic than in other systems, such as established cell lines. This chapter summarizes the various approaches used for the successful identification of RA-regulated genes in the mouse embryo, and suggests additional modifications, which may reduce the number of false positive clones and therefore facilitate the identification of true RA-regulated genes.

Chapter 4

Cloning and characterization of the mouse aldehyde reductase cDNA: *AKR1A4*

Abstract

The aldo-keto reductase (AKR) superfamily catalyzes the reduction of a broad range of aldehydes and ketones to their corresponding alcohols in a NAD(P)(H) dependent fashion. Aldehyde reductase is capable of reducing toxic aldehydes that are produced in both physiological and pathological conditions and is thought to act as a general detoxifier *in vivo*. This enzyme has been isolated, and the cDNAs cloned from, human, rat, and pig tissues. Although the mechanism of catalytic activity has been elucidated through extensive biochemical and structural studies relatively little is known regarding the role of aldehyde reductase during embryonic development. This chapter describes the cloning of the *mouse aldehyde reductase* cDNA and its embryonic pattern of expression. From stages E7.5 to E13.5 *aldehyde reductase* is expressed at high levels in several tissues, including the neural ectoderm, gut endoderm, somites, branchial arches, otic vesicles, limb buds, and tail bud. In adult mice this enzyme was expressed, at various levels, in all tissues examined. *Aldehyde reductase* does not appear to have the ability to reduce retinaldehyde as assessed by a RARE-β–galactosidase reporter cell line.

4.2. Introduction

The aldo-keto reductase (AKR) superfamily consists of 59 highly conserved enzymes that reduce a wide variety of aldehydes and ketones to their corresponding alcohols (Bohren *et al.*, 1989; Jez *et al.*, 1997a). These proteins (M_w ~35,000) are monomeric, cytosolic, and require NADP(H) as a co-factor for catalytic activity. The AKR superfamily has been divided into seven families based on amino acid homology (Jez *et al.*, 1997b; Jez *et al.*, 1997c). The largest of these families is composed of several sub-families including the mammalian aldose reductases; mammalian aldehyde reductases; hydroxysteroid dehydrogenases; D4-3-ketosteroid-5β-reductases; and the plant aldehyde reductases.

While the physiological roles of many of these enzymes remain to be established, biological functions are known, or have been proposed, for several members. For example, aldose reductase (ADR) is involved in the control of cellular osmoregulation. Transcription of the ADR gene in renal tubular cells is significantly induced by hyperosmotic stress (Garcia-Perez *et al.*, 1989; Petrash *et al.*, 1992), and an osmotic response element has been identified in the human, rabbit and rat ADR promoters (Ruepp *et al.*, 1996; Ferraris *et al.*, 1996; Aida *et al.*, 1999). ADR, as the first enzyme in the polyol pathway, increases intracellular tonicity by converting glucose into sorbitol, an organic osmolyte. Under physiological conditions glucose is phosphorylated by hexokinase, which has a much higher affinity for glucose than ADR (reviewed in Tomlinson *et al.*, 1994), and the accumulation of sorbitol is negligible. However, patients with diabetes mellitus have elevated blood levels of glucose and the flux through the polyol pathway increases, thereby producing excess amounts of sorbitol. The tissue-specific accumulation of sorbitol has been implicated in secondary complications arising from diabetes mellitus, including the development of cataracts and neuropathy (van Heyningen, 1959; Gabbay, 1973). Moreover, transgenic mice over-expressing aldose reductase develop galactose-induced complications similar to those seen in diabetic animals (Lee *et al.*, 1995; Yamaoka *et al.*, 1995; Yagihashi *et al.*, 1996). Aldehyde reductase (ALR) is also capable of reducing glucose to sorbitol and therefore may also play a role in diabetic complications (Kinoshita, 1974). It is apparent that inhibition of these enzymes would be highly desirable for the prevention of some diabetes-related

complications. Over the past two decades several chemical inhibitors of ADR have been designed. Although many of the drugs assessed in clinical trials showed considerable promise for the treatment of diabetic complications, serious side effects were also noted (Handelsman and Turtle, 1981; Pitts *et al.*, 1986). As members of the aldo-keto superfamily are highly conserved, and many of the ADR inhibitors are equally effective inhibitors of ALR (Srivastava *et al.*, 1982; Barski *et al.*, 1995) it is possible that non-specific inhibition may account for some of the observed side effects. Alternatively, the attenuation of the normal physiological function(s) of ADR or the production of toxic intermediates (Spielberg *et al.*, 1991) may also contribute to the deleterious effects of these agents.

Aldehyde reductase (ALR) is more widely expressed than ADR (Bohren *et al.*, 1989) and less is known about its physiological role(s). One proposed function for ALR is the detoxification of potentially harmful aldehydes produced by endogenous metabolic pathways (Bachur, 1976). For example, ALR isolated from several species reduces 3-deoxyglucosone (3-DG; a 2-*oxo*-aldehyde) to 3-deoxyfructose (Kanazu *et al.*, 1991; Takahashi *et al.*, 1993). 3-DG is a highly reactive intermediate produced by degredation of the Amadori product in the advanced Maillard reaction. This reaction, which involves the glycation of proteins by glucose and fructose, ultimately leads to the production of advanced glycation end products (AGEs), and is associated with symptoms, such as cataracts and browning of the skin, that are correlated with diabetes and aging (Monnier *et al.*, 1984; Szwergold *et al.*, 1990, Brownlee, 2000). AGEs bind to receptors (RAGEs) of the immunoglobulin superfamily resulting in increased superoxide formation (Schmidt *et al.*, 1996). Another 2-*oxo*-aldehyde substrate of ALR, methylglyoxal, is produced non-enzymatically and/or enzymatically from triose phosphates (Ohmori *et al.*, 1989; Pompliano *et al.*, 1990) and is thought to contribute to the secondary complications arising from diabetes mellitus (Vander Jagt *et al.*, 1992). Hence, a potential physiological function of ALR is to protect tissues from the damaging effects of these, and other, reactive endogenous aldehydes.

Although this family of enzymes has been studied extensively at the biochemical level in adult tissues and cell culture models, there has been no examination of their potential roles during development. In a differential display screen to identify retinoic

acid regulated genes in the mouse embryo (Chapter 3) a cDNA fragment was isolated that had very high homology to several members of the aldo-keto reductase superfamily. This chapter describes the cloning of the full-length mouse aldehyde reductase cDNA and its expression pattern in the mouse embryo and adult tissues. Additionally, the ability of this enzyme to utilize retinaldehyde as a substrate was assessed.

4.3. Results

4.3a. Cloning of the mouse aldehyde reductase cDNA.

In a differential display screen to identify retinoic acid-regulated genes in the mouse embryo (Chapter 3), a 257 bp cDNA fragment (DC43) that exhibited homology to several members of the AKR superfamily was isolated. Although transcriptional regulation of DC43 by retinoic acid was not consistent, its dynamic pattern of expression during embryogenesis and high homology to aldehyde reductase cDNAs cloned from human, pig and rat, prompted further study. To this end, a mouse E8.5 cDNA library was screened with the DC43 fragment in an attempt to isolate the corresponding full-length cDNA. Three positive plaques were identified, one of which contained the entire mouse aldehyde reductase ORF, as determined by end-sequencing. This clone was completely sequenced on both strands and the full-length nucleic acid and the deduced amino acid sequences are shown in Figure 4.1. The open reading frame from nucleotides 248 to 1225 of the 1320 bp cDNA encodes a predicted polypeptide of 325 amino acids, which is terminated by a TGA stop codon. The 5'- and 3'-UTRs are 247 bp and 95 bp in length, respectively. The 257-bp cDNA fragment isolated by differential display is underlined, and the putative polyadenylation signal (AATAAA) is shown in bold.

Comparison of the deduced amino acid sequence to that of the predicted coding regions of previously cloned aldehyde reductase cDNAs indicated that the mouse clone was 97%, 93%, and 91% identical to the rat, human, and pig sequences, respectively (Figure 4.2). The structural domains of the enzyme, as determined by X-ray crystallography of pig muscle aldehyde reductase (AKR1A2) (El Kabbani *et al.*, 1995), are indicated above the amino acid sequence. All members of the AKR superfamily, for which the three-dimensional structures have been solved, adopt an identical $(\alpha/\beta)_8$-barrel

Fig. 4.1. Nucleic acid and deduced amino acid sequence of *mouse aldehyde reductase (AKR1A4).* Nucleic acids are numbered on the right and amino acids on the left. The 1320 bp cDNA encodes a predicted 325 amino acid polypeptide. The underlined sequence corresponds to the 257 bp cDNA fragment number isolated by differential display. The *AKR1A4* cDNA sequence has been deposited into the GenBank database, accession number AF225564.

```
                        ttcggcacgagggaatgtgcaaagtcccagctttggcttctactcc   46
ctcttctacttcgcaggacagtgggggtctcctccgtcctgcgcgtagttctgggagccgggccctc  113
gctcctccctggggtggggctgccgcttctccgcccggacttaagtcgggccctgttgcctcagtac  180
tggagtgcagagctgaattcgggccactttgtcttttccacagcctgtgctcactgccaaggggaca  247

     atg acg gcc tcc agt gtc ctc ctg cac act gga cag aag atg cct ctg att  298
  1  Met Thr Ala Ser Ser Val Leu Leu His Thr Gly Gln Lys Met Pro Leu Ile

     ggt ctg ggg aca tgg aag agt gag cct ggt cag gtg aaa gca gcc att aaa  349
 18  Gly Leu Gly Thr Trp Lys Ser Glu Pro Gly Gln Val Lys Ala Ala Ile Lys

     cat gcc ctt agc gca ggc tac cgc cac att gat tgt gct tct gta tat ggc  400
 35  His Ala Leu Ser Ala Gly Tyr Arg His Ile Asp Cys Ala Ser Val Tyr Gly

     aat gaa act gag att ggg gag gcc ctg aag gag agt gtg ggg tca ggc aag  451
 52  Asn Glu Thr Glu Ile Gly Glu Ala Leu Lys Glu Ser Val Gly Ser Gly Lys

     gca gtc cct cga gag gag ctg ttt gtg aca tcc aag ctg tgg aat act aag  502
 69  Ala Val Pro Arg Glu Glu Leu Phe Val Thr Ser Lys Leu Trp Asn Thr Lys

     cac cac cct gag gat gta gaa cct gcc ctc cgg aag aca ctg gct gat ctg  553
 86  His His Pro Glu Asp Val Glu Pro Ala Leu Arg Lys Thr Leu Ala Asp Leu

     caa ctg gag tat ttg gac ctc tat ttg atg cac tgg cct tat gcc ttt gag  604
103  Gln Leu Glu Tyr Leu Asp Leu Tyr Leu Met His Trp Pro Tyr Ala Phe Glu

     cgg gga gac aat ccc ttt ccc aag aat gcc gat gga act gtc aga tat gac  655
120  Arg Gly Asp Asn Pro Phe Pro Lys Tyr Asp Ser Thr His Asn Ala Asp Gly

     tca act cac tat aaa gag acc tgg aag gct ctg gag gta ctg gtg gca aag  706
137  Thr Val Arg Tyr Lys Glu Thr Trp Lys Ala Leu Glu Val Leu Val Ala Lys

     ggg ctg gtg aaa gcc ctg ggc ttg tcc aac ttc aac agt cgg cag att gat  757
154  Gly Leu Val Lys Ala Leu Gly Leu Ser Asn Phe Asn Ser Arg Gln Ile Asp

     gat gtc ctc agt gtg gcc tct gtg cgc cca gct gtc ttg cag gtg gaa tgc  808
171  Asp Val Leu Ser Val Ala Ser Val Arg Pro Ala Val Leu Gln Val Glu Cys

     cat cca tac ctg gct cag aat gag ctc att gcc cac tgt cac gca cgg ggc  859
188  His Pro Tyr Leu Ala Gln Asn Glu Leu Ile Ala His Cys His Ala Arg Gly

     ttg gag gtg act gct tat agc ccc ttg ggt tcc tct gac cgt gct tgg cgc  910
205  Leu Glu Val Thr Ala Tyr Ser Pro Leu Gly Ser Ser Asp Arg Ala Trp Arg

     cat cct gat gag cca gtc ctg ctt gaa gaa cca gta gtc ttg gca cta gct  961
222  His Pro Asp Glu Pro Val Leu Leu Glu Glu Pro Val Val Leu Ala Leu Ala

     gaa aaa cat ggc cga tct cca gct cag atc ttg ctt aga tgg cag gtt cag 1012
239  Glu Lys His Gly Arg Ser Pro Ala Gln Ile Leu Leu Arg Trp Gln Val Gln

     cgg aaa gtg atc tgc atc ccc aaa agc atc aat cct tcc cgc atc ctt cag 1063
256  Arg Lys Val Ile Cys Ile Pro Lys Ser Ile Asn Pro Ser Arg Ile Leu Gln

     aac att cag gta ttt gat ttc acc ttt agc cca gag gag atg aaa caa tta 1114
273  Asn Ile Gln Val Phe Asp Phe Thr Phe Ser Pro Glu Glu Met Lys Gln Leu

     gat gct ctg aac aaa aat tgg cgg tat att gtg ccc atg att acg gtg gat 1165
290  Asp Ala Leu Asn Lys Asn Trp Arg Tyr Ile Val Pro Met Ile Thr Val Asp

     ggg aag agg gtt ccc aga gat gct gga cac cct ctg tat ccc ttt aat gac 1216
307  Gly Lys Arg Val Pro Arg Asp Ala Gly His Pro Leu Tyr Pro Phe Asn Asp

     cca tac tga gacctatagtttctcagcttccctttcagttctcctgctaagcattgcctgctac 1280
324  Pro Tyr End

     tccccagaaagaaggaatcaataaagccattgaagtgtaa                           1320
```

(TIM-barrel) fold. Additionally, three loops of variable size (A, B, and C), that are located on the C-terminal side of the barrel, are involved in substrate specificity and binding affinity. The amino acids that compose the α-helices and β-strands of the barrel, two β-strands and α-helices external to the barrel, and loops A, B and C, are indicated in Figure 4.2. Eleven amino acids involved in co-factor binding, structural integrity of the enzyme, and in the active site are conserved across all known AKR family members (Jez *et al.*, 1997a). These residues are also present in the predicted mouse aldehyde reductase protein (shaded residues, Figure 4.2). An additional eight amino acids, conserved in 41 of the 42 AKR family members, are also found in the mouse homologue (boxed residues, Figure 4.2.). Based on the high degree of homology to aldehyde reductase cDNAs from other species, we have named this clone *mouse aldehyde reductase* or *AKR1A4* in accordance with the proposed nomenclature for the aldo-keto reductase superfamily (Jez *et al.*, 1997b; 1997c). The cDNA sequence has been deposited in GenBank (accession number AF225564), and submitted to the AKR superfamily homepage (http://www.med.upenn.edu/akr).

4.3b. Expression of AKR1A4 during development.

Expression of *AKR1A4* was assessed by whole mount *in situ* hybridization from E7.5 to E13.5 (Figure 4.3). At E7.5 *AKR1A4* was weakly but broadly expressed (Figure 4.3B). One day later, *AKR1A4* transcripts became more restricted with the highest levels of expression observed in neural ectoderm (Figure 4.3C-3F) and gut endoderm (Figure 4.3E). In the neural ectoderm, there appeared to be a concentration of *AKR1A4* transcripts localized to a narrow region adjacent to the mesenchyme (Figure 4.3D-3F). In the closed neural tube, *AKR1A4* transcripts were excluded from the ventral most region (Figure 4.3F). Lower levels of message were detected at this stage in mesenchyme at the level of the open neural tube (Figure 4.3C and 4.3D), and in the somites (Figure 4.3F). At E9.0 expression of *AKR1A4* was maintained along the entire neural axis and in the gut endoderm (Figure 4.3G-J). High levels of expression were also observed in the ectoderm overlying the first branchial arch (Figure 4.3H), the otic placodes (Figure 4.3G and 4.3H), and in the tail bud mesenchyme (Figure 4.3J). At E9.5 and E10.5 *AKR1A4* was strongly expressed in the limb buds (Figure 4.3K and 4.4E), fronto- nasal mass, branchial arches,

Figure 4.2. Comparison of the predicted *AKR1A4* coding region to the amino acid sequences of aldehyde reductases isolated from other species. Amino acids are numbered on the left. Amino acids identical to the mouse AKR1A4 sequence are indicated by a dash. Differences in amino acid sequence are identified by the appropriate single letter code. Residues shaded in gray are conserved between all known AKR family members. Boxed residues are conserved between 41 of the 42 known AKR family members. Distinct structural regions of the protein, as determined by crystallographic studies, are indicated above the amino acid sequence. B and H indicate β-sheets and α-helices outside of the α/β-barrel core.

```
                        B1        B2        β1          α1          β2
AKR1A4(Mouse)   1   MTASSVLLHT GQKMPLIGLG TWKSEPGQVK AAIKHALSAG YRHIDCASVY
AKR1A3(Rat)         ---------- ---------- ---------- ----Y---V- ----------
AKR1A1(Human)       -A--C----- ---------- ---------- --V-Y---V- -------AI-
AKR1A2(Pig)         -A--C----- ---------- ---------- ----Y--TV- -------AI-

                          α2                    β3                  α3
AKR1A4(Mouse)  51   GNETEIGEAL KESVGSGKAV PREELFVTSK LWNTKHHPED VEPALRKTLA
AKR1A3(Rat)         ---------- -----A---- ---------- ---------- ----V-----
AKR1A1(Human)       ---P------ --D--P---- ---------- ---------- ----------
AKR1A2(Pig)         ---L------ T-T--P---- ---------- ---------- ----------

                        β4                Loop A                  α4
AKR1A4(Mouse)  101  DLQLEYLDLY LMHWRYAFER GDNPFPKNAD GTVRYDSTHY KETWKALEVL
AKR1A3(Rat)         ---------- ---------- ---------- ---K------ --------A-
AKR1A1(Human)       ---------- ---------- ---------- --IC------ --------A-
AKR1A2(Pig)         ---------- ---------- ---------- --I---A--- -D------A-

                        β5          α5                  β6          α6
AKR1A4(Mouse)  151  VAKGLVKALG LSNFNSRQID DVLSVASVRP AVLQVECHPY LAQNELIAHC
AKR1A3(Rat)         ---------- ----S----- ---------- ---------- ----------
AKR1A1(Human)       ------Q--- ---------- -I-------- ---------- ----------
AKR1A2(Pig)         ------R--- ----S----- ---------- ---------- ----------

                        β7        Loop B        HA          α7
AKR1A4(Mouse)  201  HARGLEVTAY SPLGSSDRAW RHPDEPVLLE EPVVLALAEK HGRSPAQILL
AKR1A3(Rat)         Q--------- ---------- ---------- ---------- ----------
AKR1A1(Human)       Q--------- ---------- -D-------- ---------- Y---------
AKR1A2(Pig)         Q--------- ---------- -D-N------ ----Q----- YN--------

                    α7      β8      α8                  HB       Loop C
AKR1A4(Mouse)  251  RWQVQRKVIC IPKSINPSRI LQNIQVFDFT FSPEEMKQLD ALNKNWRYIV
AKR1A3(Rat)         ---------- -----T---- ---------- ---------- ----------
AKR1A1(Human)       ---------- -----T---- ----K----- ---------N ----------
AKR1A2(Pig)         ---------- ----VT---- P--------- ---------- -----L-F--

                          Loop C
AKR1A4(Mouse)  301  PMITVDGKRV PRDAGHPLYP FNDPY*
AKR1A3(Rat)         ---------- ---------- ------
AKR1A1(Human)       --L------- ---------- ------
AKR1A2(Pig)         --L------- ---------- ------
```

% Identity
97.23
93.23
91.08

otic vesicle and tail bud (Figure 4.3K-3M). Expression in the neural tube was diminished at E9.5 (Figure 4.3L) and was no longer detectable by E10.5. At E11.5 high levels of *AKR1A4* transcripts were localized in the ectoderm and underlying mesoderm of the limb buds (Figure 4.3N, 4.3O, 4.4A and 4.4F) as well as in the tail (Figure 4.3N), with weaker expression in the surface ectoderm and adjacent mesenchyme of the trunk (Figure 4.3N-P). From E12.5 to E13.5, expression levels of *AKR1A4* in the facial region declined (Figure 4.3N, 4.3Q and 4.3S), and transcripts in the developing limbs became more restricted to the distal ectoderm and interdigital mesenchyme (Figure 4.3Q-T, 4.4B, 4.4C, 4.4G and 4.4H). By E14.5 expression in the forelimbs was absent (data not shown) and was restricted to the edges of the presumptive digits in the hindlimbs (Figure 4.4D). Analysis of *AKR1A4* expression in the developing lungs at E13.5 and E14.5 revealed a low background level throughout the mesenchyme, with markedly elevated expression in the segmental (Figure 4.5A and 4.5B) and terminal bronchi (Figure 4.5C and 4.5D).

4.3c. Expression of AKR1A4 in adult tissues.

Northern blot analysis revealed the presence of *AKR1A4* transcripts in all adult tissues examined (Fig. 4.6). However, levels varied markedly, with highest expression in the kidney and lowest in muscle and spleen. This expression pattern is similar to that observed for the cognate rat homologue (Takahashi *et al.*, 1993).

4.3d. Assessment of AKR1A4 function in the vitamin A metabolic pathway.

Retinoic acid is generated from its precursor, vitamin A or retinol (ROL), through a two step process. Alcohol dehydrogenase is capable of catalyzing the reduction of ROL to retinaldehyde (RAL), which is susbsequently reduced to RA by retinaldehyde dehydrogenase. As members of the AKR superfamily reduce a wide variety of aldehydes to alcohols, it was tempting to speculate that there may be a role for AKR1A4 in the vitamin A metabolic pathway. To test this hypothesis, F9 teratocarcinoma cells, stably transfected with the Sil-REM/β-gal-Neo reporter construct (Wagner *et al.*, 1992), were used. This reporter construct consists of a 64-bp region of the human RARβ promoter, containing a RARE, situated upstream of the gene encoding β-galactosidase (de The *et al.*, 1990; Sucov *et al.*, 1990). If AKR1A4 is able to convert RAL to ROL,

Figure 4.3. Expression of *AKR1A4* during mouse development. Whole mount *in situ* hybridization of antisense *AKR1A4* shown on intact (B-C, G, K, M-O, and Q-T) and sectioned (D-F, H-J, L, and P) mouse embryos. A negative control using sense *AKR1A4* riboprobe is shown in (**A**). (**B**) E7.5, anterior is . (**C**) E8.5, anterior is top. (**D-F**) Sections of E8.5 embryo as depicted in (C), dorsal is top. (**G**) E9.0, anterior is left. (**H-J**) Sections of E9.0 embryo as depicted in (G). (**H**) Anterior is top. (**I**) Dorsal is top. (**J**) Anterior is top. (**M**) E10.5, dorsal is right. (**N**) E11.5, dorsal is left. (**O**) E11.5, dorsal is facing viewer. (**P**) Transverse section of E11.5 embryo through trunk at the level of the hindlimb bud. (**Q-T**) Anterior is top. (**Q**) E12.5, dorsal is left. (**R**) E12.5, dorsal is facing viewer. (**S**) E13.5, dorsal is left. (**T**) E13.5, dorsal is facing viewer. **Scale Bars:** (A and G) 0.5 mm. (B and C) 0.25 mm. (D-F, H-J, L, and P) 0.1 mm. (K, M-O, and Q-T) 1 mm. **Abbreviations:** ba, branchial arch; fg, foregut; flb, forelimb bud; fnm, fronto-nasal mass; h, heart; hg, hindgut; hlb, hindlimb bud; ic, intra-embryonic coelomic cavity; mg, midgut; ne, neural epithelium; np, neural plate; oc, optic cup; op, otic placode; ov, otic vesicle; pc, pericardio-peritoneal canal; pnp, posterior neuropore; s, somite; se, surface ectoderm; tb, tailbud.

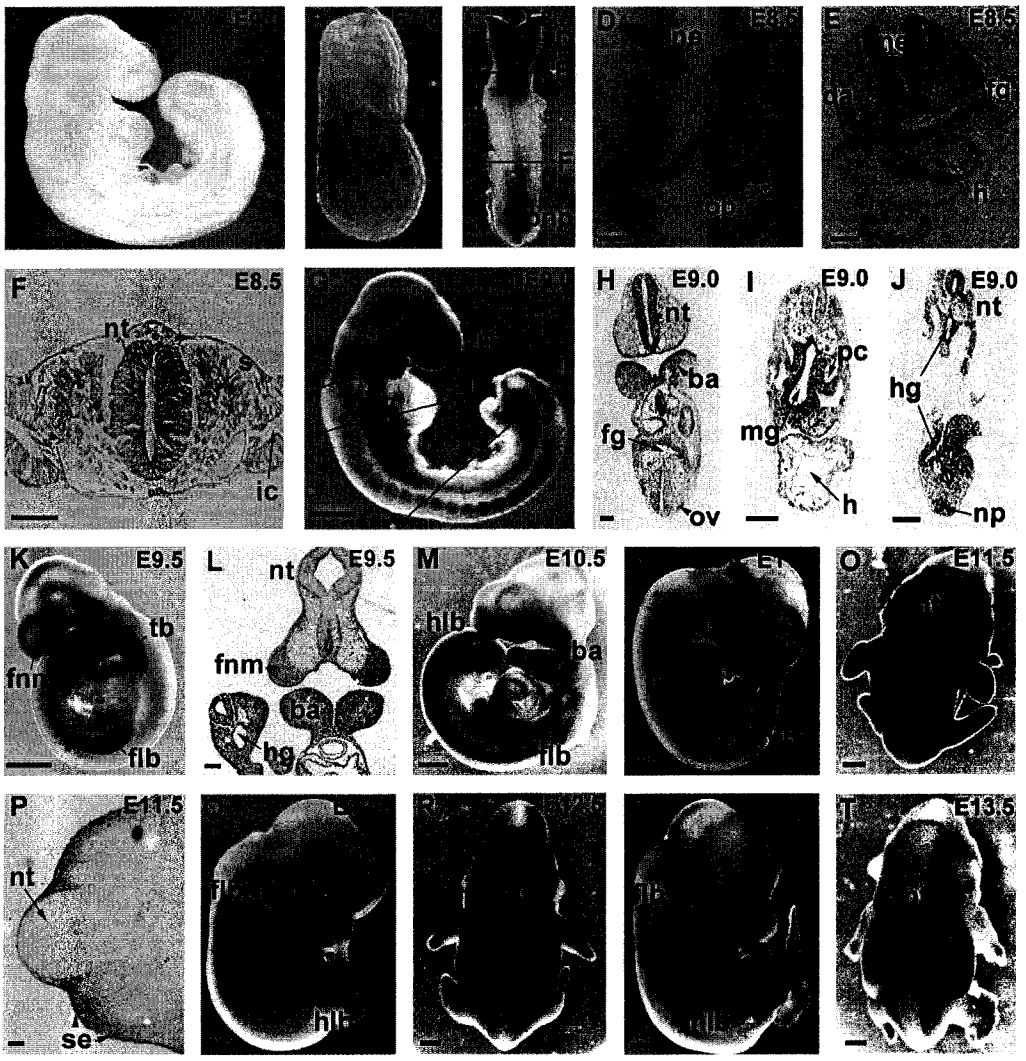
D
E8.5
E
E8.5
F
E8.5
nt
s
ic
H
E9.0
nt
ba
fg
ov
I
E9.0
pc
mg
h
J
E9.0
nt
hg
np
K
E9.5
tb
fnm
flb
L
E9.5
nt
fnm
ba
hg
M
E10.5
hlb
ba
flb
O
E11.5
P
E11.5
nt
se
hlb
T
E13.5

Figure 4.4. Expression of *AKR1A4* during development of the limbs. Whole mount *in situ* hybridization of antisense *AKR1A4* riboprobe shown on intact (A-D) and sectioned (E-H) limbs. (A-D) Distal is top. (**A**) E11.5, forelimb. (**B**) E12.5, forelimb. (**C**) E13.5, forelimb. (**D**) E14.5, hindlimb. (**E**) Frontal section of E9.5 forelimb bud, distal is left. (**F**) Transverse section of E11.5 forelimb, distal is left. (**G**) Frontal section through the three middle digits of an E12.5 limb, dorsal is top-left. (**H**) Frontal section through the three middle digits of an E13.5 limb, dorsal is top-left. **Scale Bars:** (A-D) 1 mm. (E-H) 0.1 mm. **Abbreviations:** idz, inter-digital zone; mc, mesenchymal condensation; se, surface ectoderm.

Figure 4.5. Expression of AKR1A4 during lung development. Whole mount *in situ* hybridization of antisense *AKR1A4* riboprobe shown on intact lungs (A-D). (A-D) Anterior is top. (**A** and **B**) E13.5 lungs. (**C** and **D**) E14.5 lungs. **Scale Bars**: (A-D) 1 mm. **Abbreviations**: sb, segmental bronchi; tb, terminal bronchi/bronchiole

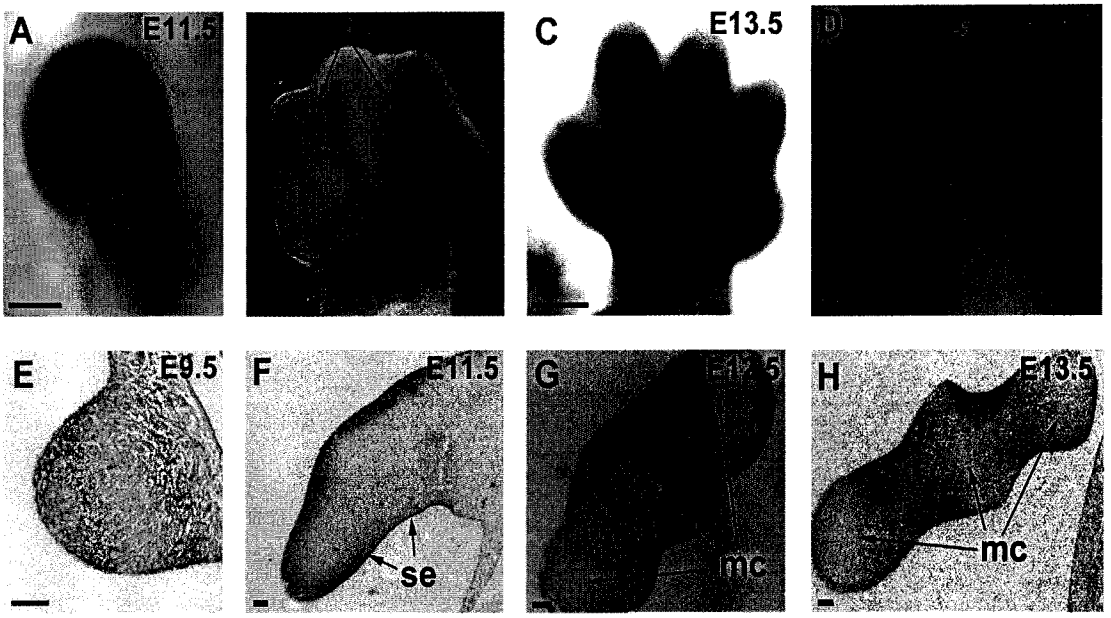
A
E11.5
C
E13.5
E
E9.5
F
E11.5
se
G
mc
H
E13.5
mc

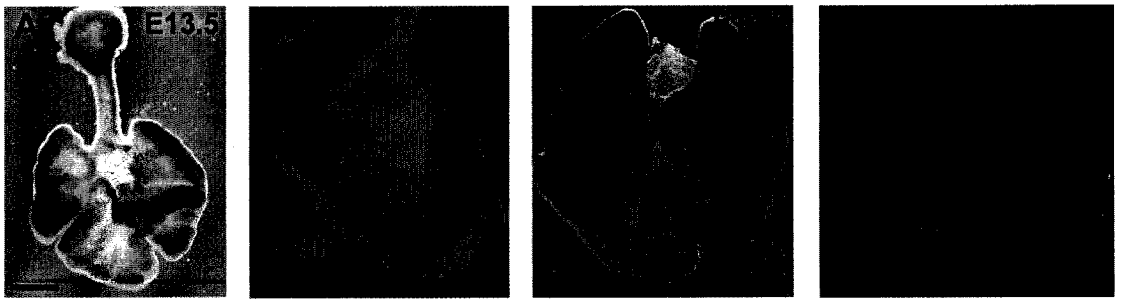
A
E13.5

Figure 4.6. Levels of *AKR1A4* mRNA in adult mouse tissues. A northern blot was prepared using 15 μg of total RNA isolated from adult mouse tissues. The blot was probed with ^{32}P-labeled *AKR1A4* cDNA, which hybridized to a single band of approximately 1.4 kb in size. Oligonucleotide hybridization to 18s ribosomal RNA was used to control for sample loading.

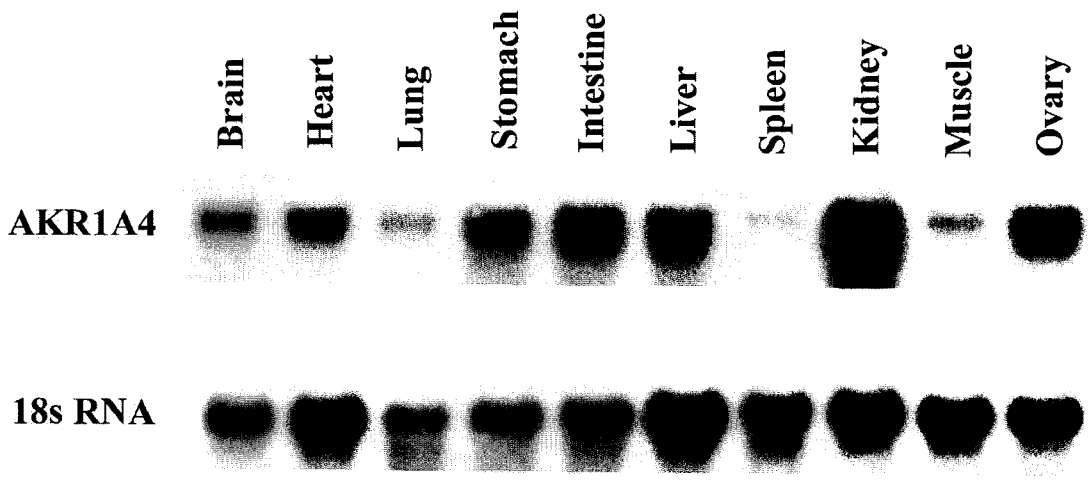
Brain
Heart
Lung
Stomach
Intestine
Liver
Spleen
Kidney
Muscle
Ovary
AKR1A4
18s RNA

diminished amounts of RAL would be present in cells that over-express this enzyme, as compared to control cells. Hence, less RA would be produced by retinaldehyde dehydrogenase resulting in decresed activity of the reporter gene. The role of AKR1A4 in vitamin A metabolism can also be assesed by supplementation of the media with excess retinoids (ROL, RAL, and RA). That is, if AKR1A4 reduces RAL, the addition of either ROL or RAL to the media of *AKR1A4*-over-expressing cells would result in lower levels of reporter gene activity than that achieved with ROL- or RAL-treated control cells. However, excess RA would result in similar levels of induction of the reporter gene in both cell lines as RA can not be converted into RAL.

The reporter cells were electroporated with a plasmid conferring puromycin resistance (pD503) and a 10-fold molar excess of either *AKR1A4* cDNA in a modified pSG5 expression vector (Green *et al.*, 1988), or the expression vector alone. One or two days following electroportation, puromycin was added to the media, in order to select for clones containing the pD503 plasmid. As a large excess of the expression vector was co-transfected along with pD503, it was probable that most of the puromycin resistant clones would have also incorporated the expression vector. After 7 to 10 days of selection, the resistant clones were pooled and plated into 96-well plates. At this point, puromycin was removed from the media. In order to determine whether *AKR1A4* overexpression had an effect on retinoid-induction of the RARE, cells were treated with retinoic acid, retinal, or retinol for various lengths of time ranging from 30 minutes to 24 hours (Figure 4.7). No significant difference was observed between cells transfected with the *AKR1A4* expression vector or empty vector at any of the time points. Similarly, F9 reporter cells transiently transfected with the *AKR1A4* expression construct, or empty vector, were treated with different concentrations of retinoid (retinoic acid, retinal, or retinol) ranging from 10^{-5} to 10^{-11} M for 24 hours (Figure 4.8). Again, no significant difference was observed due to the transfection of *AKR1A4*. Additionally, various concentrations (10^{-6} to 10^{-12} M) of an aldose reductase inhibitor (AL1576, Alcon Laboratories) which has also been shown to inhibit aldehyde reductase (IC_{50} = 0.06 μM, Barski *et al*, 1995) was added to the media of the F9 Sil-REM/β-gal-Neo reporter cells. After a 24-hour treatment with 10^{-8} to 10^{-6} M retinoic acid, retinal, or retinol, the β–galactosidase activity was assessed, and found to be the same irrespective of the

Figure 4.7. Fold-activation of the RARE-β-galactosidase reporter construct in response to length of retinoid treatment. F9 teratocarcinoma cells stably transfected with the Sil-REM/β-gal-Neo construct were co-transfected by electroporation with 50 μg of AKR1A4 cDNA in a modified pSG5 expression vector, or vector alone, and 5 μg of a plasmid conferring puromycin resistance (pD503). Puromycin resistant cells were treated with 10^{-6} M retinol, retinal, or retinoic acid in DMSO for the indicated length of time. Cells that were not treated with retinoids were treated with an equivalent amount of DMSO for 24 hours. Relative β-galactosidase activity was assessed by O.D. at 405 nm after incubation with ONPG. Results are expressed as the mean (+/- S.D.) of 4 samples, relative to the untreated sample transfected with empty vector (arbitrarily set to a value of 1). All values were corrected for protein concentration.

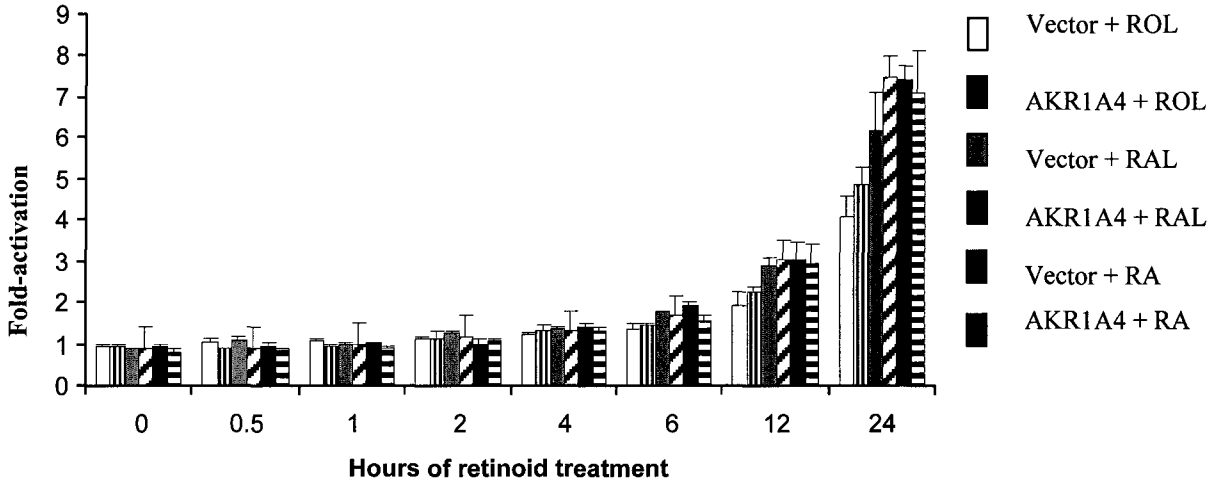
Fold-activation
9
8
7
6
5
4
3
2
1
0
0
0.5
1
2
4
6
12
24
Hours of retinoid treatment
Vector + ROL
AKR1A4 + ROL
Vector + RAL
AKR1A4 + RAL
Vector + RA
AKR1A4 + RA

Figure 4.8. Fold-activation of the RARE-β-galactosidase reporter construct in response to retinoid concentration. F9 SIL 15 cells transiently transfected with either the AKR1A4 expression vector, or vector alone, were treated with 10^{-11} to 10^{-5} M retinol (A), retinal (B), or retinoic acid (C) for 24 hours. Cells that were not treated with retinoids were treated with an equivalent amount of DMSO for 24 hours. Relative β-galactosidase activity was assessed by O.D. at 405 nm after incubation with ONPG. Results are expressed as the mean (+/- S.D.) of 4 samples, relative to the untreated sample transfected with empty vector (arbitrarily set to a value of 1). All values were corrected for protein concentration.

A

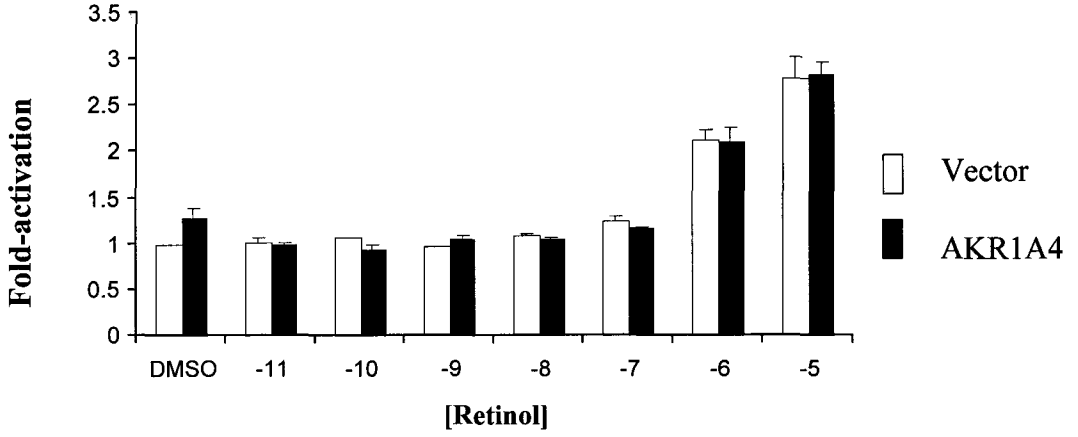
Fold-activation
3.5
3
2.5
2
1.5
1
0.5
0
DMSO
-11
-10
-9
-8
-7
-6
-5
[Retinol]
Vector
AKR1A4

B

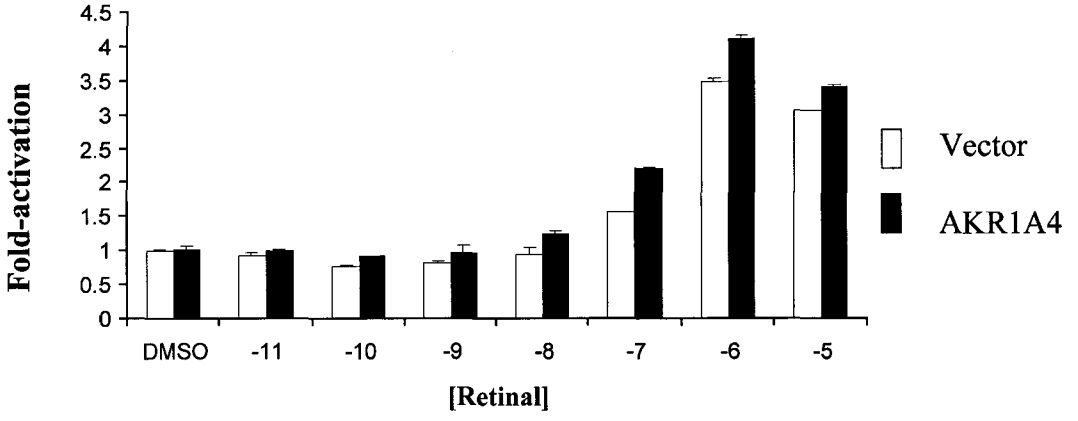
Fold-activation
4.5
4
3.5
3
2.5
2
1.5
1
0.5
0
DMSO
-11
-10
-9
-8
-7
-6
-5
[Retinal]
Vector
AKR1A4

C

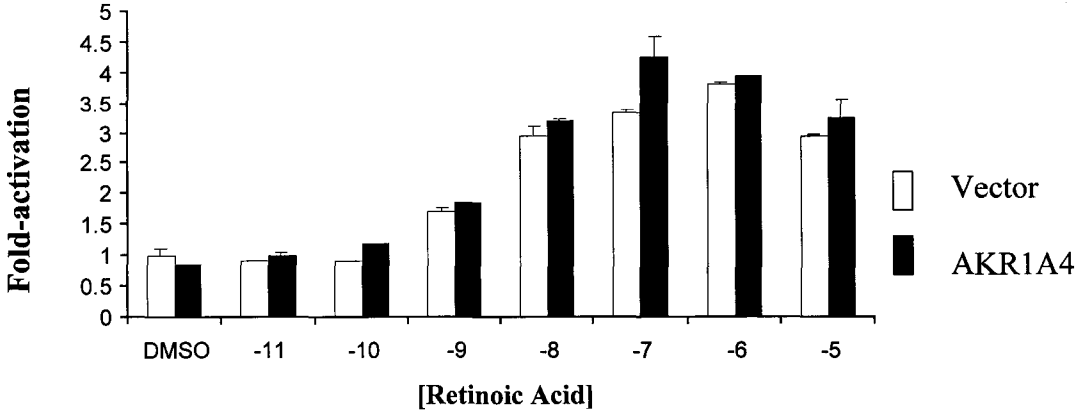
Fold-activation
5
4.5
4
3.5
3
2.5
2
1.5
1
0.5
0
DMSO
-11
-10
-9
-8
-7
-6
-5
[Retinoic Acid]
Vector
AKR1A4

presence of AL1576 (data not shown). Finally, AKR1A4 was not able to utilize retinaldehyde or retinol as a substrate as assessed by HPLC (Dr. Glenn Jones, Queen's University). Taken together, these results indicate that AKR1A4 does not alter the bio-available levels of retinoic acid in F9 teratocarcinoma cells.

4.4. Discussion

4.4a. Summary

A cDNA fragment encoding a portion of the mouse homologue of aldehyde reducatse, a member of the aldo-keto reductase superfamily, was cloned by differential display PCR (Chapter 3). The full-length cDNA (designated *AKR1A4*) was isolated, sequenced, and its expression during development was analyzed by whole mount *in situ* hybridization. *AKR1A4* was expressed in several distinct tissues and structures of the developing embryo including the limb buds, neural tube, branchial arches, gut, and lungs. In the adult, *AKR1A4* messages were detected in all tissues examined, however, the levels of expression were varied. The ability of AKR1A4 to metabolize retinaldehyde was assessed by measuring the bio-available levels of retinoic acid in F9 cells in the presence or absence of exogenous *AKR1A4* cDNA. The results obtained with this system suggest that AKR1A4 is not involved in the vitamin A metabolic pathway.

4.4b. A potential role for AKR1A4 during development

The expression pattern of *AKR1A4* during development appears to be pronounced in some structures undergoing high rates of growth. For example, transcripts are abundant in the branchial arches, limb buds, and tail bud, all of which contain rapidly dividing cells. As ALR catalyzes the reduction of toxic 2-oxo-aldehydes (Kanazu *et al.*, 1991; Vander Jagt *et al.*, 1992; Takahashi *et al.*, 1993), and these metabolites are likely produced in regions of pronounced growth, it is conceivable that AKR1A4 may play a protective role during embryonic development. In support of this hypothesis, the frequency of infants with congenital malformations born to diabetic mothers is two- to four-fold higher than that of the normal population (Kucera, 1971; Soler *et al.*, 1976; Mills, 1982). The spectrum of defects includes transposition of the great vessels,

ventricular septal defect, situs inversus, caudal regression syndrome, anencephaly, ureteral duplication, renal agenesis and anal-rectal atresia (Gabbe, 1977; Mills *et al.*, 1979). Some of these defects can be elicited in animal models by experimentally induced diabetes (Eriksson, 1988), or by culturing embryos in the presence of high concentrations of glucose (Cockroft *et al.*, 1977; Fine *et al.*, 1999). Significantly, Eriksson *et al.* (1998) found that the levels of 3-deoxyglucosone (3-DG) were seventeen times higher in rat embryonic tissues cultured in the presence of 50 mM glucose compared to those cultured in media alone, indicating that this protein cross-linker may be involved in hyperglycemia-induced malformations. Indeed, cultured rat embryos exhibited a malformation score that positively correlated with the amount of 3-DG in the media (Eriksson *et al.*, 1998). The severity and frequency of the defects were lessened if superoxide dismutase was also added to the media, presumably due to the reduction of reactive oxygen species that are produced by advanced glycation end products (AGEs; Yan *et al.*, 1994). Consistent with these findings, several antioxidants have previously been shown to inhibit hyperglycemia-induced embryo malformations *in vitro* and *in vivo* (Eriksson and Borg, 1991; Hagay *et al.*, 1995; Siman and Eriksson, 1997; Yang *et al.*, 1998). Recently, methylglyoxal was shown to induce malformations when administered to the common toad, *Bufo bufo*, during development (Amicarelli *et al.*, 1998). The authors concluded that the methylglyoxal-induced malformations are likely due to inhibition of cell division during earlier stages of development.

Several studies have been published that document the effect of ALR, and other members of the AKR superfamily, on aldehyde-induced cytotoxicity. For example, PC12 cells are protected against the cytotoxic effect of methlyglyoxal and 3-DG when rat ALR (AKR1A3) is overexpressed (Suzuki *et al.*, 1998). Conversely, inhibition of ADR by ONO-2235 reduces the viability of hepatoma cells treated with 3-DG (Takahashi *et al.*, 1995). In addition to potentially harmful metabolic products, ALR is also capable of reducing xenobiotics used in the treatment of cancer, such as daunorubicin and acetohexamide (Ahmed *et al.*, 1981; Ohara *et al.*, 1995).

Together these results demonstrate that high levels of 2-oxo-aldehydes are detrimental to the developing embryo and that AKR1A4 is capable of detoxifying such substances. The generation of mice that are homozygous null for *ADR* (*AKR1B3*) has

recently been described (Ho *et al.*, 2000). Although these mice suffer from a partial inability to concentrate urine, they have no detectable developmental or reproductive abnormalities. The expression pattern of this enzyme has not been studied during embryogenesis, therefore it is not known whether *AKR1B3* transcripts, if expressed, are co-localized with those of *AKR1A4*. If the expression patterns overlap this might suggest that these two enzymes are functionally redundant during development as ADR is also capable of metabolizing 2-oxo-aldehydes (Vander Jagt *et al.*, 1992; Sato *et al.*, 1993). However, if *AKR1B3* does not overlap with *AKR1A4*, this may indicate that AKR1A4 has a unique role in embryogenesis. To this end, it would be interesting to generate *AKR1A4* null mice by homologous recombination, and to observe whether such embryos exhibit malformations similar to those that are induced by excess 3-DG. An alternative hypothesis is that mouse embryos may develop properly in the absence of AKR1A4 under normal conditions, however, they may be more sensitive to malformations induced by 2-oxo-aldehydes in pathological situations, such as diabetes mellitus.

4.4c. Retinoids and AKR1A4

As members of the aldo-keto reductase superfamily reduce a wide variety of aldehydes to alcohols, AKR1A4 was assessed for its ability to reduce retinaldehyde to retinol. This was accomplished using a F9 cell reporter cell line that measures the bio-available levels of RA. It was hypothesized that if AKR1A4 has an effect on the vitamin A metabolic pathway it would be reflected by a decrease in the amount of the final product, that is, RA. No significant difference of reporter activity was observed in the presence of AKR1A4 irrespective of the level, or time, of incubation with any retinoids. In this regard, *AKR1A4* is abundantly expressed in F9 cells (data not shown) which may confound the interpretation of these results. However, the ability of AKR1A4 to reduce retinaldehyde was also assessed by HPLC in a different system (Dr. Glenn Jones, Queen's University) and again, no such activity was observed. Consistent with these data, it has never been demonstrated that other members of the AKR superfamily can utilize retinaldehyde as a substrate.

4.4d. Conclusions

Although the expression of *AKR1A4* does not appear to be regulated by RA, and this enzyme is not apparently involved in the vitamin A metabolic pathway, its interesting pattern of expression in the mouse embryo suggests that AKR1A4 may play an important role in the development of several structures. It would be very interesting to determine the extent of this role, and whether this enzyme is involved in diabetes-induced congenital malformations.

Chapter 5

RARγ and *Cdx1* act synergistically in vertebral patterning

5.1 Abstract

Retinoic acid signaling is involved in antero-posterior patterning of the vertebral column. Disruption of the *RAR* genes during development results in anterior homeotic transformations of the cervical vertebrae. Conversely, posterior homeotic transformations and malformations are evident in the vertebrae of newborn mice that were exposed to excess RA at E7.5. *Hox* genes are expressed to distinct rostral boundaries in the somites and prevertebrae, and are instrumental in antero-posterior patterning of the vertebral column. RA-induced transformations are correlated with anteriorizations of the limit of *Hox* gene expression in the prevertebrae. However, many of the *Hox* genes that are affected by RA treatment do not appear to contain RAREs, suggesting that the effect of RA on *Hox* gene expression is mediated through another transcription factor. The members of the *Cdx* family in the mouse are homologues of the *Drosophila caudal* gene, and are involved in antero-posterior specification of the vertebral column. The *Cdx* genes encode transcription factors that are capable of binding elements present in the promoters of some *Hox* genes. *Cdx1* homozygous null mutants exhibit anterior homeotic transformations that are reminiscent of those observed in RARγ null offspring, and *Cdx1* null embryos display posteriorized limits of *Hox* gene expression in the somites and prevertebrae. *Cdx1* has recently been demonstrated to be a direct target of RA signaling in the mouse embryo. However, the contribution of *Cdx1* downstream of RAR signaling *in vivo* is unknown. This chapter describes the generation and skeletal analysis of a complete allelic series of *Cdx1/RARγ* mutants. The results demonstrate that *Cdx1* is likely required downstream of RA-signaling, but also that *Cdx1* and *RARγ* also act in parallel to affect the specification of certain vertebrae. Moreover, the interaction between *Cdx1* and *RARγ* appears to be synergistic. These findings further support a model by which RA can affect the expression of *Hox* genes that do not have functional RAREs in their regulatory regions.

5.2 Introduction

In the mouse, formation of the body axis commences on the sixth day of gestation with the induction of the primitive streak in the posterior region of the embryo (reviewed in Beddington and Robertson, 1999). Ectodermal cells that ingress through the anterior region of the primitive streak during gastrulation give rise to paraxial mesoderm, which subsequently segments and differentiates into somites (Wilson and Beddington, 1996; Tam and Behringer, 1997). These epithelial structures give rise to demomyotome, which will form dermis and striated muscle, and sclerotome, which forms the components of the vertebrae. Each vertebral unit in the axial column is unique with respect to its antero-posterior (AP) position, which is reflected by distinct, although often subtle, morphological characteristics. Following the discovery that *Hox* genes are expressed in the developing vertebral column, and that their anterior boundaries of expression are staggered along the length of the axis, it was suggested that vertebral AP identity may be imparted through the expression of a combination of *Hox* genes; such that each distinct vertebra is specified by a unique '*Hox* code' (Kessel and Gruss, 1991). This hypothesis is strongly supported by the skeletal phenotypes of mice that have altered *Hox* gene expression. In general, ectopic activity of a *Hox* gene anterior to its normal limit of expression, results in posterior transformations of the vertebrae, while loss of expression leads to anterior transformations. However, several exceptions to this rule have been documented, and in some cases both anterior and posterior transformations occur due to the loss of a single *Hox* gene (i.e. Horan *et al.*, 1994, 1995a; Saegusa *et al.*, 1996).

Apart from *Hox* genes themselves, loss, or diminished activity, of several different gene products, including *Fgfr1* (Partanen *et al.*, 1998), *ActRIIB* (Oh and Li, 1997), *Mll* (Yu *et al.*, 1995), and *Cdx1* and *Cdx2* (Subramanian *et al.*, 1995: Chawengsaksophak *et al.*, 1997), leads to abnormal vertebral specification. Administration of retinoic acid (RA) to pregnant mice at various stages of gestation also results in homeotic transformations of the vertebrae (Kessel and Gruss, 1991; Kessel, 1992). The direction of transformation, and the axial level affected, is dependent on the developmental stage at which the embryos are exposed to RA. Posterior transformations induced by RA-treatment at E7.5 are correlated with anteriorized limits of *Hox* gene expression in the prevertebrae, while anterior transformations induced at later stages are

correlated with posteriorized expression boundaries of *Hox* genes located more 5' in the *Hox* clusters. Skeletal analysis of mice lacking specific *RARs* has demonstrated the requirement of these receptors for normal vertebral specification. *RARγ* null mice exhibit anterior transformations of the cervical vertebrae at a relatively low incidence (Lohnes *et al.*, 1993), and the frequency of these transformations increases in a gene-dosage-dependent manner when additional *RAR* genes are also non-functional (Lohnes *et al.*, 1994). Therefore, a precise level of RA signaling appears to be necessary for correct AP specification of the vertebral column.

RARs form heterodimeric complexes with RXRs and activate transcription by binding to retinoic acid response elements (RAREs) in the promoters or enhancer regions of target genes (reviewed in Mangelsdorf *et al.*, 1995). RAREs have been identified in the 5' or 3' regions of *Hox* genes belonging to paralogue groups 1 and 4. Point mutation or deletion of these elements leads to reduced expression of the corresponding *Hox* gene in the CNS and lateral plate mesoderm, confirming a direct level of *Hox* regulation by RARs (Langston and Gudas, 1992; Moroni *et al.*, 1993; Pöpperl and Featherstone, 1993; Marshall *et al.*, 1994; Studer *et al.*, 1994; Frasch *et al.*, 1995; Morrison *et al.*, 1996; Dupé *et al.*, 1997; Gould *et al.*, 1998; Huang *et al.*, 1998; Packer *et al.*, 1998). However, the anterior limit of *Hox* expression in the somites is not affected in any of these mutants, although a 5' RARE in the mouse *Hoxd4* gene is part of a paraxial mesoderm enhancer (Zhang *et al.*, 1997a).

The *caudal* family of homeobox-containing transcription factors is conserved across several species and appears to be required for correct segmentation, and for the specification of the posterior-most portion of the developing embryo (reviewed in Freund *et al.*, 1998). In the mouse, the *caudal*-related gene family consists of three members, *Cdx1*, *Cdx2* and *Cdx4*, each of which are expressed in an overlapping, nested expression pattern in the caudal embryo (Meyer and Gruss, 1993; Gamer and Wright, 1993; Beck *et al.*, 1995). *Cdx1* homozygous null, and *Cdx2* heterozygous skeletons exhibit multiple anterior homeotic transformations in the cervical and thoracic regions of the vertebral column (Subramanian *et al.*, 1995; Chawengsaksophak *et al.*, 1997). Moreover, the anterior limit of expression of several *Hox* genes is shifted posteriorly by one or two prevertebra in the *Cdx1* null mutant embryos (Subramanian *et al.*, 1995). Several

homeotic transformations observed in the *Cdx1* mutants are also exhibited in *RARγ* mutant skeletons, although at a lower incidence (Lohnes *et al.*, 1993). Recently, Houle *et al.,* (2000) demonstrated that *Cdx1* is positively regulated by excess RA in the caudal embryo from E7.5 to E9.5. Moreover, in *RARα1γ* double mutant embryos both the endogenous, and RA-induced, expression of *Cdx1* is reduced compared to untreated and RA-treated wild type embryos, respectively. A RARE is present in the region 5' to the *Cdx1* transcriptional start site, and is capable of binding RAR/RXR heterodimers (Houle *et al.*, 2000). Taken together, these results suggest that *Cdx1* may directly mediate the RAR signal that results in homeotic transformations of the vertebral column.

In order to investigate the relationship between *Cdx1* and *RARγ*, the complete series of *Cdx1/RARγ* compound mutant mice was generated and their skeletons scored for vertebral transformations and malformations. Additionally, the involvement of *Cdx1* in RA-induced homeotic transformations initiated at E7.4, and the effect of RA on the anterior transformations characteristic of *Cdx1* null skeletons was also examined. The results suggest that *Cdx1* acts both downstream of, and in parallel to, retinoid signaling in vertebral specification.

5.3 Results

5.3a. Generation of compound RARγ/Cdx1 mutant mice

For the sake of brevity, the symbols $^{+/-}$ and $^{-/-}$ will be used to designate heterozygous and homozygous null genotypes, respectively. *Cdx1*$^{-/-}$ (Subramanian *et al.*, 1995) and *RARγ*$^{+/-}$ (Lohnes *et al.*, 1993) mice were mated to generate *Cdx1*$^{+/-}$ and *Cdx1*$^{+/-}$ *RARγ*$^{+/-}$ offspring. From these progeny, the appropriate crosses were established to produce a complete allelic series of *Cdx1* and *RARγ* compound mutant mice on the same mixed genetic background (i.e. wild type, *RARγ*$^{+/-}$, *RARγ*$^{-/-}$, *Cdx1*$^{+/-}$, *Cdx1*$^{-/-}$, *Cdx1*$^{+/-}$ *RARγ*$^{+/-}$, *Cdx1*$^{+/-}$*RARγ*$^{-/-}$, *Cdx1*$^{-/-}$*RARγ*$^{+/-}$ and *Cdx1*$^{-/-}$*RARγ*$^{-/-}$). Newborn mice, or E18.5 fetuses, were collected and prepared for skeletal analysis as described in Chapter 2, Section 2.2.

As originally reported by Subramanian *et al.* (1995), all *Cdx1*$^{-/-}$ mice were viable and fertile, and the loss of one allele of the *RARγ* gene had no detrimental effect on the

ability to survive to adulthood or reproduce. Genotypic analysis of 55 newborn mice, generated from *Cdx1*$^{-/-}$*RARγ*$^{+/-}$ intercrosses, indicated that there were 13 (24%) *Cdx1*$^{-/-}$, 26 (47%) *Cdx1*$^{-/-}$*RARγ*$^{+/-}$, and 16 (29%) *Cdx1*$^{-/-}$*RARγ*$^{-/-}$ offspring. These numbers are in concordance with those predicted by Mendelian genetics, therefore, the *Cdx1/RARγ* double mutant genotype does not appear to result in embryonic lethality. Newborn mice of different genotype were not distinguishable by their outward appearance, except for the presence of shiny skin that is correlated with the loss of *RARγ* (unpublished observations). Occasionally, the double mutants appeared slightly smaller and sometimes exhibited a hunched posture (data not shown). The vertebral homeotic transformations and malformations observed in the *Cdx1/RARγ* compound mutants are summarized in Table 5.1 and are discussed in detail below.

In the mouse, the wild type vertebral column is typically composed of seven cervical (C1-C7), thirteen thoracic (T1–T13), six lumbar (L1-L6), three or four sacral (S1-S4), and thirty-one caudal vertebrae that form the tail. Some of the vertebrae possess unique characteristics that facilitate their identification (refer to Figure 5.1A-D and Figure 5.6). For example, the first cervical vertebra (C1 or atlas) has thick neural arches, lacks a true vertebral body, and possesses a ventrally located tubercle termed the anterior arcus atlantis (AAA). The neural arches of C2 (axis) are not as broad as those of C1; however, they are thicker than those of the more posterior cervical vertebrae. Additionally, C2 possesses two vertebral bodies, the second of which (the dens axis) is composed of material derived from C1, and is located directly anterior to the vertebral body of the axis. Vertebrae C3 to C5 are virtually identical to one another and can be identified by the presence of a foramen transversum, and articular processes that extend in the plane of the body. C6 carries two ventral structures, the anterior tuberculi, and C7 closely resembles C3 to C5, except it lacks the foramen transversum. Each of the thoracic vertebrae bears one pair of ribs, and the first seven of these pairs (T1-T7) attach to the sternum. The second thoracic vertebra can be distinguished by a large dorsally protruding spinous process. In this study, only the cervical, thoracic and lumbar vertebrae were examined.

5.3b. Cdx1 homozygous null mutant phenotype

The skeletal phenotype of *Cdx1*$^{-/-}$ mice has been previously described (Subramanian *et al.*, 1995). *Cdx1* null mutants exhibit transformations of the entire cervical region such that each vertebra displays a morphology characteristic of the next most anterior vertebra (Table 5.1 and Figure 5.1). This results in the loss of the C7 morphology, as vertebra eight (T1) always carries a rib in these mutants. However, it was noted that the vertebral body of T1 displayed some characteristics of C7, indicating a partial anterior transformation (Subramanian *et al.*, 1995). The first cervical vertebra is transformed to resemble, and is also frequently fused to, the occipital bones of the skull (Figure 5.1E-H). Additionally, the AAA of vertebra 1 is incorporated into the basioccipital, and is correlated with an increase in the length of this bone (Figure 5.1G and H). Anterior transformations were also observed in the anterior thoracic vertebrae, and the first two ribs were often fused to each other before joining to the sternum. The types of vertebral transformations observed in the present study were identical to those reported by Subramanian *et al.*, however, an increased penetrance of all of the transformations was noted (Table 5.1). Additionally, a higher expressivity of the T1 to C7 anterior transformation was observed, as detected by the absence of ribs on vertebra 8 in 38% of the *Cdx1* null specimens (Table 5.1). As the penetrance of homeotic transformations and malformations in the vertebrae of *Cdx1* null mice is different between genetic strains (i.e. C57BL/6 vs. 129/SV; Subramanian *et al.*, 1995) the increased penetrance and expressivity observed in this study may be due to modifiers in the mixed genetic background.

5.3c. Cdx1 heterozygous mice

In concordance with the higher penetrance of homeosis observed in the *Cdx1*$^{-/-}$ skeletons in this study, anterior transformations and vertebral malformations were observed in 82% of the *Cdx1*$^{+/-}$ mice on this background; whereas no abnormalities were detected in the previously described heterozygotes (Subramanian *et al.*, 1995). Caudal extension of the basioccipital or the fusion of this bone to the AAA of C1 was observed in 18% and 13% of the skeletons, respectively (Figure 5.2B and E). Malformation of the neural arches was observed in both C1 (16%) and C2 (42%) (Figure 5.2C and F), and

Table 5.1. Vertebral phenotypes of compound Cdx1/RARγ mutant mice

	Genotype								
	WT	$\gamma^{+/-}$	$\gamma^{-/-}$	$Cdx1^{+/-}$	$Cdx1^{-/-}$	$Cdx1^{+/-}\gamma^{+/-}$	$Cdx1^{+/-}\gamma^{-/-}$	$Cdx1^{-/-}\gamma^{+/-}$	$Cdx1^{-/-}\gamma^{-/-}$
	n=23	n=38	n=27	n=38	n=29	n=42	n=15	n=32	N=20
Abnormal phenotype	(%)	(%)	(%)	(%)	(%)	(%)	(%)	(%)	(%)
Basioccipital									
Fusion to AAA	-	-	1 (4)	5 (13)	29 (100)	3 (7)	6 (40)	32 (100)	20 (100)
Extension	-	-	2 (7)	7 (18)	-	16 (38)	3 (20)	-	-
Vertebrae 1									
Fusion to occipitals[f]	-	-	-	-	29 (100)	-	-	32 (100)	20 (100)
Malformed NA[g]	-	-	-	6 (16)[d]	-	4 (10)[c]	9 (60)[e]	1 (3)[a]	-
Fusion to V2									
Dorsal	-	-	-	-	-	2 (5)[a]	7 (47)[e]	4 (13)[c]	-
Ventral[h]	-	-	1 (4)	4 (11)	-	1 (2)	6 (40)	1 (3)	-
Vertebrae 2									
Complete C1 identity	-	-	-	-	29 (100)	-	-	32 (100)	20 (100)
Partial C1 identity									
AAA	-	-	3 (11)	17 (44)	-	21 (50)	13 (87)	-	-
Thick NA	-	3 (8)[a]	11 (41)[d]	17 (44)[d]	-	34 (81)[d]	5 (33)[d]	-	-
Malformed NA	-	-	-	16 (42)[e]	-	11 (26)[c]	8 (53)[d]	4 (13)[c]	1 (5)[a]
Fusion to V3									
Dorsal	-	-	-	3 (8)[a]	-	3 (7)[a]	4 (27)[d]	-	-
Ventral	-	-	-	7 (18)	4 (14)	7 (17)	1 (7)	2 (6)	-
Vertebrae 3									
Complete C2 identity	-	-	-	-	29 (100)	-	-	32 (100)	20 (100)
Malformed/Thick NA	-	-	-	-	-	2 (5)[c]	8 (53)[d]	-	-
Vertebrae 6									
No TA	-	-	-	1 (4)[a]	29(100)	5 (12)[a]	2 (13)[a]	31 (97)[b]	20 (100)
Vertebrae 7									
TA	-	-	-	-	28 (97)[b]	4 (10)[a]	2 (13)[a]	32 (100)[d]	20 (100)
Rib	-	1 (3)[a]	-	-	-	-	-	-	-
Vertebrae 8									
C7 identity (+/ - buds)	-	-	-	-	11 (38)[d]	-	-	16 (50)[c]	16 (80)[d]
Incomplete rib	-	-	-	-	18 (62)[d]	-	-	16 (50)[e]	4 (20)[b]
Spinous process on:									
V10	-	-	-	-	6 (27)[i]	-	1 (7)	7 (22)	9 (45)
V8 and V9	-	1 (3)	1 (4)	-	-	-	-	-	-
V9 and V10	-	1 (3)	2 (7)	-	6 (27)[i]	-	4 (27)	15 (47)	8 (40)
Cervical vertebrae:									
6	-	1 (3)[a]	-	-	-	-	-	-	-
8	-	-	-	-	11 (38)[d]	-	-	15 (47)[c]	16 (80)[d]
Rib-bearing vertebrae: 12	-	-	-	-	13 (45)[e]	-	-	14 (44)[e]	8 (40)[d]
14	1 (4)[b]	4 (11)[a]	15 (56)[e]	-	2 (7)[e]	-	9 (60)[e]	4 (13)[e]	3 (15)[a]
Ribs attached to sternum: 6	-	-	-	-	6 (21)[a]	-	-	1 (3)[a]	-
8	4 (17)[a]	6 (16)[c]	21 (78)[c]	9 (24)[c]	4 (14)[a]	16 (38)[d]	14 (93)[d]	6 (19)[a]	-
Lumbar vertebrae:									
5	4 (17)	4 (11)	15 (56)	4 (11)	6 (21)	6 (14)	9 (60)	6 (19)	15 (75)
Vertebral pattern:									
C6/T14/L6	-	1 (3)[a]	-	-	-	-	-	-	-
C7/T12/L6	-	-	-	-	-	-	-	-	-
C7/T13/L5	3 (13)[c]	2 (5)[b]	-	4 (11)[d]	2 (7)[e]	6 (14)[d]	-	1 (3)[a]	-
C7/T13/L6	19 (83)[d]	32 (84)[d]	12 (44)[d]	34 (89)[d]	14 (48)[d]	36 (86)	6 (40)[b]	14 (44)[b]	2 (10)[b]
C7/T14/L5	1 (4)[b]	2 (5)[a]	15 (56)[e]	-	2 (7)[e]	-	9 (60)[e]	4 (13)[e]	6 (30)[a]
C7/T14/L6	-	1 (3)[a]	-	-	-	-	-	1 (3)[a]	-
C8/T12/L5	-	-	-	-	-	-	-	1 (3)[a]	-
C8/T12/L6	-	-	-	-	10 (34)[c]	-	-	11 (34)[c]	5 (25)[c]
C8/T13/L5	-	-	-	-	2 (7)[a]	-	-	3 (9)[c]	13 (65)[e]
C8/T13/L6	-	-	-	-	1 (3)[b]	-	-	1 (3)[a]	-

a, all unilateral; **b**, all bilateral, **c**, mostly unilateral; **d**, mostly bilateral; **e**, equal number of unilateral and bilateral; **f**, includes incorporation of AAA; **g**, includes fusions; **h**, fusion of AAA to vertebral body of C2; **i**, only 22 skeletons were scored for this phenotype, the percentages are based on the number scored.

Figure 5.1. Wild type and *Cdx1* homozygous null skeletal phenotypes. (A-D) Wild type skeletons. (**A**) Lateral view of cervical vertebrae; dorsal is right. (**B**) Upper specimen: ventral view of basioccipital and exoccipitals; anterior is top. Lower specimen: anterior view of vertebrae 1; ventral is top. (**C**) Lateral view of thoracic vertebrae; dorsal is top. (**D**) Ventral view of lumbar vertebrae; anterior is top. (E-H) *Cdx1* homozygous null skeletons. (**E** and **F**) Lateral view of cervical vertebrae; dorsal is right. Note the fusion of the first and second ribs (arrow). (**G** and **H**) Ventral view of basioccipital, exoccipitals, and vertebrae 1 (fused to occipitals); anterior is top. (E and G) *Cdx1*$^{-/-}$ skeleton that exhibits a low degree of fusion between C1 and the occipitals. (F and H) *Cdx1*$^{-/-}$ skeleton that exhibits a high degree of fusion between C1 and the occipitals. **Abbreviations**: AAA, anterior arcus atlantis; BO, basioccipital; C, cervical vertebra; EO, exoccipital; T, thoracic vertebra; TA, tuberculum anterium;

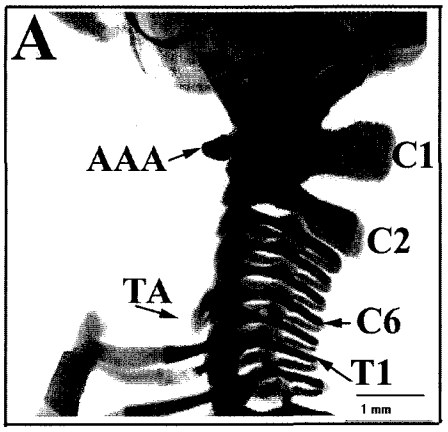
A
AAA
C1
C2
TA
C6
T1
1 mm

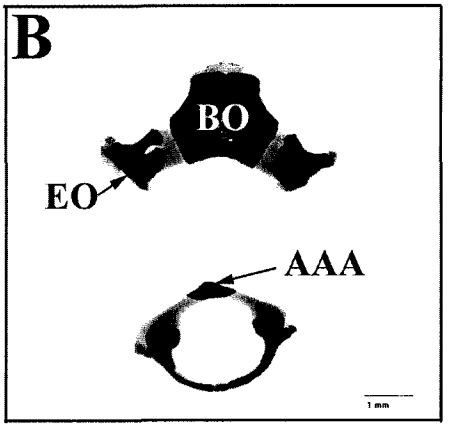
B
BO
EO
AAA
1 mm

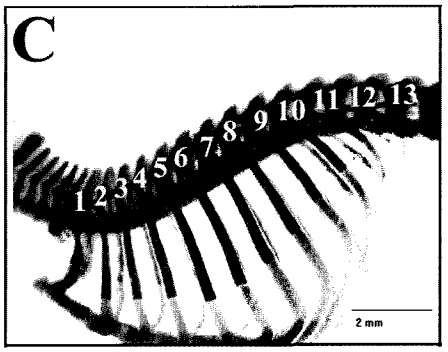
C
1 2 3 4 5 6 7 8 9 10 11 12 13
2 mm

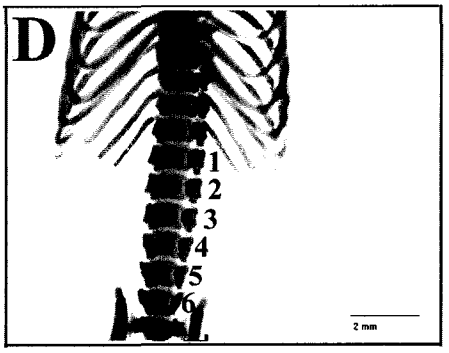
D
1
2
3
4
5
6
2 mm

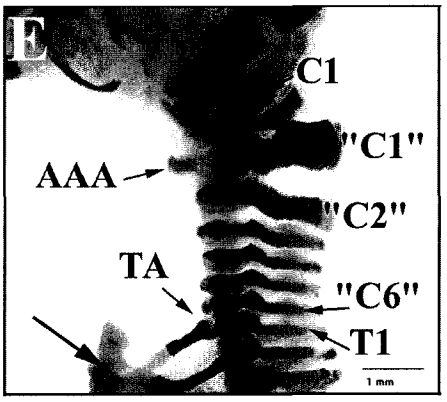
E
C1
"C1"
AAA
"C2"
TA
"C6"
T1
1 mm

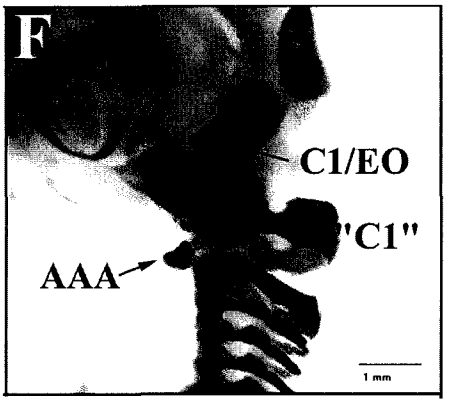
F
C1/EO
"C1"
AAA
1 mm

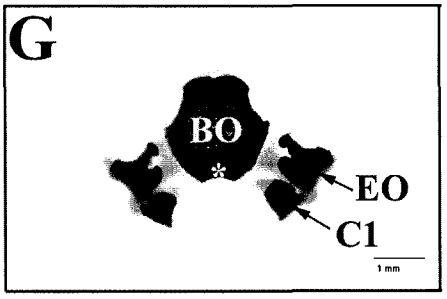
G
BO
*
EO
C1
1 mm

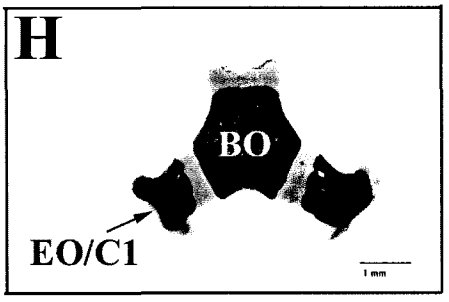
H
BO
EO/C1
1 mm

both dorsal and ventral fusions of C2 to C3 were occasionally detected. Additionally, C2 often exhibited certain characteristics of C1, including the presence of an ectopic AAA (44%), and thick neural arches (44%) (Figure 5.2A and D). However, the formation and specification of all the remaining vertebrae was normal in the *Cdx1* heterozygotes. Therefore, it appears that the anterior-most cervical vertebrae are particularly sensitive to the loss of a single *Cdx1* allele.

5.3d. Cdx1/RARγ double heterozygous mice

The homeotic transformations observed in *RARγ* mutants have been previously described (Lohnes *et al.*, 1993; Iulianella and Lohnes, 1997) and are consistent with those observed for the $RAR\gamma^{+/-}$ and $RAR\gamma^{-/-}$ mice used in this study. In brief, caudal extensions of the basioccipital bone and fusions of this bone to the AAA of C1 were observed in 7% and 4% of $RAR\gamma^{-/-}$ skeletons, respectively. Partial C2 to C1 anterior transformations were detected by ectopic AAAs (11%) and thickened neural arches (41%). The latter transformation was also observed in 8% of $RAR\gamma^{+/-}$ skeletons. These malformations and transformations are strikingly similar to those observed in $Cdx1^{+/-}$ and $Cdx1^{-/-}$ skeletons, therefore, mice that were heterozygous for both *RARγ* and *Cdx1* were examined for combined effects on vertebral patterning.

The incidence of several homeotic transformations and malformations was increased in the $Cdx1^{+/-}RAR\gamma^{+/-}$ skeletons. For example, caudal extension of the basioccipital bone was observed in 38% of the double heterozygotes (Figure 5.3A), while this phenotype was never detected in $RAR\gamma^{+/-}$ skeletons, and in only 18% of $Cdx1^{+/-}$ skeletons. Additionally, a significant increase (p=0.1) in the number of specimens with thickened C2 neural arches was observed in the double heterozygotes. This phenotype was noted in 8% of $RAR\gamma^{+/-}$, 44% of $Cdx1^{+/-}$, and 81% of $Cdx1^{+/-}RAR\gamma^{+/-}$ skeletons. Also observed at a higher frequency in the double heterozygous samples were the C6 to C5 (12%), and the C7 to C6 (10%) transformations, as detected by the loss or gain of the anterior tuberculi, respectively (Figure 5.3C). Neither of these transformations was observed in $RAR\gamma^{+/-}$ skeletons, and only the C6 to C5 transformation was observed in 4% of the $Cdx1^{+/-}$ specimens. Finally, dorsal fusion of C1 to C2 was observed in 5% of the

Figure 5.2. Phenotypes of *Cdx1* heterozygous null skeletons. Wild type (A-C) and *Cdx1* heterozygous null mutant (D-F) skulls and cervical vertebrae. (**A** and **D**) Lateral view of cervical vertebrae; dorsal is right. Note the ectopic AAA, and wide neural arches, on C2 in D. (**B** and **E**) Ventral view of basioccipital and cervical vertebrae, anterior is top. Note the fusion of the basioccipital to the AAA of C1 (arrow in E). (**C** and **F**) Dorsal view of cervical vertebrae; anterior is top. Note the malformations of C1 and C2 neural arches. **Abbreviations**: AAA, anterior arcus altantis; BO, basioccipital; C, cervical vertebra; "C", vertebra with characteristics of the designated cervical vertebra.

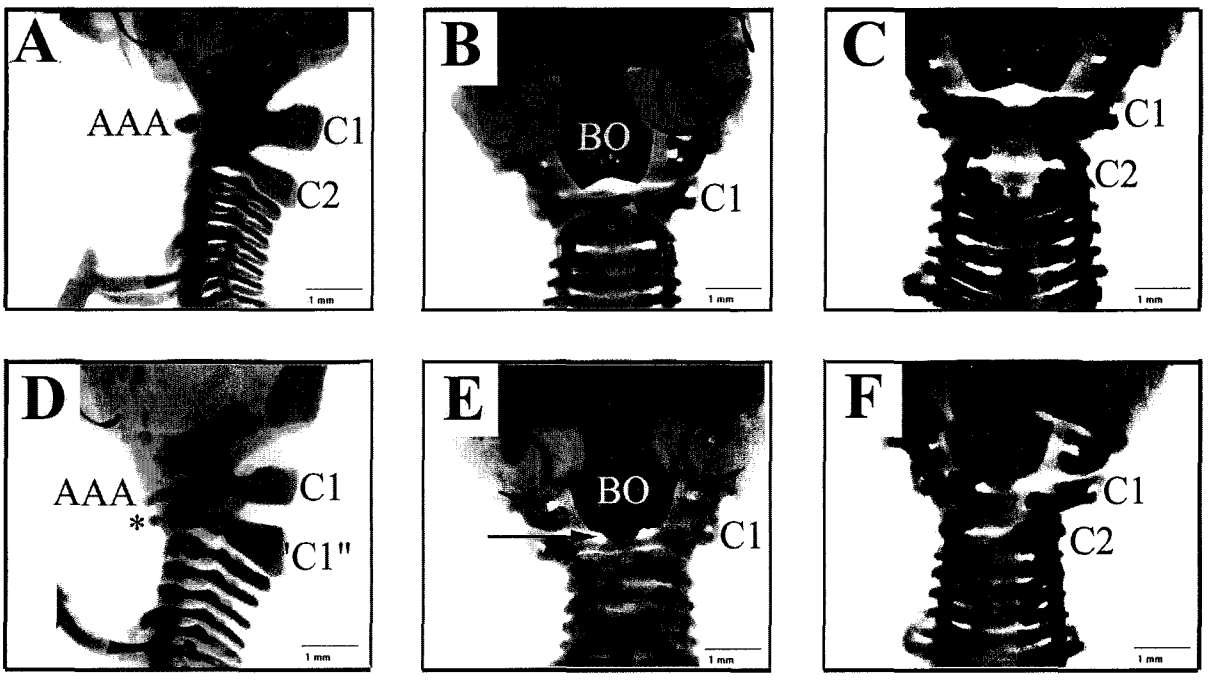
A
AAA
C1
C2
1 mm
B
BO
C1
1 mm
C
C1
C2
1 mm
D
AAA
*
C1
"C1"
1 mm
E
BO
C1
1 mm
F
C1
C2
1 mm

Cdx1$^{+/-}$*RARγ*$^{+/-}$ skeletons (Figure 5.3D), but never in either of the single heterozygotes. Taken together, these results suggest that *RARγ* and *Cdx1* act synergistically to pattern certain regions of the vertebral column.

5.3e. Cdx1$^{+/-}$*RARγ*$^{-/-}$ *mice*

The skeletal phenotype of mice that were homozygous null for *RARγ* on a *Cdx1*$^{+/-}$ background was more severe than that of *Cdx1*$^{+/-}$*RARγ*$^{+/-}$mice. An increased incidence of homeotic transformations, malformations, and fusions was observed in the basioccipital bone and the first three cervical vertebrae. For example, 40% of the *Cdx1*$^{+/-}$*RARγ*$^{-/-}$ skeletons exhibited fusion of the basioccipital bone to the AAA of C1, while an additional 20% exhibited caudal extension (Figure 5.4D). In contrast, fusion between the basioccipital and AAA was detected in only 4% of the *RARγ*$^{-/-}$, 13% of the *Cdx1*$^{+/-}$, and 7% of the *Cdx1*$^{+/-}$*RARγ*$^{+/-}$ skeletons. The basioccipital to AAA fusion in *Cdx1*$^{+/-}$*RARγ*$^{-/-}$ skeletons occurs significantly more frequently than would be expected if this was due to an additive effect of the two genes ($p<0.025$).

The first cervical vertebra was severely affected in 73% of the *Cdx1*$^{+/-}$*RARγ*$^{-/-}$ mice. Sixty percent of the skeletons exhibited malformed neural arches, which were often fused to the neural arches of C2 (Figure 5.4B). An ectopic AAA on C2 was observed in 87% of the specimens (Figure 5.4D), and in 46% of these cases this structure was fused to the endogenous AAA on C1. Eighty percent of *Cdx1*$^{+/-}$*RARγ*$^{-/-}$ skeletons had affected C2 neural arches. In contrast to the double heterozygous genotype where 81% of the C2 neural arches displayed characteristics normal to C1, the majority of the affected *Cdx1*$^{+/-}$*RARγ*$^{-/-}$ C2 neural arches were either malformed, dorsally fused to C1 and/or C3, or both. Additionally, whereas only 5% of the *Cdx1*$^{+/-}$*RARγ*$^{+/-}$ C3 vertebrae were affected, 53% of the neural arches of the *Cdx1*$^{+/-}$*RARγ*$^{-/-}$ C3 vertebral units were malformed, dorsally fused to C2 (Figure 5.4D), or exhibited a C2-like morphology. It is apparent that the effect of *RARγ* mutation on the vertebral column is enhanced in the *Cdx1*$^{+/-}$ background. This evidence further supports the findings that *Cdx1* and *RARγ* act synergistically in vertebral patterning.

Figure 5.3. Cervical phenotype of *Cdx1/RARγ* double heterozygotes. (**A**) Ventral view of the cervical region; anterior is top. Note the caudal extension of the basioccipital bone (arrow). (B-D) Lateral view of the cervical region; dorsal is right. (**B**) Asterix marks an ectopic AAA on C2. Note the wide neural arches. (**C**) The tuberculum anterium is located on C7, indicating an anterior transformation of C7 to C6. (**D**) Note the dorsal fusions and malformations of C1 and C2 neural arches. **Abbreviations**: AAA, anterior arcus atlantis; BO, basioccipital; C, cervical vertebra; TA, tuberculum anterium.

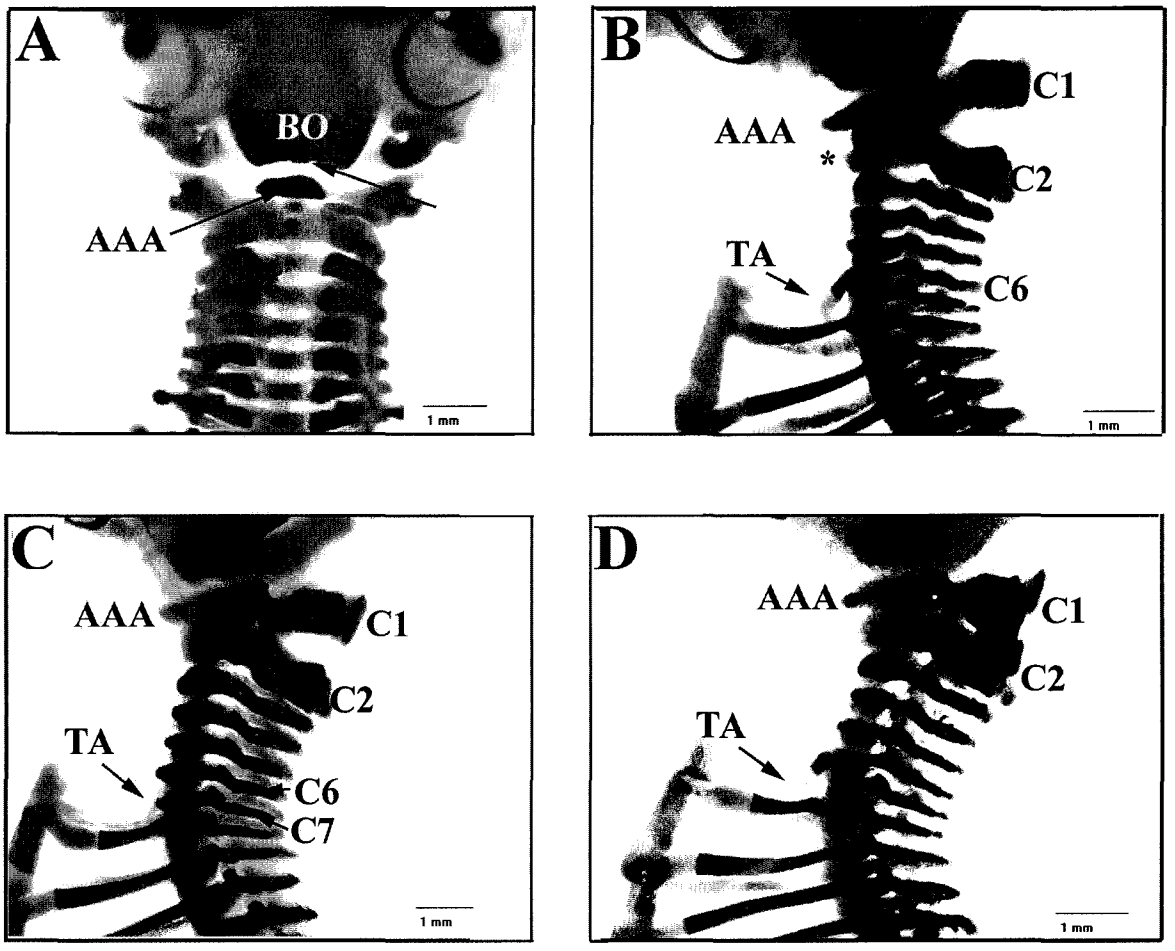
A
BO
AAA
1 mm
B
C1
AAA
*
C2
TA
C6
1 mm
C
AAA
C1
C2
TA
C6
C7
1 mm
D
AAA
C1
C2
TA
1 mm

Figure 5.4. Malformations and dorsal fusions of *Cdx1*$^{+/-}$*RARγ*$^{-/-}$ cervical vertebrae. (**A** and **C**) Wild type cervical region. (B and D) *Cdx1*$^{+/-}$*RARγ*$^{-/-}$ cervical region. (A and B) Dorsal view; anterior is top. (C and D) Lateral view; dorsal is left. (**B**) Note the malformations and dorsal fusion of C1 and C2 neural arches. (**D**) Arrowhead indicates fusion of the basioccipital to the AAA of C1. Asterix marks an ectopic AAA on C2. Note the dorsal fusions of C1, C2 and C3 neural arches. Abbreviations: C, cervical vertebra.

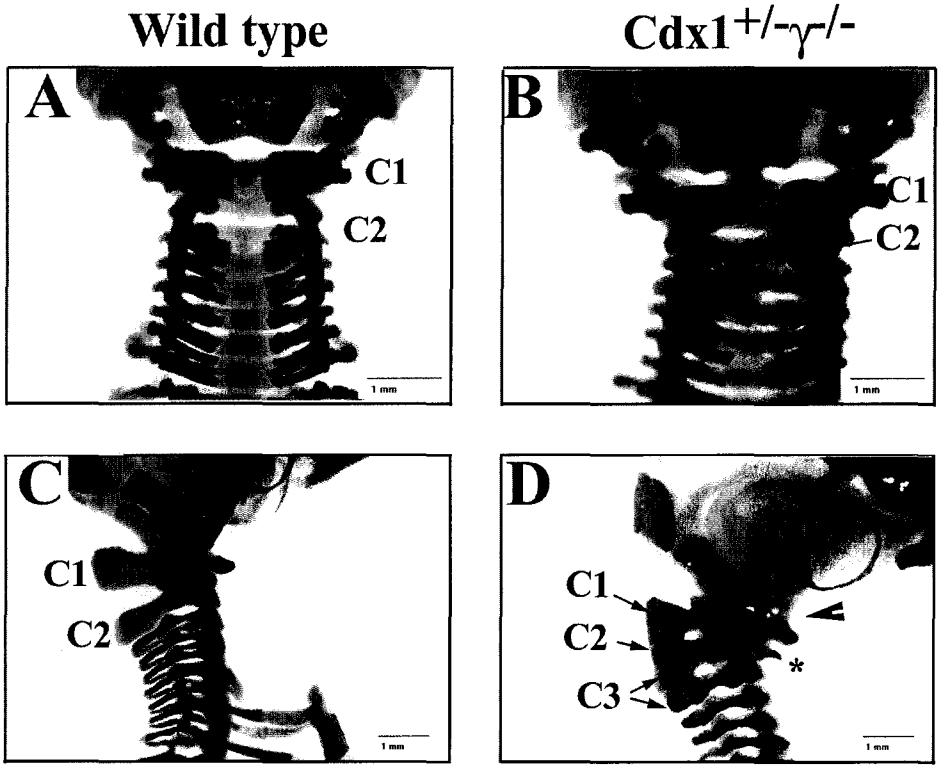
Wild type
Cdx1+/-γ-/-
A
C1
C2
1 mm
B
C1
C2
1 mm
C
C1
C2
1 mm
D
C1
C2
C3
*
1 mm

5.3f. Cdx1/RARγ double homozygotes

The loss of the remaining *Cdx1* allele from the *Cdx1*$^{+/-}$*RARγ*$^{-/-}$ background had dramatic effects on the morphology and specification of the vertebral column. The phenotype of double homozygous null skeletons closely resembles that of the *Cdx1*$^{-/-}$ mice, with complete anterior transformations of C1 through C7. However, the T1 to C7 transformation observed in 38% of the *Cdx1*$^{-/-}$ skeletons was present in 50% of *Cdx1*$^{-/-}$ *RARγ*$^{+/-}$ and 80% of *Cdx1*$^{-/-}$*RARγ*$^{-/-}$ mice (Figure 5.5D and Figure 5.6). Although this transformation was never observed in *RARγ*$^{+/-}$ or *RARγ*$^{-/-}$ skeletons these data demonstrate that *RARγ* significantly increases the incidence of this homeosis in the *Cdx1*$^{-/-}$ background in a dose-dependent manner. The reappearance of a C7-like vertebral phenotype was not due to an insertion of an extra vertebral unit, as all affected *Cdx1*$^{-/-}$*RARγ*$^{-/-}$ skeletons possessed only 12 thoracic, or 5 lumbar vertebrae, thus maintaining the number of pre-sacral vertebrae at 26 (Figure 5.5E-H). The majority of the *Cdx1*$^{-/-}$*RARγ*$^{-/-}$ skeletons with T1 to C7 transformations exhibited vertebral patterns of C8/T13/L5 (Table 5.1). This is in contrast to the majority of *Cdx1*$^{-/-}$ skeletons with the same transformation, which had vertebral patterns of C8/T12/L6. Therefore, the loss of *RARγ* from the *Cdx1*$^{-/-}$ background results in an increased incidence of anterior homeotic transformations at more posterior levels in the vertebral column.

Due to this additional transformation, the majority of double mutant cervical regions appeared superficially identical to the wild type cervical region (compare Figure 5.5A and D). This is especially striking when compared to the *Cdx1*$^{+/-}$*RARγ*$^{-/-}$ cervical region, which is highly malformed (Figure 5.4). Notably, such malformations tend occur in skeletons where *Cdx1* is heterozygous (irrespective of the *RARγ* genotype), or when *Cdx1* is homozygous null and *RARγ* is heterozygous. Conversely, *Cdx1* null, or *Cdx1/RARγ* double null skeletons rarely exhibit malformations, but do exhibit complete homeotic transformations. The increased incidence of vertebral malformation in the intermediate genotypes may be due to slight alterations in the expression levels of CDX1 and/or RARγ target genes. For example, decreased levels of target genes may provide mixed signals to the sclerotome, resulting in a "confused" identity, whereas loss of expression in a particular unit would lead to homeotic transformation.

Figure 5.5. A significantly higher incidence of T1 to C7 anterior transformation is observed in *Cdx1/RARγ* double homozygotes. (A-D) Lateral view of the cervical region; dorsal is right. (**A**) Wild type. (**B**) *Cdx1*$^{-/-}$. (**C**) *Cdx1*$^{-/-}$ *RARγ*$^{+/-}$. (**D**) *Cdx1*$^{-/-}$*RARγ*$^{-/-}$. Note the higher degree of fusion between C1 and the exoccipitals as compared to *Cdx1*$^{-/-}$ (B) or *Cdx1*$^{-/-}$*RARγ*$^{+/-}$ (C) skeletons. Vertebra 8 exhibits characteristics of the seventh cervical vertebra, instead of the first thoracic vertebra, and is designated "C7" in (D). Asterix in B-D indicates an ectopic AAA on Vertebra 2, which has acquired all of the normal characteristics of C1. (E and G) Lateral view of thoracic vertebrae. (E) Wild type. (G) *Cdx1*$^{-/-}$ *RARγ*$^{-/-}$. (F and H) Ventral view of lumbar vertebrae. (F) Wild type. (H) *Cdx1*$^{-/-}$ *RARγ*$^{-/-}$. Note the loss of one thoracic vertebra, for a total number of 12 (G); or one lumbar vertebra, for a total number of 5 (H) in the double mutants, as compared to wild type. **Abbreviations**: C, cervical vertebra; "C", vertebra with characteristics of the designated cervical vertebra; EO, exoccipital; T, thoracic vertebra; TA, tuberculum anterium.

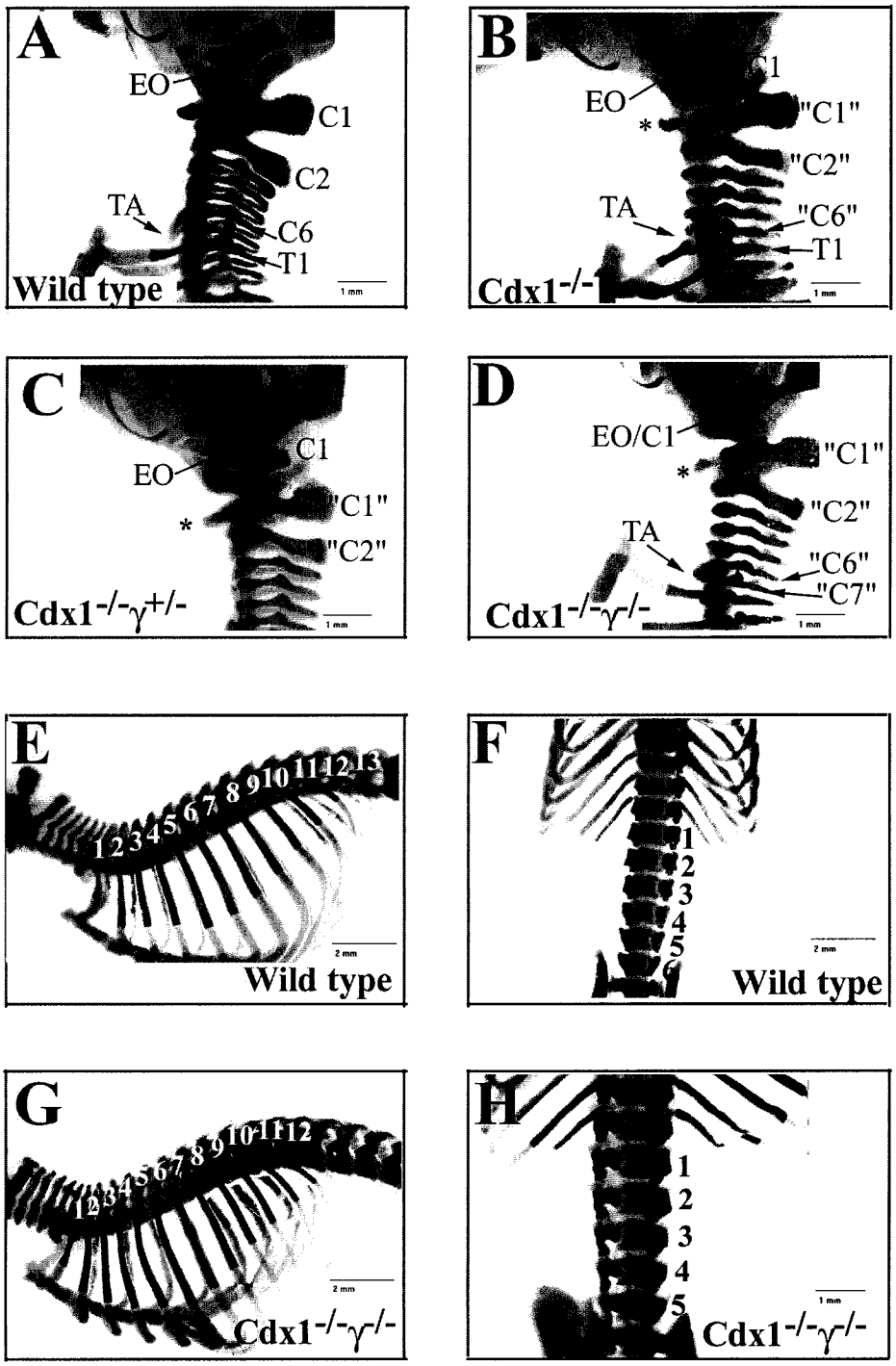
A
EO
C1
C2
TA
C6
T1
Wild type
1 mm
B
EO
"C1"
"C2"
TA
"C6"
T1
Cdx1-/-
1 mm
C
EO
C1
"C1"
"C2"
Cdx1-/-γ+/-
1 mm
D
EO/C1
"C1"
"C2"
TA
"C6"
"C7"
Cdx1-/-γ-/-
1 mm
E
1 2 3 4 5 6 7 8 9 10 11 12 13
2 mm
Wild type
F
1
2
3
4
5
6
2 mm
Wild type
G
1 2 3 4 5 6 7 8 9 10 11 12
2 mm
Cdx1-/-γ-/-
H
1
2
3
4
5
1 mm
Cdx1-/-γ-/-

Figure 5.6. Phenotypes of individual cervical vertebrae from wild type and mutant mice. Views of all vertebrae are anterior (ventral is top), except for Vertebra 1 of *Cdx1*$^{-/-}$, and *Cdx1*$^{-/-}$*RARγ*$^{-/-}$ samples, which are viewed ventrally (anterior is top). Views of the occipital bones are ventral; anterior is top. Asterix on *RARγ*$^{-/-}$ vertebra 2 indicates the partial formation of an ectopic AAA. Note the fusion of vertebra 1 to the occipitals in *Cdx1*$^{-/-}$ and *Cdx1*$^{-/-}$*/RARγ*$^{-/-}$ specimens. Vertebrae 2 through 7 exhibit complete anterior transformations in both *Cdx1*$^{-/-}$ and *Cdx1*$^{-/-}$*RARγ*$^{-/-}$ specimens. Vertebra 8 exhibits an anterior transformation only in the *Cdx1/RARγ* double mutants (compare Vertebra 8 of *Cdx1*$^{-/-}$*RARγ*$^{-/-}$ to wild type and *RARγ*$^{-/-}$ Vertebra 7). **Abbreviations**: FT, foramen transversum; TA, tuberculi anterior.

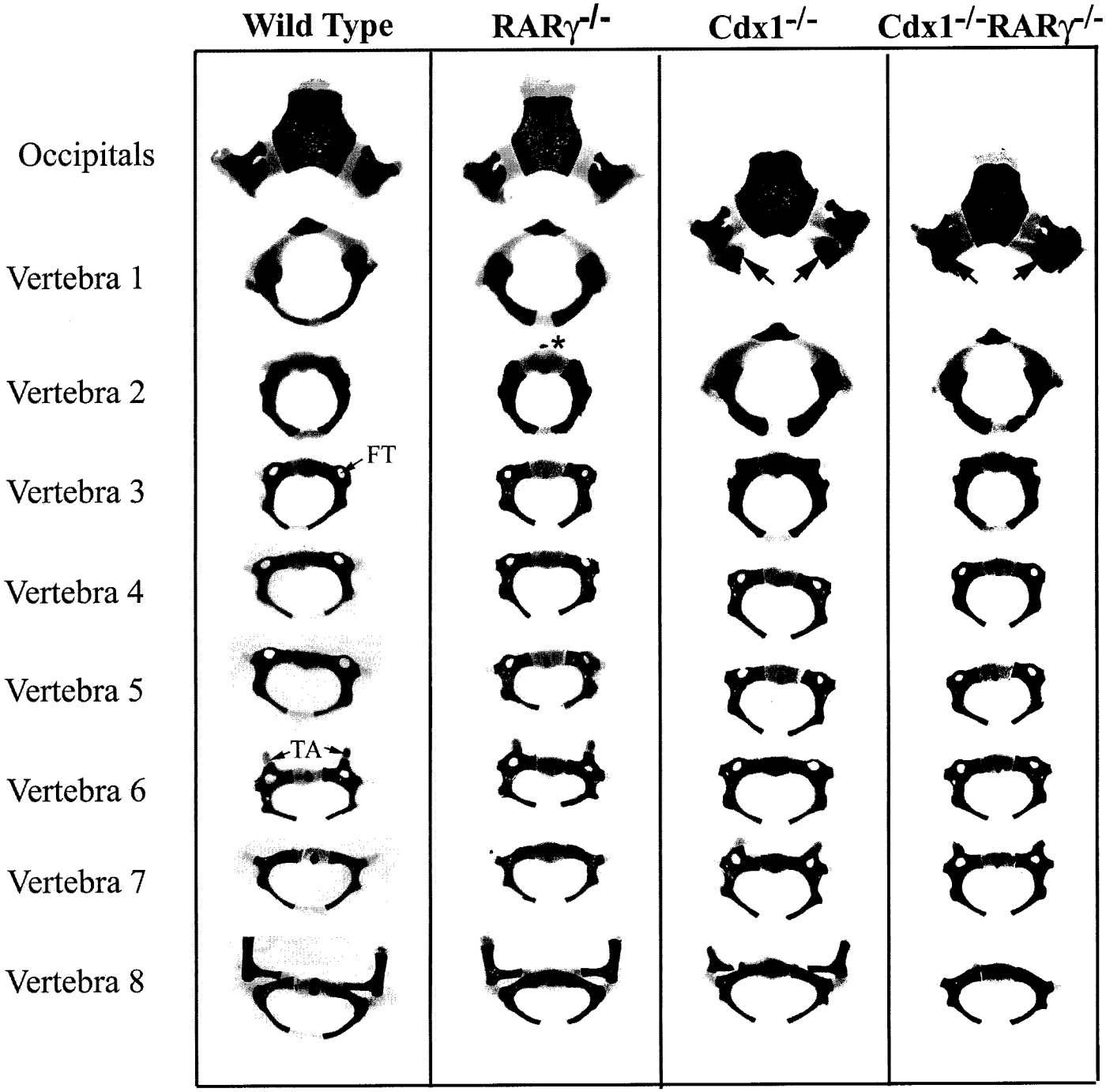
Wild Type
RARγ-/-
Cdx1-/-
Cdx1-/-RARγ-/-
Occipitals
Vertebra 1
Vertebra 2
Vertebra 3
Vertebra 4
Vertebra 5
Vertebra 6
Vertebra 7
Vertebra 8
FT
TA
*

5.3g. Expression of Hox genes in Cdx1$^{-/-}$RARγ$^{-/-}$ embryos

The anterior expression limits of certain *Hox* genes are posteriorized by one or two prevertebra in *Cdx1* null mice (Subramanian *et al.*, 1995). Conversely, RA treatment at E7.5 anteriorizes *Hox* expression boundaries and it was proposed that these altered expression patterns lead to the observed anterior or posterior homeotic transformations (Kessel and Gruss, 1991). Hence, aberrant *Hox* gene expression is a likely mechanism for the additional homeotic transformations and malformations observed in the compound *Cdx1/RARγ* mutant skeletons. In this regard, the expression patterns of *Hoxd3* and *Hoxd4* were examined in wild type, *Cdx1*$^{-/-}$ and *Cdx1*$^{-/-}$*RARγ*$^{-/-}$ E9.5 embryos (Figure 5.7A-D). The anterior boundary of *Hoxd3* expression in the paraxial mesoderm normally lies between somites 4 and 5 (Condie and Capecchi, 1993). In *Cdx1*$^{-/-}$ embryos *Hoxd3* expression is shifted posteriorly by one somite (Subramanian *et al.*, 1995 and Figure 5.7A). *Cdx1/RARγ* double mutant embryos did not display any further alteration of this pattern of expression (Figure 5.7B). Additionally, in *Cdx1*$^{+/-}$ embryos, the anterior boundary of *Hoxd3* expression was identical to that observed in wild type embryos (data not shown). Therefore, the basioccipital/AAA fusions in *Cdx1* heterozygotes, and the higher degree of fusion of vertebra 1 to the occipitals in *Cdx1/RARγ* double null skeletons, does not correlate with an alteration of the level, or boundary, of *Hoxd3* expression, as assessed by *in situ* hybridization.

Hoxd4 has an anterior limit of strong expression in somite 6, with weaker expression in somite 5, at E9.5 (Folberg *et al.*, 1997). *Hoxd4* null embryos exhibit many of the same homeotic transformations that are observed in *Cdx1*$^{+/-}$ and *RARγ*$^{-/-}$ skeletons (Horan *et al.*, 1995a). Moreover, *RARγ* and *Hoxd4* null mutations are synergistic in the promotion of fusion between the basioccipital bone and the AAA, and the appearance of an ectopic AAA on C2 (Folberg *et al.*, 1999a). Hence, it follows that the synergistic effects of *Cdx1* and *RARγ* on the incidence of these same defects may be explained by decreased expression of *Hoxd4* in the *Cdx1* mutants. However, *Hoxd4* expression was not affected in *Cdx1*$^{-/-}$ or *Cdx1*$^{-/-}$*RARγ*$^{-/-}$ embryos compared to wild type offspring (Figure 5.7C and D).

Figure 5.7. Expression of *Hoxd3* and *Hoxd4* in *Cdx1/RARγ* double mutant embryos. Whole mount *in situ* hybridization of E9.5 mouse embryos using *Hoxd3* (A and B) and *Hoxd4* (C and D) riboprobes. Anterior is top. White dashes indicate the position of the forelimb bud. (**A**) *Hoxd3* expression in wild type and *Cdx1*$^{-/-}$ embryos. The anterior limit of expression in *Cdx1*$^{-/-}$ embryos is one somite posterior to that of wild type embryos (arrows point to somite 5). (**B**) *Hoxd3* expression in *Cdx1*$^{-/-}$ and *Cdx1*$^{-/-}$*RARγ*$^{-/-}$ embryos. Note the anterior limit of expression is identical (somite 6) in both genotypes. (**C**) *Hoxd4* expression in wild type and *Cdx1*$^{-/-}$ embryos. The anterior limit of expression (somite 6) is the same in both embryos (arrows). (**D**) *Hoxd4* expression in *Cdx1*$^{-/-}$ and *Cdx1*$^{-/-}$*RARγ*$^{-/-}$ embryos. The anterior limit of expression in *Cdx1*$^{-/-}$*RARγ*$^{-/-}$ embryos was identical to that observed for wild type and *Cdx1*$^{-/-}$ embryos (arrows).

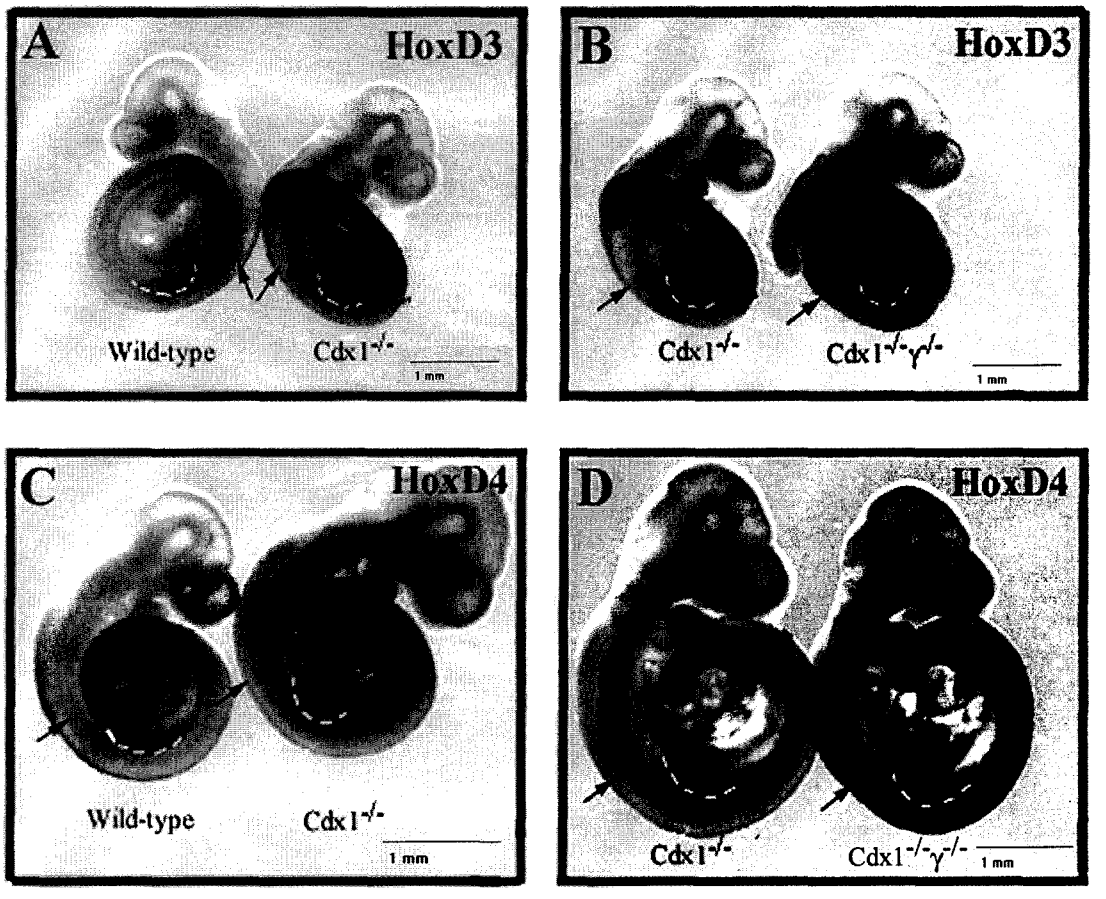
A
HoxD3
Wild-type
Cdx1-/-
1 mm
B
HoxD3
Cdx1-/-
Cdx1-/-γ-/-
1 mm
C
HoxD4
Wild-type
Cdx1-/-
1 mm
D
HoxD4
Cdx1-/-
Cdx1-/-γ-/-
1 mm

5.3h. RA treatment of Cdx1/RARγ compound mutant mice at E7.4

Malformations, and homeosis of several vertebrae, particularly those located in the cervical region, are induced by RA treatment at E7.3-7.5 (Kessel and Gruss, 1991; Kessel, 1992). Recently, Iulianella and Lohnes (1997) demonstrated that *RARγ* is required to fully elicit some of these abnormalities, including craniofacial malformations, neural tube defects, and certain posterior transformations. However, all of the RA-induced abnormalities were not eliminated in these mutants, therefore, some of the effects of RA must also be mediated through the remaining RARs. *Cdx1* transcripts increase in the caudal portion of the embryo (in the vicinity of the primitive streak) one hour post RA-treatment *in utero* (Houle *et al.*, 2000). At E7.5 both the endogenous, and RA-induced, levels of *Cdx1* message are significantly reduced in *RARα1γ* null embryos, and these mutants exhibit a higher incidence of anterior homeotic transformations (Lohnes *et al.*, 1994). Moreover, a RARE was identified in the promoter of *Cdx1* which is essential for RA induction in F9 cells (Houle *et al.*, 2000). Therefore, it was hypothesized that *Cdx1* may directly mediate some of the posteriorizing effects of RA excess on the vertebral column. To assess this *Cdx1/RARγ* compound mutants, treated at E7.4 with 10mg/kg of RA, were generated, and their skeletal phenotype analyzed (Table 5.2)

The effects of 10mg/kg of RA, administered at E7.3-7.5 on wild type and *RARγ* mutant vertebral columns have been documented (Kessel and Gruss, 1991, Iulianella and Lohnes, 1997) and similar abnormalities were observed in this study (summarized in Table 5.2). In general, RA-treatment at this stage results in posterior transformations and malformations of the cervical vertebrae. An additional vertebral unit, the proatlas, located directly anterior to the normal first vertebra, was observed in 32% of the RA-treated wild type embryos (Table 5.2 and Figure 5.8B-D). This structure derives from cells of the 4th and 5th somites, which normally contribute to the basioccipital bone and the tip of the dens axis. As the proatlas closely resembles the normal first vertebra, the appearance of this structure can be interpreted as a posterior homeotic transformation (Kessel *et al.*, 1990, Kessel and Gruss, 1991). Posterior transformations were also observed in C1 through C6 resulting in the deletion of one or two cervical vertebrae (see vertebral pattern in Table 5.2). Although the types of RA-induced homeotic transformations, and the reduction of cervical vertebrae observed in the skeletons of this

Table 5.2. Vertebral phenotypes of compound Cdx1/RARγ mutant mice treated with RA at E7.4

	Genotype								
	WT	$\gamma^{+/-}$	$\gamma^{-/-}$	$Cdx1^{+/-}$	$Cdx1^{-/-}$	$Cdx1^{+/-}\gamma^{+/-}$	$Cdx1^{+/-}\gamma^{-/-}$	$Cdx1^{-/-}\gamma^{+/-}$	$Cdx1^{-/-}\gamma^{-/-}$
	n=19	n=9	n=8	n=7	N=7	n=10	n=5	n=3	n=9
Abnormal phenotype	(%)	(%)	(%)	(%)	(%)	(%)	(%)	(%)	(%)
Basioccipital									
Fusion to: AAA	1 (5)	-	-	1 (14)	-	-	3 (60)	3 (100)	9 (100)
Dens	2 (11)	-	-	-	-	-	1 (20)	-	-
Extension	1 (5)	-	-	2 (29)	1 (14)	-	-	-	-
Proatlas									
Evidence for	-	1 (11)[b]	2 (25)[a]	3 (43)[e]	2 (29)[e]	-	-	-	-
Complete	6 (32)[b]	1 (11)[b]	-	-	-	-	-	-	-
Fused to occipitals	1 (5)[a]	2 (22)[e]	-	2 (29)[b]	2 (29)[e]	-	-	-	-
Fused to V1									
Dorsal	2 (11)[e]	1 (11)[b]	-	1 (14)[a]	1 (14)[b]	-	-	-	-
Ventral[g]	3 (16)	-	-	-	-	-	-	-	-
Vertebra 1									
Fusion to occipitals[f]	-	-	-	-	-	-	-	2 (67)[b]	5 (56)[d]
Partial C2 identity									
Vertebral body	3 (16)	1 (11)	-	-	-	-	-	-	-
Thin NA	1 (5)[a]	-	1 (13)[a]	1 (14)[b]	1 (14)[b]	-	-	-	-
Fusion to V2									
Dorsal	-	1 (11)[a]	-	-	-	-	2 (40)[e]	-	5 (56)[e]
Ventral[g]	4 (21)	1 (11)[a]	-	2 (29)	4 (57)	-	-	1 (33)	3 (33)
Malformed NA[h]	3 (16)[c]	4 (44)[d]	2 (25)[a]	2 (29)[e]	3 (43)[b]	1 (10)[a]	3 (60)[c]	-	-
Vertebra 2									
Complete C1 identity	-	-	-	-	-	-	-	3 (100)	8 (89)
Partial C1 identity									
AAA	-	-	-	1 (14)	3 (43)[I]	2 (20)	4 (80)	-	1 (11)
Thick NA	-	-	-	1 (14)[b]	3 (43)[b]	1 (10)[b]	1 (20)[b]	-	1 (11)[b]
Complete C3 identity	3 (16)	-	-	-	-	-	-	-	-
Partial C3 identity									
Thin NA	6 (32)[d]	-	-	-	1 (14)[b]	-	-	-	-
Malformed NA[h]	3 (16)[c]	2 (22)[e]	-	4 (57)[e]	3 (43)[c]	1 (10)[b]	3 (60)[b]	1 (33)[b]	-
Fusion to V3									
Dorsal	-	-	-	-	1 (14)[a]	-	2 (40)[e]	-	2 (22)[e]
Ventral	-	-	-	-	-	-	-	-	1 (11)
Vertebra 3									
Complete C2 identity	-	-	-	-	-	-	-	3 (100)	8 (89)
Partial C2 identity									
Thick NA	-	-	-	-	-	-	-	-	1 (11)[b]
Malformed NA[h]	-	-	-	-	-	-	3 (60)[d]	-	-
Vertebra 5									
TA	6 (32)[d]	3 (33)[b]	4 (50)[d]	4 (57)[d]	2 (29)[a]	-	-	-	-
Vertebra 6									
C5 identity	-	-	-	-	-	-	3 (60)[e]	2 (67)[b]	5 (56)[b]
C7 identity	6 (32)[d]	3 (33)[b]	4 (50)[d]	3 (43)[b]	2 (29)[a]	-	-	-	-
Rib	1 (5)[b]	-	-	1 (14)[b]	-	-	-	-	-
Vertebra 7									
TA	-	-	-	-	-	-	3 (60)[e]	2 (67)[b]	5 (56)[b]
Rib: Incomplete	2 (11)[b]	-	-	1 (14)[b]	2 (29)[a]	2 (20)[e]	1 (20)[a]	-	-
Complete	7 (37)[b]	3 (33)[b]	4 (50)[b]	4 (57)[b]	4 (57)[b]	1 (10)[a]	-	-	-
Vertebra 8									
C7 identity	-	-	-	-	-	-	1 (20)[a]	1 (33)[a]	3 (33)[b]
Incomplete rib	1 (5)[b]	-	-	-	-	-	1 (20)[a]	2 (67)[e]	2 (22)[e]
Spinous process on:									
V7	1 (5)	-	-	1 (14)	-	-	-	-	-
V8	6 (32)	3 (33)	4 (50)	4 (57)	5 (71)	2 (20)	-	-	-
V10	-	-	-	-	-	-	-	-	3 (33)
V8 and V9	2 (11)	-	-	-	1 (14)	-	-	-	-
V9 and V10	-	-	-	-	-	1 (10)	3 (60)	1 (33)	1 (11)

Table 5.2. cont'd. Vertebral phenotypes of compound Cdx1/RARγ mutant mice treated with RA at E7.4

	Genotype								
	WT	**$\gamma^{+/-}$**	**$\gamma^{-/-}$**	**$Cdx1^{+/-}$**	**$Cdx1^{-/-}$**	**$Cdx1^{+/-}\gamma^{+/-}$**	**$Cdx1^{+/-}\gamma^{-/-}$**	**$Cdx1^{-/-}\gamma^{+/-}$**	**$Cdx1^{-/-}\gamma^{-/-}$**
	n=19	n=9	n=8	n=7	N=7	n=10	n=5	n=3	n=9
Abnormal phenotype	(%)	(%)	(%)	(%)	(%)	(%)	(%)	(%)	(%)
Cervical Vertebrae									
5	1 (5)[b]	-	-	1 (14)[b]	-	-	-	-	-
6	8 (42)[b]	3 (33)[b]	4 (50)[b]	4 (57)[b]	6 (86)[d]	2 (20)[e]	-	-	-
8	-	-	-	-	-	-	1 (20)[a]	1 (33)[a]	3 (33)[b]
Ribs attached to sternum									
6	2 (11)[e]	-	1 (13)[a]	-	-	-	-	-	-
8	3 (16)[e]	3 (33)[a]	5 (63)[e]	1 (14)[b]	-	7 (70)[d]	3 (60)[e]	-	1 (11)[a]
Rib-bearing vertebrae									
12	1 (5)[b]	-	-	1 (14)[b]	1 (14)[b]	-	-	1 (33)[a]	2 (22)[b]
14	6 (32)[d]	1 (11)[a]	4 (50)[d]	1 (14)[b]	-	7 (70)[d]	4 (80)[e]	-	1 (11)[b]
Lumbar vertebrae									
5	11(53)[d]	3 (33)[d]	4 (50)[e]	3 (43)[b]	4 (57)[d]	5 (50)[e]	1 (20)[a]	1 (33)[b]	6 (67)[b]
Vertebral pattern[j]									
C5/T13/L5	-	-	-	1 (14)[b]	-	-	-	-	-
C5/T14/L5	1 (5)[b]	-	-	-	-	-	-	-	-
C6/T13/L5	3 (16)[b]	2 (22)[b]	-	2 (29)[b]	3 (43)[b]	-	-	-	-
C6/T13/L6	3 (16)[b]	1 (11)[b]	2 (25)[e]	2 (29)[b]	3 (43)[e]	2 (20)[e]	-	-	-
C6/T14/L5	2 (11)[b]	-	3 (38)[e]	-	-	1 (10)[a]	1 (20)[a]	-	-
C6/T14/L6	-	-	1 (13)[a]	-	-	-	-	-	-
C7/T12/L5	1 (5)[a]	-	-	-	-	-	-	-	-
C7/T12/L6	1 (5)[a]	-	-	1 (14)[b]	1 (14)[b]	-	-	-	2 (22)[b]
C7/T13/L5	1 (5)[a]	-	-	-	1 (14)[a]	1 (10)[b]	1 (20)[a]	1 (33)[b]	2 (22)[b]
C7/T13/L6	5 (26)	5 (56)	3 (38)	-	-	1 (10)	1 (20)	1 (33)	1 (11)
C7/T14/L5	3 (16)[c]	1 (11)[a]	1 (13)[b]	-	-	3 (30)[e]	3 (60)[e]	-	1 (11)[b]
C7/T14/L6	-	-	-	1 (14)[b]	-	3 (30)[b]	-	-	-
C8/T13/L5	-	-	-	-	-	-	1 (20)[a]	1(33)[a]	3 (33)[b]

[a] unilateral
[b] bilateral
[c] mostly unilateral
[d] mostly bilateral
[e] equal unilateral and bilateral
[f] including incorporation of AAA
[g] fusion of AAA to AAA, or vertebral body
[h] includes fusions of neural arches
[i] AAA shared with vertebra 1
[j] not including proatlas

study were similar to those previously reported, the frequency at which they appeared was reduced. This could be due to slight differences in the stage at which the developing embryos were exposed to RA, or to differences in genetic background.

The resistance of *RARγ* mutant embryos to RA-induced transformations and malformations, described by Iulianella and Lohnes (1997), was also observed in this study. For example, the appearance of a proatlas was detected in 25% of the $RAR\gamma^{-/-}$ skeletons, however this structure was not well developed and typically consisted only of incomplete neural arches (data not shown). Posterior transformations of C1 and C2 were not detected in the *RARγ* mutants. The loss of one cervical vertebra (C3, C4, or C5) was observed in 50% of these mutants, but the more severe cervical reductions that occurred in wild type RA-treated specimens (i.e. C4 to C6, or C3 to C6) were not detected, consistent with prior observations (Iulianella and Lohnes, 1997).

$Cdx1^{+/-}$ and $Cdx1^{-/-}$ skeletons exhibited the same incidence of RA-induced homeotic transformations observed in wild type skeletons, with the exceptions of proatlas formation, and posterior transformations of C1 and C2 (Table 5.2). A proatlas was detected in 43% of the *Cdx1* heterozygotes (Figure 5.10B) and 29% of the homozygotes (Figure 5.8F), however, similar to *RARγ* mutants, this structure was not completely formed and was detected as an extra pair of neural arches above C1. Therefore, the expressivity of this transformation depends on *Cdx1* dosage. The C1 to C2 transformation observed in 16% of the RA-treated wild type skeletons was not detected in the *Cdx1* mutants. Moreover, the presence of C3-like neural arches on C2, indicative of a partial homeotic transformation, was only observed in one $Cdx1^{-/-}$ skeleton (14%), as compared to 32% of wild type specimens. There was no significant difference in the penetrance of C5 to C6, and C6 to C7 posterior transformations in the $Cdx1^{+/-}$ or $Cdx1^{-/-}$ treated skeletons, however, these transformations only occurred unilaterally in the latter genotype. This evidence demonstrates that *Cdx1*, at E7.4, is required for the full effect of RA-induced homeotic transformations.

All of the $Cdx1^{+/-}RAR\gamma^{+/-}$, $Cdx1^{+/-}RAR\gamma^{-/-}$, $Cdx1^{-/-}RAR\gamma^{+/-}$ and $Cdx1^{-/-}RAR\gamma^{-/-}$ embryos were remarkably more resistant to RA-induced homeotic transformations than

Figure 5.8. *RARγ* is required for the effect of RA treatment on specification of *Cdx1*$^{-/-}$ cervical vertebrae. All treated skeletons (TR) were exposed to 10mg/kg of RA at E7.4. (A-L) Lateral view of the cervical region, dorsal is left. (**A**) Wild type untreated control. (**B-D**) Wild type skeletons treated with RA. Note the formation of a proatlas above the normal first vertebra and the reduction of the exoccipitals. (**D**) The proatlas is fused ventrally and dorsally to vertebra 1. (**E**) Untreated *Cdx1*$^{-/-}$ control (F-H) *Cdx1*$^{-/-}$ skeletons treated with RA. Note the RA-rescue of the C1/exoccipital fusion that is characteristic of untreated *Cdx1* nulls. (**F**) Proatlas formation can be detected by the presence of ectopic neural arches above C1. Note the dorsal fusion of the proatlas to C1 and fusion of the AAA to C2. (**G**) Intermediate rescue of the *Cdx1*$^{-/-}$ phenotype. Note that C1 is not fused to the occipitals. (**H**) Nearly complete rescue of the *Cdx1*$^{-/-}$ phenotype (compare A to H). (**I**) Untreated *Cdx1*$^{-/-}$*/RARγ*$^{+/-}$ skeleton. (**J**) *Cdx1*$^{-/-}$*RARγ*$^{+/-}$ skeleton treated with RA. Note the limited rescue of the C1/exoccipital fusion and anterior homeotic transformations. (**K**) Untreated *Cdx1*$^{-/-}$*/RARγ*$^{-/-}$ control skeleton. (**L**) RA treated *Cdx1*$^{-/-}$*/RARγ*$^{-/-}$ skeleton. Note the partial rescue of the C1/exoccipital fusion, but not the C2 to C1 homeotic transformation. **Abbreviations**: AAA, anterior arcus atlantis; AAA*, ectopic anterior arcus atlantis; C, cervical vertebra; "C", vertebra with characteristics of the designated cervical vertebra; EO, exoccipital; P, proatlas.

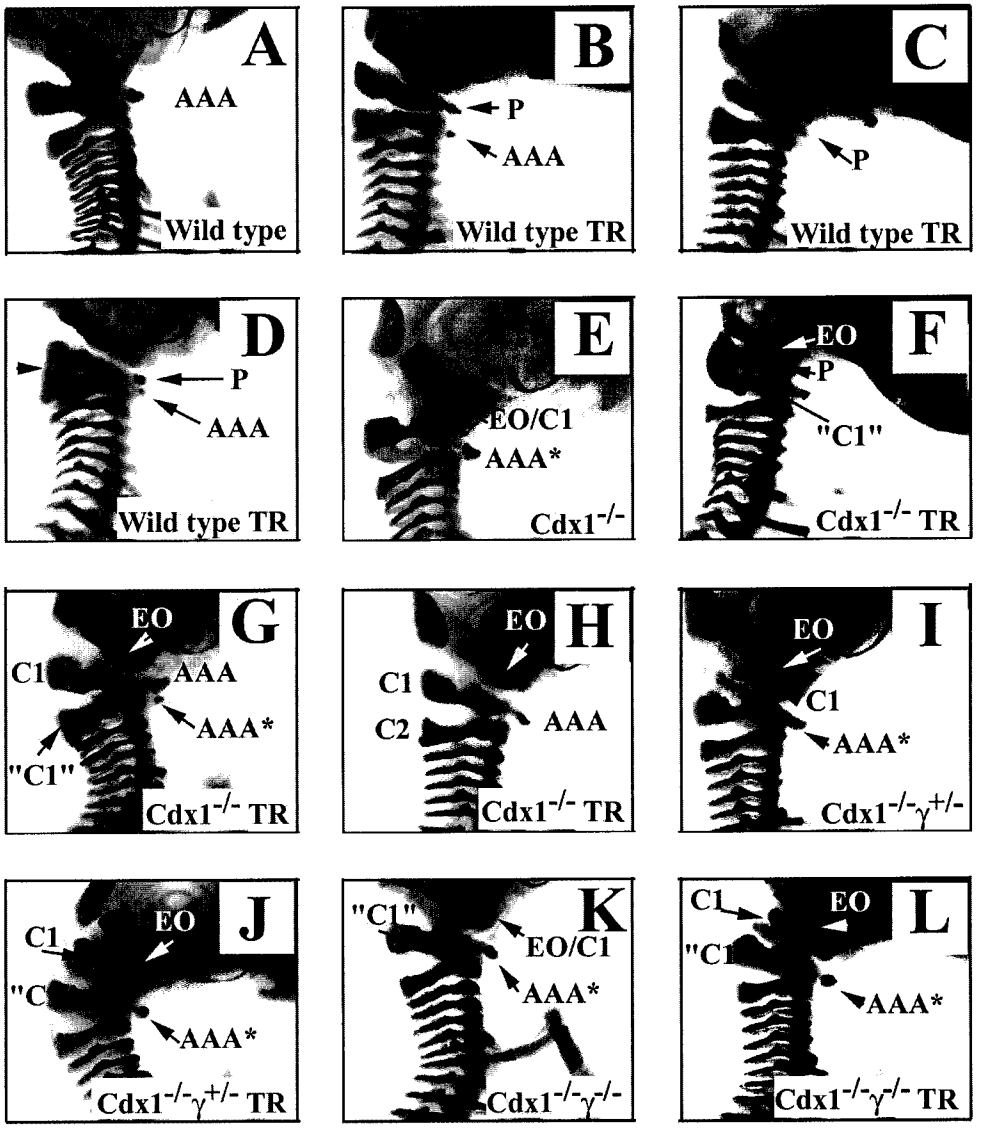
A
AAA
Wild type
B
P
AAA
Wild type TR
C
P
Wild type TR
D
P
AAA
Wild type TR
E
EO/C1
AAA*
Cdx1-/-
F
EO
P
"C1"
Cdx1-/- TR
G
EO
C1
AAA
AAA*
"C1"
Cdx1-/- TR
H
EO
C1
C2
AAA
Cdx1-/- TR
I
EO
C1
AAA*
Cdx1-/-γ+/-
J
C1
EO
"C
AAA*
Cdx1-/-γ+/- TR
K
"C1"
EO/C1
AAA*
Cdx1-/-γ-/-
L
C1
EO
"C1
AAA*
Cdx1-/-γ-/- TR

those lacking either gene alone (Table 5.2). Induction of a proatlas, and posterior transformations of C1 and C2, were never observed in the RA-treated compound *Cdx1/RARγ* mutants. Furthermore, C5 to C6, and C6 to C7, homeotic transformations were abolished in these mutants, although the loss of either *Cdx1* or *RARγ* alone had no effect on these transformations (compare Figure 5.10B to Figure 5.10D). A posterior transformation of C7 to T1 was observed in 30% of the $Cdx1^{+/-}RAR\gamma^{+/-}$ and 20% of the $Cdx1^{+/-}RAR\gamma^{-/-}$ skeletons. In addition to the lower incidence of this transformation, as compared to the wild type treated skeletons (48%), the majority of the ribs observed on C7 in the compound mutants were incomplete, indicating a decreased level of expressivity.

5.3i. RA rescue of Cdx1-associated anterior transformations

The basioccipital was either caudally extended or fused to the AAA of C1 in 31% of the untreated $Cdx1^{+/-}$ skeletons. The incidence of the basioccipital extension/fusion was not affected by RA-treatment in $Cdx1^{+/-}$ offspring (29%), but was completely eliminated in *Cdx1* null mutants (compare Figure 5.9C to Figure 5.9E and F). Moreover, in RA-treated *Cdx1* null skeletons, the appearance of C1 was relatively normal (Figure 5.8F-H). This is dramatically different than the untreated *Cdx1* null phenotype where the dorsal neural arches are not formed, the lateral masses are fused to the exoccipitals, and the AAA is completely incorporated into the basioccipital bone (Figure 5.8E). Conversely, RA treatment of $Cdx1^{-/-}RAR\gamma^{+/-}$, and $Cdx1^{-/-}RAR\gamma^{-/-}$embryos had no effect on the incidence of this anterior transformation, although the extent of the exoccipital-C1 neural arch fusion appeared to be reduced (compare Figure 5.8 I and J, and K and L). Taken together, these results indicate that RARγ is required to mediate the RA-induced rescue of the C1 to occipital anterior transformation that is characteristic of *Cdx1* mutant skeletons.

Nearly half of the $Cdx1^{+/-}$ skeletons examined in this study exhibited an ectopic AAA and wide neural arches on C2 (i.e. a C2 to C1 transformation. In contrast, this transformation was observed in only 14% of such skeletons following treatment with RA at E7.4. The loss of a single *RARγ* allele resulted in an increased frequency of this C2

Figure 5.9. *RARγ* is required for the effect of RA treatment on the occipitals of *Cdx1*$^{-/-}$ skeletons. (A-L) Ventral view of the cervical region; anterior is top. (**A**) Wild type untreated control. (**B**) Wild type treated skeleton. Note the caudal extension of the basioccipital, and the malformation of the AAA. (**C**) Untreated *Cdx1*$^{-/-}$ control. (D-F) *Cdx1*$^{-/-}$ treated skeletons exhibiting different degrees of RA-rescue. (**D**) Proatlas formation between the occipitals and C1. Note the ventral fusion of the proatlas to the basioccipital. (**E**) C1 is not fused to the occipitals, AAA is fused to C2. Note the more posterior location of the AAA relative to C2. (**F**) Nearly complete rescue of the *Cdx1*$^{-/-}$ phenotype (compare to A). (**G**) *Cdx1*$^{-/-}$*RARγ*$^{+/-}$ untreated control. (H-I) *Cdx1*$^{-/-}$*RARγ*$^{+/-}$ skeletons treated with RA. (**H**) Partial rescue of the *Cdx1*$^{-/-}$*RARγ*$^{+/-}$ phenotype. Note the fusion of the basioccipital, AAA, and C2. The AAA appears to be shared between C1 and C2 ("C1"). (**I**) The *Cdx1*$^{-/-}$*RARγ*$^{+/-}$ phenotype is not rescued by RA. (**J**) Untreated *Cdx1*$^{-/-}$*RARγ*$^{-/-}$ control. (K-L) RA treated *Cdx1*$^{-/-}$*RARγ*$^{-/-}$ skeletons demonstrating no (**K**) and limited (**L**) RA-rescue. Note the lower degree of fusion between C1 and the occipitals (L) compared to untreated double mutants (J). **Abbreviations**: AAA, anterior arcus atlantis; BO, basioccipital; C, cervical vertebra; "C", vertebrae with characteristics of the designated cervical vertebra; EO, exoccipital; P, proatlas.

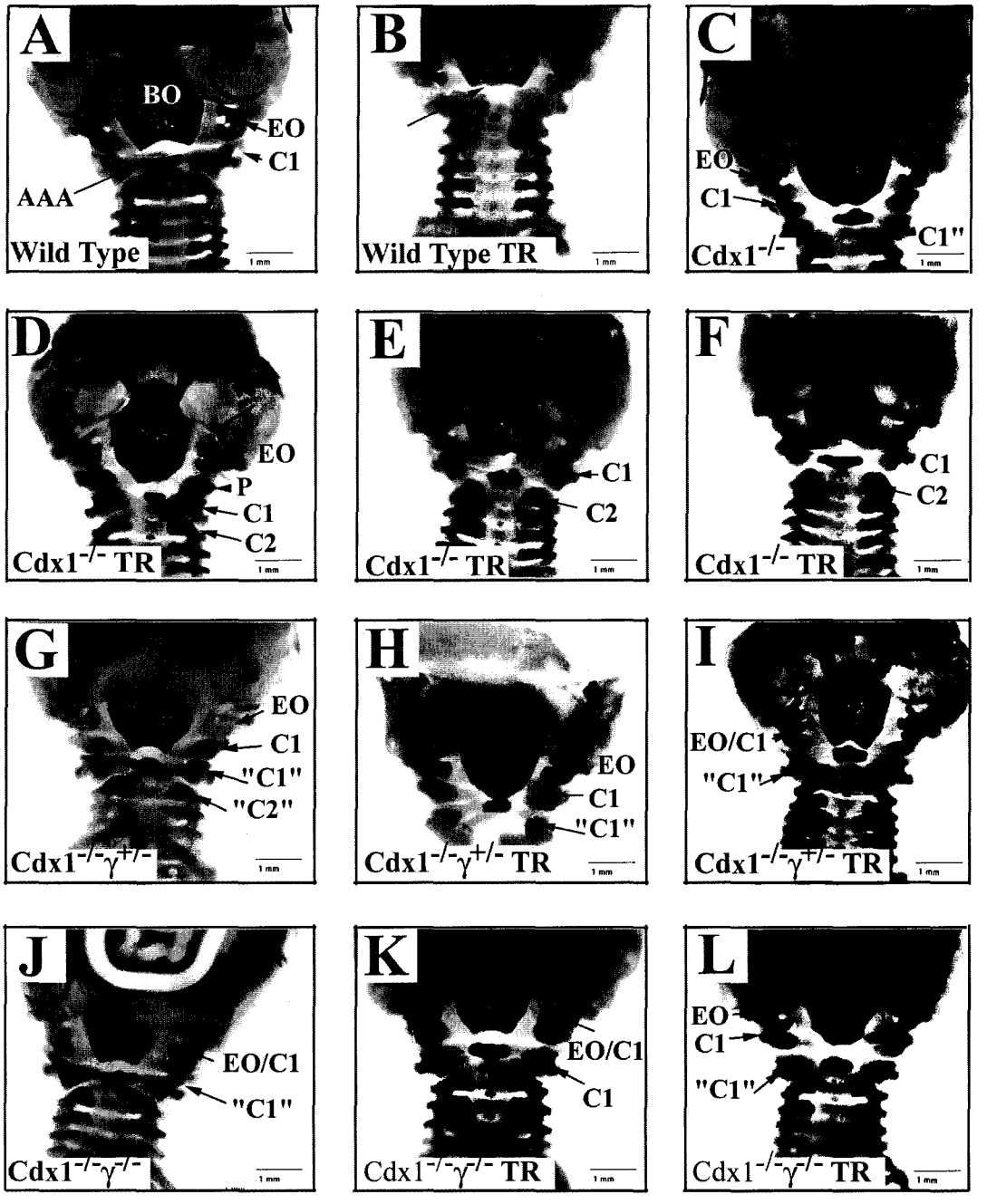
A
BO
EO
C1
AAA
Wild Type
1 mm
B
Wild Type TR
1 mm
C
EO
C1
C1"
Cdx1-/-
1 mm
D
EO
P
C1
C2
Cdx1-/- TR
1 mm
E
C1
C2
Cdx1-/- TR
1 mm
F
C1
C2
Cdx1-/- TR
1 mm
G
EO
C1
"C1"
"C2"
Cdx1-/-γ+/-
1 mm
H
EO
C1
"C1"
Cdx1-/-γ+/- TR
1 mm
I
EO/C1
"C1"
Cdx1-/-γ+/- TR
1 mm
J
EO/C1
"C1"
Cdx1-/-γ-/-
1 mm
K
EO/C1
C1
Cdx1-/-γ-/- TR
1 mm
L
EO
C1
"C1"
Cdx1-/-γ-/- TR
1 mm

transformation (50% AAA and 81% thick neural arches), which was also partially rescued by treatment (20% AAA and 10% thick neural arches). However, the loss of both *RARγ* alleles from the *Cdx1* heterozygous background significantly impaired this RA-rescue (87% untreated vs. 80% treated AAA, and 33% untreated vs. 20% treated thick neural arches). This relationship was even more striking in the *Cdx1* null homozygotes, where 100% of these skeletons typically exhibit a complete transformation of C2 to C1. RA-treatment partially inhibited this transformation such that 57% of the C2 vertebrae appeared virtually normal (compare Figure 5.8A and H). The remainder either shared an AAA with C1 (Figure 5.8F) or possessed an ectopic AAA fused to the AAA of C1 (Figure 5.8G). Again, loss of *RARγ* inhibited the RA-rescue of the C2 to C1 transformation, as 100% of $Cdx1^{-/-}RAR\gamma^{+/-}$, and 89% of the $Cdx1^{-/-}RAR\gamma^{-/-}$, skeletons exhibited complete C2 to C1 anterior transformations following treatment. Similarly, RA-rescue of the C3 to C2 anterior transformation also appeared to require *RARγ* (Table 5.2, and Figure 5.8I and J, and K and L).

The RA-rescue of more caudal cervical transformations in the $Cdx1^{-/-}$ mutant skeletons appeared to be less dependent on *RARγ*. For example, C6 to C5 and C7 to C6 transformations were observed in nearly all of the untreated $Cdx1^{-/-}$, $Cdx1^{-/-}RAR\gamma^{+/-}$ and $Cdx1^{-/-}RAR\gamma^{-/-}$ skeletons. Treatment with RA completely inhibited these transformations in the $Cdx1^{-/-}$ specimens, and partially inhibited them in $Cdx1^{-/-}RAR\gamma^{+/-}$ (67% with transformations) and $Cdx1^{-/-}RAR\gamma^{-/-}$ (56% with transformations) mice. Therefore, unlike the nearly complete resistance to RA-rescue of C1, C2, and C3 transformations, the sixth and seventh vertebrae of the $Cdx1^{-/-}RAR\gamma^{+/-}$ and $Cdx1^{-/-}RAR\gamma^{-/-}$ mutants were only partially resistant to the effects of RA. These results indicate that the RA signal is transduced through another RAR to partially rescue the specification of these vertebrae.

The incidence of T1 to C7 anterior transformation, which occurred at a higher frequency in *Cdx1/RARγ* double mutants, was also reduced by RA treatment at E7.4. Only 33% of the treated double mutants exhibited this transformation, while it occurred in 80% of the untreated skeletons of the same genotype. Moreover, treated $Cdx1^{-/-}$ $RAR\gamma^{+/-}$ skeletons also exhibited a reduced incidence of this transformation (50%

Figure 5.10. Effect of RA treatment, and requirement of *RARγ*, on the cervical phenotypes of *Cdx1*$^{+/-}$ skeletons. (A-F) Lateral view of the cervical region, dorsal is left. Treated (TR) skeletons were exposed to 10mg/kg of RA at E7.4. (**A**) Untreated *Cdx1*$^{+/-}$ control. Note the ectopic AAA, and wide neural arches on C2. (B) Treated *Cdx1*$^{+/-}$ skeleton. Note the formation of a proatlas and the rescue of an ectopic AAA on C2. Arrowhead indicates malformation of the C1 neural arch. The tuberculum anterium is located on vertebra 5 instead of vertebra 6. (**C**) *Cdx1*$^{+/-}$*RARγ*$^{+/-}$ untreated control. Note the ectopic AAA on C2. (D) RA-treated *Cdx1*$^{+/-}$*RARγ*$^{+/-}$ skeleton. The tuberculum anterium is located on vertebrae 6 (normal). (E) Untreated *Cdx1*$^{+/-}$*RARγ*$^{-/-}$ skeleton. Note the fusion of neural arches, and presence of ectopic AAA on C2. (F) RA-treated *Cdx1*$^{+/-}$*RARγ*$^{-/-}$ skeleton. Note the presence of TA on vertebra 6, and the fusion of neural arches of C3 and C4. This specimen represents the minority of RA-treated *Cdx1*$^{+/-}$*RARγ*$^{-/-}$ skeletons. The majority did not show an altered phenotype compared to the untreated controls.

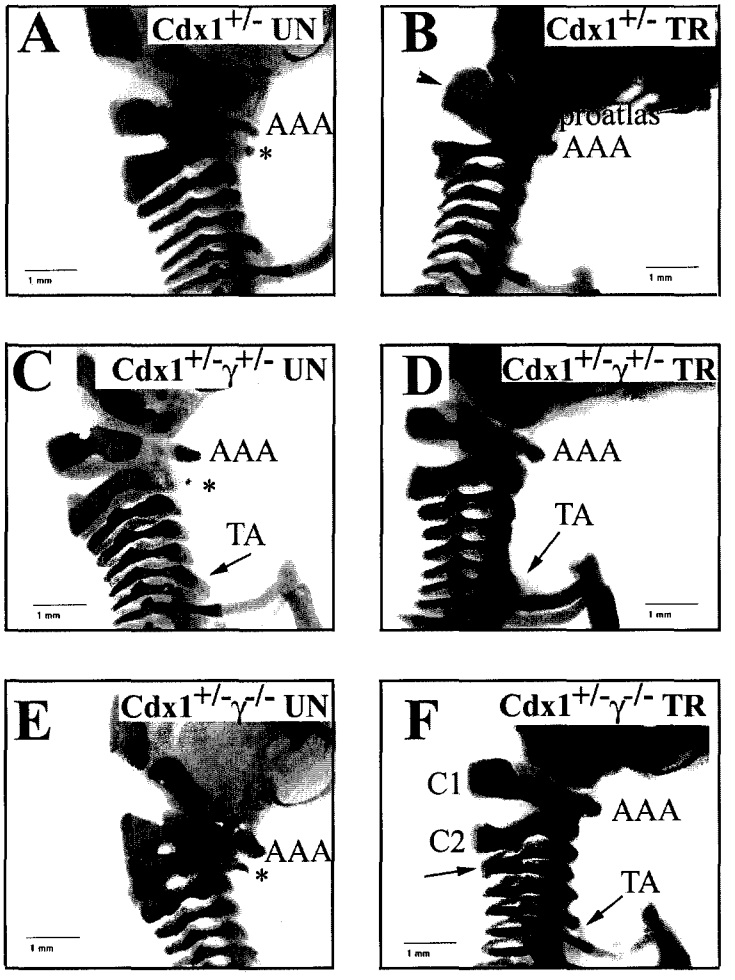
A
Cdx1+/- UN
AAA
*
1 mm
B
Cdx1+/- TR
proatlas
AAA
1 mm
C
Cdx1+/-γ+/- UN
AAA
*
TA
1 mm
D
Cdx1+/-γ+/- TR
AAA
TA
1 mm
E
Cdx1+/-γ-/- UN
AAA
*
1 mm
F
Cdx1+/-γ-/- TR
C1
C2
AAA
TA
1 mm

untreated vs. 33% treated), and the eighth vertebra never displayed a C7 phenotype in treated *Cdx1*$^{-/-}$ mutants, as compared to 38% of untreated controls.

5.3j. Sensitivity to RA-induced malformations

Excess RA, administered at E8.5, results in precocious truncation of the axial column, and neural tube defects (Tibbles and Wiley, 1988: Kessel and Gruss, 1991; Kessel, 1992). These malformations require RARγ, as RARγ$^{-/-}$ mutant embryos are completely resistant to these teratogenic effects (Lohnes *et al.*, 1993). *Cdx1* message levels increase in the caudal region of the embryo following RA treatment at E8.5, and ectopic expression of *caudal* family members in *Xenopus* and the mouse results in axial truncation and neural tube defects, respectively (Epstein *et al.*, 1997; Isaacs *et al.*, 1998; Charité *et al.*, 1998). As *RARγ* and *Cdx1* are required for the full effects of excess RA on the vertebral column at E7.4, it is possible that *Cdx1* may also be involved in RA-induced caudal truncation. To assess this, *Cdx1* heterozygous crosses were established and pregnant females gavaged with 100mg/kg of RA at E8.5. All of the resultant newborn offspring were similarly affected by the RA treatment and exhibited the same degree of caudal truncation, irrespective of genotype (data not shown).

RA treatment between E9.5 and E10.5 results in severe malformation of the limbs (Wood *et al.*, 1996). As *Cdx1* is expressed in the limb bud mesenchyme at these stages of development, the involvement of this gene in the RA-induced limb malformations was also tested. Again, RA treatment resulted in limb malformations in both wild type and *Cdx1* null embryos. Therefore, although *Cdx1* is required to mediate some of the RA-induced homeosis of the vertebral column, it is not essential for these other congenital abnormalities.

5.4 Discussion

5.4a. Cdx1 heterozygotes

The loss of both copies of *Cdx1* in the mouse has profound effects on AP patterning of the vertebral column. Previous results suggested that *Cdx1* is not haploinsufficient as heterozygotes display no discernable phenotype (Subramanian *et al.*, 1995). However, the findings presented in this study demonstrate that two copies of a

functional *Cdx1* gene are required for correct specification of the first two vertebral units, the atlas and the axis. Several lines of evidence indicate that members of the caudal gene family are transcriptional regulators of *Hox* genes. In *Xenopus*, over expression of *Xcad2* and *Xcad3* results in anteriorization of certain *Hox* expression domains along the AP axis (Pownall *et al.*, 1996; Epstein *et al.*, 1997; Isaacs *et al.*, 1998). Conversely, expression of a dominant negative *Xcad* inhibits the induction of several *Hox* genes (Isaacs *et al.*, 1998). In the mouse, *Cdx1* null embryos exhibit posterior shifts of multiple *Hox* expression domains in the prevertebrae (Subramanian *et al.*, 1995). Moreover, putative CDX binding sites have been identified in the promoters and enhancers of several *Hox* genes (Subramanian *et al.*, 1995; Charité *et al.*, 1998).

Cdx1 homozygous null embryos display a posteriorization of *Hoxd3* expression by one somite at E9.5 (Subramanian *et al.*, 1995). This is consistent with the phenotype of *Hoxd3* null embryos, which exhibit C1 transformation to an occipital-like structure, and C2 to a partial C1 identity (Condie and Capecchi, 1993). *Hoxd3* heterozygotes exhibit a milder anterior transformation of the atlas such that the basioccipital is fused to the AAA by an ossified bridge. A posterior shift of *Hoxd3* expression in *Cdx1* heterozygotes was not observed (data not shown). However, in light of the similarity of the $Cdx1^{+/-}$ and $Hoxd3^{+/-}$ phenotypes, it seems plausible that reduced levels of *Hoxd3* expression (which may not be detectable by *in situ* hybridization methods) may account for the basioccipital-AAA fusion in *Cdx1* heterozygotes.

Hoxd4 mutant skeletons exhibit a caudal extension of the basioccipital bone, or an ossified bridge between this bone and the AAA (Horan *et al.*, 1995a). Moreover, an ectopic AAA and widened neural arches frequently appear on C2. As the *Cdx1* heterozygotes phenocopy these *Hoxd4* null defects, it is tempting to speculate that *Cdx1* may control the expression of *Hoxd4*. However, as with *Hoxd3*, no difference in *Hoxd4* expression was observed in the *Cdx1* heterozygous or homozygous E9.5 mutant embryos. Given these findings, it is possible that CDX1 may regulate paralogues of *Hox*d3 or *Hox*d4 (i.e. *Hox*a3 or *Hox*b4), as paralogous genes are often functionally redundant. Additionally, subtle changes in individual *Hox* expression may not be detectable by *in situ* hybridization, and it is possible that the expression of multiple *Hox* genes may be

diminished by the loss of one *Cdx1* allele. The net effect of this combined reduction could be a partial anterior transformation of the atlas and the axis.

5.4b. Cdx1 is downstream of RA-signaling in vertebral specification

It has recently been demonstrated that *Cdx1* is a direct target of RA excess in the developing embryo (see Introduction and Houle *et al.*, 2000). As a transcription factor downstream of retinoid signaling, *Cdx1* may potentially be involved in RA-induced congenital malformations. In support of this hypothesis, *Cdx1* expression is increased in the region of the primitive streak following exposure to RA at E8.5, and in the forelimb buds following RA treatment at E9.5 (Houle *et al.*, 2000). Both of these sites are targets for RA-induced developmental abnormalities (reviewed in Ross *et al.*, 2000). However, *Cdx1* null embryos are as susceptible as wild type embryos to retinoid induced malformations of both the body axis and the limb. Therefore, *Cdx1* does not appear to play a significant role in mediating these teratogenic effects.

Since the abnormal phenotype of *Cdx1* null mice appears to be limited to the vertebral column, a more likely role for *Cdx1* may be in mediating RA-induced homeotic transformations of the vertebrae. The results of this study further support this hypothesis, as *Cdx1* null embryos are resistant to cervical posterior transformations induced by RA at E7.4. This is the first evidence that *Cdx1* is an essential downstream component of the retinoid signaling pathway *in vivo*, and offers an explanation as to how excess RA can induce the expression of *Hox* genes that do not have RAREs.

5.4c. RARγ regulates additional target genes involved in vertebral patterning

Although *Cdx1* partially mediates the posteriorizing effects of excess RA at E7.4, it was not clear whether this gene is the only target of RARγ required for normal vertebral patterning. The increase in penetrance of the T1 to C7 transformation in *Cdx1/RARγ* double mutant skeletons, as compared to either single mutant, demonstrates that RARγ regulates the expression of additional factors involved in vertebral specification. This also demonstrates a role for RARγ in patterning the posterior cervical and anterior thoracic vertebrae, a function that is masked by the presence of CDX1. Further evidence that RARγ regulates target genes distinct from the *Cdx1* pathway is

provided by the observation that *Cdx1* null skeletons display increased resistance to RA-induced transformations when at least one *RARγ* allele is disrupted. For example, the formation of a proatlas is never observed in RA-treated compound *Cdx1/RARγ* mutant skeletons. Moreover, RA-treatment of *Cdx1* null embryos results in a rescue of the anteriorized cervical region, such that the morphology of these vertebrae become relatively normal. This effect requires RARγ, as mutation of this gene nearly abolishes the RA-mediated rescue. The residual RA-mediated posteriorization observed in *Cdx1/RARγ* double null skeletons suggests that some effects are mediated via another RAR, likely RARα as it is broadly expressed during development.

5.4d. Cdx1 and RARγ act synergistically in vertebral patterning

The significant increase in penetrance and expressivity of the cervical anterior transformations in *Cdx1/RARγ* double heterozygotes, as compared to single heterozygotes, demonstrates that these transcription factors act synergistically to specify vertebral identity. There are several potential mechanisms by which this synergistic action could be explained. For example, RARγ and CDX1 may bind to the same enhancer region of a target gene(s) leading to a greater-than-additive effect on the transcriptional machinery (Carey, 1998). In this regard, a putative CDX binding site has been identified 2 bp downstream of a RARE in the 3' region of the *Hoxd4* gene (Zhang *et al.*, 2000). However, this site does not bind human CDX1 *in vitro*, and this RARE is not required for *Hoxd4* expression in the somites. Moreover, the expression of *Hoxd4* in the somites at E9.5 is not altered in *RARγ* mutants (Folberg *et al.*, 1999a) or *RARγ/Cdx1* double mutants (Figure 5.7). Therefore, it is unlikely that this particular combination of elements is involved in the specification of vertebral patterning. However, this does not rule out the existence of a similar combination of regulatory elements in the promoter/enhancer regions of other *Hox* genes.

It is also possible that RARγ and CDX1 regulate the expression of distinct target genes, either directly or through a cascade, which affect the same physiological processes. Alteration of expression of genes that control cellular proliferation, migration, and apoptosis may ultimately re-direct shaping of the vertebral unit. Alternatively, given that expression of *Cdx1* is dependent on *RARs* (Houle *et al.*, 2000), the loss of functional

RARγ alleles could result in lower levels of *Cdx1* transcripts. This effect may not be significant if two *Cdx1* alleles are functional, however, in the case of *Cdx1* heterozygotes this could further reduce the quantity of transcripts below the level necessary for sufficient activation of CDX1 target genes. As *Cdx1* is haploinsufficient, it is conceivable that a greater reduction in the number of *Cdx1* transcripts could lead to an increased incidence of homeotic transformations.

5.4e. Potential targets of RARγ and Cdx1

The increased penetrance of the T1 to C7 anterior transformation in *Cdx1/RARγ* double mutants suggests that the level of *Hox* gene expression in this region is altered in these embryos. *Hoxb5* and *Hoxb6* are candidate targets for this, as the cognate null mutants exhibit transformations of C6 to C5, C7 to C6, and T1 to C7 (Rancourt *et al.*, 1995), and their expression in *Cdx1* null and *Cdx1/RARγ* double null embryos is currently under investigation. *Hoxb5* and *Hoxb6* appear to act together, as transheterozygotes exhibit these transformations at the same frequency as either single null mutant. Although expression analysis may be informative, the latter finding also suggests that a slight decrease in the expression of these (and potentially other) *Hox* genes may be functionally significant, yet may not be detectable by *in situ* hybridization. Other *Hox* genes have also been demonstrated to be required for correct patterning of the cervical-thoracic region, including members of the 4th, 5th and 6th paralogous groups (Jeannotte *et al.*, 1993; Horan *et al.*, 1994, 1995a, 1995b; Kostic and Capecchi, 1994; Boulet and Capecchi, 1996; Aubin *et al.*, 1997, 1998). These represent additional candidate *Cdx1/RARγ* targets potentially necessary for specification of the first thoracic vertebra.

RA-treatment at E7.4 rescues much of the *Cdx1* null phenotype. Perhaps one of the most striking differences is the restoration of a relatively normal atlas, as opposed to complete fusion of this vertebra with the occipitals in untreated *Cdx1* mutants. *Hoxd3* is posteriorized by one somite in E9.5 *Cdx1* null embryos, and *Hoxd3* mutants phenocopy this vertebral fusion (Condie and Capecchi, 1993; Subramanian *et al.*, 1995). However, in the *Hoxd3* null mutants, reduced neural arches of the atlas persist, while they are absent in *Cdx1* null skeletons. This implies that additional genes involved in patterning

of the atlas are affected by the loss of *Cdx1*. In this regard, *Hoxa3/d3* and *Hoxb3/d3* double mutants display a complete loss of the atlas (Condie and Capecchi, 1994; Manley and Capecchi, 1997). Therefore, *Cdx1* may also control the regulation of *Hoxa3* or *Hoxb3*. RA treatment at E7.5 anteriorizes the expression of *Hoxa3* by one prevertebra, and this anteriorization is correlated with the induction of a proatlas (Kessel and Gruss, 1991). Therefore the group 3 *Hox* genes are potential targets for RA-mediated rescue of the atlas-occipital fusion in *Cdx1* null embryos. The anterior expression limit of *Hoxd3* in the somites remains posteriorized following RA treatment of *Cdx1* null embryos at E7.4 (M. Houle, D. Allan, and D. Lohnes unpublished observations), although it is anteriorized in the CNS, as previously observed (Conlon and Rossant, 1992). As *Hoxa3* is anteriorized in the paraxial mesoderm by RA-treatment (Kessel and Gruss, 1991), it is possible that this gene mediates the RA-induced rescue. This is supported by the finding that *Hoxa3* and *Hoxd3* can functionally substitute for one another (Greer *et al.*, 2000). The expression of *Hoxa3* in wild type and *Cdx1* null (untreated and RA-treated) embryos is currently under investigation.

5.4f. Conclusions

In conclusion, the results presented in this chapter support a model by which RA regulates the expression of some *Hox* genes via *Cdx1*. *Cdx1* is required to exert some of the RA-induced effects on the vertebral column, demonstrating that this transcription factor functions downstream of RA-signaling *in vivo*. In addition to this linear pathway, *Cdx1* and *RARγ* also interact in parallel to synergistically influence vertebral specification. Finally, these results also provide evidence of a novel role for *RARγ* in vertebral patterning not revealed by disruption of the *RARγ* gene alone, or in combination with other *RARs*.

Chapter 6

Discussion

6.1 Regulation of *Hox* expression by retinoic acid

It has been well established that exposure of the developing vertebrate embryo to excess RA leads to severe congenital defects, which include alterations in anteroposterior identity of the hindbrain and vertebral column (Durston *et al.*, 1989; Kessel and Gruss, 1991; Conlon and Rossant, 1992; Kessel, 1992). In general, excess RA causes posteriorizations, and in some cases deletions, of anterior structures. These abnormalities are correlated with changes in both the expression levels and domains of various *Hox* genes. In human EC cells, it was noted that the *Hox* genes respond to RA differently depending on their location in the cluster. Those situated closer to the 3' end respond more rapidly and to lower concentrations of RA than *Hox* genes located in more 5' regions of the cluster (Simeone *et al.*, 1990, 1991).

Given the spatial colinearity of *Hox* expression that is observed along the anteroposterior axis, it has been proposed that a gradient of RA is present in the developing embryo, with the highest concentrations found in the posterior end (reviewed in Marshall *et al.*, 1996). In this model RA would function as a morphogen, inducing the expression of different *Hox* genes at different concentrations. While this model is attractive, no evidence of such a gradient has been found in the mouse. Instead, RA is present in all three germ layers of the posterior end of the embryo at the headfold stage (E7.75), and at high levels in the trunk with sharp anterior and posterior boundaries at E8.5 (Rossant *et al.*, 1991; Horton and Maden, 1995).

An alternative hypothesis is that the length of time that cells are exposed to RA while in the primitive streak is critical to the expression of specific *Hox* genes. In this model, cells that exit the streak at later stages would have been exposed to RA for a longer period of time, thereby resulting in the activation of more 5' *Hox* genes. Hence, excess RA in the primitive streak mesoderm may mimic the effect of a longer exposure time, and lead to the premature activation of *Hox* expression.

6.2 RA regulation of endogenous *Hox* expression

The identification of RAREs in the promoters of several *Hox* genes strongly suggested that RA regulates endogenous *Hox* expression. This has been confirmed by mutation of the *Hoxa1* 3'RARE which results in lower levels of *Hoxa1* expression and a

delay in its anterior spreading at E7.75 (Dupé *et al.*, 1997). Compared to wild type embryos, much lower levels of *Hoxa1* transcript are detected at E8-E8.5 in *Hoxa1* 3'RARE mutant embryos. Therefore, proper initiation, spreading, and maintenance of *Hoxa1* expression in the spinal cord and paraxial mesoderm are dependent, either directly or indirectly, on the 3'RARE. In addition to *Hoxa1*, the expression of *Hoxa2* in rhombomere 5 is also affected in *Hoxa1* 3'RARE null mutant embryos (Dupé *et al.*, 1997). However, it is not clear whether this is due to a direct effect of the *Hoxa1* 3'RARE on *Hoxa2* expression, or to an indirect effect *via* cross-regulation by the *Hoxa1* gene product. The *Hoxa1* 3'RARE is also necessary for the proper initiation of *Hoxb1* expression in the primitive streak in the absence of the *Hoxb1* 3'RARE (Studer *et al.*, 1998). Furthermore, mutation of the *Hoxd4* 3'RARE, which is located in a region of the promoter which contains a neural enhancer, results in a dramatic delay and downregulation of *Hoxd4* transgene expression in the CNS (Zhang *et al.*, 2000). Taken together, these results demonstrate that RA has an important role in the direct initiation of *Hox* expression, and likely in the initiation of auto- and cross-regulatory loops that maintain *Hox* expression at later stages. The alterations in *Hox* expression which occur following the disruption of the *Hoxa1* 3' RARE alone or in combination with the 3' RARE of *Hoxb1* lead to milder versions of the phenotypes observed in *Hoxa1* and *Hoxb1* null mice. Therefore, RA signaling is required to initiate at least some of the normal developmental roles that are performed by the *Hox* gene products.

Given that RARE mutations significantly affect *Hox* expression, it could be anticipated that *RAR* null mutant mice, which exhibit homeotic transformations of the vertebral column, would exhibit altered anterior boundaries of *Hox* expression. However, there has been no report of abnormal *Hox* expression boundaries in the somites or prevertebrae of *RAR* mutant embryos. It is possible that *Hox* expression patterns may have not been extensively characterized in these mutants, and differences in the anterior boundaries may indeed exist. Alternatively, the loss of a *RAR* may decrease the level of transcription from a certain *Hox* promoter without affecting its anterior border of expression, and this reduction may be sufficient to account for the low frequency of vertebral transformations observed in the single *RAR* mutants. Presumably, in double *RAR* mutants the transcription rates of these *Hox* genes would be further reduced, thus

increasing the incidence and expressivity of the homeotic transformations. Additionally, with respect to vertebral patterning, most *Hox* expression analysis is performed at E9.5, before somite differentiation, or at E12.5 after the formation of the prevertebrae. Given the phenotypes obtained following mutation of the *Hox* RAREs it may be important to examine the early expression levels and patterns of *Hox* genes in the *RAR* mutant embryos. Perhaps a delay in the induction or establishment phase could lead to altered vertebral identity even though the final *Hox* expression pattern is unaffected.

6.3 At what stage is RA required for Hox expression?

Hox expression in the vertebrate embryo can be divided into three major phases: initiation, establishment and maintenance (Deschamps *et al.*, 1999). All *Hox* expression is initiated in the same region of the embryo: the posterior-most portion of the primitive streak. Following initiation, the *Hox* expression domains spread anteriorly along the streak, and into the neuroectoderm, lateral plate mesoderm, and paraxial mesoderm. During this establishment phase, the anterior boundaries of *Hox* expression become more rostral as development proceeds. This progressive anteriorization is not due to cellular interactions, as insertion of a physical barrier does not block *Hox* 'spreading' in any of these tissues. Instead, these cells appear to be pre-programmed to initiate *Hox* expression when they reach a certain developmental stage, or after a certain length of time. Moreover, this temporal delay is inversely correlated with the physical order of the cells along the axis, such that more anterior cells (i.e. the first to leave the primitive streak) express a given *Hox* gene at a later time-point relative to more posterior cells (i.e. those which left the primitive streak at a later stage). Once the pre-determined anterior boundary of expression for a particular *Hox* gene is reached, the expression domain is maintained, and persists in the progeny of these cells.

Studies on the effects of excess RA on the developing vertebral column strongly indicate that the final *Hox* expression domains are influenced by RA while the epiblast cells are ingressing though the primitive streak (Kessel and Gruss, 1991; Kessel, 1992). Exposure to RA at E7.5 affects vertebrae along the entire length of the axis, while exposure at E8.5 affects thoracic and more posterior vertebrae. Notably, *Hoxa3* expression is anteriorized in the prevertebrae following RA exposure at E7.5, however it

is unaffected by treatment at later stages. As *RAR* null mutant mice exhibit homeotic transformations of the cervical vertebrae, this suggests that the RARs function between E7.5 and E8.0, as the precursors to these vertebrae are ingressing through the primitive streak. This is supported by the observation that RA is only detectable in this region of the embryo during the same developmental stages.

It is also possible that RA influences *Hox* expression in the somites as they contain high levels of RA. Accordingly, *Hoxa1* expression is initiated in *Raldh2* null embryos in the region of the primitive streak, but is not maintained in the paraxial mesoderm at later stages (Neiderreither *et al.*, 1999). However, it is not clear whether the lack of maintained *Hoxa1* expression is due to the absence of RA in the somites, or whether other factors, whose expression is also initiated by RA in the primitive streak, are required at later stages to perform necessary cross-regulation of *Hoxa1*. In order to address this issue, *Raldh2* null embryos could be dosed with RA at E7.5 to determine whether the presence of RA at this stage is sufficient to induce the later maintenance functions. Alternatively, a temporal-specific disruption of *Raldh2* at E8.5 would determine whether the continued presence of RA throughout the initiation and establishment phase is required for normal *Hox* expression.

Analysis of *Hoxb4* regulation in the CNS has demonstrated that RA, and another factor from the paraxial mesoderm, are required at early stages to set the proper anterior expression boundary at the rhombomere 6/7 junction (Gould *et al.*, 1998). A DR5 RARE is present in an early neural enhancer (NE), and is required for initiation of a *Hoxb4* transgene in the CNS. Following rhombomeric segmentation, a late NE is activated and functions to maintain the appropriate *Hoxb4* expression domain. This late NE has been identified as an auto- and cross-regulatory element, and HOX proteins from several paralogous groups can bind to this region (Gould *et al.*, 1997). While the early NE is required for the initial response of *Hoxb4* expression to exogenous RA, the late NE is necessary for the maintenance of ectopic expression at later stages. Perhaps a similar regulatory mechanism operates in the paraxial mesoderm, such that RA initiates expression of *Hox* genes in the paraxial mesoderm, and auto-, cross-, and para-regulatory mechanisms maintain this expression following somite segmentation.

6.4 Indirect regulation of Hox expression by RA: *Cdx1*

Although RA may not be acting as a morphogen *per se*, it is possible that it may control the expression of other genes that are expressed along the axis in a gradient. There is evidence to support a gradient within the paraxial mesoderm that controls *Hox* expression in the CNS. For example, rhombomeres that are transplanted to more posterior regions of the spinal cord are induced to express more 5' *Hox* genes, and the factors that mediate this induction originate from the paraxial mesoderm (Grapin-Bottin *et al.*, 1995, 1997). Additionally, the premature activation and anterior expression of *Hox* genes that occurs following the removal of a repressor region at the 5' end of the *HoxD* complex is not sustained later in development (Kondo and Duboule, 1999). This indicates that although *Hox* expression can be initiated in ectopic regions, other factors are required to maintain this expression, and that these factors are absent from more anterior mesoderm. It is important to note that the 'gradient' need not be composed of a single protein. For example, different combinations of transcription factors may activate the expression of specific *Hox* genes, and an increased number of factors may be necessary for the induction of more 5' *Hox* genes.

There is growing evidence to support a role for CDX1 as one of these factors. Excess RA induces *Cdx1* expression at several stages of development. Moreover, the levels of *Cdx1* are dramatically reduced in *RARα1/γ* double mutant E7.5 embryos. However, at E8.5, *Cdx1* expression is not affected by the loss of these two receptors, indicating that another pathway supports *Cdx1* expression at this stage of development. This is in concordance with the absence of detectable RA in the open posterior neuropore at this time (Rossant et al., 1991; Horton and Maden, 1995). While the increased incidence of homeotic transformations observed in *Cdx1/RARγ* double heterozygotes demonstrates that these transcription factors act synergistically in the specification of vertebral identity, it is not clear how this occurs. As RA regulates the expression of *Cdx1* it is possible that a reduction in RA signaling, by the inactivation of one *RARγ* allele, would lead to a further reduction of *Cdx1* expression in the *Cdx1* heterozygous background. This reduction may bring *Cdx1* levels below a certain threshold that is required for sufficient *Hox* expression. Alternatively, RARγ and CDX1 may regulate the

expression of a common set of target genes, or different genes that are involved in common developmental processes.

As with the RARs, it has not been determined at which stage CDX1 affects *Hox* expression. The earliest time point at which *Hox* expression has been examined in *Cdx1* null mutant embryos is E9.5 (Subramanian *et al.*, 1995), and at this stage *Hoxd3* expression is already posteriorized. The posterior shift in the *Hoxd3* anterior boundary could be due to the absence of *Cdx1* at the initiation stage, such that initiation is delayed and *Hoxd3* expression does not reach its anterior-most domain by the time/stage *Hox* expression patterns become fixed. Alternatively, *Cdx1* could be required to maintain *Hoxd3* expression in the anterior-most somite and its absence could lead to the loss of established *Hoxd3* expression from this somite. This is analogous to the late NE function discussed in Section 6.3. However, *Cdx1* is expressed very weakly throughout the somites until E9.5, when it is detected in the dermomyotome (Meyer and Gruss, 1993; Houle *et al.*, 2000). A clue regarding the site of action of CDX1 may be provided by the expression pattern of *Cdx2*. This gene is also required for proper anteroposterior specification of the vertebrae although it is never expressed in the somites (Beck *et al.*, 1995; Chawengsaksophak *et al.*, 1997). Therefore, CDX2 must specify vertebral identity in the cells of the primitive streak or unsegmented paraxial mesoderm. A careful analysis of *Hox* expression patterns from initiation to maintenance stages may help clarify the role of *Cdx1* in the regulation of *Hox* expression.

While it is likely that *RARγ* and *Cdx1* function together during the early stages of gastrulation as *Hox* gene expression is initiated, the possibility that these two transcription factors act at different stages of vertebral specification can not be excluded. In addition to *RARγ* expression in the region of the primitive streak, these transcripts are detected in the sclerotome beginning at E10.5 (Ruberte *et al.*, 1990). Therefore CDX1 and RARγ could function in different tissues, as well as at different stages. For example, anterior transformations may arise due to the absence of *Cdx1* expression in the primitive streak and/or the somites, and may be exacerbated by the absence of *RARγ* during migration of the sclerotome to form the vertebrae.

RA treatment at E7.4 is capable of rescuing some of the anteriorizations that are characteristic of *Cdx1* null embryos. These data can be interpreted in several ways. First,

RA could increase and/or anteriorize the expression of the same *Hox* genes that are affected by the loss of *Cdx1*. This would imply that the relationship between CDX1 and RA is not only linear, but that they act in parallel to control the expression of common target genes. There is some evidence that does not support this model. Exposure of E7.4 embryos to excess RA results in the anteriorization of the *Hoxd3* expression domain in the neural tube and an increase in *Hoxd3* expression levels in the paraxial mesoderm at E9.5. In *Cdx1* null mutant embryos, the induction of *Hoxd3* expression levels by RA in the paraxial mesoderm is compromised, although RA is able to anteriorize expression of *Hoxd3* in the neural tube (M. Houle, D. Allan and D. Lohnes, unpublished observations). While this supports a linear relationship between RA and *Cdx1* in the regulation of *Hox* expression, it does not provide an answer as to how RA rescues the *Cdx1*$^{-/-}$ associated anteriorizations. A second model of RA-rescue could involve the anteriorization and/or increased expression of different *Hox* genes that can functionally compensate for the loss of *Cdx1*. In this regard, the RA-induced expression pattern of *Hoxa3* is presently being characterized in *Cdx1* null mutant embryos (M. Houle, D. Allan, and D. Lohnes unpublished observations). Of course, it is entirely possible that a combination of these two models is correct, such that RARγ and CDX1 cooperate to activate some genes, and act independently, or in concert with other factors, to regulate the expression of other genes.

6.5 RA regulation of Hox expression through other intermediary factors

Studies in *Xenopus* have demonstrated that ectopic expression of *Xcad2* and *–3* results in transcriptional activation of some of the same *Hox* genes (Pownall *et al.*, 1996; Epstein *et al.*, 1997; Isaacs *et al.*, 1998). Additionally, overexpression of *Cdx1, -2*, or *-4* results in ectopic expression of *Hoxb8* (Charité *et al.*, 1998). These data suggest that CDX proteins are able to perform some of the same functions *in vivo*. In this case, it could be suggested that the RA rescue of the *Cdx1*-null phenotype is mediated by an increase in *Cdx2* and/or *Cdx4* expression. However, recent evidence has demonstrated that the expression levels of both *Cdx2* and *Cdx4* are downregulated in the embryo following RA treatment (Iulianella *et al.*, 1999; Prinos *et al.*, manuscript in preparation).

There are several other candidates that could be involved in the indirect regulation of *Hox* expression by RA. PBX and MEIS transcription factors are members of the TALE family of homeodomain proteins that are required as cofactors for the efficient binding of HOX proteins to DNA (Bürglin, 1997). In addition, MEIS, PBX, and HOX proteins can form trimeric complexes on heterodimeric DNA-binding sites (Shanmugam *et al.*, 1999; Shen *et al.*, 1999). RA treatment results in an increase of *Meis1* and *Meis2* expression in P19 cells and the developing limb (Oulad-Abdelghani *et al.*, 1997; Mercader *et al.*, 2000), and the protein levels of PBX transcription factors are increased following RA induced differentiation of P19 cells (Knoepfler and Kamps, 1997). Therefore, RA may alter the transcriptional activity of HOX proteins by regulating the levels of their binding partners.

DNA-binding partners for CDX2/3, such as HNF1α and Pax6, have recently been identified *in vitro* (Andersen *et al.*, 1999; Hussain and Habener, 1999; Ritz-Laser *et al.*, 1999; Mitchelmore *et al.*, 2000). As these transcription factors act synergistically with CDX2/3 to promote transcriptional activation, it is likely that heterodimeric partners of CDX proteins are also involved in vertebral specification. Regulation of the genes encoding these proteins could be another mechanism by which RA indirectly influences *Hox* expression.

6.6 The FGF signaling pathway and Hox expression

6.6a FGFR1, Cdx, and anteroposterior patterning

Fibroblast growth factor receptor 1 (Fgfr1) null embryos do not survive past E9.5, and their anteroposterior axes are truncated due to the inability of gastrulating cells to traverse the primitive streak (Deng *et al.*, 1994; Yamaguchi *et al.*, 1994; Ciruna *et al.*, 1997; Deng *et al.*, 1997). In contrast, mice carrying hypomorphic *Fgfr1* alleles exhibit a much milder phenotype, which allows the completion of gestation (Partanen *et al.*, 1998). These mice have a reduced number of caudal vertebrae, resulting in a short to absent tail, and a high incidence of vertebral homeotic transformations. The majority of these are anterior transformations, similar to those observed in *Cdx1* null and *Cdx2* heterozygous mice (Subramanian *et al.*, 1995; Chawengsaksophak *et al.*, 1997). *In situ* hybridization

analysis at E8.5 demonstrated that the anterior limit of *Hoxd4* expression is posteriorized by one somite in these embryos.

In *Xenopus*, a linear relationship between FGFs, Xcads, and *Hox* expression has been demonstrated (Pownall *et al.*, 1996; Isaacs *et al.*, 1998). From these observations, it could be hypothesized that FGF regulation of *Hox* expression through CDX is conserved in the mouse. However, at E8.5, *Cdx1* and *Cdx4* expression patterns are unaltered in *Fgfr1* hypomorphic mice (Partanen *et al.*, 1998).

There are several possible explanations for this discrepancy. The first is simply that FGF regulation of *Cdx* is not conserved between the mouse and *Xenopus* and that FGF signaling regulates the expression of *Hox* genes by other means in the mouse. Given the wide array of homeotic transformations observed in *Fgfr1* hypomorphic mice, FGF signaling would likely control the expression or activation other global regulators of *Hox* expression. Second, it is possible that FGF may influence *Cdx* expression at stages other than E8.5. It has previously been demonstrated that *Cdx* regulation is stage-specific as the loss of *RARα1* and *RARγ* results in a decrease in *Cdx1* transcript levels at E7.5, but by E8.5 *Cdx1* expression levels are relatively normal (Houle *et al.*, 2000). This would suggest that another mechanism, besides RAR and FGF signaling, is responsible for *Cdx* expression at E8.5. Recent evidence suggests the WNT pathway may be involved at this stage (Prinos *et al.*, manuscript in preparation). Third, it is possible that FGF signaling regulates the transcription of *Cdx2*, the expression of which was not examined in *Fgfr1* hypomorphic mice. Like these mice, *Cdx2* heterozygotes also have shortened tails, however the early lethality of *Cdx2* homozygous null embryos precludes the identification of a potentially more severe gastrulation defect (Chawengsaksophak *et al.*, 1997).

Finally, it has been proposed that cellular proliferation may be directly linked to the colinear expression of *Hox* genes (Duboule, 1994, 1995). This model is based on the fact that axial formation takes place concomitantly with anteroposterior patterning, such that a particular axial identity can only be established following the formation of the more anterior regions. The chromatin configuration of the *Hox* clusters is thought to open progressively as development proceeds, however, it is not clear what regulates this process during gastrulation. One alternative is that the cells in the region of the primitive

streak may sense their anteroposterior identity by the number of times they have undergone cell division. Only the 3' most *Hox* genes would be accessible to transcription factors in cells have divided relatively few times before exiting the streak, while those that have undergone extensive proliferation would be competent to express *Hox* genes located in more 5' regions of the cluster. Therefore, altered proliferation that may arise due to abnormal FGF signaling may be sufficient to respecify the anteroposterior identity of cells as they leave the streak.

6.6b RA and FGF signaling at E8.5

Axial truncations in *Fgfr1* hypomorphic mice are frequently accompanied by spina bifida, and this phenotype closely resembles that which is induced by RA excess at E8.5 (Tibbles and Wiley, 1988: Kessel and Gruss, 1991; Kessel, 1992). This similarity may suggest that FGF- and RA-signaling affect the same pathways involved in axial patterning. As somites formation commences, RA becomes excluded from the region of the developing caudal neuropore such that, by the 8 to 10 somite stage a sharp boundary just posterior to the last formed somite is evident. It has been proposed that P450RAI, which is expressed in the open caudal neuropore by E8.5, functions to keep the level of RA very low in these tissues (Iulianella *et al.*, 1999). Indeed, *P450RAI* null mice exhibit caudal truncations that are very similar to those elicited by RA treatment (Abu-Abed *et al.*, 2001; Sakai *et al.*, 2001). The caudal region of the embryo is protected from exogenous RA by the rapid induction of *P450RAI* expression in the caudal neuropore following RA exposure. In contrast, high levels of RA, produced by RALDH2, are present in the newly formed somites. Furthermore, studies with VAD quails, and *Raldh2* null mutant mice, have demonstrated that RA is necessary for proper somite development (Neiderreither *et al.*, 1999; Maden *et al.*, 2000).

The relationship between FGF- and RA-signaling has recently been examined in two developing structures in the embryo: the chick limb bud and the mouse lungs (Mapel *et al.*, 2000; Mercader *et al.*, 2000). In both cases, RA is necessary for the proper development of proximal structures while it inhibits the differentiation of more distal structures. The restriction of RA signaling to the proximal region of the limb bud or lung bud is accomplished by two mechanisms: control of available RA, and control of RAR

mediated transcriptional activation. The expression of *Raldh2* is localized to the proximal region, and *P450RAI* is expressed at the distal tip of both structures. The complementary expression pattern of these two enzymes controls the spatial distribution of RA. Additionally, the RA signaling pathway is inhibited in the distal portion of the bud, as detected by the lack of *RARE-lacZ* transgene response in this region. In the limb bud, FGF signaling from the apical ectodermal ridge (AER), located at the distal tip of the bud along the anteroposterior axis, rapidly attenuates RA signaling, and inhibits the expression of *Raldh2*. Inhibition of the FGF signaling pathway results in increased RA synthesis and signaling in the distal region of the limb bud, and leads to a limb with a more proximal phenotype (Mercader *et al.*, 2000). Similarly, in the developing lung excess RA in the distal region of the lung bud inhibits the expression of genes involved in distal patterning, such as *Fgf10* and *Bmp4*. Moreover, excess RA in culture media results in a reduced number of terminal branches and epithelial tubules with a more proximal appearance (Cardoso *et al.*, 1995; Malpel *et al.*, 2000). Taken together, the downregulation of RA signaling appears to be necessary for generation of distal structures, and in both cases FGF signaling plays a significant role in this process.

Given the similar phenotypes of RA-excess and FGF attenuation it is tempting to speculate that the production of mesoderm from the tail bud is controlled by a similar mechanism. Perhaps a role of FGF signaling in the region of the primitive streak involves the inhibition of RA signaling, thereby allowing the formation of more distal structures. Hence, hypomorphic *Fgfr1* alleles would result in increased RA signaling and proximalization (or truncation) of the axial column. In this regard, it would be interesting to examine the expression of a *RARE-lacZ* reporter transgene in the caudal neuropore of *Fgfr1* hypomorphic embryos.

6.6c RA and FGF signaling at E7.5

It is clear that the proposed interactions between FGF and RA at E8.5 are probably not operating at E7.5. As both RAR and FGF signaling influence the specification of the vertebrae in the cervical region, it is possible that these two pathways may be involved in the regulation of the same genes. Alternatively, they could regulate the expression of different genes, with the loss of either set resulting in vertebral

transformations. There is at least some evidence that the latter hypothesis may be correct. For example, in *Fgfr1* hypomorphic embryos the anterior limit of *Hoxd4* expression is posteriorized by one somite at E8.5 (Partanen *et al.*, 1998). However, in *RARγ* null, *Cdx1* null, and *RARγ/Cdx1* double null E9.5 embryos, the anterior border if *Hoxd4* expression is identical to that of wild type embryos (Folberg *et al.*, 1999a and Figure 5.7). However is cannot be ruled out that the cohort of *Hox*, and perhaps other, genes regulated by RA and FGFs may partially overlap, such that they cooperate to regulate the expression of some genes, while they independently regulate others.

6.7 WNT signaling and *Cdx1* expression

It has recently been reported that WNT signaling directly regulates *Cdx1* expression in the developing intestine and in P19 cells (Lickert *et al.*, 2000; Prinos *et al.*, manuscript in preparation). Furthermore, *Cdx1* expression levels are diminished in the nascent mesoderm of *vestigial tail* (a hypomorphic allele of *Wnt3a*) mutant mice, and can be induced following *ex vivo* culture with WNT-containing media (Prinos *et al.*, manuscript in preparation). Evidence from *C.elegans* suggests that WNT-signaling may be involved in axial patterning, as the expression of some *Hox* genes is dependent on WNT-signaling. Moreover, a link between WNT-signaling, *pal-1* (the *C.elegans caudal* homologue), and *Hox* expression has been demonstrated (Hunter *et al.*, 1999; Zhang and Emmons, 2000). Although vertebral homeotic transformations have not been reported in any WNT-signaling deficient mice, it is possible that functional redundancy between components of the WNT pathway, or early phenotypes that preclude vertebral analysis may mask such a role.

RA treatment at E8.5 leads to a downregulation of *Wnt3a* expression, and WNT3a signaling is required for proper expression of *Cdx1*. However, *Cdx1* is strongly upregulated by exogenous RA at this stage of development, indicating that the direct regulation of *Cdx1* expression by RA can overcome a reduction in WNT3a signaling. As diminished levels of *Wnt3a* and *Brachyury* expression are thought to be responsible for the caudal truncations elicited by RA treatment (Iulianella et a., 1999; Shum et al., 1999), *Cdx1* does not appear to be critically involved in this process. This is supported by the

observation that *Cdx1* homozygous null embryos are not resistant to RA-induced caudal truncations (Chapter 5).

6.8 Summary and Perspectives

Formation and patterning of the vertebrate axial column is a complex process that involves the coordination of several different signaling pathways. However, it is largely unknown how the molecules of these pathways interact to specify the anteroposterior identity of nascent mesoderm. It is evident that some of these pathways converge on common targets, for example regulation of *Cdx1* by RA and Wnt signaling. Although there is no data that directly supports FGF regulation of *Cdx* expression in the mouse, evidence from *Xenopus* strongly suggests that this is possible. In this regard, it is interesting to note that RA, WNTs, and FGFs have all been implicated as posteriorizing factors in the 'activation-transformation' model proposed by Nieuwkoop. In addition, these three signaling pathways are interdependent in axis formation of the limb bud (reviewed in Vogt and Duboule, 1999). Therefore, it is possible that similar regulatory interactions may occur during the process of formation and patterning of the vertebral column. The identification of additional genes and molecular pathways involved in these processes will lead to a greater understanding of the mechanisms that govern normal development, and lead to congenital malformations, of the vertebrate embryo.

References

Abu-Abed, S.S., Beckett, B.R., Chiba, H., Chithalen, J.V., Jones, G., Metzger, D., Chambon, P., and Petkovich, M. (1998) Mouse P450RAI (CYP26) expression and retinoic acid-inducible retinoic acid metabolism in F9 cells are regulated by retinoic acid receptor γ and retinoid X receptor α. *J. Biol. Chem.* **273**: 2409-2415.

Abu-Abed, S., Dollé, P., Metzger, D., Beckett, B., Chambon, P., and Petkovich, M. (2001) The retinoic acid-metabolizing enzyme, CYP26A1, is essential for normal hindbrain patterning, vertebral identity, and development of posterior structures. *Genes Dev.* **15**: 226-240.

Ahmed, N.K., Felsted, R.L., Bachur, N.R. (1981) Daunorubicin reduction mediated by aldehyde and ketone reductases. *Xenobiotica* **11**: 131-136.

Aida, K., Tawata, M., Ikegishi, Y., Onaya, T. (1999) Induction of rat aldose reductase gene transcription is mediated through the cis-element, osmotic response element (ORE): increased synthesis and/or activation by phosphorylation of ORE-binding protein is a key step. *Endocrinology* **140**: 609-617.

Alkasaka, T., Kanno, M., Balling, R., Mieza, M.A., Taniguchi, M., and Koseki, H. (1996) A role for mel-18, a Polycomb group-related vertebrate gene, during the anteroposterior specification of the axial skeleton. *Development* **122**: 1513-1522.

Allenby, G., Bocquel, M.-T., Saunders, M., Kazmer, S., Speck, J., Rosenberger, M., Lovey, A., Kastner, P., Grippo, J.F., Chambon, P., and Levin, A.A. (1993) Retinoic acid receptors and retinoid X receptors: interactions with endogenous retinoic acids. *Proc. Natl. Acad. Sci. USA* **90**: 30-34.

Alles, A.J. and Sulik, K.K. (1990) Retinoic acid-induced spina bifida: evidence for a pathogenetic mechanism. *Development* **108**: 73-81.

Amicarelli, F., Bonfigli, A., Colafarina, S., Bucciarelli, T., Principato, G., Ragnelli, A.M., Di Ilio, C., and Miranda, M. (1998) Effect of methylglyoxal on Bufo bufo embryo development: morphological and biochemical aspects. *Chem. Biol. Interact.* **114:** 177-189.

Andersen, F.G., Heller, R.S., Petersen, H.V., Jensen. J., Madsen, O.D., and Serup, P. (1999) Pax6 and Cdx2/3 form a functional complex on the rat glucagon gene promoter G1-element. *FEBS Lett.* **445**: 306-310.

Ang, H.L., Deltour, L., Hayamizu, T.F., Zgombic-Knight, M., and Duester, G. (1996a) Retinoic acid synthesis in mouse embryos during gastrulation and craniofacial development linked to class IV alcohol dehydrogenase gene expression. *J. Biol. Chem.* **271**: 9526-9534.

Ang, H.L., Deltour, L., Zgombic-Knight, M., Wagner, M.A., and Duester, G. (1996b) Expression patterns of class I and class IV alcohol dehydrogenase genes in developing epithelia suggest a role for alcohol dehydrogenase in local retinoic acid synthesis. *Alcohol. Clin. Exp. Res.* **20**: 1050-1064.

Ang, H.L., and Duester, G. (1999) Retinoic acid biosynthetic enzyme ALDH1 localizes in a subset of retinoid-dependent tissues during *Xenopus* development. *Dev. Dyn.* **215**: 264-272.

Arnold, S.J., Stappert, J., Bauer, A., Kispert, A., Herrmann, B.G., and Kremler, R. (2000) *Brachyury* is a target gene of the Wnt/β-catenin signaling pathway. *Mech. Dev.* **91**: 249-258.

Aubin, J., Lemieux, M., Tremblay, M., Bérard, J., Jeannotte, L. (1997) Early postnatal lethality in *Hoxa-5* mutant mice is attributable to respiratory tract defects. *Dev. Biol.* **192**: 432-445.

Aubin, J., Lemieux, M., Tremblay, M., Behringer, R.R., and Jeannotte, L. (1998) Transcriptional interferences at the *Hoxa4/Hoxa5* locus: Importance of correct *Hoxa5* expression for proper specification of the axial skeleton. *Dev. Dynam.* **212**: 141-156.

Bachur, N.R. (1976) Cytoplasmic aldo-keto reductases: a class of drug metabolizing enzymes. *Science* **193**: 595-597.

Bachvarova, R. (1988) Small B2 RNAs in mouse oocytes, embryos, and somatic tissues. *Dev. Biol.* **130**: 513-523.

Bailey, J.S., and Siu, C.H. (1988) Purification and partial characterization of a novel binding protein for retinoic acid from neonatal rat. *J. Biol. Chem.* **263**: 9326-9332.

Baniahmad, A., Kohne, A.C., and Renkawitz, R. (1992) A transferable silencing domain is present in the thyroid hormone receptor, in the *v-erbA* oncogene and in the retinoic acid receptor. *EMBO J.* **11**: 1015-1023.

Bannister, A.J., and Kouzarides, T. (1996) The CBP co-activator is a histone acetyltransferase. *Nature* **384**: 641-643.

Barrow, J.R., Stadler, H.S., and Capecchi, M.R. (2000) Roles of *Hoxa1* and *Hoxa2* in patterning the early hindbrain of the mouse. *Development* **127**: 933-944.

Barski, O.A., Gabbay, K.H., Grimshaw, C.E., Bohren, K.M. (1995) Mechanism of human aldehyde reductase: characterization of the active site pocket. *Biochemistry* **34**: 11264-11275.

Bastein, J., Adam-Sitah, S., Riedl, T., Egly, J.M., Chambon, P., and Rochette-Egly, C. (2000) TFIIH interacts with the retinoic acid receptor gamma and phosphorylates its AF-1-activating domain through cdk7. *J.Biol. Chem.* **275**: 21896-21904.

Beato, M., Herrlich, P., and Schutz, G. (1995) Steroid hormone receptors: many actors in search of a plot. *Cell* **83**: 851-857.

Beck, F., Erler, T., Russell, A., James, R. (1995) Expression of Cdx-2 in the mouse embryo and placenta: possible role in patterning of the extra-embryonic membranes. *Dev. Dyn.* **204**: 219-27

Beck, F., Chawengsaksophak, K., Waring, P., Playford, R.J., and Furness, J.B. (1999) Reprogramming of intestinal differentiation and intercalary regeneration in *Cdx2* mutant mice. *Proc. Natl. Acad. Sci. USA* **96**: 7318-7323.

Beddington, R.S.P., and Robertson, E.J. (1999) Axis development and early asymmetry in mammals. *Cell* **96**: 195-209.

Bel, S., Coré, N., Djabali, M., Kieboom, K., van der Lugt, N., Alkema, M.J., and Van Lohuizen, M. (1998) Genetic interactions and dosage effects of polycomb group genes in mice. *Development* **125**: 3453-3551.

Bel-Vialar, S., Coré, N., Terranova, R., Goudot, V., Boned, A., and Djabali, M. (2000) Altered retinoic acid sensitivity and temporal expression of Hox genes in Polycomb-M33-deficient mice. *Dev. Biol.* **224**: 238-249.

Bennett, K.L., Hill, R.E., Pietras, D.F., Woodworth-Gutai, M., Kane-Haas, C., Houston, J.M., Heath, J.K., Hastie, N.D. (1984) Most highly repeated dispersed DNA families in the mouse genome. *Mol Cell Biol.* **8**:1561-71

Bladon, T.S., Fregeau, C.J., and McBurney, M.W. (1990) Synthesis and processing of small B2 transcripts in mouse embryonal carcinoma cells. *Mol. Cell. Biol.* **10**: 4058-4067.

Bladon, T.S., and McBurney, M.W. (1991) The rodent B2 sequence can affect expression when present in the transcribed region of a reporter gene. *Gene* **98**: 259-263.

Blanco, J.C., Minucci, S., Lu, J., Yang, X.J., Walker, K.K., Chen, H., Evans, R.M., Nakatani, Y., and Ozato, K. (1998) The histone acetylase PCAF is a nuclear receptor coactivator. *Genes Dev.* **12**: 1638-1651.

Bliss, A.F. (1951) The equilibrium between vitamin A alcohol and aldehyde in the presence of alcohol dehydrogenase. *Arch. Biochem.* **31**: 197-204.

Blomhoff, R.B. (1994) In Blomhoff, R. (ed) Vitamin A in Health and Disease, Marcel Dekker Inc., New York.

Blumberg, B., Bolado, J., Jr., Moreno, T.A., Kinter, C., Evans, R.M., and Papalopulu, N. (1997) An essential role for retinoid signaling in anteroposterior neural patterning. *Development.* **124**: 373-379.

Bohren, K.M., Bullock, B., Wermuth, B., Gabbay, K.H. (1989) The aldo-keto reductase superfamily. cDNAs and deduced amino acid sequences of human aldehyde and aldose reductases. *J. Biol. Chem.* **264**: 9547-9551

Boulet, A.M., and Capecchi, M.R. (1996) Targeted disruption of *Hoxc-4* causes esophageal defects and vertebral transformations. *Dev. Biol.* **177**: 232-249.

Bourguet, W., Vivat, V., Wurtz, J.M., Chambon, P., Gronemeyer, H., and Moras, D. (2000) Crystal structure of a heterodimeric complex of RAR and RXR ligand-binding domains. *Mol. Cell.* **5**: 289-298.

Brocard, J., Kastner, P., and Chambon, P. (1996) Two novel RXR alpha isoforms from mouse testis. *Biochem. Biophys. Res. Commun.* **229**: 211-218.

Brooke, N.M., Garcia-Fernàndez, J., and Holland, P.W.H. (1998) The ParaHox gene cluster is an evolutionary sister of the Hox gene cluster. *Nature* **392**: 920-922.

Brownlee, M. (2000) Negative consequences of glycation. *Metabolism* **49**(2 Suppl 1): 9-13.

Bürglin, T. (1997) Analysis of TALE superclass homeobox genes (MEIS, PBC, KNOX, Iroqois, TGIF) reveals a novel domain conserved between plants and animals. *Nucleic Acids Res.* **23**: 4173-4180.

Caelles, C., Gonzalez-Sancho, J.M., and Munoz, A. (1997) Nuclear hormone receptor antagonism with AP-1 by inhibition of the JNK pathway. *Genes. Dev.* **11**: 3351-3364.

Carey, M. (1998) The enhanceosome and transcriptional synergy. *Cell* **92**: 5-8.

Chalifour, L.E., Fahmy, R., Holder, E.L., Hutchinson, E.W., Osterland, C.K., Schipper, H.M., and Wang, E. (1994) A method for analysis of gene expression patterns. *Anal. Biochem.* **216**: 299-304.

Charité, J., de Graaff, W., Consten, D., Reijnen, M.J., Korving, J., and Deschamps, J. (1998) Transducing positional information to the *Hox* genes: critical interaction of *cdx* gene products with position-sensitive regulatory elements. *Development* **125**: 4349-4358.

Chawengsaksophak, K., James, R., Hammond, V.E., Köntgen, F., and Beck, F. (1997) Homeosis and intestinal tumours in *Cdx2* mutant mice. *Nature* **386**: 84-87.

Chen, D., and Evans, R.M. (1995) A transcriptional co-repressor that interacts with nuclear hormone receptors. *Nature* **377**: 454-457.

Chen, H., Lin, R.J., Schiltz, R.L., Chakravarti, D., Nash, A., Nagy, L., Privalsky, M.L., Nakatani, Y., and Evans, R.M. (1997) Nuclear receptor coactivator ACTR is a novel histone acetyltransferase and forms a multimeric activation complex with P/CAF and CBP/p300. *Cell* **90**: 569-580.

Chiba, H., Clifford, J., Metzger, D., and Chambon, P. (1997) Distinct retinoid X receptor-retinoic acid receptor heterodimers are differentially involved in the control of expression of retinoid target genes in F9 embryonal carcinoma cells. *Mol. Cell Biol.* **17**: 3013-3020.

Ciruna, B.G., Schwartz, L., Harpal, K., Yamaguchi, T.P., and Rossant, J. (1997) Chimeric analysis of *fibroblast growth factor receptor-1* (*Fgfr1*) function: a role for FGFR1 in morphogenetic movement through the primitive streak. *Development* **124**: 2829-2841.

Clemens, M.J. (1987) A potential role for RNA transcribed from B2 repeats in the regulation of mRNA stability. Cell 49: 157-158

Cockroft, D.L., Coppola, P.T. (1977) Teratogenic effects of excess glucose on head-fold rat embryos in culture. *Teratology* **16**: 141-146.

Cohlan, S.Q. (1953) Excessive intakes of vitamin A as a cause of congential anomalies in the rat. *Science* **117**: 535-536.

Condie, B.G., and Capecchi, M.R. (1993) Mice homozygous for a targeted disruption of *Hoxd-3 (Hox-4.1)* exhibit anterior transformations of the first and second cervical vertebrae, that atlas and axis. *Development* **119**: 579-595.

Condie, B.G., and Capecchi, M.R. (1994) Mice with targeted disrptions in the paralogous genes hoxa-3 and hoxd-3 reveal synergistic interactions. *Nature* **370**: 304-307.

Conlon, R.A. (1995) Retinoic acid and pattern formation in vertebrates. *Trends Genet.* **11**: 314-319.

Conlon, R.A., and Rossant, J. (1992) Exogenous retinoic acid rapidly induces anterior ectopic expression of murine *Hox-2* genes in vivo. *Development* **116**: 357-368.

Creech Kraft, J. (1992) Pharmacokinetics, placental transfer, and teratogenicity of 13-cis-retinoic acid, its isomer and metabolites. In Retinoids in Normal Development and Teratogenesis, G.M. Morriss-Kay, ed. (Oxford: Oxford University Press), pp. 267-280.

Darimont, B.D., Wagner, R.L., Apriletti, J.W., Stallcup, M.R., Kushner, P.J., Baxter, D., Fletterick, R.J., and Yamamoto, K.R. (1998) Structure and specificity of nuclear receptor-coactivator interactions. *Genes Dev.* **12**: 3343-3356.

Dearolf, C.R., Topol, J., and Parker, C.S. (1989) The *caudal* gene product is a direct activator of *fushi tarazu* transcription during *Drosophila* embryogenesis. *Nature* **341**: 340-343.

Delmotte, M.H., Tahayato, A., Formstecher, P., and Lefebvre, P. (1999) Serine 157, a retinoic acid receptor alpha residue phosphorylated by protein kinase C in vitro, is involved in RXR.RARalpha heterodimerization and transcriptional activity. *J. Biol. Chem.* **274**: 38225-38231.

Deltour, L., Foglio, M.H., and Duester, G. (1999a) Metabolic deficiencies in alcohol dehydrogenase *Adh1*, *Adh3*, and *Adh4* null mutant mice: Overlapping roles of *Adh1* and *Adh4* in ethanol clearance and metabolism of retinol to retinoic acid. *J. Biol. Chem.* **274**: 16796-16801.

Deltour, L., Foglio, M.H., and Duester, G. (1999b) Impaired retinol utilization in *Adh4* alcohol dehydrogenase mutant mice. *Dev. Genet.* **25**: 1-10.

Deng, C., Bedford, M., Li, C., Xu, X., Yand, X., Dunmore, J., and Leder, P. (1997) Fibroblast Growth Factor Receptor-1 (FGFR-1) is essential for normal neural tube and limb development. *Dev. Biol.* **185**: 42-54.

Deng, C.X., Wynshaw-Boris, A., Shen, M.M., Daugherty, C., Ornitz, D.M., and Leder, P. (1994) Murine FGFR-1 is required for early postimplantation growth and axial organization. *Genes Dev.* **8**: 3045-3057.

de Roos, K., Sonneveld, E., Compaan, B., ten Berge, D., Durston, A.J., and van der Saag, P.T. (1999) Expression of retinoic acid 4-hydroxylase (CYP26) during mouse and Xenopus laevis embryogenesis. *Mech Dev* **82**: 205-211.

Dersch, H., and Zile, M.H. (1993) Induction of normal cardiovascular development in the vitamin A-deprived quail embryo by natural retinoids. *Dev. Biol.* **160**: 424-433.

Deschamps, J., and Wijgerde, M. (1993) Two phases in the establishment of HOX expression domains. *Dev. Biol.* **156**: 473-480.

Deschamps, J., van den Akker, E., Forlani, S., de Graff, W., Oosterveen, T., Roelen, B., and Roelfsema, J. (1999) Initiation, establishment, and maintenance of *Hox* gene expression patterns in the mouse. *Int. J. Dev. Biol.* **43**: 635-650.

de The, H., Vivanco-Ruiz, M.M., Tiollais, P., Stunnenberg, H., and Dejean, A. (1990) Identification of a retinoic acid responsive element in the retinoic acid receptor beta gene. *Nature* **343:** 177-180.

Diatchenko, L., Lau, Y.F., Campbell, A.P., Chenchik, A., Mogadam, F., Huang, B., Lukyanov, S., Lukyanov, K., Gurskaya, N., Sverdlov, E.D., and Siebert, P.D. (1996)

Suppression subtractive hybridization: a method for generating differentially regulated or tissue specific cDNA probes and libraries. *Proc. Natl. Acad. Sci. U.S.A.* **93**: 6025-6030.

Dickman, E.D., Thaller, C., and Smith, S.M. (1997) Temporally-regulated retinoic acid depletion produces specific neural crest, ocular and nervous system defects. *Development* **124**: 3111-3121.

Dillworth, F.J., Fromental-Ramain, C., Yamamoto, K., and Chambon, P. (2000) ATP-driven chromatin remodeling activity and histone acetyltransferases act sequentially during transactivation by RAR/RXR in vitro. *Mol. Cell.* **6**: 1049-1058.

Dockham, P.A., Lee, M.-O., and Sladek, N.E. (1992) Identification of human liver aldehyde dehydrogenases that catalyze the oxidation of aldophosphamide and retinaldehyde. *Biochem. Pharmacol.* **43**: 2453-2469.

Dollé, P., Ruberte, E., Kastner, P., Petkovich, M., Stoner, C.M., Gudas, L.J., Chambon, P. (1989) Differential expression of the genes encoding the retinoic acid receptors α, β, γ and CRABPI in the developing limbs of the mouse. *Nature* **342**: 702-705.

Dollé, P., Ruberte, E., Leroy, P., Morriss-Kay, G.M., and Chambon, P. (1990) Retinoic acid receptors and cellular retinoid binding proteins. I. A systematic study of their differential pattern of transcription during mouse organogenesis. *Development* **110:** 1133-1151.

Dollé, P., Fraulob, V., Kastner, P., and Chambon, P. (1994) Developmental expression of murine retinoid X receptor (RXR) genes. *Mech. Dev.* **45**: 91-104.

Donovan, M., Olofsson, B., Gustafson, A.-L., Dencker, L., and Eriksson, U. (1995) The cellular retinoic acid binding proteins. *J. Steroid Biochem. Molec. Biol.* **53**: 459-465.

Drager, U.C., McCaffery, P. (1995) Retinoic acid synthesis in the developing spinal cord. *Adv. Exp. Med. Biol.* **372**: 185-192.

Duboule, D., and Dollé, P. (1989) The structural and functional organization of the murine *HOX* gene family resembles that of *Drospohila* homeotic genes. *EMBO J.* **8**: 1497-1505.

Duester, G. Farrés, J., Felder, M.R., Holmes, R.S., Höög, J.-O., Parés, X., Plapp, B.V., Yin, S.-J., and Jörnvall, H. (1999) Recommended nomenclature for the vertebrate alcohol dehydrogenase gene family. *Biochem. Pharmacol.* **58**: 389-395.

Duester, G. (2000) Families of retinoid dehydrogenases regulating vitamin A function: Production of visual pigment and retinoic acid. *Eur. J. Biochem.* **267**: 4315-4324.

Dupé, V., Davenne, M., Brocard, J., Dollé, P., Mark, M., Dierich, A., Chambon, P., and Rijli, F.M. (1997) In vivo functional analysis of the *Hoxa1* 3' retinoic acid response element (3' RARE). *Development* **124**: 399-410.

Dupé, V., Ghyselinck, N.B., Wendling, O., Chambon, P., and Mark, M. (1999) Key roles of retinoic acid receptors alpha and beta in the patterning of the caudal hindbrain, pharyngeal arches and otocyst in the mouse. *Development* **126**: 5051-5059.

Durston, A.J., Timmermans, J.P.M., Hage, W.J.,Hendriks, H.F.J., de Vries, N.J., Heidiveld, M., and Nieuwkoop, P.D. (1989) Retinoic acid causes an anteroposterior transformation in the developing central nervous system. *Nature* **340**: 140-144.

Dyson, E., Sucov, H.M., Kubalak, S.W., Schmid-Schonbein, G., Delano, F.A., Evans, R.M., Ross, J., Jr. and Chien, K.R. (1995) Atria-phenotype is associated with embryonic ventricular failure in retinoid X receptor α-/- mice. *Proc. Natl. Acad. Sci. USA* **92**: 7386-7390.

Easwaran, V., Pishvaian, M., Salimuddin, and Byers, S. (1999) Cross-regulation of β-catenin-LEF/TCF and retinoid signaling pathways. *Curr. Biol.* **9**: 1415-1418.

Egea, P.F., Klaholz, B.P., and Moras, D. (2000) Ligand-protein interactions in nuclear receptors of hormones. *FEBS Letters* **476**: 62-67.

El-Kabbani, O., Judge, K., Ginell, S.L., Myles, D.A.A., DeLucas, L.J., and Flynn, T.G. (1995) Structure of porcine aldehyde reductase holoenzyme. *Nature Struct. Biol.* **2**: 687-692.

Epstein, M., Pillemer, G., Yelin, R., Yisraeli, J.K., Fainsod, A. (1997) Patterning of the embryo along the antero-posterior axis: the role of the *caudal* genes. *Development* **124**: 3805-3814.

Eriksson, U.J. (1988) Importance of genetic predisposition and maternal environment for the occurrence of congenital malformations in offspring of diabetic rats. *Teratology* **37**: 365-374.

Eriksson, U.J., and Borg, L.A. (1991) Protection by free oxygen radical scavenging enzymes against glucose-induced embryonic malformations in vitro. *Diabetologia* **34**: 325-331.

Eriksson, U.J., Wentzel, P., Minhas, H.S., and Thornalley, P.J. (1998) Teratogenicity of 3-deoxyglucosone and diabetic embryopathy. *Diabetes* **47**:1960-1966.

Evans. R. (1988) The steroid and thyroid hormone receptor family. *Science* **240**: 889-895.

Fawcett, D., Pasceri, P., Fraser, R., Colbert, M., Rossant, J., and Giguère, V. (1995) Postaxial polydactyly in forelimbs of CRABP-II mutant mice. *Development* **121**: 671-679

Feldman, B., Poueymirou, W., Papaioannou, V.E., DeChiara, T.M., and Goldfarb, M. (1995) Requirement of FGF-4 for postimplantation mouse development. *Science* **267**: 246-249.

Feng, W., Ribeiro, R.C., Wagner, R.L., Nguyen, ., Apriletti, J.W., Fletterick, R.J., Baxter, J.D., Kushner, P.J., and West, B.L. (1998) Hormone-dependent coactivator binding to a hydrophobic cleft on nuclear receptors. *Science* **280**: 1747-1749.

Ferraris, J.D., Williams, C.K., Jung, K.Y., Bedford, J.J., Burg, M.B., and Garcia-Perez, A. (1996) ORE, a eukaryotic minimal essential osmotic response element. The aldose reductase gene in hyperosmotic stress. *J. Biol. Chem.* **271**: 18318-18321.

Fine, E.L., Horal, M., Chang, T.I., Fortin, G., and Loeken, M.R. (1999) Evidence that elevated glucose causes altered gene expression, apoptosis, and neural tube defects in a mouse model of diabetic pregnancy. *Diabetes* **48**: 2454-2462

Fiorella, P., and Napoli, J. (1991) Expression of cellular retinoic acid binding protein (CRABP) in Escherichia coli: Characterization and evidence that holo-CRABP is a substrate in retinoic acid-metabolism. *J. Biol. Chem.* **266**: 16572-16579.

Fiorella, P.D., Giguère, V., and Napoli, J.L. (1993) Expression of cellular retinoic acid binding protein (type II) in *Escherichia coli*: characterization and comparison to cellular retinoic acid binding protein (type I). *J. Biol. Chem.* **268**: 21545-21552.

Folberg, A., Nagy Kovács, E.N., and Featherstone, M.S. (1997) Characterization and retinoic acid responsiveness of the murine *Hoxd4* transcription unit. *J.Biol.Chem.* **272**: 29151-29157.

Folberg, A., Nagy Kovács, E.N., Huang, H., Houle, M., Lohnes, D., and Featherstone, M.S. (1999a) *Hoxd4* and *RARγ* interact synergistically in the specification of the cervical vertebrae. *Mech. Dev.* **89**: 65-74.

Folberg, A., Nagy Kovács, E.N., Luo, J., Giguère, V., and Featherstone, M.S. (1999b) *RARβ* mediates the response of *Hoxd4* and *Hoxb4* to exogenous retinoic acid. *Dev. Dyn.* **215**: 96-107.

Folkers, G.E., van der Leede, B.-jM., van der Saag, P.T. (1993) The retinoic acid receptor-β2 contains two separable cell-specific transactivation domains, at the N-terminus and in the ligand-binding domain. *Mol. Endocrinol.* **7**: 616-627.

Fondell, J.D., Ge, H., and Roeder, R.G. (1996) Ligand induction of a transcriptionally active thyroid hormone receptor coactivator complex. *Proc. Natl. Acad. Sci. USA* **93**: 8329-8333.

Forman, B.M., Yange, C.R., Au, M., Casanova, J., Ghysdael, J., Samuels, H.H. (1989) A domain containing leucine-zipper-like motifs mediate novel in vivo interactions between the thyroid hormone and retinoic acid receptors. *Mol. Endocrinol.* **3**: 1610-1626.

Frasch, M., Chen, X., and Lufkin, T. (1995) Evolutionary-conserved enhancers direct region-specific expression of the murine Hoxa1 and Hoxa2 loci in both mice and Drosophila. *Development* **121**: 957-974.

Freund, J.N., Domon-Dell, C., Kedinger, M., and Duluc, I. (1998) The *Cdx1* and *Cdx2* homeobox genes in the intestine. *Biochem. Cell Biol.* **76**: 957-969.

Frohman, M.A., Martin, G.R., Cordes, S., Halamek, L.P., and Barsh, G.S. (1993) Altered rhombomere-specific gene expression and hyoid bone differentiation in the mouse segmentation mutant *kreisler* (*kr*). *Development* **117**: 925-936.

Fujii, H., Sato, T., Kaneko, S., Gotoh, O., Fujii-Kuriyama, Y., Osawa, K., Kato, S., and Hamada, H. (1997) Metabolic inactivation of retinoic acid by a novel P450 differentially expressed in developing mouse embryos. *EMBO J.* **16**: 4163-4173.

Gabbay, K.H. (1973) The sorbitol pathway and the complications of diabetes. *N. Engl. J. Med.* **288**: 831-836.

Gabbe, S.G. (1977) Congenital malformations in infants of diabetic mothers. *Obstet. Gynecol. Surv.* **32**: 125-132.

Galceran, J., Farinas, I., Depew, M.J., Clevers, H., and Grosschedl, R. (1999) *Wnt3a*$^{-/-}$-like phenotype and limb deficiency in *Lef1*$^{-/-}$*Tcf1*$^{-/-}$ mice. *Genes Dev.* **13**: 709-717.

Gale, E., Zile, M., Maden, M. (1999) Hindbrain respecification in the retinoid-deficient quail. *Mech. Dev.* **89**: 43-54.

Gamer, L.W., and Wright, C.V. (1993) Murine Cdx-4 bears striking similarities to the Drosophila caudal gene in its homeodomain sequence and early expression pattern. *Mech. Dev.* **43**: 71-81.

Gampe, R.T. Jr., Montana, V.G., Lambert, M.H., Miller, A.B., Bledsoe, R.K., Milburn, M.V., Kliewer, S.A., Willson, T.M., and Xu, H.E. (2000) Asymmetry in the PPARgamma/RXRalpha crystal structure reveals the molecular basis of heterodimerization among nuclear receptors. *Mol Cell* **5**: 545-555.

Garcia-Perez, A., Martin, B., Murphy, H.R., Uchida, S., Murer, H., Cowley, B.D. Jr, Handler, J.S., and Burg, M.B. (1989) Molecular cloning of cDNA coding for kidney aldose reductase. Regulation of specific mRNA accumulation by NaCl-mediated osmotic stress. *J. Biol. Chem.* **264**: 16815-16821

Gaunt, S.J., Dean, W., Sang, H., and Burton, R.D. (1999) Evidence that Hoxa expression domains are evolutionarily transposed in neuroectoderm, and that they are established by a forward spreading mechanism in paraxial mesoderm. *Mech. Dev.* **82**: 109-118.

Gaunt, S.J., and Strachan, L. (1994) Forward spreading in the establishment of a vertebrate *Hox* expression boundary: the expression domain separates into anterior and posterior zones, and the spread occurs across implanted glass barriers. *Dev. Dyn.* **199**: 229-240.

Ghyselinck, N.B., Dupé, V., Dierich, A., Messaddeq, N., Garnier, J.M., Rochette-Egly, C., Chambon, P., and Mark, M. (1997) Role of the retinoic acid receptor beta (RARβ) during mouse development. *Int. J. Dev. Biol.* **41**: 425-447.

Ghyselinck, N.B., Wendling, O., Messaddeq, N., Deirich, A., Lampron, C., Décimo, D., Viville, S., Chambon, P and Mark, M. (1998) Contribution of retinoic acid receptor β isoforms to the formation of the conotruncal septum of the embryonic heart. *Dev. Biol.* **198**: 303-318.

Ghyselinck, N.B., Bavik, C., Sapin, V., Mark, M., Bonnier, D., Hindelang, C., Dierich, A., Nilsson, C.B., Hakansson, H., Sauvant, P., Azais-Braesco, V., Frasson, M., Picaud, S., and Chambon, P. (1999) Cellular retinol-binding protein I is essential for vitamin A homeostasis. *EMBO J* **18**: 4903-4914.

Giguere, V. (1994) Retinoic acid receptors and cellular tetinoid binding proteins: complex interplay in retinoid signaling. *Endocrine Rev.* 15: 61-78.

Giguère, V., Hollenberg, S.M., Rosenfeld, M.G., and Evans, R.M. (1986) Functional domains of the human glucocorticoid receptor. *Cell* **46**: 645-652.

Giguère, V., Ong, E.S., Segui, P., and Evans, R.M. (1987) Identification of a receptor for the morphogen retinoic acid. *Nature* **330**: 624-629.

Glass, C.K., and Rosenfeld, M.G. (2000) The coregulator exchange in transcriptional functions of nuclear receptors. *Genes Dev.* **14**: 121-141.

Godbout, R. (1992) High levels of aldehyde dehydrogenase transcripts in the undifferentiated chick retina. *Exp. Eye Res.* **54**: 297-305.

Goodman, R.H., and Smolik, S. (2000) CBP/p300 in cell growth, transformation, and development. *Genes Dev.* **14**: 1553-1577.

Gorry, P., Lufkin, T., Dierich, A., Rochette-Egly, C., Décimo, D., Dollé, P., Mark, M., Durand, B., and Chambon, P. (1994) The cellular retinoic acid binding protein I (CRABPI) is dispensable. *Proc. Natl. Acad. Sci. USA* **90**: 932-936.

Göttlicher, M., Heck, S., and Herrlich, P. (1998) Transcriptional cross-talk, the second mode of steroid hormone receptor action. *J. Mol. Med.* **76**: 480-489.

Gould, A., Itasaki, N., and Krumlauf, R. (1998) Initiation of rhombomeric *Hoxb4* expression requires induction by somites and a retinoid pathway. *Neuron* **21**: 39-51.

Gould, A., Morrison, A., Sproat, G., White, R.A.H., and Krumlauf, R. (1997) Positive cross-regulation and enhancer sharing: two mechanisms for specifying overlapping *Hox* expression patterns. *Genes Dev.* **11**: 900-913.

Gradl, D., Kühl, M., and Wedlich, D. (1999) Keeping a close eye on Wnt-1/wg signaling in *Xenopus*. *Mech. Dev.* **86**: 3-15.

Graham, A., Papalopulu, N., and Krumlauf, R. (1989) The murine and *Drosophila* homeobox clusters have common features of organization and expression. *Cell* **57**: 367-378.

Greco, T.L., Takada, S., Newhouse, M.M., McMahon, J.A., McMahon, A.P., and Camper, S.A. (1996) Analysis of the *vestigial tail* mutation demonstrates that *Wnt-3a* gene dosage regulates mouse axial development. *Genes. Dev.* **10**: 313-324.

Greenamyre, J.T., MacKenzie, G., Peng, T.I., and Stephans, S.E. (1999) Mitochondrial dysfunction in Parkinson's disease. *Biochem. Soc. Symp.* **66**: 85-97.

Green, S., and Chambon, P. (1988) Nuclear receptors enhance our understanding of transcriptional regulation. *Trends Genet.* **4**: 309-314.

Green, S., Issemann, I., and Sheer, E. (1988) A versatile in vivo and in vitro eukaryotic expression vector for protein engineering. *Nucleic Acids Res.* **16**: 369

Greer, J.M., Puetz, J., Thomas, KR., and Capecchi, M.R. (2000) Maintenance of functional equivalence during paralogous Hox gene evolution. *Nature* **403**: 661-665.

Grondona, J.M., Kastner, P., Gansmuller, A., Décimo, D., and Chambon, P. (1996) Retinal dysplasia and degeneration in *RARβ2/RARγ2* compound mutant mice. *Development* **122**: 2173-2188.

Gruber, P.J., Kubalak, S.W., Pexieder, T., Sucov, H.M., Evans, R.M., and Chien, K.R. (1996) RXRα deficiency confers susceptibility for aortic sac, conotruncal, atrioventricularcushion, and ventricular muscle defects in mice. *J. Clin. Invest.* **98**: 1332-1343.

Gustafson, A.-L., Dencker, L., and Eriksson, U. (1993) Non-overlapping expression of CRBPI and CRABPI during pattern formation of limbs and craniofacial structures in the early mouse embryo. *Development* **117**: 451-460.

Hagay, Z.J., Weiss, Y., Zusman, I., Peled-Kamar, M., Reece, E.A., Eriksson, U.J., and Groner, Y. (1995) Prevention of diabetes-associated embryopathy by overexpression of the free radical scavenger copper zinc superoxide dismutase in transgenic mouse embryos. *Am. J. Obstet. Gynecol.* **173**: 1036-104.1

Hale, F. (1937) Relation of maternal vitamin A deficiency to microphthalmia in pigs. *Texas State J. Med.* **33**: 228-232.

Handelsman, D.J., and Turtle, J.R. (1981) Clinical trial of an aldose reductase inhibitor in diabetic neuropathy. *Diabetes* **30**: 459-464.

Haselbeck, R.J., Hoffmann, I., and Duester, G. (1999) Distinct functions for *Aldh1* and *Raldh2* in the control of ligand production for embryonic retinoid signaling pathways. *Dev. Genet.* **25**: 353-364.

Hathcock, J.N., Hattan, D.G., Jenkins, M.Y., McDonald, J.T., Sundaresan, P.R., and Wilkening, V.L. (1990) Evaluation of vitamin A toxicity. *Am. J. Clin. Nutr.* **52**: 183-202.

Haynes, S.R. and Jelinek, W.R. (1981) Low molecular weight RNAs transcribed in vitro by RNA polymerase III from Alu-type dispersed repeats in Chinese hamster DNA are also found in vivo. *Proc. Natl. Acad. Sci. U S A* **78**: 6130-6134.

Heinzel, Y., Lavinsky, R.M., Mullen, T.M., Soderstrom, M., Laherty, C.D., Torchia, J., Yang, Y.M., Brard, G., Ngo, S.D., Davie, J.R., et al. (1997) A complex containing N-CoR, mSin3 and histone deacetylase mediates transcriptional repression. *Nature* **387**: 43-48.

Henrique, D., Adam, J., Myat, A., Chitnis, A., Lewis, J., and Ish-Horowicz, D. (1995) Expression of a Delta homologue in prospective neurons in the chick. *Nature* **375**: 787-790.

Hermann, B.G., Labeit, S., Poustka, A., King, T.R., and Lehrach, H. (1990) Cloning of the *T* gene required in mesoderm formation in the mouse. *Nature* **343**: 617-622.

Heyman, R.A., Mangelsdorf, D.J., Dyck, J.A.., Stein, R.B., Eichele, G., Evans, R.M., and Thaller, C. (1992) 9-*cis* retinoic acid is a high affinity ligand for the retinoid X receptor. *Cell* **68**: 397-406.

Hill, J., Clarke, J.D.W., Vargesson, N., Jowett, T., and Holder, N. (1995) Exogenous retinoic acid causes specific alterations in the development of the midbrain and hindbrain of the zebrafish embryo including positional respecification of the Mauthner neuron. *Mech. Dev.* **50**: 3-16.

Ho, H.T., Chung, S.K., Law, J.W., Ko, B.C., Tam, S.C., Brooks, H.L., Knepper, M.A., and Chung, S.S. (2000) Aldose reductase-deficient mice develop nephrogenic diabetes insipidus. *Mol. Cell. Biol.* **20**: 5840-5846.

Hogan, B., Beddington, R., Constantini, F., and Lacy, E. (1994) In "Manipulating the Mouse Embryo. A Laboratory Manual." Cold Spring Harbor Laboratory Press, New York.

Holder, N., and Hill, J.(1991) Retinoic acid modifies development of the midbrain-hindbrain border and affect cranial ganglion formation in zebrafish embryos. *Development* **113**: 1159-1170.
Hollemann, T., Chen, Y., Grunz, H., and Pieler, T. (1998) Regionalized metabolic activity establishes boundaries of retinoid signaling. *EMBO J.* **17**: 7361-7372.

Hoopes, C.W., Taketo, M., Ozato, K., Liu, Q., Howard, T.A., Linney, E., and Seldin, M.F. (1992) Mapping of the *Rxr* loci encoding nuclear retinois X receptors RXRα, RXRβ and RXRγ. *Genomics* **14**: 611-617.

Horan, G.S., Wu, K., Wolgemuth, D.J., and Behringer, R.R. (1994) Homeotic transformation of cervical vertebrae in *Hoxa4* mutant mice. *Proc. Natl. Acad. Sci. USA* **91**: 12644-12648.

Horan, G.S.B., Nagy Kovács, E., Behringer, R.R., and Featherstone, M.S. (1995a) Mutations in paralogous Hox genes result in overlapping hometoic transformations of the axial skeleton: evidence for unique and redundant function. *Dev. Biol.* **169**: 359-372.

Horan, G.S., Ramirez-Solis, R., Featherstone, M.S., Wolgemuth, D.J., Bradley, A., Behringer, R.R. (1995b) Compound mutants for the paralogous *Hoxa-4*, *Hoxb-4*, and *Hoxd-4* genes show more complete homeotic transformations and a dose-dependent increase in the number of vertebrae transformed. *Genes Dev.* **9**: 1667-1677.

Hörlein, A.J., Naar, A.M., Heinzel, T., Torchia, J., Gloss, B., Kurokawa, R., Ryan, A., Kamei, Y., Soderstrom, M., Glass, C.K., and et al., (1995) Ligand-independent repression by the thyroid hormone receptor mediated by a nuclear receptor co-repressor. *Nature* **377**: 397-404.

Horton, C., Maden, M. (1995) Endogenous distribution of retinoids during normal development and teratogenesis in the mouse embryo. *Dev. Dyn.* **202**: 312-323.

Houle, M., Prinos, P., Iulianella, A., Bouchard, N., and Lohnes, D. (2000) Retinoic acid regulation of Cdx1: an indirect mechanism for retinoids and vertebral specification. *Mol. Cell Biol.* **20**: 6579- 6586.

Howell, J. McC., Thompson, J.N., and Pitt, G.A. (1963) Histology of the lesions produced in the reproductive tract of animals fed a diet deficient in vitamin A alcohol but containing vitamin A acid. I. The male rat. *J. Reprod. Fertil.* **5**: 159-167.

Huang, D., Chen, S.W., Langston, A.W., and Gudas, L.J. (1998) A conserved retinoic acid responsive element in the murine *Hoxb-1* gene is required for expression in the developing gut. *Development* **125**: 3235-3246.

Huang, E.Y., Zhang, J., Miska, E.A., Guenther, M.G., Kouzarides, T., and Lazar, M.A. (2000) Nuclear receptor corepressors partner with class II histone deacetylases in a Sin3-independent repression pathway. *Genes Dev* **14**: 45-54.

Hunter, C.P., Harris, J.M., Maloof, J.N., and Kenyon, C. (1999) Hox gene expression in a single *Caenorhabditis elegans* cell is regulated by a *caudal* homolog and intercellular signals that inhibit *Wnt* signaling. *Development* **126:** 805-814.

Hussain, M.A., and Habener, J.F. (1999) Glucagon gene transcription activation mediated by synergistic interactions of pax-6 and cdx-2 with the p300 co-activator. *J. Biol. Chem.* **274**: 28950-28957.

Isaacs, H.V., Pownall, M.E., and Slack, J.M.W. (1998) Regulation of Hox gene expression and posterior development by the *Xenopus* caudal homologue Xcad3. *EMBO J.* **17**: 3414-3427.

Ishiguro, T., Nakajima, M., Naito, M., Muto, T., and Tsuruo, T. (1996) Identification of genes differentially expressed in B16 murine melanoma sublines with different metastatic potentials. *Cancer. Res.* **56**: 875-879.

Ishiguro, T., Nagawa, H., Naito, M., and Tsuruo, T. (2000) Analysis of novel metastasis-associated gene TI-227. *Jpn. J. Cancer. Res.* **91**: 390-394.

Iulianella, A., and Lohnes, D. (1997) Contribution of retinoic acid receptor gamma to retinoid-induced craniofacial and axial defects. *Dev. Dynam.* **209**: 92-104.

Iulianella, A., Beckett, B., Petkovich, M., and Lohnes, D. (1999) A molecular basis for retinoic acid-induced axial truncation. *Dev. Biol.* **205**: 33-48.

Jeannotte, L., Lemieux, M., Charron, J., Poirier, F., and Robertson, E.H. (1993) Specification of axial identity in the mouse: role of the *Hoxa-5* (*Hox1.3*) gene. *Genes Dev.* **7**: 2085-2096.

Jez, J.M., Bennett, M.J., Schlegel, B.P., Lewis, M., and Penning, T.M. (1997a) Comparative anatomy of the aldo-keto reductase superfamily. *Biochem. J.* **326**: 625-636.

Jez, J.M., Flynn, T.G., and Penning, T.M. (1997b) A new nomenclature for the aldo-keto reductase superfamily. *Biochem. Pharmacol.* **54**: 639-647.

Jez, J.M., Flynn, T.G., and Penning, T.M. (1997c) A nomenclature system for the aldo-keto reductase superfamily. *Adv. Exp. Med. Biol.* **414**: 579-600.

Kadonaga, J.T. (1998) Eukaryotic transcription: an interlaced network of transcription factors and chromatin-modifying machines. *Cell* **92**: 307-313.

Kamei, Y., Xu, L., Heinzel, T., Torchia, J., Kurokawa, R., Gloss, B., Lin, S.-C., Heyman, R.A., Rose, D.W., Glass, C.K., and Rosenfeld, M.G. (1996) A CBP integrator complex mediates transcriptional activation and AP-1 inhibition by nuclear receptors. *Cell* **85**: 403-414.

Kanazu, T., Shinoda, M., Nakayama, T., Deyashiki, Y., Hara, A., and Sawada, H. (1991) Aldehyde reductase is a major protein associated with 3-deoxyglucosone reductase activity in rat, pig and human livers. *Biochem. J.* **279**: 903-906.

Kao, H.Y., Downes, M., Ordentlich, P., and Evans, R.M. (2000) Isolation of a novel histone deacetylase reveals that class I and class II deacetylases promote SMRT-mediated repression. *Genes Dev.* 14: 55-66.

Kastner, P., Grondona, J., Mark, M., Gansmuller, A., LeMeur, M., Decimo, D., Vonesch, J.L., Dolle, P., and Chambon, P. (1994) Genetic analysis of RXRα developmental function: convergence of RXR and RAR signaling pathways in heart and eye morphogenesis. *Cell* **78**: 987-1003.

Kastner, P., Mark, M., Leid, M., Gansmuller, A., Chin, W., Grondona, J.M., Décimo, D., Krezel, W., Dierich, A., and Chambon, P. (1996) Abnormal spermatogenesis in RXRβ mutant mice. *Genes Dev.* **10**: 80-92.

Kastner, P., Mark, M., Ghyselinck, N., Krezel, W., Dupe, V., Grondona, J.M., and Chambon, P. (1997) Genetic evidence that the retinoid signal is transduced by heterodimeric RXR/RAR functional units during mouse development. *Development* **124**: 313-326.

Kataoka, A., Kubota, M., Wantanabe, K., Sawada, M., Koishi, S., Lin, Y.W., Usami, I., Akiyama, Y., Kitoh, T., and Furusho, K. (1997) NADH dehydrogenase deficiency in an apoptosis resistant mutant isolated from a human HL-60 leukemia cell line. *Cancer Res.* **57**: 5243-5245.

Kaufman, T.C., Seeger, M., and Olsen, G. (1990) Molecular and genetic organization of the *Antennapedia* gene complex of *Drosophila melanogaster*. *Adv. Genet.* **27**: 309-362.

Kenyon, C. (1994) If birds can fly, why can't we? Homeotic genes and evolution. *Cell* **78**: 175-180.

Kessel, M. (1992) Respecification of vertebral identities by retinoic acid. *Development* **115**: 487-501.

Kessel, M., Balling, R., and Gruss, P. (1990) Variations of cervical vertebrae after expression of a *Hox1.1* (*A7*) transgene in mice. *Cell* **61**: 301-308.

Kessel, M. and Gruss, P. (1991) Homeotic transformations of murine vertebrae and concomitant alteration of *Hox* codes induced by retinoic acid. *Cell* **67**: 89-104.

Kieny, M., Mauger A., and Sengel, P. (1972) Early regionalization of the somitic mesoderm as studied by the development of the axial skeleton of the chick embryo. *Dev. Biol.* **28**: 142-161.

Kinoshita, J.H. (1974) Mechanisms initiating cataract formation. Proctor Lecture. *Invest Ophthalmol* **13**: 713-724.

Kliewer, S.A., Umesono, K., Noonan, D.J., Heyman, R.A., and Evans, R.M. (1992) Convergence of 9-cis retinoic acid and peroxisome proliferator signaling pathways through heterodimer formation of their receptors. *Nature* **358**: 771-774.

Kmita, M., van der Hoeven, F., Zákány, J., Krumlauf, R., and Duboule, D. (2000) Mecahanisms of *Hox* gene colinearity: transposition of the anterior *Hoxb1* gene into the posterior *HoxD* complex. *Genes Dev.* **14**: 198-211.

Knittel, T., Kessel, M., Kim, M.H., and Gruss, P. (1995) A conserved enhancer of the human and murine *Hoxa7* gene specifies the anterior boundaries of expression during embryonal development. *Development* **121**: 1077-1088.

Kochhar, D.M. (1967) Teratogenic activity of retinoic acid. *Acta. Pathol. Microbiol. Immunol. Scand.* **70**: 398-404.

Kochhar, D.M. (1973) Limb development in mouse embryos. I. Analysis of teratogenic effects of retinoic acid. *Teratology* 7: 289-298.

Kolm, P.J., Apekin, V., and Sive, H. (1997) *Xenopus* hindbrain patterning requires retinoid signaling. *Dev. Biol.* **192**: 1-16.

Kondo, T., and Duboule, D. (1999) Breaking colinearity in the mouse *HoxD* complex. *Cell* **97**: 407-417.

Korzus, E., Torchia, J., Rose, D.W., Xu, L., Kurokawa, R., McInerney, E.M., Mullen, T.M., Glass, C.K., and Rosenfeld, M.G. (1998) Transcription factor-specific requirements for coactivators and their acetyltransferase functions. *Science* **279**: 703-707.

Kostic, D., and Capecchi, M. (1994) Targeted disruptions of the murine *Hoxa-4* and *Hoxa-6* genes result in homeotic transformations of components of the vertebral column. *Mech. Dev.* **46**: 231-247.

Knoepfler, P.S., and Kamps, M.P. (1997) The Pbx family of proteins is strongly upregulated by a post-transcriptional mechanism during retinoic acid-induced differentiation of P19 embryonal carcinoma cells. *Mech. Dev.* **63**: 5-14.

Kramerov, D.A., Grigoryan, A.A., Ryskov, A.P., and Georgiev, G.P. (1979) Long double-stranded sequences (dsRNA-B) of nuclear pre-mRNA consist of a few highly

abundant classes of sequences: evidence from DNA cloning experiments. *Nucleic Acids Res.* **6**: 697-713.

Kramerov, D.A., Tillib, S.V., Lekakh, I.V., Ryskov, A.P., and Georgiev, G.P. (1985) Biosynthesis and cytoplasmic distribution of small poly(A)-containing B2 RNA. *Biochim. Biophys. Acta.* **824:** 85-98.

Krayev, A.S., Markusheva, T.V., Kramerov, D.A., and Ryskov, A.P. (1982) Ubiquitous transposon-like repeats B1 and B2 of the mouse genome: B2 sequencing. *Nucleic Acids Res.* **10**: 7461-7475.

Krezel, W., Dupé, V., Mark, M., Dierich, A., Kastner, P., and Chambon, P. (1996) RXRγ null mice are apparently normal and compound RXR$\alpha^{+/-}$/RXR$\beta^{-/-}$/RXR$\gamma^{-/-}$ mutant mice are viable. *Proc. Natl. Acad. Sci. USA* **93**: 9010-9014.

Krezel, W., Ghyselinck, N., Samad, T.A., Dupe, V., Kastner, P.,Borrelli, E., and Chambon, P. (1998) Impaired locomotion and dopamine signaling in retinoid receptor mutant mice. *Science* **279**: 863-867.

Krumlauf, R. (1992) Evolution of the vertebrate *Hox* homeobox genes. *Bioessays* **14**: 245-251.

Krumlauf, R. (1994) *Hox* genes in vertebrate development. *Cell* 78: 191-201.

Kucera, J. Rate and type of congenital anomalies among offspring of diabetic women. *J. Reprod. Med.* **7**: 73-82

Kurlandsky, S.B., Gamble, M.V., Ramakrishnan, R., and Blaner, W.S. (1995) Plasma Delivery of Retinoic Acid to Tissues in the Rat. *J. Biol. Chem.* **270**: 17850-17857.

Kurokawa, R., Söderström, M., Hörlein, A.J., Halachmi, S., Brown, M., Rosenfeld, M.G., and Glass, C.H. (1995) Polarity-specific activities of retinoic acid receptors determined by a co-repressor. *Nature* **377**: 451-454.

Kurokawa, R., Yu, V.C., Näär, A., Kyakumoto, S., Han, Z., Silverman, S., Rosenfeld, M.G., and Glasss, C.K. (1993) Differential orientations of the DNA-binding domain and carboxy-terminal dimerization interface regulate binding site selection by nuclear receptor heterodimers. *Genes Dev.* **7**: 1423-1435.

Labrecque, J., Dumas, F., Lacroix, A., and Bhat. P.V. (1995) A novel isoenzyme of aldehyde dehydrogenase specifically involved in the biosynthesis of 9-*cis* and all-*trans* retinoic acid. *Biochem J.* **305**: 681-684.

Laherty, C.D., Billin, A.N., Lavinsky, R.M., Yochum, G.S., Bush, A.C., Sun, J.M., Mullen, T.M., Davie, J.R., Rose, D.W., Glass, C.K., Rosenfeld, M.G., Ayer, D.E., and

Eisenman, R.N. (1998) SAP30, a component of the mSIN3 corepressor complex involved in N-CoR-mediated repression by specific transcription factors. *Mol. Cell.* **2**: 33-42.

Lammer, E.J., Chen, D.T., Hoar, R.M., Agnish, N.D., Benke, P.J., Braun, J.T., Curry, C.J., Fernhoff, P.M., Grix, A.W., Lott, .T., Richard, J.M., and Sun, S.C. (1985) Retinoic acid embryopathy. *N. Eng. J. Med.* **313**: 837-841.

Lampron, C., Rochette-Egly, C., Gorry, P., Dollé, P., Mark, M., Lufkin, T., LeMeur, M., and Chambon, P. (1995) Mice deficient in cellular retinoic acid binding protein II (CRABPII) or in both CRABPI and CRABPII are essentially normal. *Development* **121**: 539-548.

Langston, A.W., and Gudas, L.J. (1992) Identification of a retinoic acid responsive enhancer 3' of the murine homeobox gene Hox1.6. *Mech. Dev.* **38**: 217-227.

Lee, A.Y.W., Chung, S.K., and Chung, S.S.M. (1995) Demonstration that polyol accumulation is responsible for diabetic cataract by the use of transgenic mice expressing the aldose reductase gene in the lens. *Proc. Natl. Acad. Sci. USA* **92**: 2780-2784.

Lee, H.-Y., Sueoka, N., Hong, W.-K., Mangelsdorf, D.J., Claret, F.X., and Kurie, J.M. (1999) All-*trans*-retinoic acid inhibits jun N-terminal kinase by increasing dual-specific phosphatase activity. *Mol. Cell Biol.* **19**: 1973-1980.

Lee, H.-Y., Walsh, G.L., Dawson, M., Hong, W.K., and Kurie, J.M. (1998) All-*trans*-retinoic acid inhibits jun N-terminal kinase dependent signaling pathways. *J.Biol. Chem.* **273**: 7066-7071.

Lee, M.-O., Manthey, C.L., and Sladek, N.E. (1991) Identification of mouse liver aldehyde dehydrogenases that catalyze the oxidation of retinaldehyde to retinoic acid. *Biochem. Pharmacol.* **43**: 2453-2469.

Leid, M., Kastner, P., Lyons, R., Nakshatri, H., Saunders, M., Zacharewski, T., Chen, J.Y., Staub, A., Garnier, J.M., Mader, S., and Chambon, P. (1992) Purification, cloning and RXR identity of the HeLa cell factor with which RAR or TR heterodimerizes t bind target sequences efficiently. *Cell* **68**: 377-395.

Levin, A.A., Sturzenbecker, L.J., Kazmer, S., Bosakowski, T., Huselton, C., Allenby, G., Speck, J., Kratzeisen, C., Rosenberger, M., Lovey, A., and Grippo, J.F. (1992) 9-cis retinoic acid sterioisomer binds and activates the nuclear receptor RXRα. *Nature* **355**: 359-361.

Levine, M., Harding, K., Wedeen, C., Doyle, H., Hoey, T.,and Radomska, H. (1985) Expression of the homeo box gene family in Drosophila. *Cold Spring Harb Symp Quant Biol.* **50**: 209-222.

Lewis, E. (1978) A gene complex controlling segmentation in *Drosophila. Nature* **276**: 565-570.

Li, H., Wagner, E., McCaffery, P., Smith, D., Andreadis, A., and Dräger, U.C. (2000) A retinoic acid synthesizing enzyme in ventral retina and telencephalon of the embryonic mouse. *Mech. Dev.* **95:** 283-289.

Li, E., Sucov, H.M., Lee, K.F., Evans, R.M., and Jaenisch, R. (1993) Normal development and growth of mice carrying a targeted disruption of the α1 retinoic acid receptor gene. *Proc. Natl. Acad. Sci. USA* **90**: 1590-1594.

Liang, P., and Pardee, A.B. (1992) Differential display of eukaryotic messenger RNA by means of the polymerase chain reaction. *Science* **257**: 967-971.

Lickert, H., Domon, C., Huls, G., Wehrle, C., Duluc, I., Clevers, H., Meyer, B.I., Freund, J.N., and Kemler, R. (2000) Wnt/β-catenin signaling regulates the expression of the homeobox gene *Cdx1* in embryonic intestine. *Development* **127**: 3805-3813.

Lisitsyn, N., Lisitsina, N., and Wigler, M. (1993) *Science* **259**: 946-951.

Liu, P., Wakamiya, M., Shea, M.J., Albrecht, U., Behringer, R.R., and Bradley, A. (1999) Requirement for *Wnt3* in vertebrate axis formation. *Nature Genetics* **22**: 361-365.

Liu, Q., and Linney, E. (1993) The mouse retinoid-X receptor-gamma gene: genomic organization and evidence for functional isoforms. *Mol Endocrinol* 7: 651-658.

Lohnes, D., Dierich, A., Ghyselinck, N., Kastner, P., Lampron, C., LeMeur, M., Lufkin, T., Mendelsohn, C., Nakshatri, H., and Chambon, P. (1992) Retinoid receptors and binding proteins. *J. Cell Sci.* Suppl **16**: 69-76.

Lohnes, D., Kastner, P., Dierich, A., Mark, M., LeMeur, M., and Chambon, P. (1993) Function of retinoic acid receptor γ in the mouse. *Cell* **73**: 643-658.

Lohnes, D., Mark, M., Mendelsohn, C., Dolle, P., Dierich, A., Gorry, P., Gansmuller, A., and Chambon, P. (1994) Function of the retinoic acid receptors (RARs) during development (I). Craniofacial and skeletal abnormalities in RAR double mutants. *Development* **120**: 2723-2748.

Loudig, O., Babichuk, C., White, J., Abu-Abed, S., Mueller, C., and Petkovich, M. (2000) Cytochrome P450RAI(CYP26) promoter: a distinct composite retinoic acid response element underlies the complex regulation of retinoic acid metabolism. *Mol. Endocrinol.* **14**: 1483-1497.

Lufkin, T., Lohnes, D., Mark, M., Dierich, A., Gorry, P., Gaub, M.P., LeMeur, M., and Chambon, P. (1993) High postnatal lethality and testis degeneration in retinoic acid receptor α mutant mice. *Proc. Natl. Acad. Sci. USA* **90**: 7225-7229.

Luisi, B.F., Xu, W.X., Otinowski, Z., Freedman, L.P., Yamamoto, K.R., and Sigler, P.B. (1991) Crystallographic analysis of the interaction of the glucocorticoid receptor with DNA. *Nature* **352**: 497-505.

Luo, J., Pasceri, P., Conlon, R.A., Rossant, J., and Giguère, V. (1995) Mice lacking all isoforms of retinoic acid receptor β develop normally and are susceptible to the teratogenic effects of retinoic acid. *Mech. Dev.* **53**: 61-71.

Luo, J., Sucov, H.M., Bader, J.A., Evans, R.M., and Giguère, V. (1996) Compound mutants for retinoic acid receptor (RAR) β and RARα1 reveal developmental functions for multiple RARb isoforms. *Mech. Dev.* **55**: 33-44.

Macdonald, P.M., and Struhl, G. (1986) A molecular gradient in early *Drosophila* embryos and its role in specifying the body pattern. *Nature* **324**: 537-545.

Maconochie, M., Krishnamurthy, R., Nonchev, S., Meier, P., Manzanares, M., Mitchell, P.J., and Krumlauf, R. (1999) Regulation of *Hoxa2* in cranial neural crest cells involves members of the *AP-2* family. *Development* **126**: 1483-1494.

Maconochie, M.K., Nonchev, S., Studer, M., Chan, S.K., Popperl, H., Sham, M.H., Mann, R.S., and Krumlauf, R. (1997) Cross-regulation in the mouse Hoxb complex: the expression of Hoxb2 in rhombomere 4 is regulated by Hoxb1. *Genes Dev.* **18**: 1885-1895.

Maden, M., Gale, E., Kostetskii, I., and Zile, M. (1996) Vitamin A-deficient quail embryos have half a hindbrain and other neural defects. *Curr. Biol.* **6**: 417-426.

Maden, M., Graham, A., Gale, E., Rollinson, C., and Zile, M. (1997) Positional apoptosis during vertebrate CNS development in the absence of endogenous retinoids. *Development* **124**: 2799-2805.

Maden, M., Graham, A., Zile, M., and Gale, E. (2000) Abnormalities of somite development in the absence of retinoic acid. *Int. J. Dev. Biol.* **44**: 151-159.

Maden, M., Ong, D.E., and Chytil, F. (1990) Retinoid binding protein distribution in the developing mammalian nervous system. *Development* **109**: 75-80.

Maden, M., Sonneveld, E., van der Saag, P.T., and Gale, E. (1998) The distribution of endogenous retinoic acid in the chick embryo: implications for developmental mechanisms. *Development* **125**: 4133-4144.

Malik, S., and Roeder, R.G. (2000) Transcriptional regulation through mediator-like coactivators in yeast and metazoan cells. *Trends Biochem. Sci.* **25**: 277-283.

Mangelsdorf, D.J., and Evans, R.M. (1995) The RXR heterodimers and orphan receptors. *Cell* **83**: 841-850.

Mangelsdorf, D.J., Ong, E.S., Dyck, J.A., and Evans, R.M. (1990) Nuclear receptor that identifies a novel retinoic acid response pathway. *Nature* **345**: 224-229.

Mangelsdorf, D.J., Thummel, C., Beato, M., Herrlich, P., Schütz, G., Umesono, K., Blumberg, B., Kastner, P., Mark, M., Chambon, P., and Evans, R.M. (1995) The nuclear receptor superfamily: the second decade. *Cell* **83**: 835-839.

Mangelsdorf, D.J., Umesono, K., Kliewer, S.A., Borgmeyer, U., Ong, E.S., and Evans, R.M. (1991) A direct repeat in the cellular retinol-binding protein type II gene confers differential regulation by RXR and RAR. *Cell* **66**: 555-561.

Manley, N.R., and Capecchi, M.R. (1997) Hox group 3 paralogous genes act synergistically in the formation of somitic and neural crest-derived structures. *Dev.Biol.* **192**: 274-288.

Manzanares, M., Cordes, S., Ariza-McNaughton, L., Sadl, V., Maruthainar, K., Barsh, G., and Krumlauf, R. (1999) Conserved and distinct roles of kreisler in regulation of the paralogous Hoxa3 and Hoxb3 genes. *Development* **126**: 759-769.

Manzanares, M., Cordes, S., Kwan, C.T., Sham, M.H., Barsh, G.S., and Krumlauf, R. (1997) Segmental regulation by partially overlapping temporal and spatial patterns of expression. *Mech. Dev.* **64**: 41-52.

Margalit, Y., Yarus, S., Shapira, E., Gruenbaum, Y., and Fainsod, A. (1993) Isolation and characterization of target sequences of the chicken *CdxA* homeobox gene. *Nucl. Acids Res.* **21**: 4915-4922.

Marom, K., Shapira, E., and Fainsod, A. (1997) The chicken *caudal* genes establish an anterior-posterior gradient by partially overlapping temporal and spatial patterns of expression. *Mech. Dev.* **64**: 41-52.

Marshall, H., Morrison, A., Studer, M., Pöpperl, H., and Krumlauf, R. (1996) Retinoids and Hox genes. *FASEB J.* **10**: 969-978.

Marshall, H., Nonchev, S., Sham, M.H., Muchamore, I., Lumsden A., and Krumlauf, R. (1992) Retinoic acid alters hindbrain *Hox* code and induces transformation of rhombomeres 2/3 into a 4/5 identity. *Nature* **370**: 567-571.

Marshall, H., Studer, M., Pöpperl, H., Aparicio, S., Kuroiwa, A., Brenner, S., and Krumlauf, R. (1994) A conserved retinoic acid response element required for early expression of the homeobox gene *Hoxb1*. *Nature* **370**: 567-571.

Mason, K.E. (1935) Foetal death, prolonged gestation, and difficult parturition in the rat as a result of vitamin A deficiency. *Am. J. Anat.* **57**: 303-349.

Mattei, M.-G. Riviere, M., Krust, A., Ingvarsson, S., Vennstrom, B., Islam, M.Q., Levan, G., Kastner, P., Zelent, A., Chambon, P., Szpirer, J., Szpirer, C. (1991) Chromosomal assignment of retinoic acid receptor (RAR) genes in the human, mouse and rat genomes. *Genomics* **10**: 1061-1069.

McCaffery, P., and Dräger, U.C. (1993) Retinoic acid synthesis in the developing retina. *Adv. Exp. Med. Biol.* **328**: 181-190.

McCaffery, P., Wagner, E., O'Neil, J., Petkovich, M., and Dräger, U.C. (1999) Dorsal and ventral retinal terrirories defined by retinoic acid synthesis, break-down and nuclear receptor expression. *Mech. Dev.* **82**: 119-130.

McKay, I.J., Muchamore, I., Krumlauf, R., Maden, M., Lumsden, A., and Lewis, J. (1994) The *kreisler* mouse: a hindbrain segmentation mutant that lacks two rhombomeres. Development *121*

McMahon, A.P. and Moon, R.T. (1989) Ectopic expression of the proto-oncogene int-1 in *Xenopus* embryos leads to duplication of the embryonic axis. *Cell* **58**: 1075-1084.
Meyer, B.I., and Gruss, P. (1993) Mouse *Cdx-1* expression during gastrulation. *Development* **117**: 191-203.

Mendelsohn, C., Lohnes, D., Decimo, D., Lufkin, T., LeMeur, M., Chambon, P., and Mark, M. (1994a) Function of the retinoic acid receptors (RARs) during development. (II) Multiple abnormalities at various stages of organogenesis in RAR double mutants. *Development* **120**: 2749-2771.

Mendelsohn, C., Mark, M., Dolle, P., Dierich, A., Gaub, M.-P., Krust, A., Lampron, C., and Chambon, P. (1994b) Retinoic acid receptor β2 (RARβ2) null mutant mice appear normal. *Dev. Biol.* **166**: 246-258.

Meyer, B.I., and Gruss, P. (1993) Mouse Cdx-1 expression during gastrulation. *Development* **117**: 191-203.

Mills, J.L. (1982) Malformations in infants of diabetic mothers. *Teratology* **25**: 385-394.

Mills, J.L., Baker, L., and Goldman, A.S. (1979) Malformations in infants of diabetic mothers occur before the seventh gestational week: implications for treatment. *Diabetes* **28**: 292-293.

Mitchelmore, C., Troelsen, J.T., Spodsberg, N., Sjostrom, H., and Noren, O. (2000) Interaction between the homeodomain proteins Cdx2 and HNF1α mediates expression of the lactase-phlorizin hydrolase gene. *Biochem J.* **346**: 529-535.

Mlodzik, M., Fjose, A., and Gehring, W.J. (1985) Isolation of *caudal,* a Drosophila homeobox-containing gene with maternal expression whose transcripts form a gradient at the pre-blastoderm stage. *EMBO J.* **4**: 2961-2969.

Mlodzik, M., Gibson, G., and Gehring, W.J. (1990) Effects of ectopic expression of *caudal* during *Drosophila* development. *Development* **109**: 271-277.

Mollard, R., Viville, S., Ward, S.J., Decimo, D., Chambon, P., and Dollé, P. (2000) Tissue-specific expression of retinoic acid receptor isoform transcripts in the mouse embryo. *Mech. Dev.* **94**: 223-232.

Monnier, V.M., Kohn, R.R., and Cerami, A. (1984) Accelerated age-related browning of human collagen in diabetes mellitus. *Proc. Natl. Acad. Sci. U S A* **81**(2): 583-587.

Moon, R.T., Brown, J.D., and Torres, M. (1997) WNTs modulate cell fate and behaviour during vertebrate development. *Trends. Genet.* **13**: 157-162.

Moras, D., and Gronemeyer, H. (1998) The nuclear receptor ligand-binding domain: structure and function. *Curr. Opin. Cell Biol.* **10**: 384-391.

Moreno, E., and Morata, G. (1999) *Caudal* is the Hox gene that specifies the most posterior Drosophile segment. *Nature* **400**: 873-877.

Moroni, M.C., Vigano, M.A., Mavilio, F. (1993) Regulation of the human HOXD4 gene by retinoids. *Mech. Dev.* **44**: 139-154.

Morrison, A., Moroni, C.M., Ariza-McNaughton, L., Krumlauf, R., and Mavillio, F. (1996) In vitro and transgenic analysis of a human HOXD4 retinoid-responsive enhancer. *Development* **122**: 1895-1907.

Morrison, A., Ariza-McNaughton, L., Gould, A., Featherstone, M., and Krumlauf, R. (1997) HOXD4 and regulation of the group 4 paralog genes. *Development* **124**: 3135-3146.

Morriss-Kay, G. (1993) Retinoic acid and craniofacial development: molecules and morphogenesis. *Bioessays* **15**: 9-15.

Morriss-Kay, G.M., Murphy, P., Hill, R.E., and Davidson, D.R. (1991) Effects of retinoic acid excess on expression of Hox2.9 and Krox-20 and on morphological segmentation in the hindbrain of mouse embryos. *EMBO J.* **10**: 2985-2995.

Morriss-Kay, G.M., and Sokolova, N. (1996) Embryonic development and pattern formation. *FASEB* **10**: 961-968.

Moss, J.B., Xavier-Neto, J., Shapiro, M.D., Nayeem, S.M., McCaffery, P., Drager, U.C., and Rosenthal, N. (1998) Dynamic patterns of retinoic acid synthesis and response in the developing mammalian heart. *Dev. Biol.* **199**: 55-71.

Mou, L., Miller, H., Li, J., Wang, E., and Chalifour, L. (1994) Improvements to the differential display method for gene analysis. *Biochem. Biophys. Res. Commun.* **199**: 564-569.

Murphy, D., Brickell, P.M., Latchman, D.S., Willison, K., and Rigby, P.W. (1983) Transcripts regulated during normal embryonic development and oncogenic transformation share a repetitive element. *Cell* **35**: 865-71

Nadeau, J.H., Compton, J.G., Giguère, V., Rossant, J., Varmuza, S. (1992) Close linkage of retinoic acid receptor genes with homeobox- and keratin-encoding genes on paralogous segments of mouse chromosomes 11 and 15. *Mammalian Genome* **3**: 202-208.

Nagata, T., Kanno, Y., Ozato, K., and Taketo, M. (1994) The mouse Rxrb gene encoding RXR beta: genomic organization and two RNA isoforms generated by alternative splicing of transcripts initiated from CpG island promoters. *Gene* **142**: 183-189.

Nagpal, S., Frinat, S., Nakshatri, H., and Chambon, P. (1993) RARs and RXRs: evidence for two autonomous transactivation functions (AF-1 and AF-2) and heterodimerization *in vivo*. *EBMO J.* **12**: 2349-2360.

Nagpal, S., Saunders, M., Kastner, P., Durand, B., Nakshatri, H., and Chambon, P. (1992) Promoter context- and response element-dependent specificity of the transcriptional activation and modulating functions of retinoic acid receptors. *Cell* **70**: 1007-1019.

Nagy, L., Kao, H.Y., Chakravarti, D., Lin, R.J., Hassig, C.A., Ayer, D.E., Schreiber, S.L., and Evans, R.M. (1997) Nuclear receptor repression mediated by a complex containing SMRT, mSin3A, and histone deacetylase. *Cell* **89**: 373-380.

Napoli, J.L. (1999) Interactions of retinoid binding proteins and enzymes in retinoid metabolism. *Biochim. Biophys. Acta* **1440**: 139-162.

Niederreither, K., McCaffery, P., Dräger, U.C., Chambon, P., and Dollé, P. (1997) Restricted expression and retinoic acid-induced downregulation of the retinaldehyde dehydrogenase type 2 (RALDH-2) gene during mouse development. *Mech. Dev.* **62**: 67-78.

Niederreither, K., Subbarayan, V., Dollé, P., and Chambon, P. (1999) Embryonic retinoic acid synthesis is essential for early mouse post-implantation development. *Nature Genet.* **21**: 444-448.

Niederreither, K., Vermot, J., Schuhbaur, B., Chambon, P., and Dollé, P. (2000) Retinoic acid synthesis and hindbrain patterning in the mouse embryo. *Development* **127**: 75-85.

Nonchev, S., Vesque, C., Maconochie, M., Seitanidou, T., Ariza-McNaughton, L., Frain, M., Marshall, H., Har Sham, M., Krumlauf, R., and Charnay, P. (1996) Segmental expression of Hoxa-2 in the hindbrain is directly regulated by Krox-20. *Development* **122**: 543-554.

Nowicki, J.L., and Burke, A.C. (2000) *Hox* genes and morphological identity: axial versus lateral patterning in the vertebrate mesoderm. *Development* **127**: 4265-4275.

Ogryzko, V.V., Schlitz, R.L., Russanova, V., Howard, B.H., and Nakatani, Y. (1996) The transcriptional coactivators p300 and CBP are histone acetyltransferases. *Cell* **87**: 953-959.

Oh, S.P., and Li, E. (1997) The signaling pathway mediated by the type IIB activin receptor controls axial patterning and lateral asymmetry in the mouse. *Genes. Dev.* **11**: 1812-1826.

Ohara, H., Miyabe, Y., Deyashiki, Y., Matsuura, K., Hara, A. (1995) Reduction of drug ketones by dihydrodiol dehydrogenases, carbonyl reductase and aldehyde reductase of human liver. *Biochem. Pharmacol.* **50**: 221-227.

Ohmori, S., Mori, M., Shiraha, K., and Kawase, M.(1989) Biosynthesis and degradation of methylglyoxal in animals. *Prog. Clin. Biol. Res.* **290**: 397-412.

Ong, D.E., MacDonald, P.N., Gubitosi, A.M. (1988) Esterification of retinol in rat liver: possible participation by cellular retinol-binding protein and cellular retinol binding-protein II. *J. Biol. Chem.* **263**: 5789-5796.

Ong, D.E., Newcomer, M.E., and Chytil, F. (1994) Cellular retinoid-binding proteins. In *The Retinoids: Biology, Chemistry, and Medicine* (Sporn, M.B., Roberst, A.B., and Goodman, D.S., eds) 2nd Ed.. Raven Press, New York.

Oulad-Abdelghani, M., Chazaud, C., Bouillet, P., Sapin, V., Chambon, P., and Dolle, P. (1997) *Meis2*, A novel mouse Pbx-related homeobox gene induced by retinoic acid during differentiation of P19 embryonal carcinoma cells. *Dev. Dyn.* **210**: 173-183.

Packer, A.I., Crotty, D.A., Elwell, V.A., and Wolgemuth, D.J. (1998) Expression of the murine *Hoxa4* gene requires both autoregulation and a conserved retinoic acid response element. *Development* **125**: 1991-1998.

Partanen, J., Schwartz, L., and Rossant, J. (1998) Opposite phenotypes of hypomorphic and Y766 phosphorylation site mutations reveal a function for Fgfr1 in anteroposterior patterning of mouse embryos. *Genes Dev.* **12**: 2332-2344.

Pazin, M.J., and Kadonaga, J.T. (1997) What's up and down with histone deaetylation and transcription? *Cell* **89**: 85-94.

Penzes, P., Wang, X.S., Sperkova, A., and Napoli, J.L. (1997) Cloning of a rat cDNA encoding retinal dehydrogenase isoenzyme type I and its expression in *E.coli. Gene* **191**: 167-172.

Peralba, J.M., Cederlund, E., Crosas, B., Moreno, A., Julià, P., Martínez, S.E., Persson, B., Farrés, J., Parés, X., and Jörnvall, H. (1999) Structural and enzymatic properties of a gastric NADP(H)-dependent and retinal-active alcohol dehydrogenase. *J. Biol. Chem.* **274**: 26021-26026.

Perez-Castro, A.V., Toth-Rogler, L.E., Wei, L., Nguyen-Huu, M.C. (1989) Spatial and temporal pattern of expression of the cellular retinoic acid-binding protein and the cellular retinol-binding protein during mouse embryogenesis. *Proc. Natl. Acad. Sci. USA* **86**: 8813-8817.

Perissi, V., Staszewski, L.M., McInerney, E.M., Kurokawa, R., Krones, A., Rose, D.W., Lambert, M.H., Milturn, M.V., Glass, C.K., and Rosenfeld, M.G. (1999) Molecular determinants of nuclear receptor-corepressor interaction. *Genes Dev.* **13**: 3198-3208.

Perlmann, T., Rangarajan, P.N., Umesono, K., and Evans, R.M. (1993) Determinants for selective RAR and TR recognition of direct repeat HREs. *Genes Dev.* **7**: 1411-1422.

Persson, B., Krook, M., and Jörnvall, H. (1995) Short-chain dehydrogenases/reductases. *Adv Exp Med Biol.* **372**: 383-395.

Petkovich, M., Brand, N.J., Krust, A., and Chambon, P. (1987) A human retinoic acid receptor which belongs to the family of nuclear receptors. *Nature* **330**: 444-450.

Petrash, J.M., Flath, M., Sens, D., Bylander, J. (1992) Effects of osmotic stress and hyperglycemia on aldose reductase gene expression in human renal proximal tubule cells. *Biochem. Biophys. Res. Commun.* **187**: 201-208.

Pijnappel, W.W., Hendriks, H.F., Folkers, G.E., van den Brink, C.E., Dekker, E.J., Edelenbosch, C., van der Saag, P.T., and Durston, A.J. (1993) The retinoid ligand 4-oxo-retinoic acid is a highly active modulator of positional specification. *Nature* **366:** 340-344.

Pillemer, G., Epstein, M., Blumberg, B., Yisraeli, J.K., De Robertis, E.M., Steinbeisser, H., and Fainsod, A. (1998) Nested expression and sequential downregulation of the *Xenopus caudal* genes along the antero-posterior axis. *Mech. Dev.* **71**: 193-196.

Pitts, N.E., Vreeland, F., Shaw, G.L., Peterson, M.J., Mehta, D.J., Collier, J., Gundersen, K. (1986) Clinical experience with sorbinil-an aldose reductase inhibitor. *Metabolism* **35**: 96-100

Pompliano, D.L., Peyman, A., Knowles, J.R. (1990) Stabilization of a reaction intermediate as a catalytic device: definition of the functional role of the flexible loop in triosephosphate isomerase. *Biochemistry* **29**: 3186-3194.

Pöpperl, H., Bienz, M., Studer, M., Chan, S.K., Aparicio, S., Brenner, S., Mann, R.S., and Krumlauf, R. (1995) Segmental expression of Hoxb-1 is controlled by a highly conserved autoregulatory loop dependent upon exd/pbx. *Cell* **81**: 1031-1042.

Pöpperl, H., and Featherstone, M. (1992) An autoregulatory element of the murine Hox4.2 gene. *EMBO J.* **11**: 3673-3680.

Pöpperl, H., and Featherstone, M.S. (1993) Identification of a retinoic acid response element upstream of the murine Hox-4.2 gene. *Mol. Cell. Biol.* **13**: 257-265.

Pownall, M.E., Tucker, A.S., Slack, J.M.W., and Isaacs, H.V. (1996) *eFGF*, *Xcad3* and Hox genes form a molecular pathway that establishes the anteroposterior axis in *Xenopus*. *Development* **122**: 3881-3892.

Quadro, L., Blaner, W.S., Salchow, D.J., Vogel, S., Piantedosi, R., Gouras, P., Freeman, S., Cosma, M.P., Colantuoni, V., and Gottesman, M.E. (1999) Impaired retinal function and vitamin A availability in mice lacking retinol-binding protein. *EMBO J.* **18:** 4633-4644.

Rachez, C., Suldan, Z., Ward, J., Chang, C.P., Burakov, D., Erdjument-Bromage, H., Tempst, P., and Freedman, L.P. (1998) A novel protein complex that interacts with the vitamin D3 receptor in a ligand-dependent manner and enhances VDR transactivation in a cell-free system. *Genes Dev.* **12**: 1787-1800.

Ramírez-Solis, R., Zheng, H., Whiting, J., Krumlauf, R., and Bradley, A. (1993) Hoxb-4 (Hox2.6) mutant mice show homeotic transformation of a cervical vertebra and defects in the closure of the sternal rudiments. *Cell* **73**: 279-294.

Rancourt, D.E., Tsuzuki, T., and Capecchi, M.R. (1995) Genetic interaction between *hoxb-5* and *hoxb-6* is revealed by nonallelic noncomplementation. *Genes Dev.* **9**: 108-122.

Rastinejad, F., Perlmann, T., Evans, R.M., and Sigler, P.B. (1995) Structural determinants of nuclear receptor assembly on DNA direct repeats. *Nature* **375**: 203-211.

Ray, W.J., Bain, G., Yao, M., and Gottlieb, D.I. (1997) CYP26, a novel mammalian cytochrome P-450, is incuded by retinoic acid and defines a new family. *J. Biol. Chem.* **272**: 18702-18708.

Rigby, P.W., Brickell, P.M., Latchman, D.S., Murphy, D., Westphal, K.H., Willison, K.(1984) The activation of cellular genes in transformed cells. *Philos. Trans. R. Soc. Lond. B. Biol. Sci.* **307**: 347-51

Rijli, F.M., Gavalas, A., Chambon, P. (1998) Segmentation and specification in the branchial region of the head: the role of the Hox selector genes. *Int. J. Dev. Biol.* **42**(3 Spec No): 393-401.

Ritz-Laser, B., Estreicher, A., Klages, N., Saule, S., and Philippe, J. (1999) Pax-6 and Cdx-2/3 interact to activate glucagons gene expression on the G1-control element. *J. Biol. Chem.* **274**: 4124-4132.

Rivera-Pomar, R., Niessing, D., Schmidt-Ott, U., Gehring, W.J., and Jackle, H. (1996) RNA binding and translational suppression by bicoid. *Nature* **379**: 746-749.

Roberts, A.B., Nichols, M.D., Newton, D.L., and Sporn, M.B. (1979) In vitro metabolism of retinoic acid in hamster intestine and liver. *J. Biol. Chem.* **254**: 6296-6302.

Rochette-Egly, C., Adam, S., Rossignol, M., Egly, J.M., and Chambon, P. (1997) Stimulation of RARα activation function AF-1 through binding to the general transcription factor TFIIH and phosphorylation by CDK7. *Cell* **90**: 97-107.

Rogers, L.H. (1985) The origin and evolution of retrotransposons. *Int. Rev. Cytol.* **93**: 187-279.

Rosen, E.D., Beninghof, E.G., and Koenig, R.J. (1993) Dimerization interfaces of thyroid hormone, retinoic acid, vitamin D, and retinoid X receptors. *J. Biol. Chem.***268**: 11534-11541.

Ross, S.A., McCaffery, P.J., Drager, U.C., and De Luca, L.M. (2000) Retinoids in Embryonal Development. *Physiol. Rev.* **80**: 1021-54.

Rossant, J., Zirngibl, R., Cado, D., Shago, M., and Giguère, V. (1991) Expression of a retinoic acid response element-hsplacZ transgene defines specific domains of transcriptional activity during mouse embryogenesis. *Genes Dev.* **5**: 1333-1344.

Ruberte, E., Dolle, P., Chambon, P., and Morriss-Kay, G. (1991) Retinoic acid receptors and cellular retinoid binding proteins. II. Their differential pattern of transcription during early morphogenesis in mouse embryos. *Development* **111**: 45-60.

Ruberte, E., Dolle, P., Krust, A., Zelent, A., Morriss-Kay, G., Chambon, P. (1990) Specific spatial and temporal distribution of retinoic acid receptor gamma transcripts during mouse embryogenesis. *Development* **108**: 213-222.

Ruberte, E., Friederich, V., Chambon, P., and Morris-Kay, G. (1993) Retinoic acid receptors and cellular retinoid binding proteins. III. Their differential pattern of transcription during mouse nervous system development. *Development* **118**: 267-282.

Ruepp, B., Bohren, K.M., Gabbay, K.H. (1996) Characterization of the osmotic response element of the human aldose reductase gene promoter. *Proc. Natl. Acad. Sci. U S A* **93**: 8624-8629.

Ruiz i Altaba, A., and Jessell, T. (1991) Retinoic acid modifies the pattern of cell differentiation of the central nervous system of the neurula stage *Xenopus laevis* embryos. *Development* **112**: 945-958.

Ruiz-Lozano, P., Smith, S.M., Perkins, G., Kubalak, S.W., Boss, G.R., Sucov, H.M., Evans, R.M., and Chien, K.R. (1998) Energy deprivation and a deficiency in downstream metabolic target genes during the onset of embryonic heart failure in RXRα-/- embryos. *Development* **125**: 533-544.

Saegusa, H., Takahashi, N., Noguchi, S., and Suemori, H. (1996) Targeted disruption in the mouse *Hoxc-4* locus results in axial skeleton homeosis and malformation of the xiphoid process. *Dev. Biol.* **174**: 55-64.

Sakai, Y., Meno, C., Fujii, H., Nishino, J., Shiratori, H., Yukio, S., Rossant, J., and Hamada, H. (2001) The retinoic acid-inactivating enzyme CYP26 is essential for establishing an uneven distribution of retinoic acid along the anterio-posterior axis within the mouse embryo. *Genes Dev.* **15**: 213-225.

Sapin, V., Ward, S.J., Bronner, S., Chambon, P., and Dollé, P. (1997) Differential expression of transcripts encoding retinoid binding proteins, and retinoic acid receptors during placentation of the mouse. *Dev. Dyn.* **208:** 199-210.

Sato, K., Inazu, A., Yamaguchi, S., Nakayama, T., Deyashiki, Y., Sawada, H., and Hara, A. (1993) Monkey 3-deoxyglucosone reductase: tissue distribution and purification of three multiple forms of the kidney enzyme that are identical with dihydrodiol dehydrogenase, aldehyde reductase, and aldose reductase. *Arch. Biochem. Biophys.* **307**: 286-294.

Schmidt, A.M., Hori, O., Cao, R., Yan, S.D., Brett, J., Wautier, J.L., Ogawa, S., Kuwabara, K., Matsumoto, M., Stern, D. (1996) RAGE: a novel cellular receptor for advanced glycation end products. *Diabetes* **45** Suppl 3: S77-S80.

Schumacher, A., and Magnuson, T. (1997) Murine *Polycomb*- and t*rithorax*-group genes regulate homeotic pathways and beyond. *Trends Genet.* **13**: 167-170.

Schwabe, J.W.R., Chapman, L., Finch, J.T., and Rhodes, D. (1993) The crystal structure of the estrogen receptor DNA-binding domain bound to DNA: how receptors discriminate between their response elements. *Cell* **75**: 567-578.

Scott, W.J. Jr., Walter, R., Tzimas, G., Sass, J.O., Nau, H., and Collins, M.D. (1994) Endogenous Status of Retinoids and Their Cytosolic Binding Proteins in Limb Buds of Chick vs Mouse Embryos. *Dev. Biol.* **165**: 397-409.

Seitanidou, T., Schneider-Maunoury, S., Desmarquet, C., Wilkinson, D.G., and Charnay, P. (1997) *Krox-20* is a key regulator of rhombomere-specific gene expression in the developing hindbrain. *Mech. Dev.* **65**: 31-42.

Sham, M.H., Vesque, C., Nonchev, S., Marshall, H., Frain, M., Dasgupta, R., Whiting, J., Wilkinson, D., Charnay, P., and Krumlauf, R. (1993) The zinc finger gene krox20 regulates hoxb2 (hoxb2.8) during hindbrain segmentation. *Cell* **72**: 183-196.

Shamugam, K., Green, N.C., Rambaldi, I., Sargovi, H.U., and Featherstone, M.S. (1999) PBX and MEIS as non-DNA-binding proteins in trimeric complexes with HOX proteins. *Mol. Cell. Biol.* **19**: 7577-7588.

Shen, W.F., Rozenfeld, S., Kwong, A., Köm Ves, L.G., Lawrence, H.J., and Largman, C. (1999) HoxA9 forms triple complexes with PBX2 and MEIS1 in myeloid cells. *Mol. Cell. Biol.* **19**: 3051-3061.

Shenefelt, R.E. (1972) Morphogenesis of malformations in hamsters caused by retinoic acid: relation to dose and stage at treatment. *Teratology* **5**: 103-118.

Shum, A.S.W., Poon L.L.M., Tang, W.W.T., Koide, T., Chan, B.W.H., Leung, Y.-C.G., Shiroishi, T., and Copp, A.J. (1999) Retinoic acid induces down-regulation of *Wnt-3a*, apoptosis and diversion of tail bud cells to a neural fate in the mouse embryo. *Mech. Dev.* **84**: 17-30.

Siegenthaler, G., Tomatis, I., Chatellard-Gruaz. D., Jaconi, S., Eriksson, U., and Saurat, J.H. (1992) Expression of CRABP-I and –II in human epidermal cells. Alteration of relative protein amounts is linked to the state of differentiation. *Biochem J.* **287**: 383-389.

Siman, C.M., and Eriksson, U.J. (1997) Vitamin E decreases the occurrence of malformations in the offspring of diabetic rats. *Diabetes* **46**: 1054-1061.

Simeone, A., Acampora, D., Arcioni, L., Andrews, P.W., Boncinelli, E., and Mavilio, F. (1990) Sequential activation of HOX2 homeobox genes by retinoic acid in human embryonal carcinoma cells. Nature 346: 763-766.

Simeone, A., Acampora, D., Nigro, V., Faiella, A., D'Esposito, M., Stornaiuolo, A., Mavilio, F., and Boncinelli, E. (1991) Differential regulation by retinoic acid of the homeobox genes of the four HOX loci in human embryonal carcinoma cells. *Mech. Dev.* **33**: 215-227.

Simon, A., Hellman, U., Wernstedt, C., and Eriksson, U. (1995) The retinal pigment epithelial-specific 11-*cis*-retinol dehydrogenase belongs to the family of short chain alcohol dehydrogenases. *J. Biol. Chem.* **270**: 1107-1112.

Singh, K., Carey, M., Saragosti, S., Botchan, M. (1985) Expression of enhanced levels of small RNA polymerase III transcripts encoded by the B2 repeats in simian virus 40-transformed mouse cells. *Nature* **314**: 553-556.

Sokolova, N. (1996) The roles of vitamin A in embryonic lung development in mice. *D.Phil. thesis, University of Oxford, U.K.*

Soler, N.G., Walsh, C.H., and Malins, J.M. (1976) Congenital malformations in infants of diabetic mothers. *Q. J. Med.* **45**: 303-313.

Soprano, D.R., and Soprano, K.J. (1995) Retinoids as teratogens. *Annu Rev. Nutr.* **15**: 111-132.

Spencer, T.E., Jenster, G., Burcin, M.M., Allis, C.D., Zhou, J., Mizzen, C.A., McKenna, N.J., Onate, S.A., Tsai, S.Y., and O'Malley, B.W. (1997) Steroid receptor coactivator-1 is a histone acetyltransferase. *Nature* **389**: 194-198.

Spielberg, S.P., Shear, N.H., Cannon, M., Hutson, N.J., Gunderson, K. (1991) In-vitro assessment of a hypersensitivity syndrome associated with sorbinil. *Ann. Intern. Med.* **114**: 720-724.

Sporn, M.B., Roberts, A.B., and Goodman, D.S. (1994) In Sporn, M.B., Roberts, A.B., Goodman, D.S. (eds), The Retinoids: Biology, Chemistry and Medicine, Raven Press, New York.

Srivastava, S.K., Petrash, J.M., Sadana, I.J., Ansari, N.H., Partridge, C.A. (1982) Susceptibility of aldehyde and aldose reductases of human tissues to aldose reductase inhibitors. *Curr. Eye. Res.* **83**;2(6): 407-410.

Stratford, T., Logan, C., Zile, M., and Maden, M. (1999) Abnormal anteroposterior and dorsoventral patterning of the limb bud in the absence of retinoids. *Mech. Dev.* **81**: 115-125.

Studer, M., Gavalas, A., Marshall, H., Ariza-McNaughton, L., Rijli, F.M., Chambon, P., and Krumlauf, R. (1998) Genetic interactions between *Hoxa1* and *Hoxb1* reveal new roles in regulation of early hindbrain patterning. *Development* **125**: 1025-1036.

Studer, M., Lumsden, A., Ariza-McNaughton, L., Bradley, A., and Krumlauf, R. (1996) Altered segmental identity and abnormal migration of motor neurons in mice lacking *Hoxb-1*. *Nature* **384**: 630-634.

Studer, M., Pöpperl, H., Marshall, H., Kuroiwa, A., and Krumlauf, R. (1994) Role of a conserved retinoic acid response element in rhombomere restriction of Hoxb1. *Science* **265**: 1728-1732.

Subbarayan, V., Kastner, P., Mark, M., Dierich, A., Gorry, P., and Chambon, P. (1997) Limited specificity and large overlap of the functions of the mouse RARγ1 and RARγ2 isoforms. *Mech. Dev.* **66**: 131-142.

Subramanian, V., Meyer, B.I., and Gruss, P. (1995) Disruption of the murine homeobox gene *Cdx1* affects axial skeletal identities by altering the mesodermal expression domains of *Hox* genes. *Cell* **83**: 641-653.

Sucov, H.M., Dyson, E., Gumeringer, C.L., Price, J., Chein, K.R., and Evans, R.M. (1994) RXRα mutant mice establish a genetic basis for vitamin A signaling in heart morphogenesis. *Genes. Dev.* **8**: 1007-1018.

Sucov, H.M., Izpisua-Belmonte, J.C., Ganan, Y., and Evans, R.M. (1995) Mouse embryos lacking RXRα are resistant to retinoic-acid-induced limb defects. *Development* **121**: 3997-4003.

Sucov, H.M., Murakami, K.K., Evans, R.M. (1990) Characterization of an autoregulated response element in the mouse retinoic acid receptor type beta gene. *Proc. Natl. Acad. Sci. USA* **87**: 5392-5396.

Sugawara, A., Yen, P.M., Qi, Y., Lechan, R.M., Chin, W.W. (1995) Isoform-specific retinoid-X receptor (RXR) antibodies detect differential expression of RXR proteins in the pituitary gland. *Endocrinology* **136**: 1766-1774.

Suzuki, K., Koh, Y.H., Mizuno, H., Hamaoka, R., and Taniguchi, N. (1998) Overexpression of aldehyde reductase protects PC12 cells from the cytotoxicity of methylglyoxal or 3-deoxyglucosone. *J. Biochem.* **123:** 353-357.

Swindell, E.C., Thaller, C., Sockanathan, S., Petkovich, M., Jessell, T.M., Eichele, G. (1999) Complementary domains of retinoic acid production and degradation in the early chick embryo. *Dev Biol* **216**: 282-296.

Szwergold, B.S., Kappler, F., Brown, T.R. (1990) Identification of fructose 3-phosphate in the lens of diabetic rats. *Science* **247**: 451-454.

Takada, S., Stark, K.L., Shea, M.J., Vassileva, G., and McMahon, J.A. (1994) Wnt-3a regulates somite and tailbud formation in the mouse embryo. *Genes. Dev.* **8**: 174-189.

Takahashi, M., Fujii, J., Miyoshi, E., Hoshi, A., Taniguchi, N. (1995) Elevation of aldose reductase gene expression in rat primary hepatoma and hepatoma cell lines: implication in detoxification of cytotoxic aldehydes. *Int. J. Cancer* **62**: 749-754.

Takahashi, M., Fujii, J., Teshima, T., Suzuki, K., Shiba, T., and Taniguchi, N. (1993) Identity of a major 3-deoxyglucosone-reducing enzyme with aldehyde reductase in rat liver established by amino acid sequencing and cDNA expression. *Gene* **127**: 249-253.

Tam, P.P.L., and Behringer, R.R. (1997) Mouse gastrulation: the formation of the mammalian body plan. *Mech. Dev.* **68**: 3-25.

Taneja, R., Bouillet, P., Boylan, J.F., Gaub, M.-P., Roy, B., Gudas, L.J., and Chambon, P. (1995) Reexpression of retinoic acid receptor (RAR)γ or overexpression of RARα or RARβ in RARγ-null F9 cells reveals a partial functional redundancy between the three RAR types. *Proc. Natl.Acad. Sci. USA* **92**:7834-7858.

Thompson, J.N., Howell, J.McC., and Pitt, G.A. (1964) Vitamin A and reproduction in rats. *Proc. Royal Soc.* **159**: 510-535.

Tibbles, L., and Wiley, M.J. (1988) A comparative study of the effects of retinoic acid given during the critical period for inducing spina bifida in mice and hamsters. *Teratology* **37**: 113-125.

Tomlinson, D.R., Stevens, E.J., and Diemel, L.T. (1994) Aldose reductase inhibitors and their potential for the treatment of diabetic complications. *Trends. Pharm. Sci.* **15**: 293-297.

Torchia, J., Glass, C., and Rosenfeld, M.G. (1998) Co-activators and co-repressors in the integration of transcriptional responses. *Curr. Opin. Cell Biol.* **10**: 373-383.

van der Hoeven, F., Zákány, J., and Duboule, D. (1996) Gene transpositions in the *HoxD* complex reveal a hierarchy of regulatory controls. *Cell* **85**: 1025-1035.

Vander Jagt, D.L., Robinson, B., Taylor, K.K., and Hunsaker, L.A. (1992) Reduction of trioses by NADPH-dependent aldo-keto reductases. Aldose reductase, methylglyoxal, and diabetic complications. *J. Biol. Chem.* **267**: 4364-4369

van der Wees, J., Schilthuis, J.G., Koster, C.H., Diesveld-Schipper, H., Folkers, G.E., van der Saag, P.T., Dawson, M.I., Shudo, K., van der Burg, B., and Durston, A.J. (1998) Inhibition of retinoic acid receptor-mediated signalling alters positional identity in the developing hindbrain. *Development* **125**: 545-556.

Vasseur, M., Condamine, H., and Duprey, P. (1985) RNAs containing B2 repeated sequences are transcribed in the early stages of mouse embryogenesis. *EMBO J.* **4**: 1749-1753.

Velculescu, V.E., Zhang, L., Vogelstein, B., and Kinzler, K.W. (1995) Serial analysis of gene expression. *Science* **270**:484-487.

Vesque, C., Maconochie, M., Nonchev, S., Ariza-McNaughton, L., Kuroiwa, A., Charnay, P., and Krumlauf, R. (1996) Hoxb-2 transcriptional activation in rhombomeres 3 and 5 requires an evolutionarily conserved cis-acting element in addition to the krox-20 binding site. *EMBO J.* **15**: 71-88.

Vogel, S., Mendelsohn, C.L., Mertz, J.R., Piantedosi, R., Waldburger, C., Gottesman, M.E., Blaner, W.S. (2001) Characterization of a new member of the fatty acid-binding protein family that binds all-trans-retinol. *J. Biol. Chem.* **276**: 1353-1360.

Vogt, T.F., and Duboule, D. (1999) Antagonists go out on a limb. *Cell* **99**: 563-566.

Vonesch, J.L., Nakshatri, H., Philippe, M., Chambon, P., and Dollé, P. (1994) Stage and tissue-specific expression of the alcohol dehydrogenase 1 (Adh-1) gene during mouse development. *Dev. Dyn.* **199**: 199-213.

Wagner, M., Han, B., and Jessell, T.M. (1992) Regional differences in retinoid release from embryonic neural tissue detected by an in vitro reporter assay. *Development* **116**: 55-66.

Wang, X., Penzes, P., and Napoli, J.L. (1996) Cloning of a cDNA encoding an aldehyde dehydrogenase and its expression in *Escherichia coli*. Recognition of retinal as a substrate. *J.Biol. Chem.* **271**: 16288-16293.

Warkany, J., and Schraffenberger, E. (1946) Congenital malformations induced in rats by maternal vitamin A deficiency. I. Defects of the eye. *Arch. Opthalmol.* **35**: 150-169.

Webster, W.S., Johnston, M.C., Lammer, E.J., and Sulik, K.K. (1986) Isotretinoin embryopathy and the cranial neural crest: an in vivo and in vitro study. *J. Craniofac. Genet. Dev. Biol.* **6**: 211-222.

Weiss, H., Friedrich, T., Hofhaus, G., and Preis, D. (1991) The respiratory-chain NADH dehydrogenase (complex I) of mitochondria. *Eur. J. Biochem.* **197**: 563-576.

Welcher, A.A., Torres, A.R., Ward, D.C. (1986) Selective enrichment of specific DNA, cDNA and RNA sequences using biotinylated probes, avidin and copper-chelate agarose. *Nucleic. Acids. Res.* **14**: 10027-44

Wen, Y.-D., Perissi, V., Staszewski, L.M., Yang, W.-M., Krones, A., Glass, C.K., Rosenfeld, M.G., and Seto., E. (2000) The histone deacetylase-3 complex contains nuclear receptor corepressors. *Proc. Natl. Acad. Sci. USA* **97**: 7202-7207.

White, J.A., Guo, Y.-D., Baetz, K., Beckett-Jones, B., Bonasoro, J., Hsu, K.E., Dilworth, F.J., Jones, G., and Petkovich, M. (1996) Identification of the retinoic acid-inducible all-trans-retinoic acid 4-hydroxylase. *J. Biol. Chem.* **272**: 18538-18541.

White, J.A., Beckett-Jones, B., Guo, Y.-D., Dilworth, J., Bonasoro, J., Jones, G., and Petkovich, M. (1997) cDNA cloning of human retinoic acid-metabolizing enzyme (hP450RAI) identifies a novel family of cytochromes P450 (CYP26). *J. Biol. Chem.* **271**: 29922-29927.

White, J.A., Ramshaw, H., Taimi, M., Stangle, W., Zhang, A., Everingham, S., Creighton, S., Tam, S.-P., Jones, G., and Petkovich, M. (2000a) Identification of the human cytochrome P450, P450RAI-2, which is predominantly expressed in the adult cerebellum and is responsible for all-*trans*-retinoic acid metabolism. *Proc. Natl. Acad. Sci. USA* **97**: 6403-6408.

White, J.C., Highland, M., Kaiser, M., Clagett-Dame, M. (2000b) Vitamin A-deficiency results in the dose-dependent acquisition of anterior character and shortening of the caudal hindbrain of the rat embryo. *Dev. Biol.* **220**: 263-284.

White, J.C., Shankar, V.N., Highland, M., Epstein, M.L., DeLuca, H.F., and Clagett-Dame, M. (1998) Defects in embryonic hindbrain development and fetal resorption resulting from vitamin A deficiency in the rat are prevented by feeding pharmacological levels of all-*trans*-retinoic acid. *Proc. Natl. Acad. Sci. USA* **95**: 13459-13464.

Wilkinson, D.G. (1992) *In* "In Situ Hybridization. A Practical Approach." IRL Press, New York.

Williams, J.B., Pramanik, J.L., and Napoli, J.L. (1984) Vitamin A metabolism: analysis of steady-state neutral metabolites in rat tissues. *J. Lipid. Res.* **25**: 638-645.

Wilson, J.C., Roth, C.B., and Warkany, J. (1953) An analysis of the syndrome of maternal vitamin A deficiency. Effects of restoration of vitamin A at various times during gestation. *Am. J. Anat.* **92**: 189-217.

Wilson, J.G., and Warkany, J. (1948) Malformations in the genitourinary tract induced by maternal vitamin A deficiency in the rat. *Am. J. Anat.* **83**: 357-407.

Wilson, J.G., and Warkany, J. (1949) Aortic-arch and cardiac abnormalities on the offspring of vitamin A deficient rats. *Am. J. Anat.* **85**: 113-155.

Wilson V., and Beddington, R.S.P. (1996) Cell fate and morphogenetic movement in the late mouse primitive streak. *Mech. Dev.* **55**: 79-89.

Wolbach, S.B., and Howe, P.R. (1925) Tissue changes folowing deprivation of fat-soluble A vitamin. *J. Exp. Med.* **42**: 753-777.

Wood, H., Pall, G., and Morriss-Kay, G. (1994) Exposure to retinoic acid before or after the onset of somitogenesis reveals separate effects on rhombomeric segmentation and 3' HoxB gene expression domains. *Development* **120**: 2279-2285.

Wood, H.B., Ward, S.J., and Morriss-Kay, G.M. (1996) Effects of all-*trans*-retinoic acid on skeletal pattern, 5' HoxD gene expression, and RARβ2/β4 promoter activity in embryonic mouse limbs. *Dev. Genet.* **19**: 74-84.

Xu, L., Glass, C.K., and Rosenfeld, M.G. (1999) Coactivator and corepressor complexes in nuclear receptor function. *Curr. Opin. Genet. Dev.* **9**: 140-147.

Yagihashi, S., Yamagishi, S., Wada, R., Sugimoto, K., Baba, M., Wong, H.G., Fujimoto, J., Nishimura, C., Kokai, Y. (1996) Galactosemic neuropathy in transgenic mice for human aldose reductase. *Diabetes* **45**: 56-59.

Yamaguchi, T.P., Harpal, K., Henkemeyer, M., and Rossant, J. (1994) fgfr-1 is required for embryonic growth and mesodermal patterning during mouse gastrulation. *Genes Dev.* **8**: 3032-3044.

Yamaguchi, T.P., Takada, S., Yoshikawa, Y., Wu, N., and McMahon, A.P. (1999) T (Brachyury) is a direct target of Wnt3a during paraxial mesoderm specification. *Genes. Dev.* **13**: 3185-3190.

Yamaoka, T., Nishimura, C., Yamashita, K., Itakura, M., Yamada, T., Fujimoto, J., Kokai, Y. (1995) Acute onset of diabetic pathological changes in transgenic mice with human aldose reductase cDNA. *Diabetologia* **38**: 255-261.

Yan, S.D., Schmidt, A.M., Anderson, G.M., Zhang, J., Brett, J., Zou, Y.S., Pinsky, D., and Stern, D. (1994) Enhanced cellular oxidant stress by the interaction of advanced glycation end products with their receptors/binding proteins. *J. Biol. Chem.* **269**: 9889-9897.

Yang, X., Borg, L.A.H., Siman, C.M., and Eriksson, U.J. (1998) Maternal antioxidant treatments prevent diabetes-induced alterations of mitochondrial morphology in rat embryos. *Anat. Rec.* **251**: 303-135.

Yang, X., Ogryzko, V.V., Nishikawa, J., Howard, B.H., and Nakatani, Y. (1996) A p300/CBP-associated factor that competes with the adenoviral oncoprotein E1A. *Nature* 382: 319-324.

Yang, Z.-N., David, G.J., Hurley, T.D., Stone, C.L., Li, T.-K., and Bosron, W.F. (1994) Catalytic efficiency of human alcohol dehydrogenases for retinol oxidation and retinal reduction. *Alcohol. Clin. Exp. Res.* **18**: 587-591.

Yao, T.P., Ku, G., Zhou, N., Scully, R., and Livingston, D.M. (1996) The nuclear hormone recepto coactivator SRC-1 is a specific target of p300. *Proc. Natl. Acad. Sci. USA* **93**: 10626-10631.

Ye, Q., Hyndman, D., Li, X., Flynn, T.G., and Jia, Z. (2000) Crystal structure of CHO reductase, a member of the aldo-keto reductase superfamily. *Proteins* **38**: 41-48.

Yoshida, A., Rzhetsky, A., Hsu, L.C., and Chang, C. (1998) Human aldehyde dehydrogenase gene family. *Eur. J. Biochem.* **251**: 549-557.

Yu, B.D., Hess, J.L., Horning, S.E., Brown, G.A., and Korsmeyer, S.J. (1995) Altered Hox expression and segmental identity in Mll-mutant mice. *Nature* **378**: 505-508.

Yuan, C.X., Ito, M., Fondell, J.D., Fu, Z.Y., and Roeder, R.G. (1998) The TRAP220 component of a thyroid hormone receptor-associated protein (TRAP) coactivator complex interacts directly with nuclear receptors in a ligand-dependent fashion. *Proc. Natl. Acad. Sci. USA*. **95**: 7939-7944.

Zechel, C., Shen, X.-Q., Chen, J.-Y., Chen, Z.-P., Chambon, P., and Gronemeyer, H. (1994) The dimerization interfaces formed between the DNA binding domains of RXR, RAR and TR determine the binding specificity and polarity of the full-length receptors to direct repeats. *EMBO J.* **13**: 1425-1433.

Zelent, A., Mendelsohn, C., Kastner, P., Garnier, J.M., Ruffenach, F., Leroy, P., and Chambon, P. (1991) Differentially expressed isoforms of the mouse retinoic acid receptor β are generated by the usage of two promoters and alternative slpicing. *EMBO J.* **10**: 71-81.

Zhang, F., Pöpperl, H., Morrison, A., Kovàcs, E.N., Prideaux, V., Schwartz, L., Krumlauf, R., Rossant, J., and Featherstone, M.S. (1997a) Elements both 5' and 3' to the murine Hoxd4 gene establish anterior borders of expression in mesoderm and neuroectoderm. *Mech. Dev.* **67**: 49-58.

Zhang, F., Kovács, E.N., and Featherstone, M.S. (2000) Murine *Hoxd4* expression in the CNS requires multiple elements including a retinoic acid response element. *Mech. Dev.* **96**: 79-89.

Zhang, X.-K., Lehmann, J., Hoffmann, B., Dawson, M, Cameron, J., Graupner, G., Hermann, T., Tran, P., and Pfahl, M. (1992) Homodimer formation of retinoid X receptor induced by 9-*cis* retinoic acid. *Nature* **358**: 587-591.

Zhang, Y., Iratni, R., Erdjument-Bromage, H., Tempst, P., and Reinberg, D. (1997b) Histone deacetylases and SAP18, a novel peptide, are components of a human Sin3 complex. *Cell* **89**: 357-364.

Zhao, D., McCaffery, P., Ivins, K.J., Neve, R.L., Hogan, P., Chin, W.W., and Drager, U.C. (1996) Molecular identification of a mojor retinoic acid synthesizing enzyme, a retinaldehyde dehydrogenase. *Eur. J. Biochem.* **15**: 15-22.

Zhu, Y., Qi, C., Jain, S., Le Beau, M.M., Espinosa, R., Atkins, G.B., Lazar, M.A., Yeldandi, A.V., Rao, M.S., and Reddy, J.K. (1999) Amplification and overexpression of peroxisome proliferator-activated receptor binding protein (PBP/PPARBP) gene in breast cancer. *Proc. Natl. Acad. Sci. USA* **96**: 10848-100853.

Contributions to Original Knowledge

Chapter 4 of this thesis describes the identification and characterization of a novel member of the aldo-keto reductase superfamily. The full-length mouse *aldehyde reductase* (*AKR1A4*) cDNA was isolated and the expression pattern of this gene was assessed in the adult, and in the mouse embryo from E7.5 to E14.5. This is the first description of an *aldehyde reductase* expression pattern during development.

Chapter 5 describes the skeletal analysis of the *Cdx1/RARγ* single and compound mutants. Analysis of *Cdx1* heterozygous skeletons demonstrated that *Cdx1* is haploinsufficient in a C57BL/6/SV129 mixed genetic background. *Cdx1/RARγ* double heterozygotes exhibit a significantly higher incidence of vertebral transformations, as compared to either single heterozygote. These data suggest that *Cdx1* and *RARγ* function in the same pathway to specify vertebral identity. Additionally, double homozygous null skeletons exhibit a significantly higher incidence of a thoracic to cervical vertebral transformation as compared to either single null mutant mouse. These data demonstrate that *Cdx1* and *RARγ* act synergistically to specify the identity of the first thoracic vertebra.

RA treatment at E7.4 is able to rescue the *Cdx1* null-associated phenotype. *RARγ* is required for this rescue as RA-treated *Cdx1/RARγ* double homozygous null mutants exhibit anteriorizations of the cervical vertebrae. Additionally, *Cdx1* is required for RA-induced posterior transformations as these abnormalities were observed at a lower incidence in *Cdx1* null mice. Taken together, these data demonstrate that *Cdx1* and *RARγ* are required for the full effects of excess RA on vertebral specification.